APPENDIX A: CONDUCTED VERSUS RADIATED PATH MEASUREMENTS

A.1 Overview

As illustrated in Figure A.1.1, there are two possible methods for performing radio interference measurements; one is conducted and the other is radiated. While radiated measurements have the advantage of simulating real world conditions, conducted measurements have the distinct advantage of being able to test under highly controlled conditions. The latter were chosen as the preferred method for performing the UWB/GPS interference measurements at the Institute for Telecommunication Sciences (ITS). To impute validity for the measurements, it is imperative, however, that the effects on the signal within the frequency band of interest be nearly identical, whether conducted or radiated. As the UWB signal proceeds from A to B or from A to C (shown in Figure A.1.1), the temporal characteristics of the pulse change due to various effects on the magnitude and phase across the frequency band. Some of this is expected because filtering, attenuation, and amplification occur along the path. The phase and magnitude of the signal are represented by $X(j\omega)$ at the pulse generator output connector, and $Y_1(j\omega)$ and $Y_2(j\omega)$ at the output of the GPS antenna terminal for the radiated path and the output of the LNA for the conducted path respectively (where $X(j\omega)$, $Y_1(j\omega)$, and $Y_2(j\omega)$ are the Fourier transform of the time-domain signal at the respective locations – A, B, and C). The transfer functions of the different paths are represented by $H(j\omega)$ and $G(j\omega)$, whereby $H(j\omega) = Y_1(j\omega) / X(j\omega)$ and $G(j\omega) = Y_2(j\omega) / X(j\omega)$. Ideally, $H(j\omega)$ and $G(j\omega)$ should be identical across the frequency band of interest.

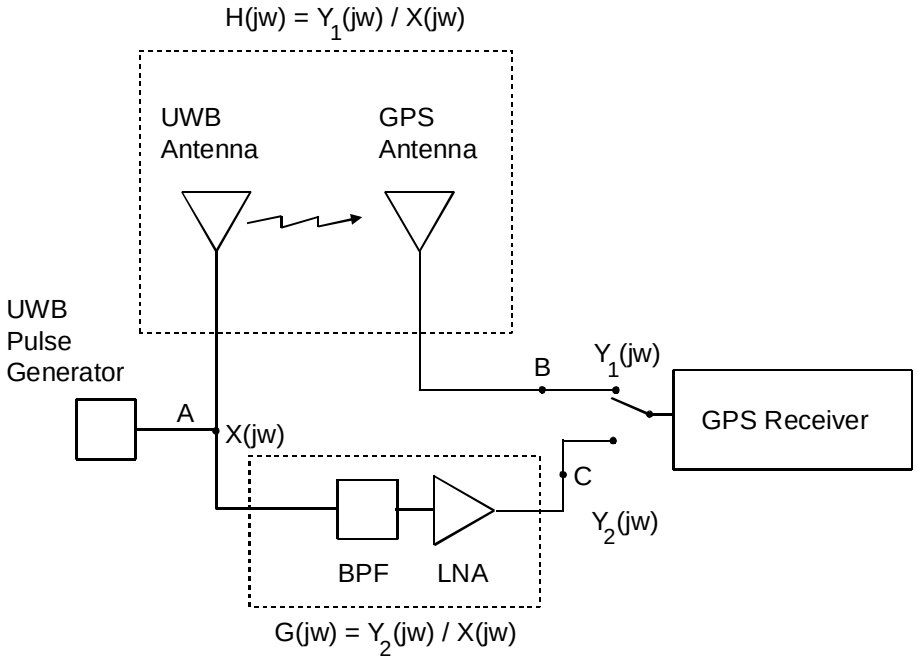

Figure A.1.1. Conducted versus radiated measurement concept.

To help match the transfer functions between the two paths, a band-pass filter (BPF) and low-noise (LNA) amplifier of bandwidth and gain, equivalent to that of the GPS antenna, were placed in the conducted path for all interference measurements. The UWB antenna is assumed to have a much wider bandwidth, making it less likely to contribute to narrowing of the bandwidth and therefore, does not require a filter to emulate its bandwidth characteristics.

Because, in real world applications, both UWB antennas and GPS antennas are used to transmit and receive pulsed or digital signals, it is assumed that the magnitude and phase distortion is minimal over the L1 band, and therefore, there should be little difference in signals (conducted or radiated) as seen in the L1 band. To verify these assumptions, measurements described herein were performed to determine the degree to which signals passed through the two paths, conducted and radiated, are likely to be the same. This was accomplished by measuring temporal characteristics of the UWB signal at points A and B as represented in Figure A.1.1. The measurements include high speed digitization of a single pulse (to determine the transfer function of the radiated path by performing Fourier analysis), as well as multiple pulse acquisitions to compare APD characteristics at points A and B for four different pulse spacing modes.

A.2 Single Pulse Measurement

High speed digitization of UWB signals emitted from a Time Domain Corporation PG-2000 pulse generator was conducted by the National Institute for Standards and Technology (NIST) Radio-Frequency Technology Division in their Time-Domain Laboratory to obtain data that represents the radiated time-domain waveform. The goal of these measurements was to capture a detailed view of a single pulse using a single-event transient digitizer capable of achieving very high sample rates. The digitizer used in this study possesses a bandwidth of 4.5 GHz with a maximum of 1,024 samples in a single shot and is designed to perform high fidelity measurements on a single pulse.

Conducted measurements were performed using the test fixture shown in Figure A.2.1. The RF output of the UWB device-under-test was connected using a coaxial transmission line to an attenuator, used to prevent overloading and damage to the measurement device from an overly strong signal level. The signal was then split into two equal amplitude levels and fed into a trigger port and a signal port on the transient digitizer.

Radiated measurements were performed using the test fixture shown in Figure A.2.2. Data was acquired in the NIST anechoic chamber using two different antennas: a UWB antenna (transmit) supplied by the manufacturer of the pulse generator, and a GPS antenna (receive) supplied with one of the receivers under test. The signal was split into two equal amplitude levels and fed into a trigger port and a signal port on the high speed transient digitizer.

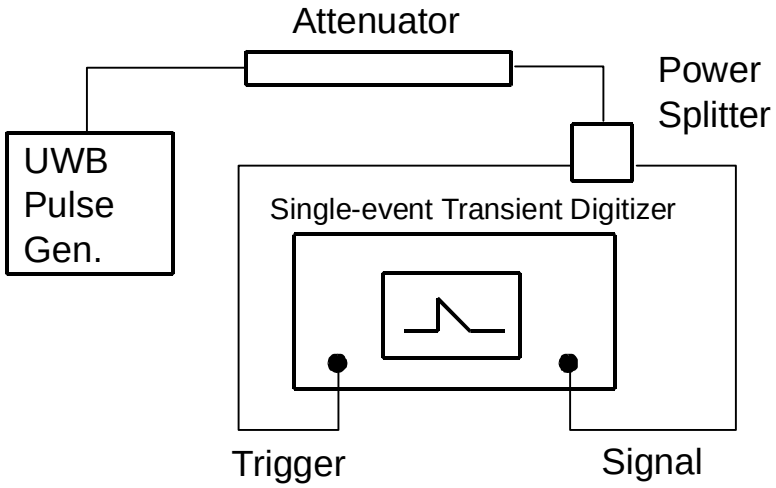

Figure A.2.1 Conducted measurement test setup.

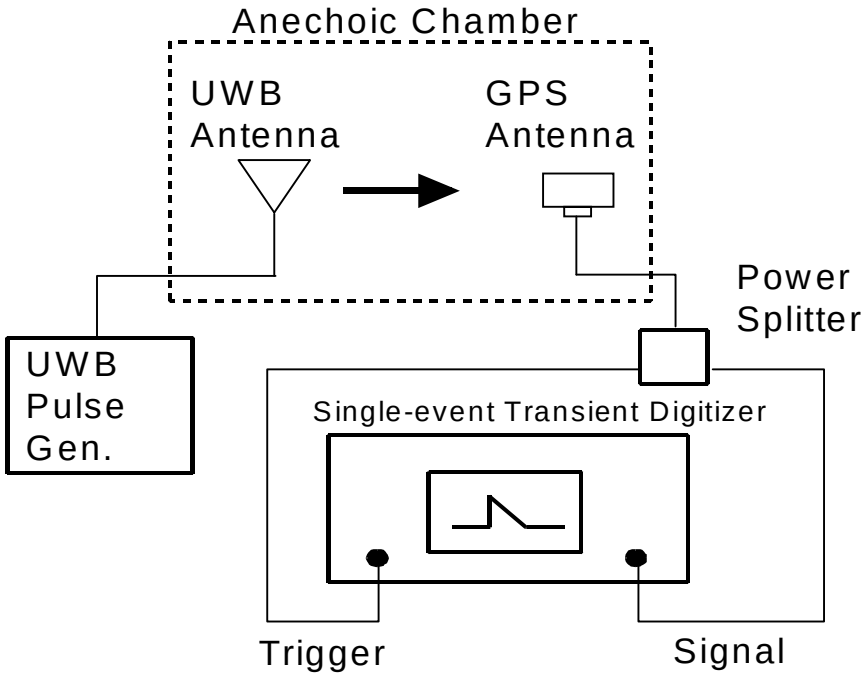

Figure A.2.2. Radiated measurement test setup.

The acquired pulses were processed to derive the complex transfer function for the radiated path ($H(j\omega)$). This was accomplished by performing a Fourier transform on the digitized time-domain radiated and conducted pulses to give $Y_1(j\omega)$ and $X(j\omega)$ respectively. To increase the frequency resolution to 150 kHz, each digitized pulse was padded with zeros (prior to applying the Fourier transform) to give a total sample size of 131,072 points. This is justified by the fact that the pulse goes to zero after full decay, and by padding with zeros, we are adding additional information that we know to be true. The complex transfer function of the radiated path was then determined by dividing $Y_1(j\omega)$ by $X(j\omega)$ to provide magnitude and group delay information across the band of interest. Since the transfer function of path A to C ($G(j\omega)$ in Figure A.1.1) is determined primarily by the inline bandpass filter (used during interference measurements), we can compare the effects of the two different paths by comparing $H(j\omega)$ (the transfer function of the radiated path) with $G(j\omega)$ (the transfer function of the filter). Figures A.2.4 through A.2.13 show the magnitude and group delay for the radiated path and for each of the inline filters used (filters F1 - F4 described in Appendix A). While there are significant differences at wider bandwidths, there is very little difference in the 20-MHz bandwidth centered at L1.

In addition to the magnitude and group delay characteristics, we can further compare the time-domain characteristics of the two different paths (A to B and A to C) by multiplying both $Y_1(j\omega)$, and $Y_2(j\omega)$ by the transfer function of a narrower filter (e.g. a 24-MHz bandpass filter) and applying the inverse Fourier transform. Figure A.2.3 illustrates the different paths used in the UWB/GPS interference measurements, each having their own transfer function. Path AB represents the radiated path, going from the UWB pulse generator to the output of the GPS antenna. Path AC represents the conducted path from the UWB pulse generator to receiver 2, and path AD for receiver 1. Assuming a maximum bandwidth of 24 MHz along each paths, as the signal ultimately passes through the preselector filter of the GPS receiver, we can compare the time-domain response at the output of each path (represented by paths ABF, ACF, and ADF). This is accomplished by multiplying the Fourier transform of the input signal at point A by the transfer function of each component along the chain (whether it be the two antennas, or inline filters) and then performing the inverse Fourier transform on the result. This is done for each of the four paths. Figure A.2.14 shows two pulses: one at the output of the UWB pulse generator and the other at the output of the GPS antenna (via the radiated path). Figure A.2.15 shows the simulated pulses at the output of each of the three paths (ABF, ACF, and ADF). While the pulses at various points along the chain (at different bandwidths) may be quite different, we can see that for the output at the end of each path, when limited in bandwidth by the same 24-MHz filter, there is very little difference in the time-domain characteristics.

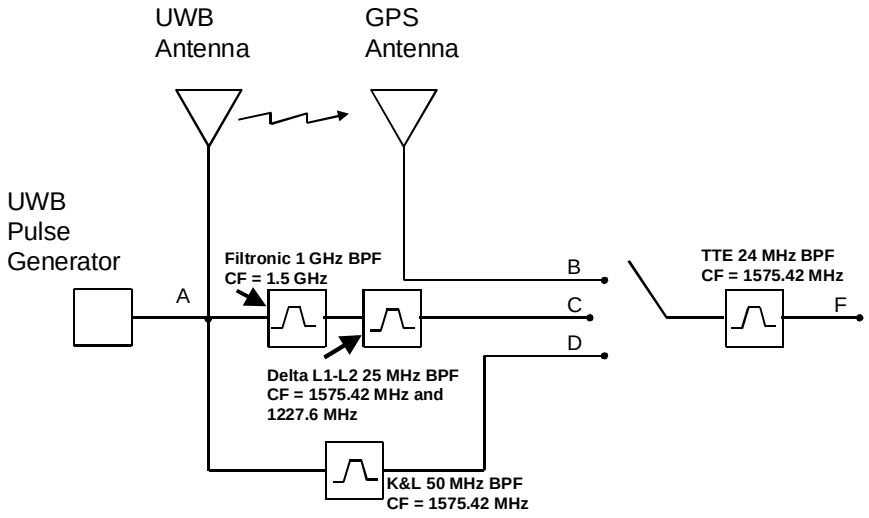

Figure A.2.3. Filter specifications for the different measurement paths.

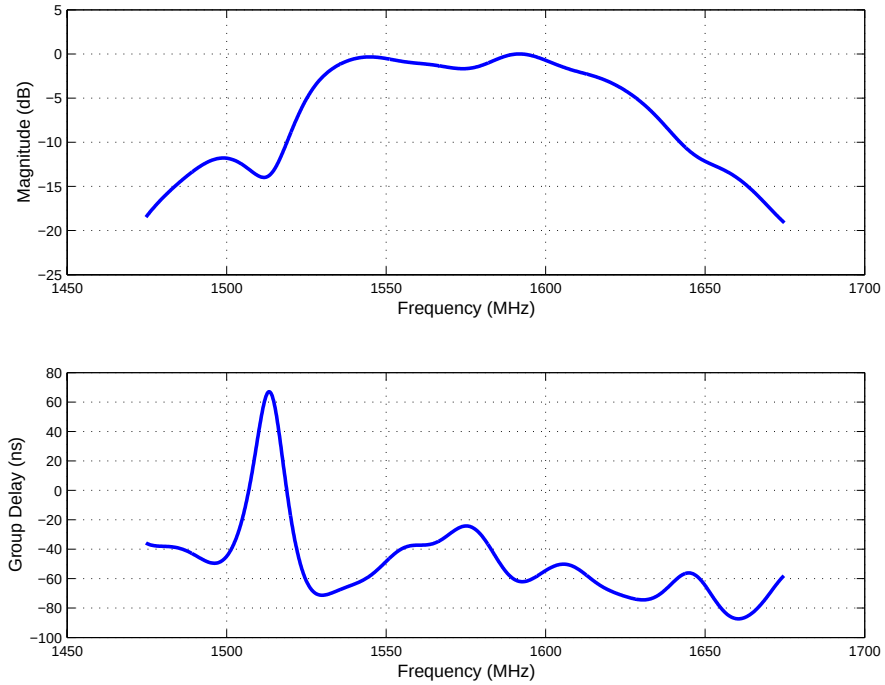

Figure A.2.4. Transfer function magnitude and group delay for radiated path - 1475 MHz to 1675 MHz.

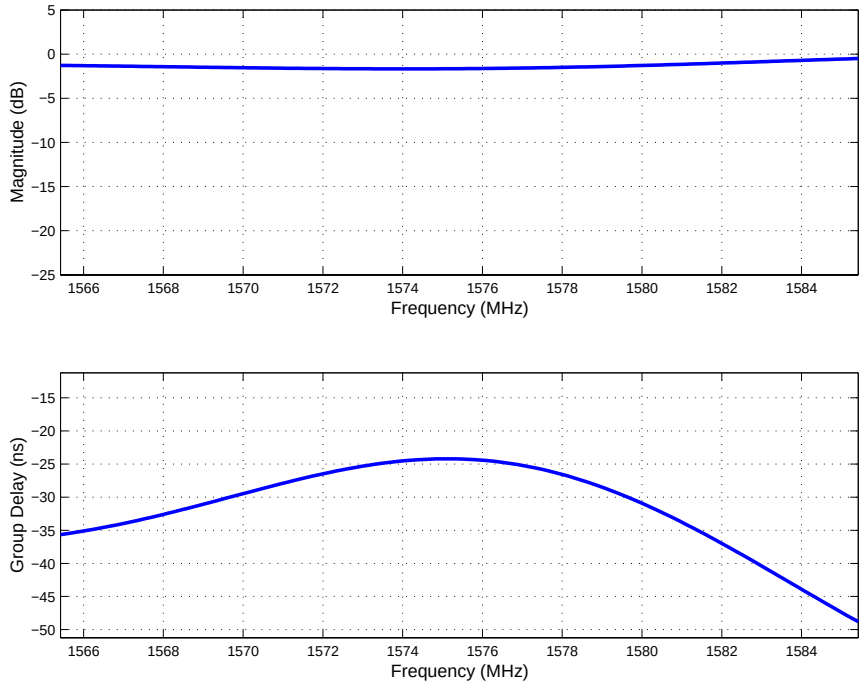

Figure A.2.5. Transfer function magnitude and group delay for radiated path - 1565 MHz to 1585 MHz.

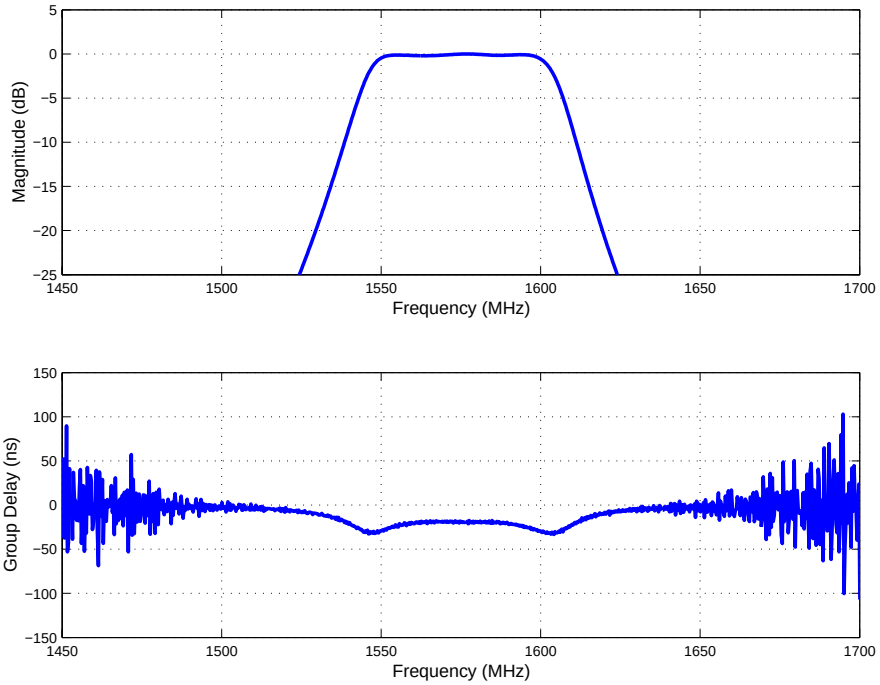

Figure A.2.6. Transfer function magnitude and group delay for filter F3 - 1475 MHz to 1675 MHz.

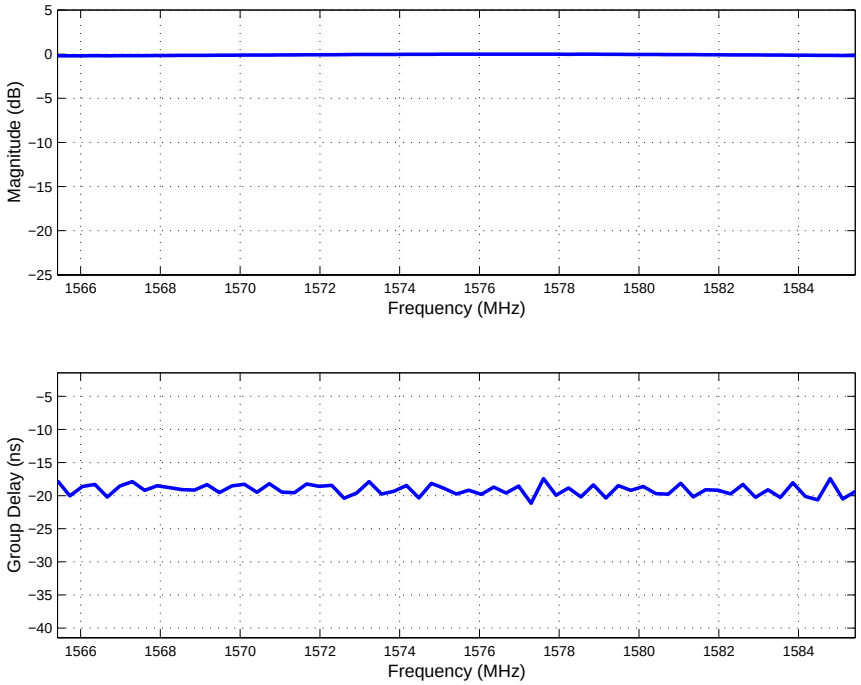

Figure A.2.7. Transfer function magnitude and group delay for filter F3 - 1565 MHz to 1585 MHz.

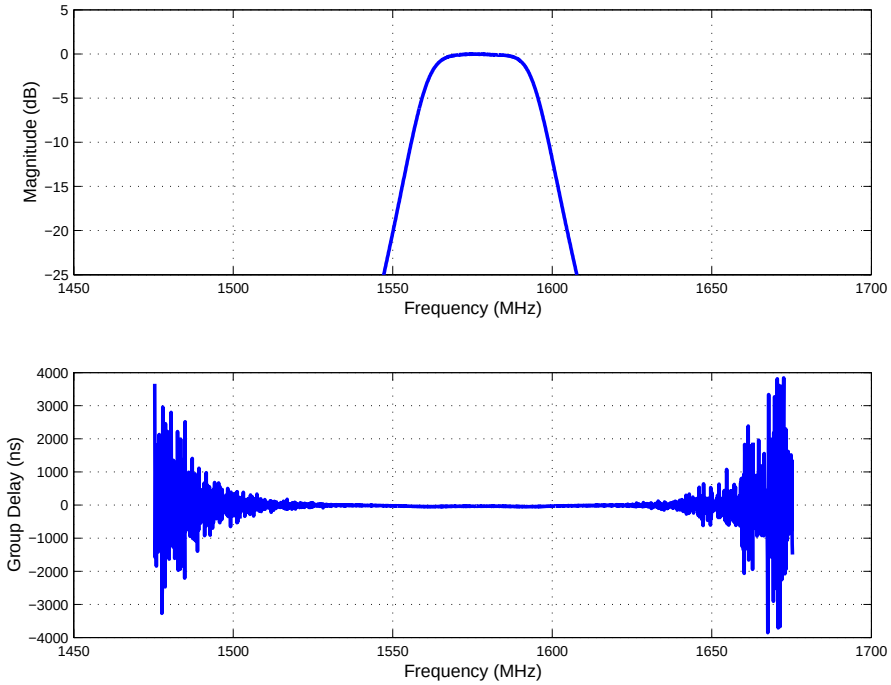

Figure A.2.8. Transfer function magnitude and group delay for filter F1 - 1475 MHz to 1675 MHz.

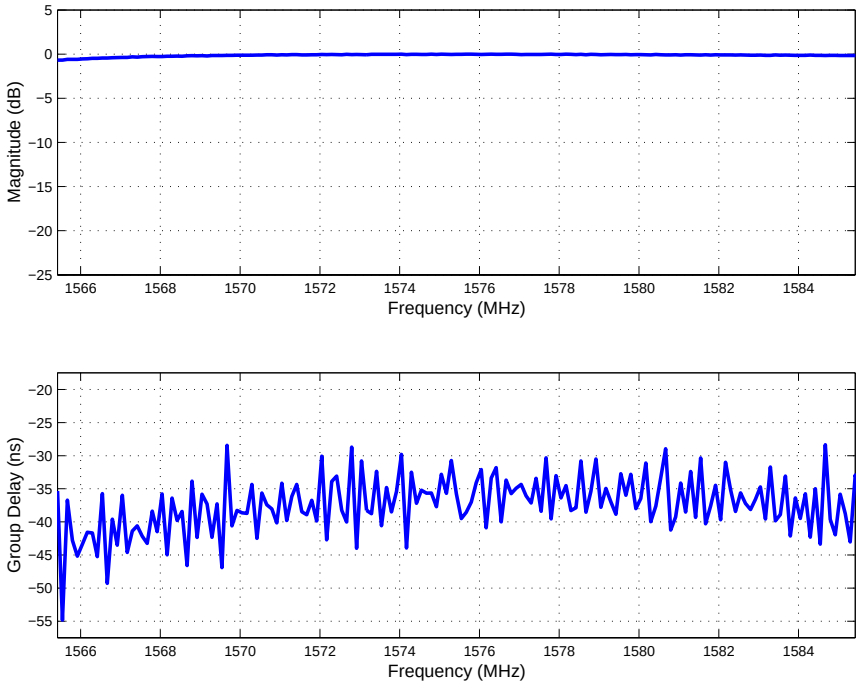

Figure A.2.9. Transfer function magnitude and group delay for filter F1 - 1565 MHz to 1585 MHz.

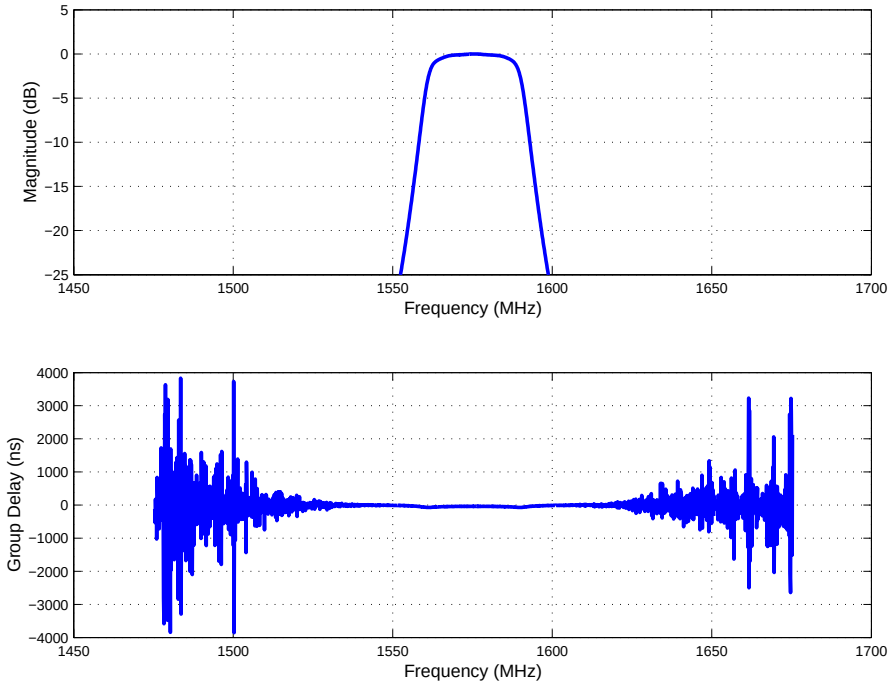

Figure A.2.10. Transfer function magnitude and group delay for filter F4 - 1475 MHz to 1675 MHz.

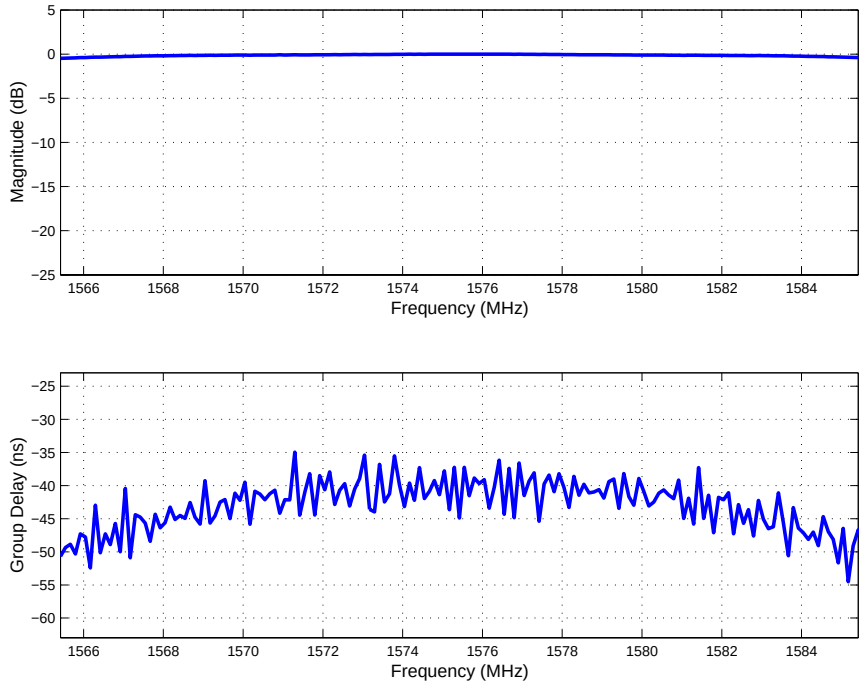

Figure A.2.11. Transfer function magnitude and group delay for filter F4 - 1565 MHz to 1585 MHz.

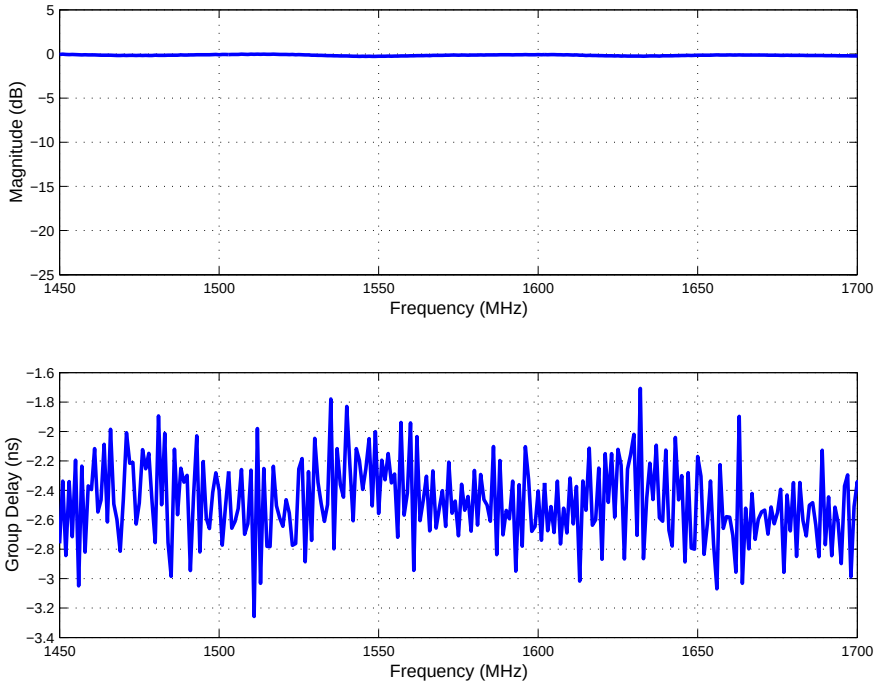

Figure A.2.12. Transfer function magnitude and group delay for filter F2 - 1475 MHz to 1675 MHz.

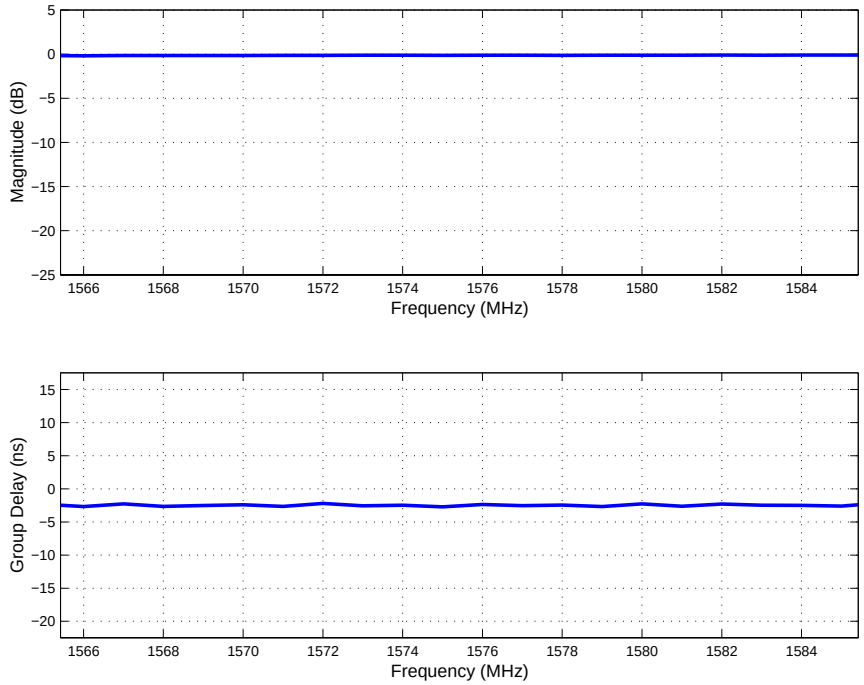

Figure A.2.13. Transfer function magnitude and group delay for filter F2 - 1565 MHz to 1585 MHz.

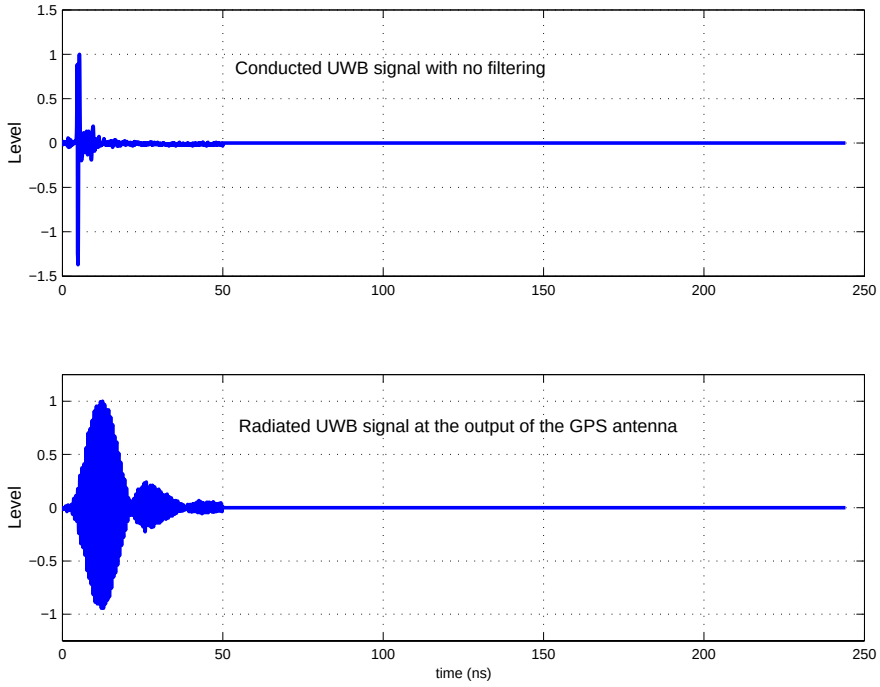

Figure A.2.14. Pulse characteristics - conducted and radiated. (Levels are normalized to peak voltage.)

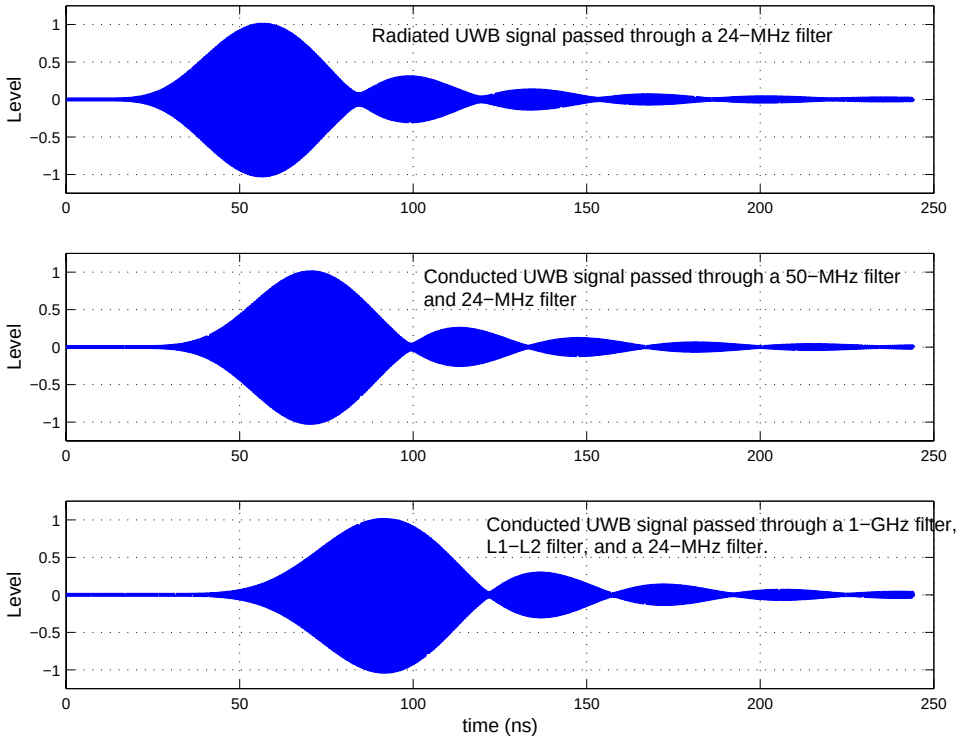

Figure A.2.15. Pulse characteristics through different measurement paths. (Levels are normalized to peak voltage.)

A.3 Multiple Pulse Measurement

Multiple pulse measurements were performed to determine the degree of signal alteration with regard to APDs, when the signal is radiated. While it is possible to have two remarkably different signals with the same amplitude distribution, if a signal, radiated and conducted, has the same amplitude distribution for the two different paths, the time-domain shape is likely to be very similar. For this reason, APD measurements were performed for two different bandwidths (3 MHz and 20 MHz centered at L1) using four different UWB signals. Results of these measurements (see Figures A.3.1 through A.3.8) show very little difference between the radiated and conducted path for the bandwidths of interest.

Data, for both conducted and radiated paths, was acquired and processed using techniques described in NTIA Report 01-383 [1].

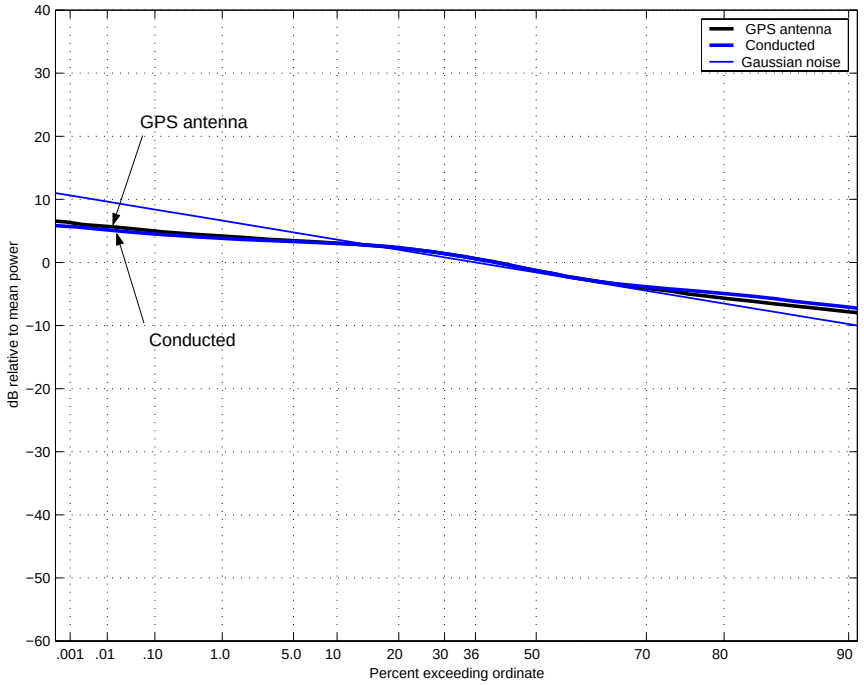

Figure A.3.1. Radiated vs. conducted APDs of 2%-RRD UWB signals (3-MHz PRF, no gating) measured in a 3-MHz bandwidth.

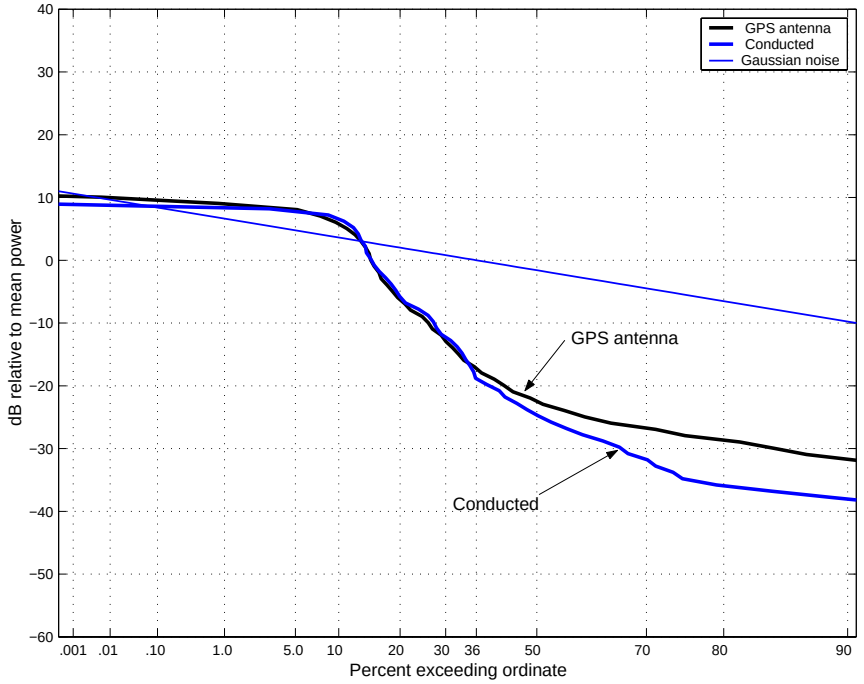

Figure A.3.2. Radiated vs. conducted APDs of 2%-RRD UWB signals (3-MHz PRF, no gating) measured in a 20-MHz bandwidth.

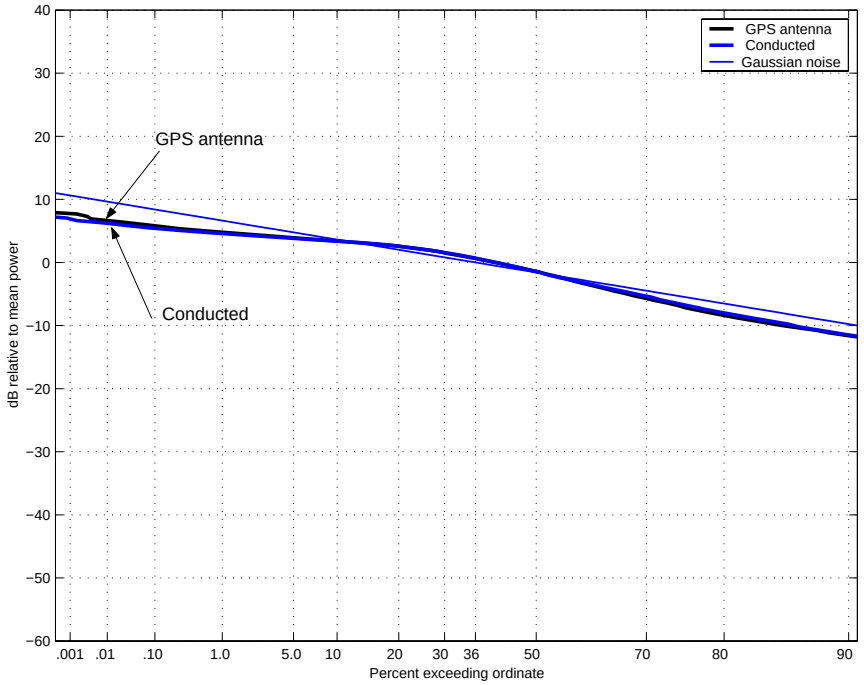

Figure A.3.3. Radiated vs. conducted APDs of 50%-ARD UWB signals (3-MHz PRF, no gating) measured in a 3-MHz bandwidth.

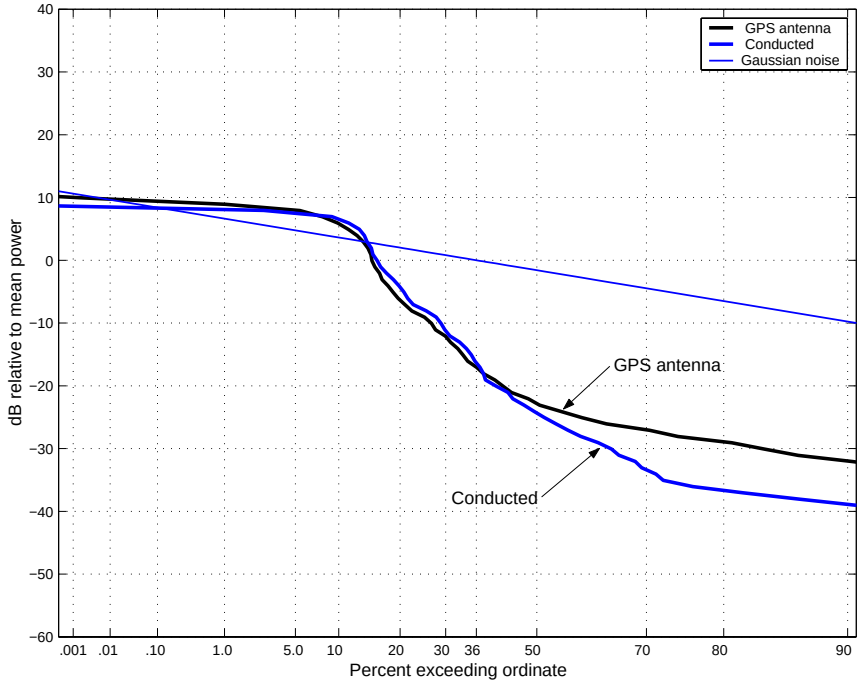

Figure A.3.4. Radiated vs. conducted APDs of 50%-ARD UWB signals (3-MHz PRF, no gating) measured in a 20-MHz bandwidth.

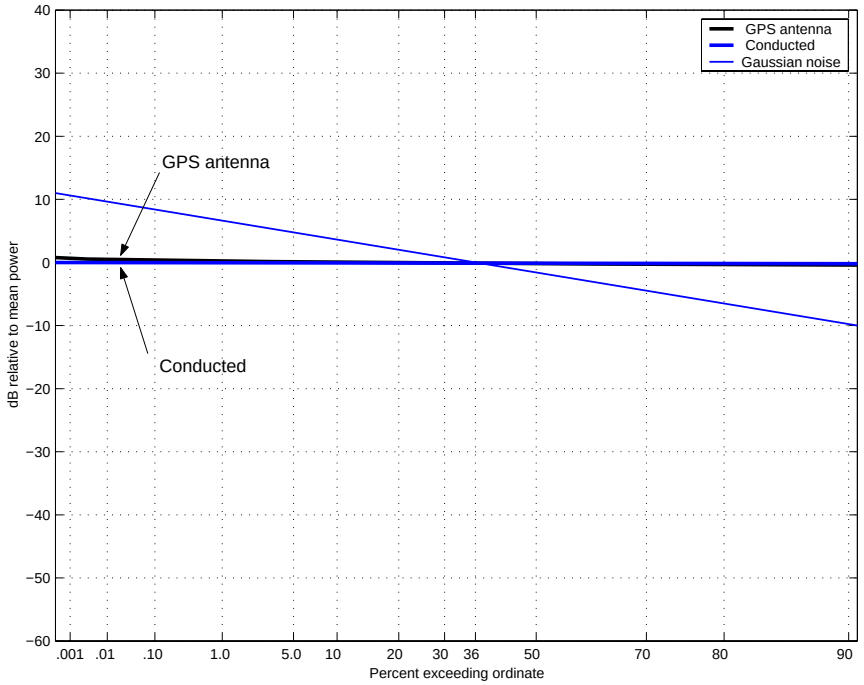

Figure A.3.5. Radiated vs. conducted APDs of UPS UWB signals (10-MHz PRF, no gating) measured in a 3-MHz bandwidth.

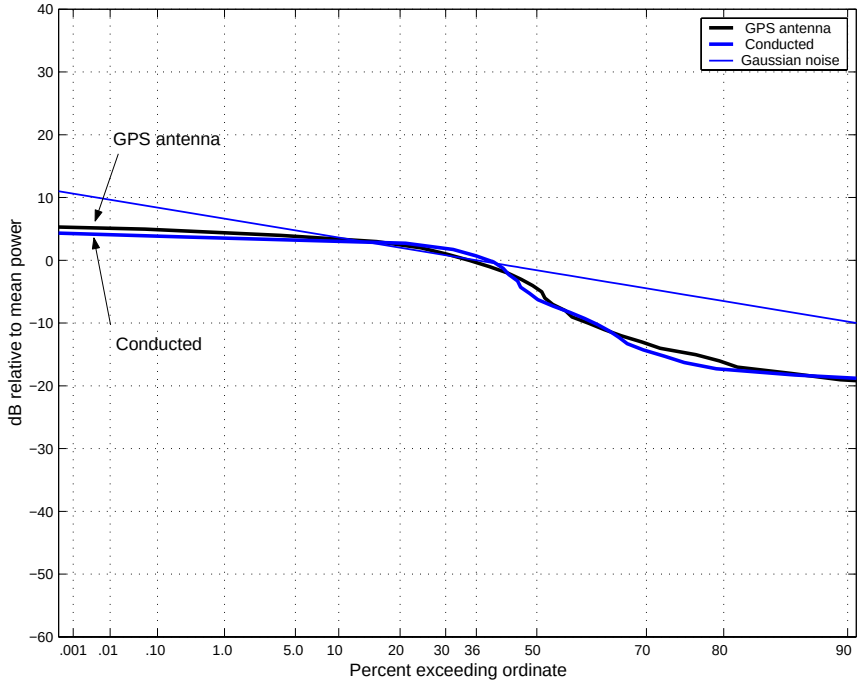

Figure A.3.6. Radiated vs. conducted APDs of UPS UWB signals (10-MHz PRF, no gating) measured in a 20-MHz bandwidth.

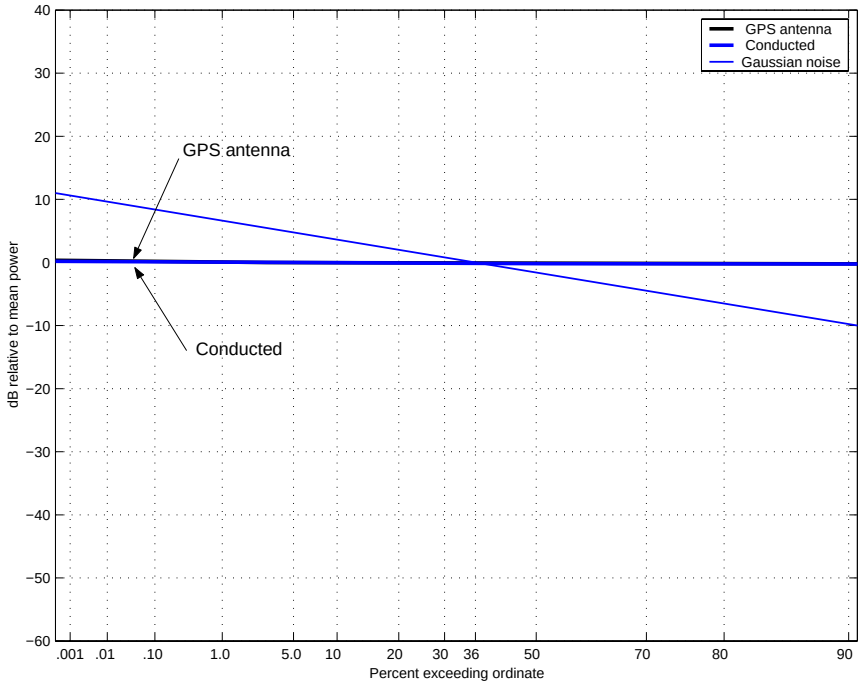

Figure A.3.7. Radiated vs. conducted APDs of UPS UWB signals (20-MHz PRF, no gating) measured in a 3-MHz bandwidth.

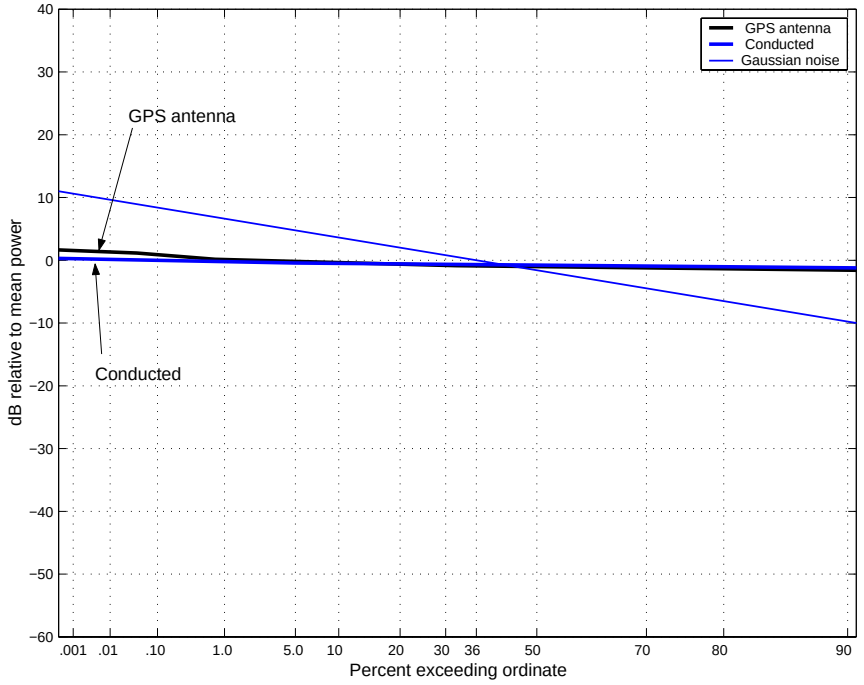

Figure A.3.8. Radiated vs. conducted APDs of UPS UWB signals (20-MHz PRF, no gating) measured in a 20-MHz bandwidth.

A.4 Conclusions

To reiterate what was discussed previously, it is necessary to verify that the conducted and radiated paths have nearly identical affects on the frequency and time-domain characteristics of the signal. Through the measurements described in this Appendix, it was shown that the magnitude and group delay characteristics, as well as the temporal characteristics (as shown through APDs time-domain pulse shapes) were similar whether radiated or conducted through a filtered path. The conclusion is that, while the GPS/UWB interference measurements were performed by transmitting signals through a conducted path, the effects should be no different than those measured during a radiated test (barring channel distortion such as multipath).

References

[1] W.A. Kissick, Ed., "The temporal and spectral characteristics of ultrawideband signals," NTIA Report 01-383, Jan. 2001.

APPENDIX B: HARDWARE SPECIFICATION

B.1 RF Components

A1 - Fixed Coaxial Attenuator
- Manufacturer: Midwest Microwave
- Model: ATT-0444-03-SMA-02
- Frequency range: 0 - 18 GHz
- Attenuation: 3 dB

A2 - Fixed Coaxial Attenuator (3x)
- Manufacturer: Midwest Microwave
- Model: ATT-0444-10-SMA-02
- Frequency range: 0 - 18 GHz
- Attenuation: 10 dB

B - DC Blocking Capacitor
- Manufacturer: Picosecond pulse Labs
- Model: 5502C
- BW(-3dB): 14 GHz
- Rise time: 24 ps
- Delay: 154 ps
- Insertion loss: < 0.5 dB @ 2 GHz

C - 3 way (0 degree) Power Combiner
- Manufacturer: Midwest Microwave
- Model: PWD-5520-03-SMA-79
- Frequency range: 0.5 - 2.0 GHz
- Isolation: 15-dB minimum
- Amplitude Balanced: 0.5 dB
- Phase Balanced: 5 degrees

DC - Directional Coupler
- Manufacturer: Mini-Circuits
- Model: ZFDC-10-5
- Frequency range: 1 - 2000 MHz
- Coupling: 10.8 dB
- Main line loss: 1.8-dB max
- Directivity: 30 dB

F1 - Tunable Bandpass Filter

Manufacturer: K&L Microwave
Model: 5BT-1500/3000-5-N/N
Frequency Range: 1500 - 3000 MHz
3-dB Bandwidth: 100 MHz
Insertion Loss: 1.0-dB max

F2 - Quadruplexer

Manufacturer: Filtronic
Type: SMX142
Passband (J2): 1.050 - 1.900 GHz
Insertion Loss: < 1.0 dB

F3 - Band Pass Filter

Manufacturer: TTE
Type: 315-1575.42M-24M-50-SMA
Center frequency (f_0): 1575.42 MHz
Passband Bandwidth: 0.015 f_0, minimum
Insertion loss at f_0: < -2 dB

F4 - GPS Filter / Amplifier

Manufacturer: Delta Microwave
Model: L5625

	L1 (1575.42 MHz)	L2 (1227.6 MHz)
1-dB Bandwidth:	26.7 MHz	26.9 MHz
Gain:	31.1 dB	32.1 dB
Noise Figure:	1.9 dB	1.8 dB

G1 - Medium Power Amplifier

Manufacturer: Mini-Circuits
Model: ZFL-2000
Frequency range: 10 - 2000 MHz
Gain at 1575.42MHz : 27 dB
Noise Figure: 7 dB
Maximum power: +16dBm

G2 - Low Noise Amplifier

Manufacturer: Mini-Circuits
Model: ZHL-1217HLN
Frequency range: 1200 - 1700 MHz
Gain at 1575.42MHz : 39 dB (measured)
Noise Figure: 1.5 dB
Maximum power: +26 dBm

ND1 - Noise Diode
Manufacturer: Noise / Com, Inc
Model: NC3108A
Serial No. E804
ENR: 27.67 dB @ 1.0 GHz
ENR: 27.09 dB @ 2.0 GHz

ND2 - Noise Diode
Manufacturer: Noise / Com, Inc
Model: NC3108A
Serial No. E574
ENR: 27.02 dB @ 1.0 GHz
ENR: 26.65 dB @ 2.0 GHz

S - 4 way, 0 deg Power Splitter
Manufacturer: Mini-Circuits
Model: ZA4PD-2
Frequency range: 1 - 2 GHz
Isolation: 25 dB
Insertion loss: 6 dB

SW - Coaxial Switch
Manufacturer: Dow-Key Microwave
Model: 401-2308
RF Circuit: SPDT
Frequency range: 0 - 26.5 GHz

T - Termination, SMA, 50 Ohm, 1 Watt
Manufacturer: Inmet
Model: TS180M
Frequency range: 0 - 18 GHz

VA1 - Step Attenuator (Programmable)
Manufacturer: Hewlett Packard
Model: HP8495G
Frequency range: 0 - 4 GHz
Attenuation range: 0 - 70 dB, 10-dB step

VA2 - Step Attenuator (Programmable)
Manufacturer: Hewlett Packard
Model: HP8494H
Frequency range: 0 - 18 GHz
Attenuation range: 0 - 11 dB, 1-dB step

VA3 - Step Attenuator (Programmable)
Manufacturer: Hewlett Packard
Model: HP8496G
Frequency range: 0 - 4 GHz
Attenuation range: 0 - 110 dB, 10-dB step

VA4 - Step Attenuator (Programmable)
Manufacturer: Hewlett Packard
Model: HP8494G
Frequency range: 0 - 4 GHz
Attenuation range: 0 - 11 dB, 1-dB step

VA5 - Step Attenuator (Manual)
Manufacturer: Hewlett Packard
Model: HP8494B
Frequency range: 0 - 18 GHz
Attenuation range: 0 - 11 dB, 1-dB step

VA6 - Step Attenuator (Manual)
Manufacturer: Hewlett Packard
Model: HP8496B
Frequency range: 0 - 18 GHz
Attenuation range: 0 - 110 dB, 10-dB step

VA7 - Step Attenuator (Manual)
Manufacturer: Midwest Microwave
Model: 1044
Frequency range: 0 - 12 GHz
Attenuation range: 0 - 60 dB, 10-dB step and 0 - 10 dB, 1-dB step

B.2 Arbitrary Waveform Generator and Pulse Generator

AWG - Arbitrary Waveform Generator
Manufacturer: Sony / Tektronix
Model: AWG520
Rise Time (10 - 90%): # 2.5 ns (amplitude > 1.0 V)
1.5 ns (amplitude # 1.0 V)
Fall Time (10 - 90%): # 2.5 ns (amplitude > 1.0 V)
1.7 ns (amplitude # 1.0 V)
Bandwidth: 500 MHz
Phase Noise: # -90 dBc/Hz (10-kHz offset)
Pulse Width: 10-ns minimum

PG1 - UWB pulse generators

Manufacturer: Time Domain
Model: Pulser PG-2000
Unit Serial Number: NTIA-004
Impulse Amplitude (50-Ù load): 5.8V
Impulse Rise Time (10 - 90%): 200 ps
Impulse Fall Time (90 - 10%): 416 ps
Impulse width (50%): 521 ps
Max. Trigger rate: 40 Mpps

PG2 - Pulse Generator

Manufacturer: MSSI
Model: TFP-1000
Serial Number: 001
Measured @ 10 Mpps
Rise Time: 269 ps
Fall Time: 127 ps
Width (rms): 245 ps
Peak-to-Peak output: 5.39 V
Max. PRF: > 50 Mpps

B.3 GPS Receivers

Rx 1 - Operating Dimension = Automatic (default)
DGPS Mode = Off
Dynamics Code = Land
Solution Mode = Weighted Over determined Fix (default)
Elevation Mask = 0E
SNR Mask = Minimum
PDOP Mask = 99
PDOP Switch = 99
Measurement Rate = 5 Hz (default)
Position Fix Rate = 1 Hz (default)
Raw Codephase Measurements (i.e., no filtering)
Dynamic filter disabled
Static filter disabled
Altitude Filter Disabled

Rx 2 - DGPS Mode = Off (default)
Elevation Mask = 0E
PDOP Mask = 255
Fastest Measurement Rate = 0.5 seconds

APPENDIX C: CHARACTERISTICS OF GENERATED UWB SIGNALS

The following sections describe details of UWB signal generation and provide APDs for each of the signal permutations used in these measurements.

C.1 Signal Description

Each of the UWB signals used in these measurements was generated using a UWB pulser triggered by either an AWG or custom designed 2%-RRD trigger circuit. Two different pulsers were utilized, each described in Appendix B.2. All single source measurements were performed using the Time Domain Corporation PG-2000 unit, and all aggregate measurements were performed using three Time Domain Corporation PG-2000 units and three MSSI TFP-1000 units. All of the 2%-RRD UWB signals with a PRF of 3 MHz or greater were generated using a custom built dithering trigger circuit.

Table C.1.1 lists parameters for each of the 39 UWB signals used for these measurements. The first 32 UWB signals in the table were used for single source conducted measurements; the remaining 7 signals were used for radiated and/or aggregate measurements.

Table C.1.1.Characteristics of Generated UWB Signals

PRF (MHz)	Pulse Spacing Mode	Duty Cycle (%)	PRL[1] Spacing (kHz)	Spectral Line Placement [2] (MHz)	LSNB [3] (Hz)	LSS [4] (Hz)	Nearest SN to L1 [5] (MHz)
0.1	UPS	100, 20	N/A	1575.570571	N/A, 500	N/A, 50	N/A
1	UPS	100, 20	N/A	1575.570571	N/A, 500	N/A, 50	N/A
3	UPS	100	N/A	1575.570571	N/A	N/A	N/A
5	UPS	100, 20	N/A	1575.570571	N/A, 500	N/A, 50	N/A
10	UPS	100	N/A	1575.570571	N/A	N/A	N/A
20	UPS	100, 20	N/A	1575.570571	N/A, 500	N/A, 50	N/A
0.1	OOK	100, 20	0.059	1575.570571	N/A, 500	N/A, 50	N/A
1	OOK	100, 20	0.017	1575.570571	N/A, 500	N/A, 50	N/A
5	OOK	100, 20	0.089	1575.570571	N/A, 500	N/A, 50	N/A
20	OOK	100, 20	0.357	1575.570571	N/A, 500	N/A, 50	N/A
0.1	50%-ARD	100, 20	0.098	N/A	N/A, 500	N/A, 50	1560
1	50%-ARD	100, 20	0.997	N/A	N/A, 500	N/A, 50	1600
3	50%-ARD	100	N/A	N/A	N/A	N/A	1650
5	50%-ARD	100, 20	4.88	N/A	N/A, 500	N/A, 50	1500
20	50%-ARD	100, 20	19.5	N/A	N/A, 500	N/A, 50	2000
0.1	2%-RRD	100, 20	0.25	N/A	N/A, 500	N/A, 50	1615
1	2%-RRD	100, 20	1.25	N/A	N/A, 500	N/A, 50	1900
3	2%-RRD	100, 20	N/A	N/A	N/A	N/A	N/A
5	2%-RRD	100, 20	N/A	N/A	N/A	N/A	N/A
10	2%-RRD	100, 20	N/A	N/A	N/A	N/A	N/A
20	2%-RRD	100, 20	N/A	N/A	N/A	N/A	N/A

[1] Pattern Repetition Lines (PRL) refer to spectral lines generated due to a repetition of the pulse pattern. (See Section C.2 for a complete discussion.)

[2] Lines due to the pulse repetition period are spaced at intervals equal to the reciprocal of PRF, but for each UWB with these spectral lines, the PRF is adjusted slightly so that one of the lines occurs at 1575.570571 MHz.

[3] Line Spreading Null-to-null Bandwidth (LSNB) refers to the null spacing of the convolving $sinc^2$ function as a result of gating, where the null-to-null bandwidth is equal to 2 times the reciprocal of the gated-on time. (See Section 4.1.2 for a complete discussion.)

[4] Line Spread Spacing (LSS) refers to the spacing between lines of the convolving $sinc^2$ function as a result of gating, where the distance between lines is equal to the reciprocal of the gating period. (See Section 4.1.2 for a complete discussion.)

[5] Spectral Node (SN) refers to a spectral feature due to the placement of the position of pulses within discrete bins. (See Section C.2 for a complete discussion.)

C.2 Residual Spectral Effects due to Signal Generation

Because the pattern of pulse spacing, whether it be OOK or dithering, is stored in the memory of an AWG and because that memory has limits with regard to size, the same pattern has to be repeated at periodic intervals. This pattern repetition results in signal power being gathered up into spectral lines with a spacing equal to the reciprocal of the period of the pattern. For those UWB cases where we would expect real world signals to have no pattern repetition, the pattern is made as long as possible so that the spectral lines are spaced very close together, and therefore, have negligible impact on the receiver. For purposes of brevity, we call these spectral lines Pattern Repetition Lines (PRL).

Also because of the limitations of memory size and sample rates of the AWG, the location of pulses (within the context of dithering) has to be confined to a limited number of discrete time bins. This is illustrated in Figure C.2.1 for the case of 50% clock-referenced dithering, in which the pulse position can be assigned to any of 19 possible discrete positions within the first 50% of the interval between reference clock periods (*t* is the size of the bins, in units of time). As opposed to a continuum of possible pulse positions, this discrete binning results in some additional spectral features worth noting. Figure C.2.2 demonstrates what we have described as a spectral node (SN), in which there is a depression in the spectral noise and the emergence of spectral lines. The spacing of these spectral nodes is directly related to the bin size *t*, where the distance between spectral nodes is 1/*t*. This phenomenon is described in greater detail in Appendix D (Theoretical Analysis of UWB Signals Using Binary Pulse-modulation and Fixed Time-base Dither). For these measurements, efforts were specifically made to place these spectral nodes in a location other than the L1 and L2 bands.

The custom built 2%-RRD circuit is analog, and therefore signals generated using this circuit do not have PRLs or SNs characteristic of signals generated digitally with an AWG.

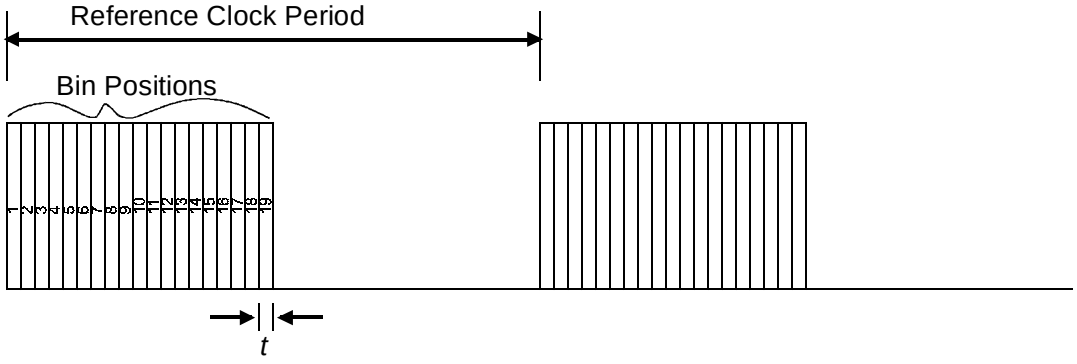

Figure C.2.1. Discrete binning of pulse position for clock referenced dithering.

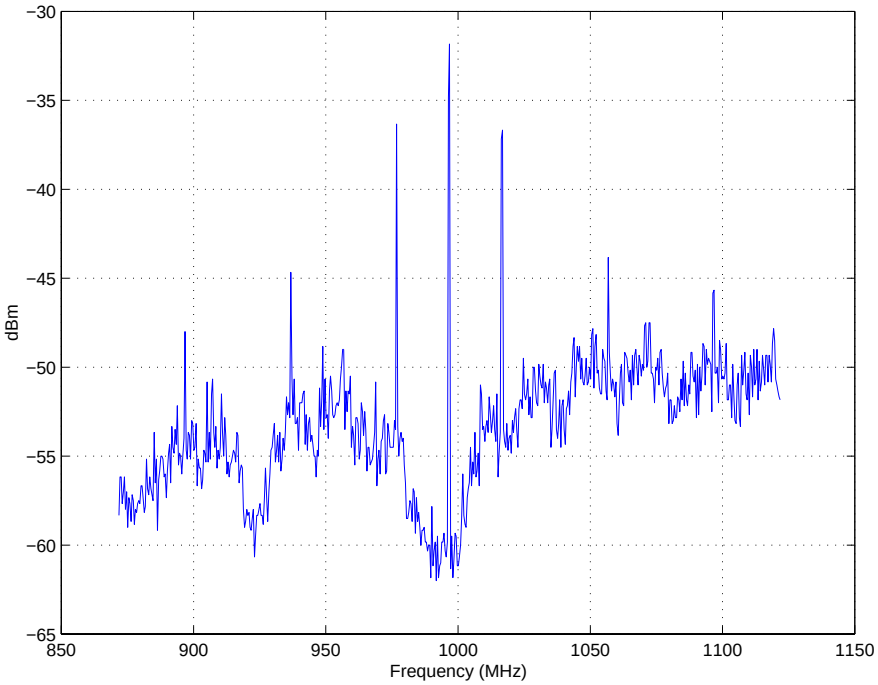

Figure C.2.2. Spectral lines due to discrete binning of pulse position.

C.3 APDs Characteristics of UWB signals

Figures C.3.1 through C.3.29 and Figures C.3.30 through C.3.31 show APDs for each of the 32 different single source UWB permutations and the 9 different aggregate signal scenarios respectively. Two different measurement bandwidths were used – 3 MHz and 20 MHz – representing a bracketing of a wide range of bandwidths. For the single source permutations, several different groupings for composite plots are shown. The four different UWB signals, each representing a different PRF, are plotted as a composite of all the different permutations of pulse spacing modes and gating. Along the other dimension, each of the pulse spacing modes (including gated and non-gated) are plotted as a composite of each of the 4 different PRFs.

For each APD, the mean power is normalized to 0 dBm/20 MHz. Note that mean power for gated signals includes both the gated on and off time. This is in contrast to the power representation of gated signals for operational and observational metrics in Section 6.

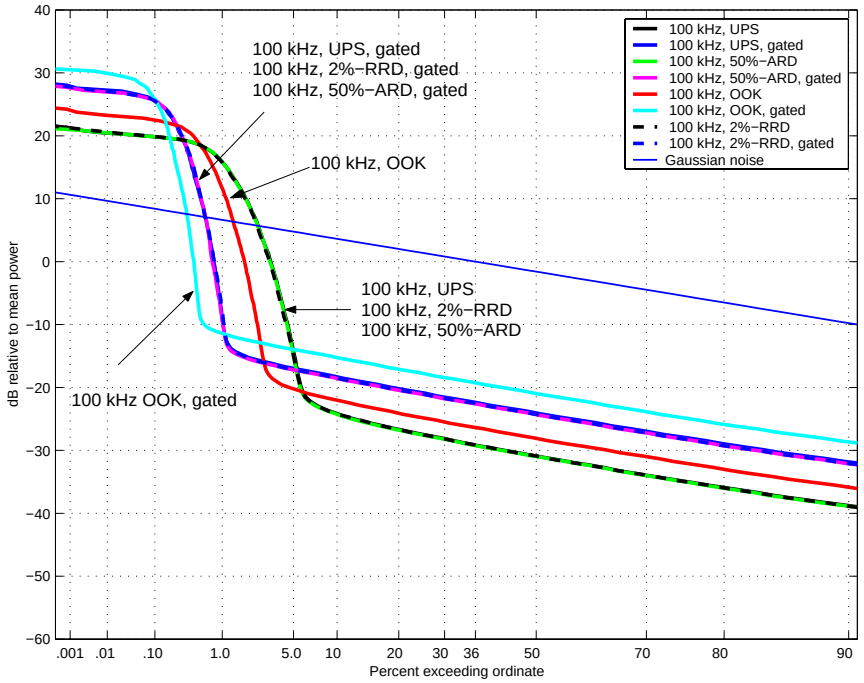

Figure C.3.1. APDs of 100-kHz PRF UWB signals measured in a 3-MHz bandwidth.

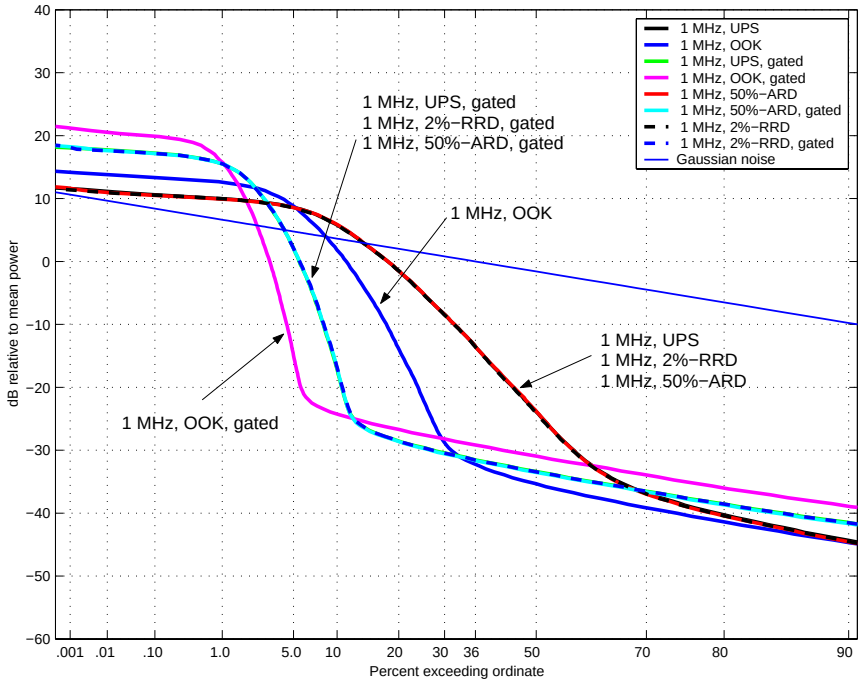

Figure C.3.2. APDs of 1-MHz UWB signals measured in a 3-MHz bandwidth.

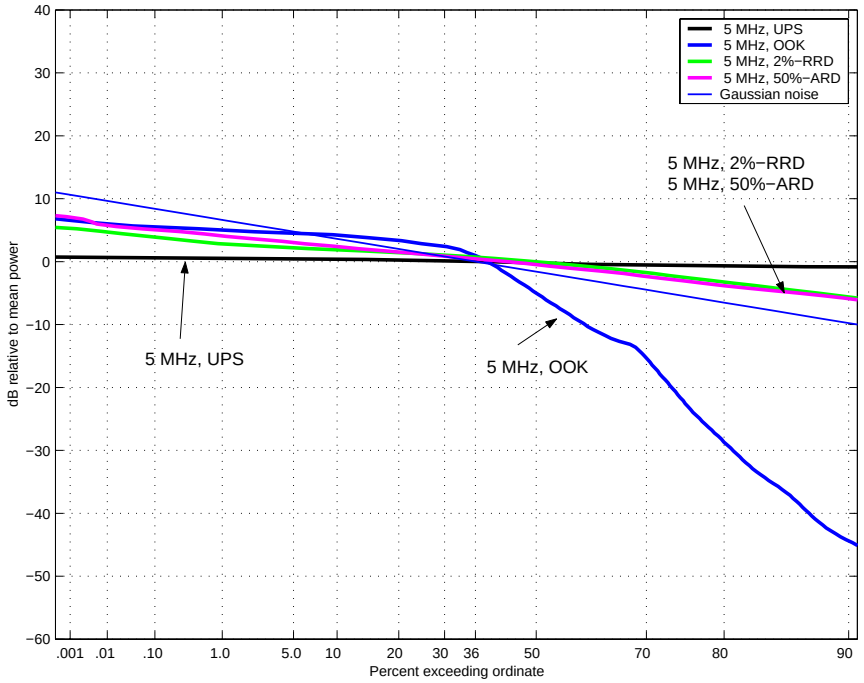

Figure C.3.3. APDs of 5-MHz PRF, non-gated UWB signals measured in a 3-MHz bandwidth.

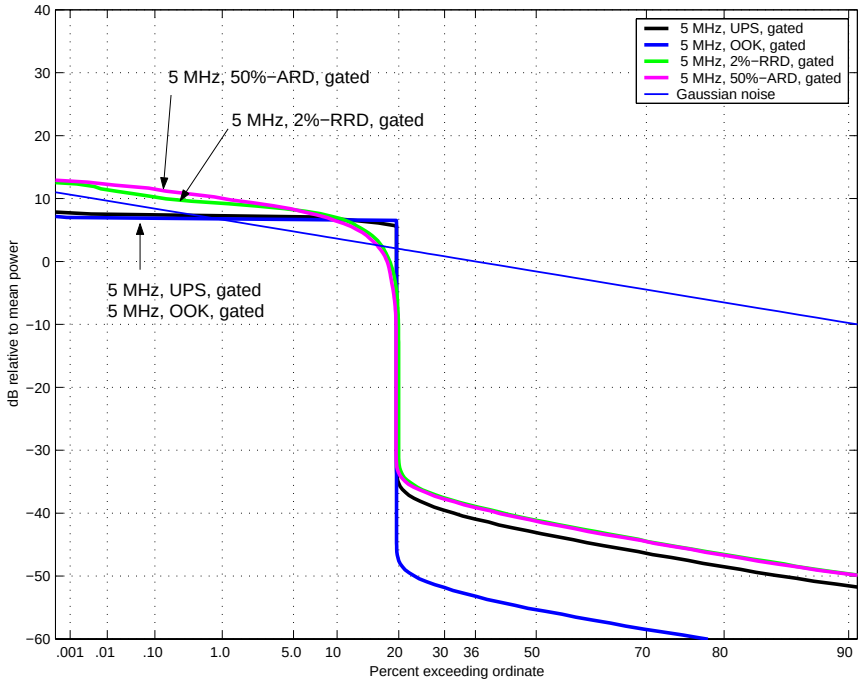

Figure C.3.4. APDs of 5-MHz PRF, gated UWB signals measured in a 3-MHz bandwidth.

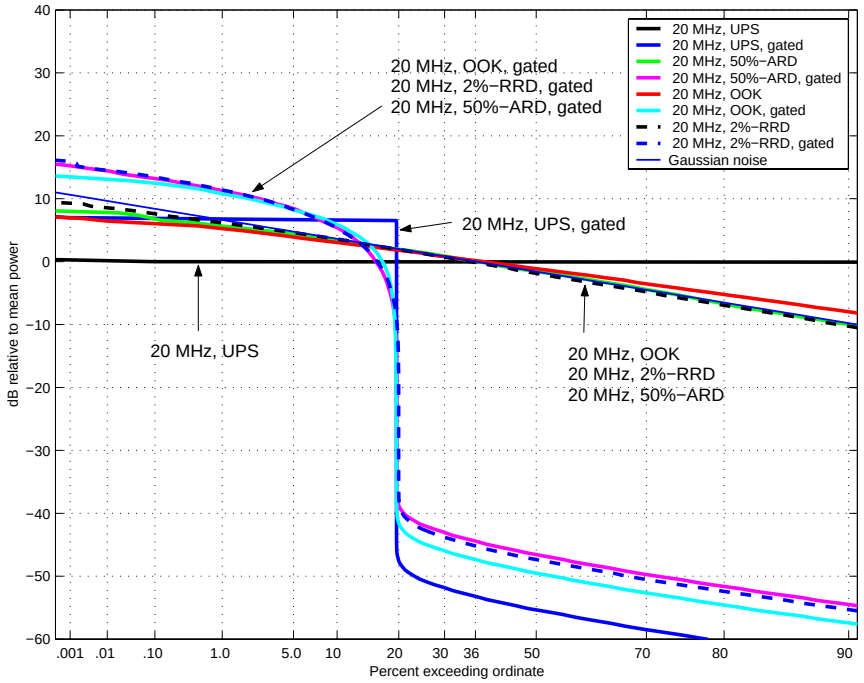

Figure C.3.5. APDs 20-MHz PRF UWB signals measured in a 3-MHz bandwidth.

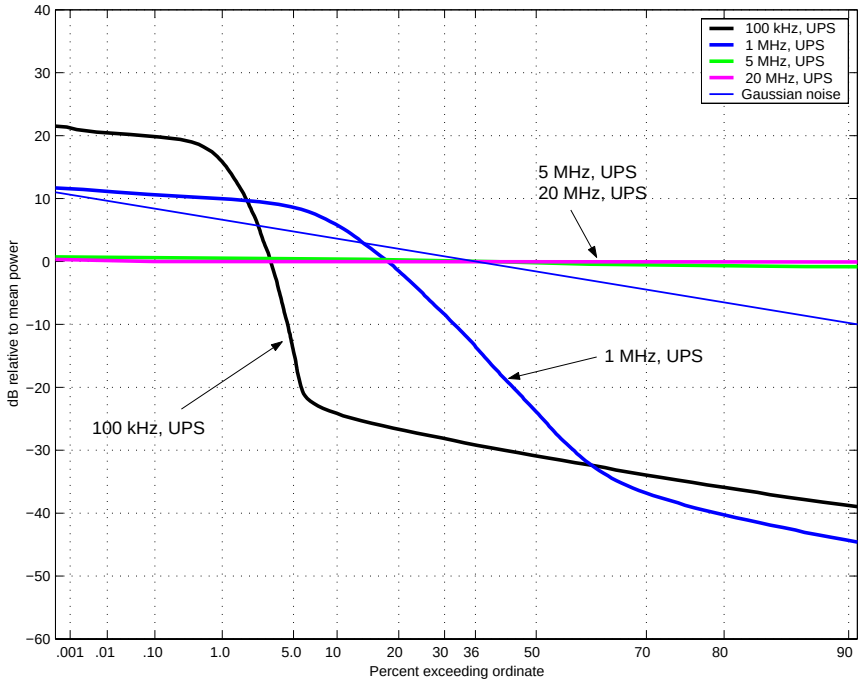

Figure C.3.6. APDs of UPS, non-gated UWB signals measured in a 3-MHz bandwidth.

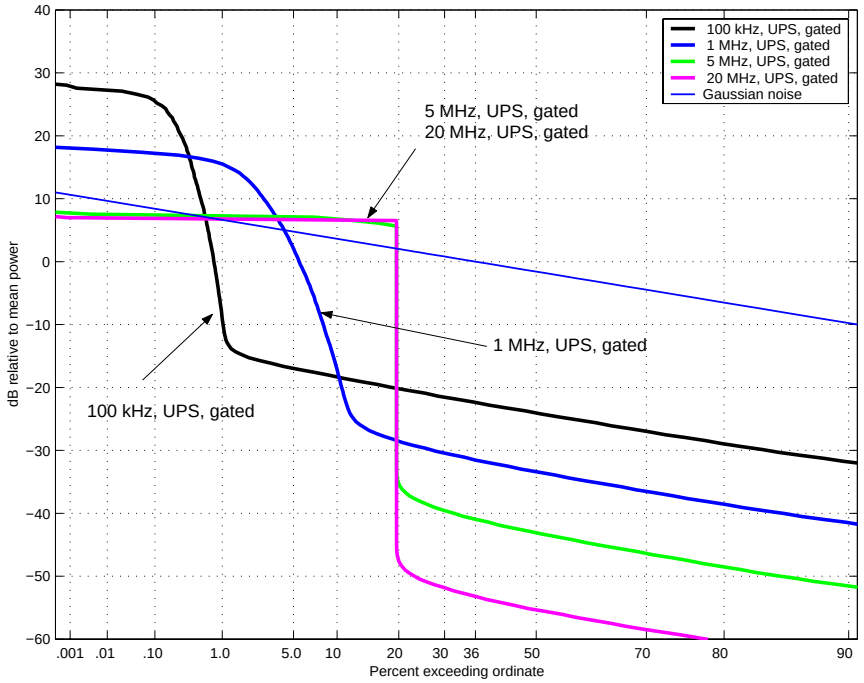

Figure C.3.7. APDs of UPS, gated UWB signals measured in a 3-MHz bandwidth.

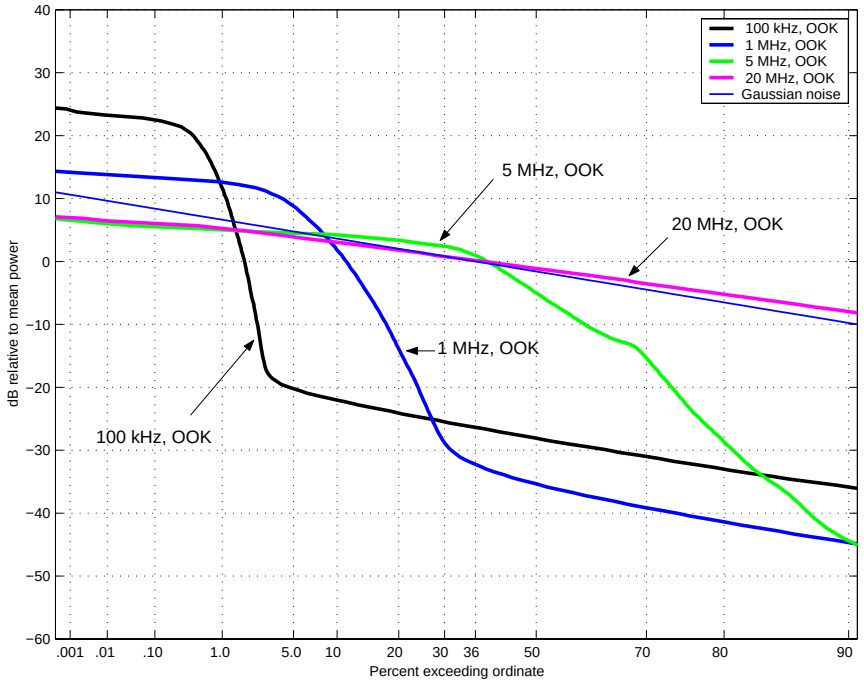

Figure C.3.8. APDs of OOK, non-gated UWB signals measured in a 3-MHz bandwidth.

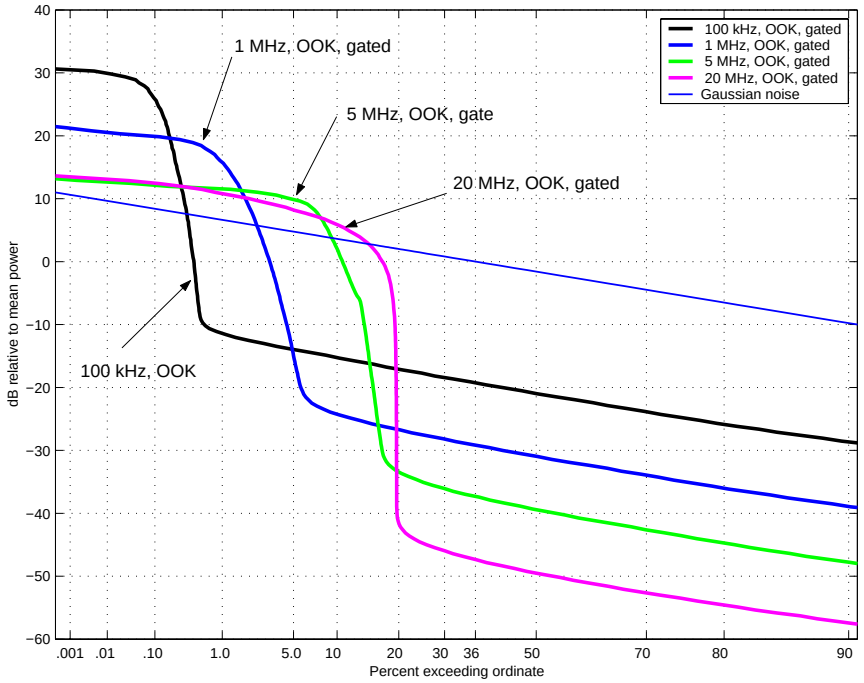

Figure C.3.9. APDs of OOK, gated UWB signals measured in a 3-MHz bandwidth.

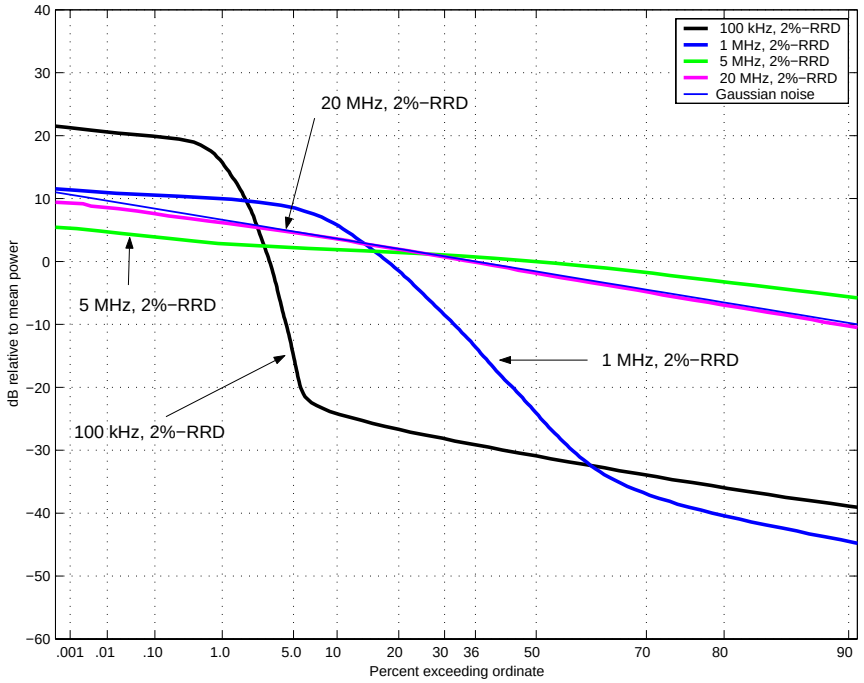

Figure C.3.10. APDs of 2%-RRD, non-gated UWB signals measured in a 3-MHz bandwidth.

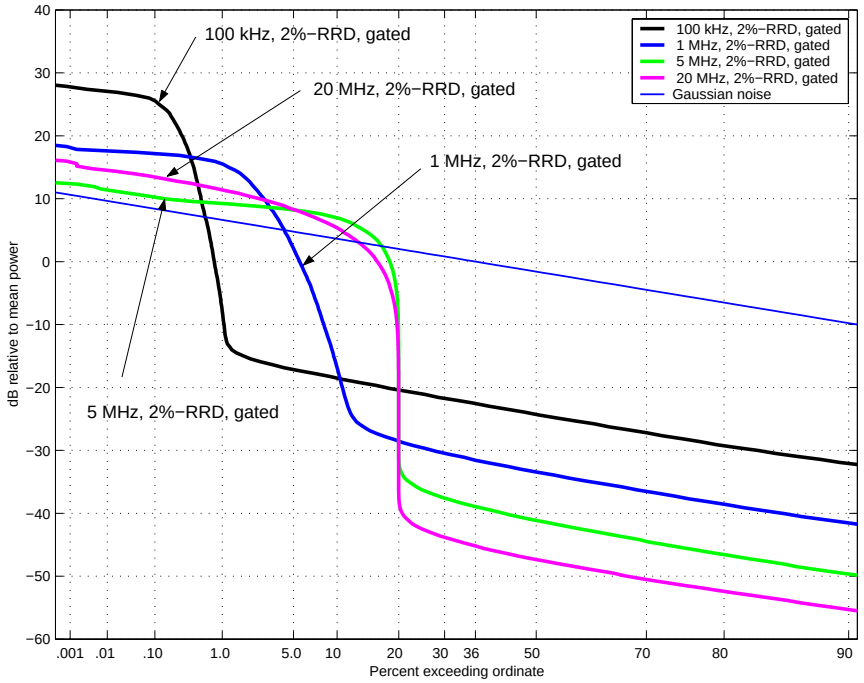

Figure C.3.11. APDs of 2%-RRD, gated UWB signals measured in a 3-MHz bandwidth.

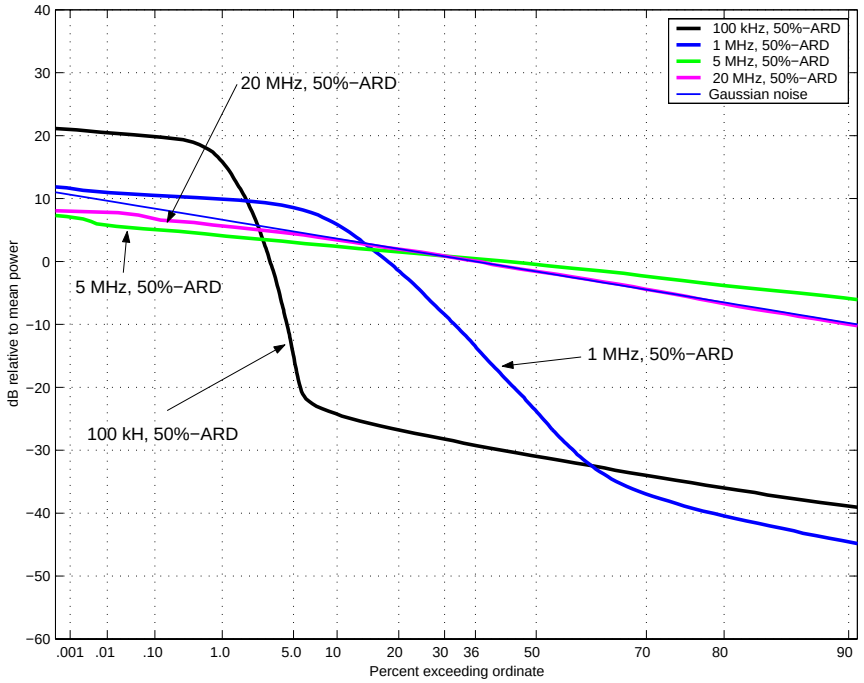

Figure C.3.12. APDs of 50%-ARD, non-gated UWB signals measured in a 3-MHz bandwidth.

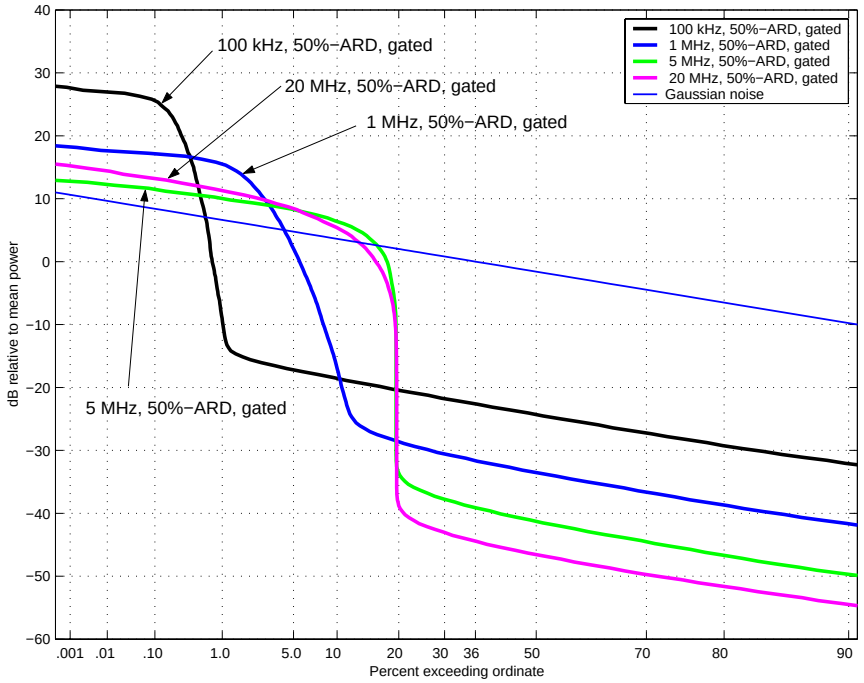

Figure C.3.13. APDs of 50%-ARD, gated UWB signals measured in a 3-MHz bandwidth.

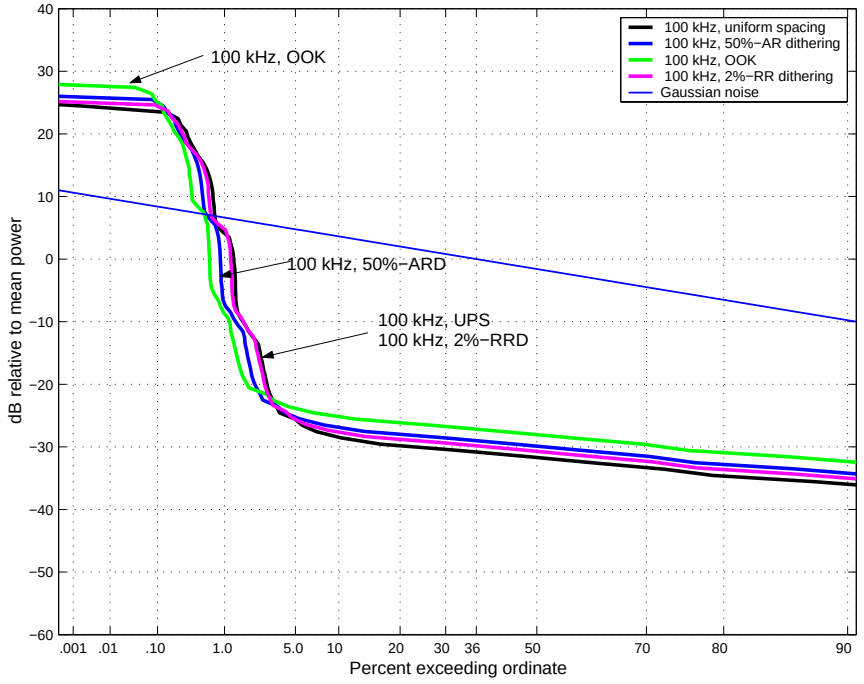

Figure C.3.14. APDs of 100-kHz PRF, non-gated UWB signals measured in a 20-MHz bandwidth.

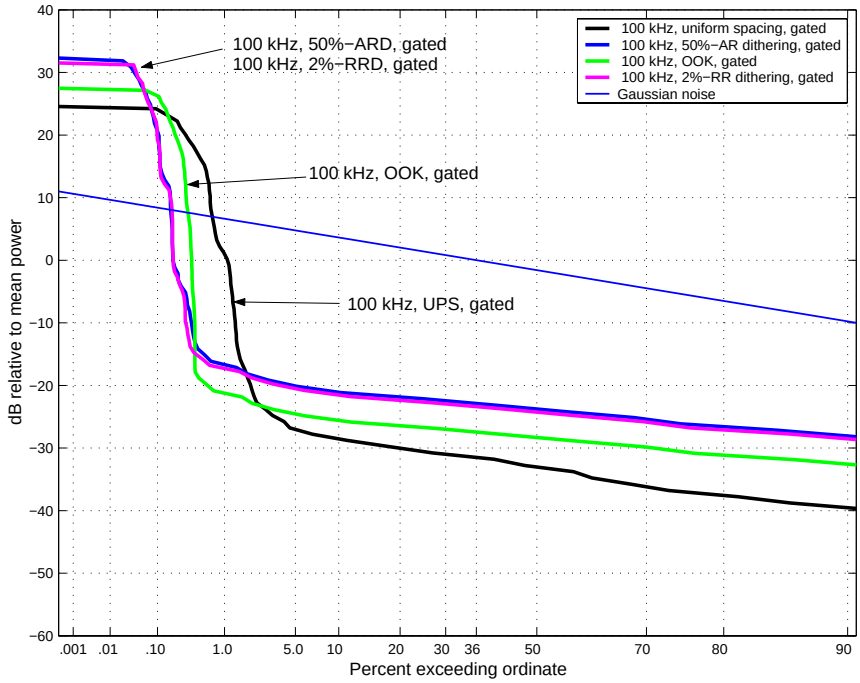

Figure C.3.15. APDs of 100-kHz PRF, gated UWB signals measured in a 20-MHz bandwidth.

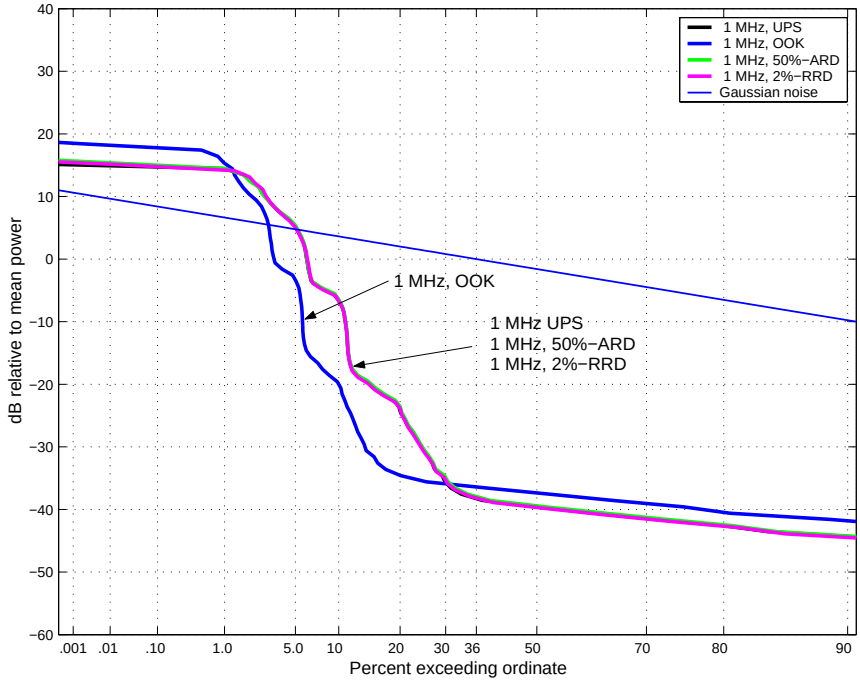

Figure C.3.16. APDs of 1-MHz PRF, non-gated UWB signals measured in a 20 MHz bandwidth.

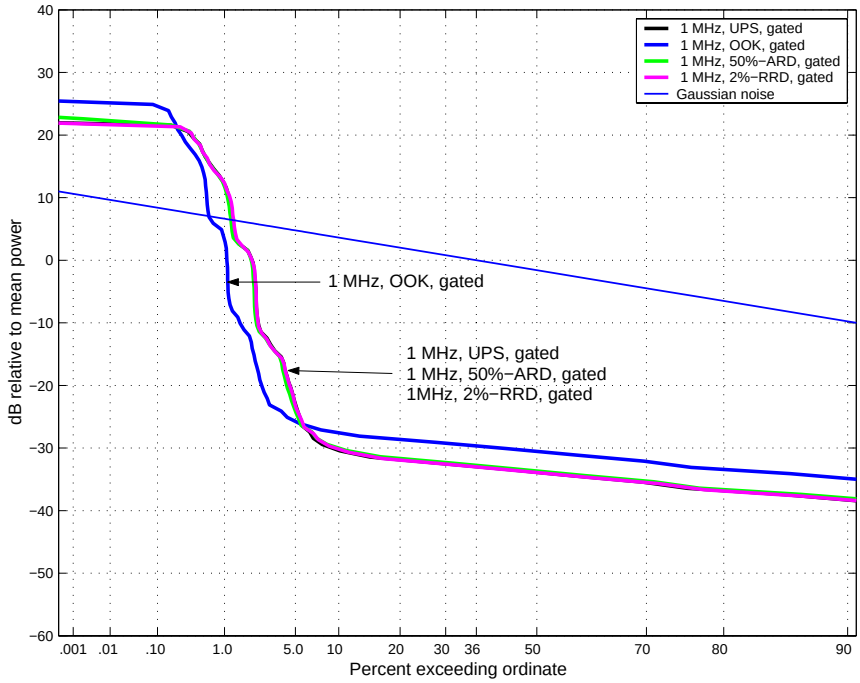

Figure C.3.17. APDs of 1-MHz PRF, gated UWB signals measured in a 20-MHz bandwidth.

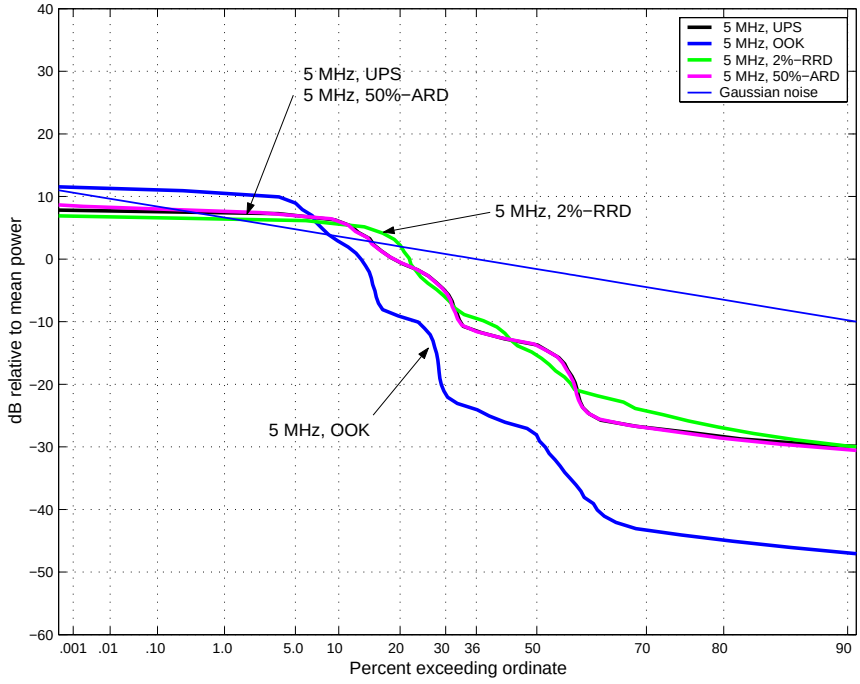

Figure C.3.18. APDs of 5-MHz PRF, non-gated UWB signals measured in a 20-MHz bandwidth.

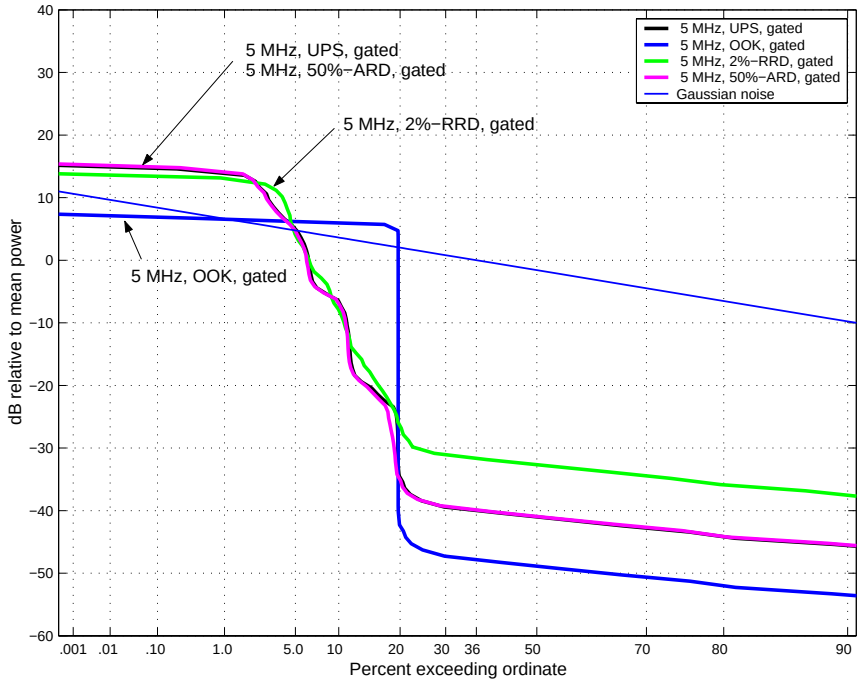

Figure C.3.19. APDs of 5-MHz PRF, gated UWB signals measured in a 20-MHz bandwidth.

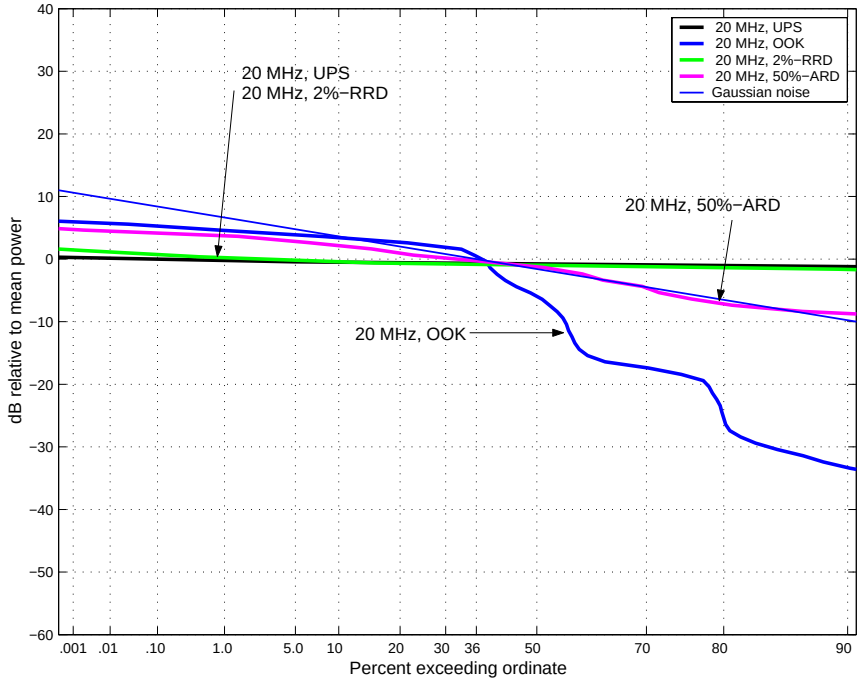

Figure C.3.20. APDs of 20-MHz PRF, non-gated UWB signals measured in a 20 MHz bandwidth.

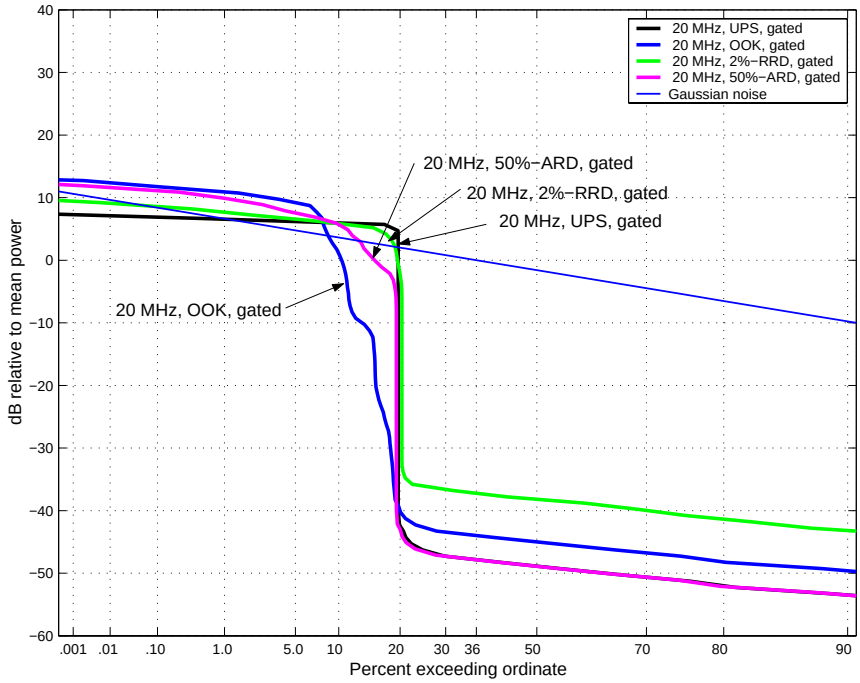

Figure C.3.21. APDs of 20-MHz PRF, gated UWB signals measured in a 20-MHz bandwidth.

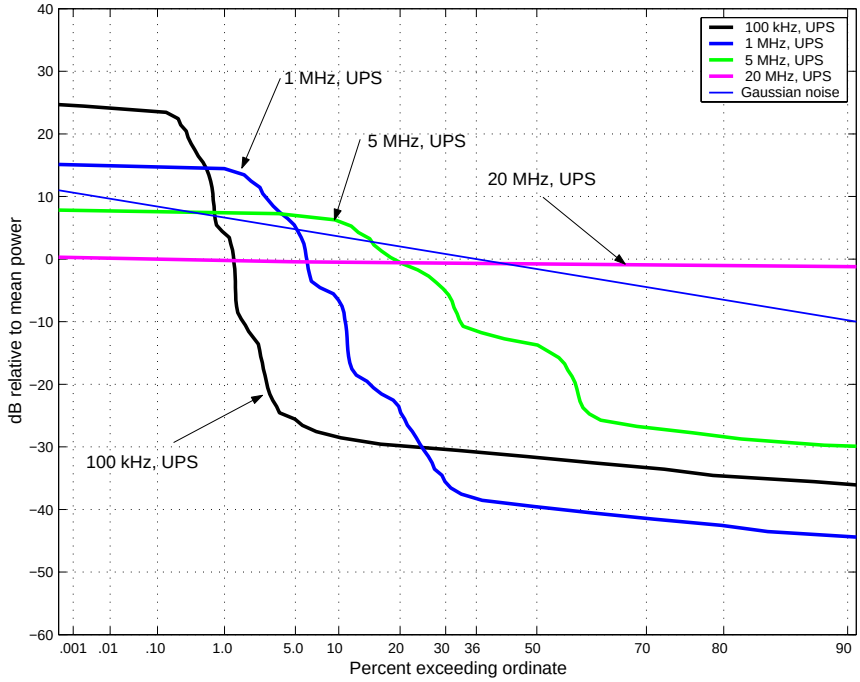

Figure C.3.22. APDs of UPS, non-gated UWB signals measured in a 20-MHz bandwidth.

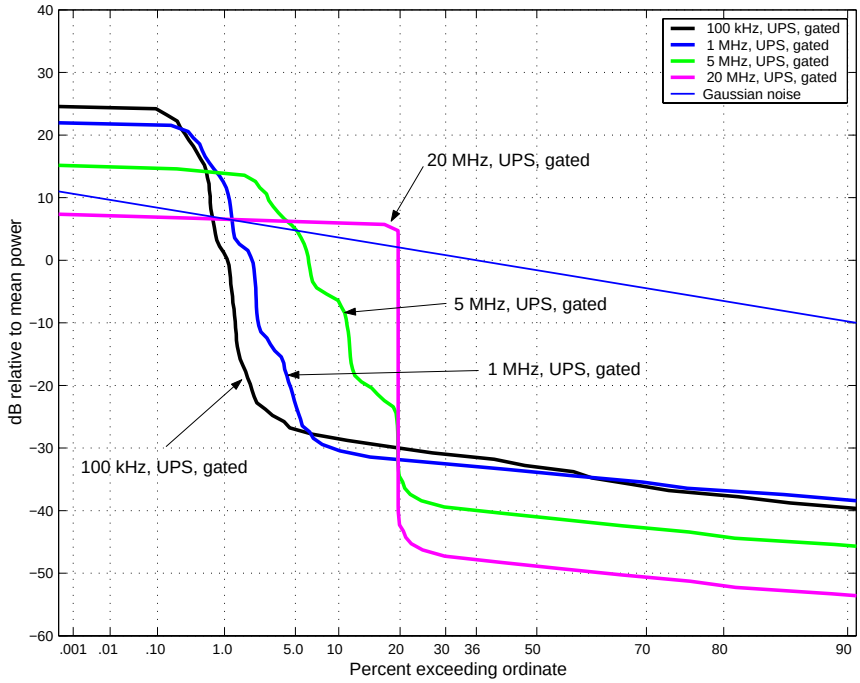

Figure C.3.23. APDs of UPS, gated UWB signals measured in a 20-MHz bandwidth.

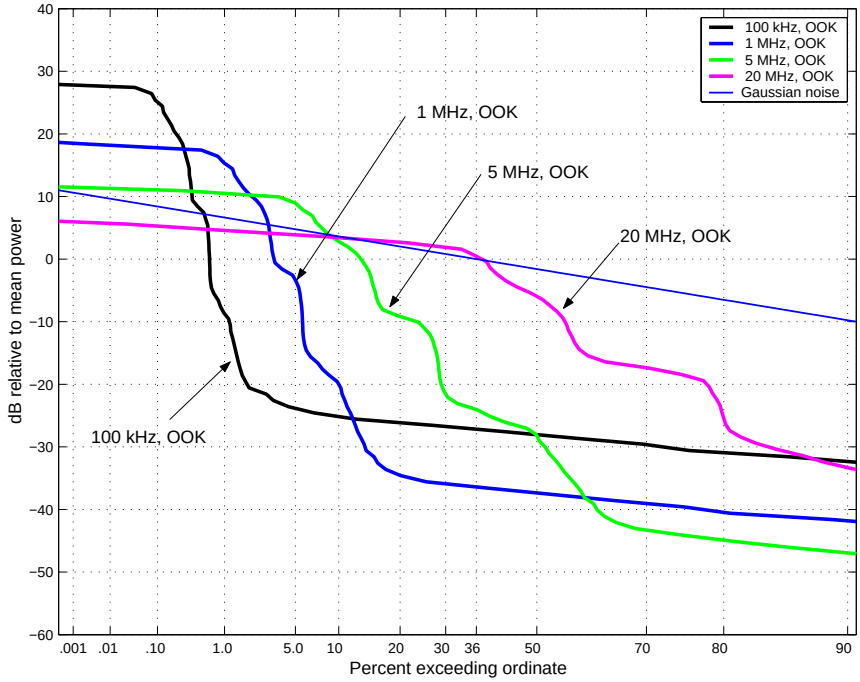

Figure C.3.24. APDs of OOK, non-gated UWB signals measured in a 20-MHz bandwidth.

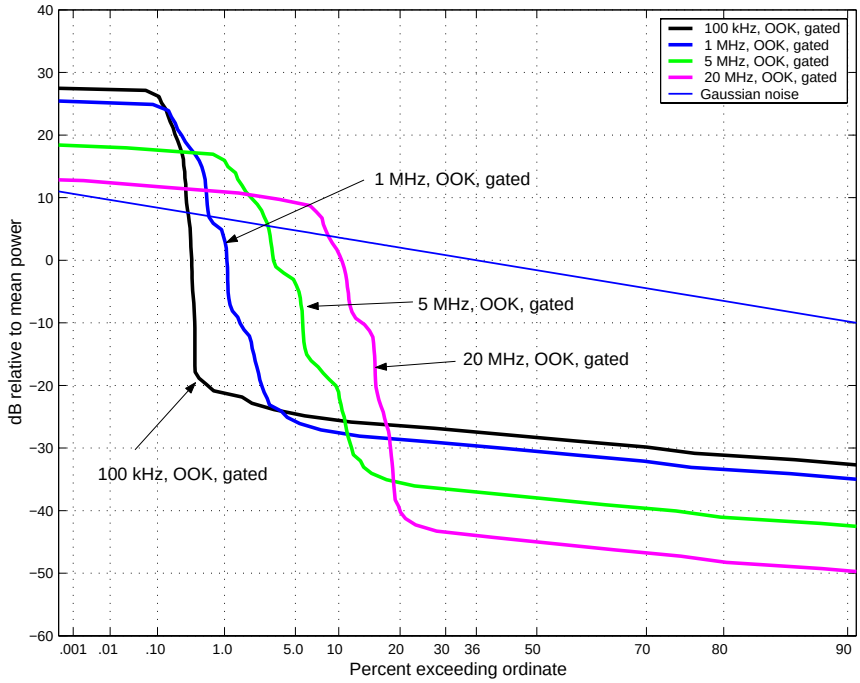

Figure C.3.25. APDs of OOK, gated UWB signals measured in a 20-MHz bandwidth.

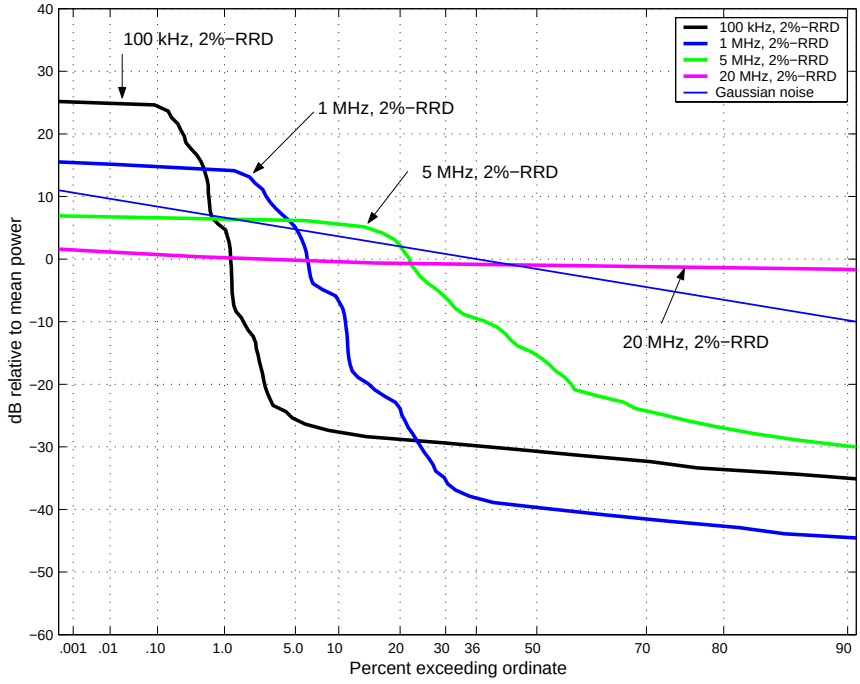

Figure C.3.26. APDs of 2%-RRD, non-gated UWB signals measured in a 20-MHz bandwidth.

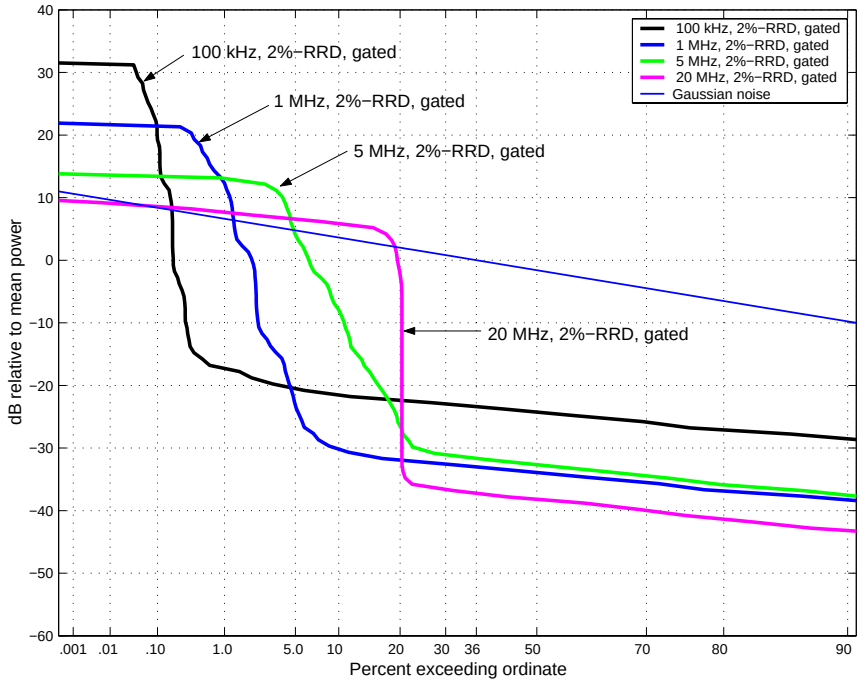

Figure C.3.27. APDs of 2%-RRD, gated UWB signals measured in a 20-MHz bandwidth.

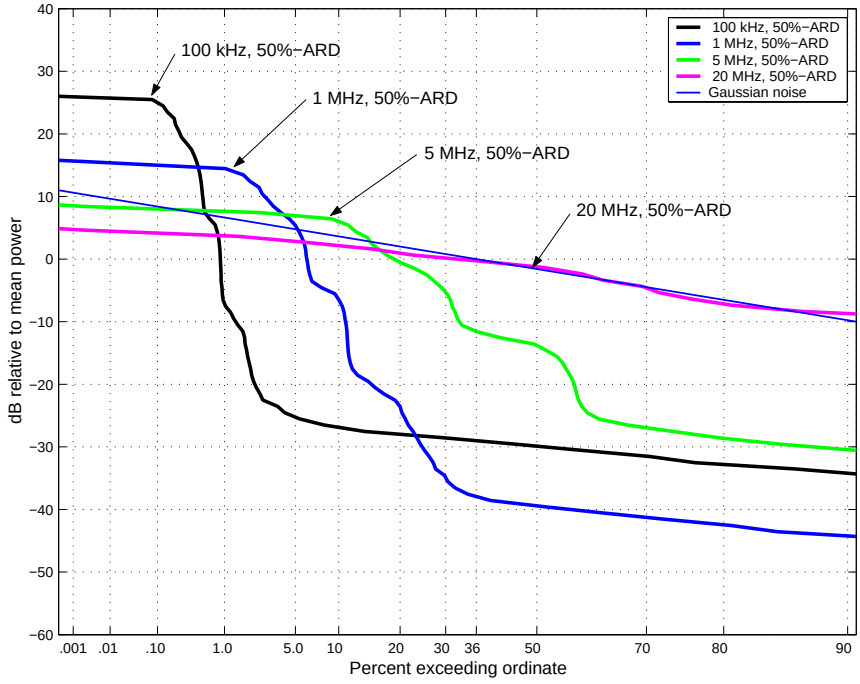

Figure C.3.28. APDs of 50%-ARD, non-gated UWB signals measured in a 20-MHz bandwidth.

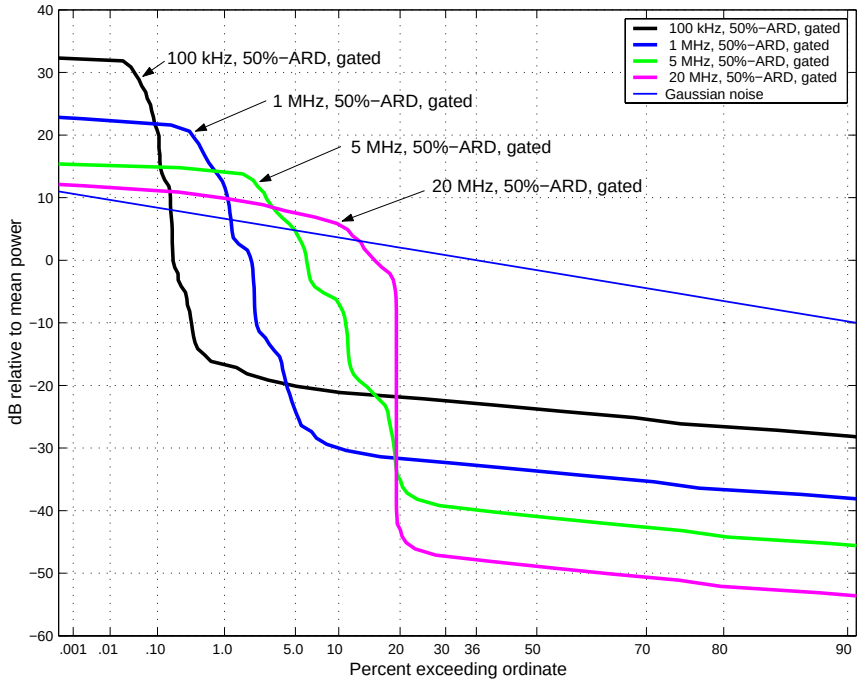

Figure C.3.29. APDs of 50%-ARD, gated UWB signals measured in a 20-MHz bandwidth.

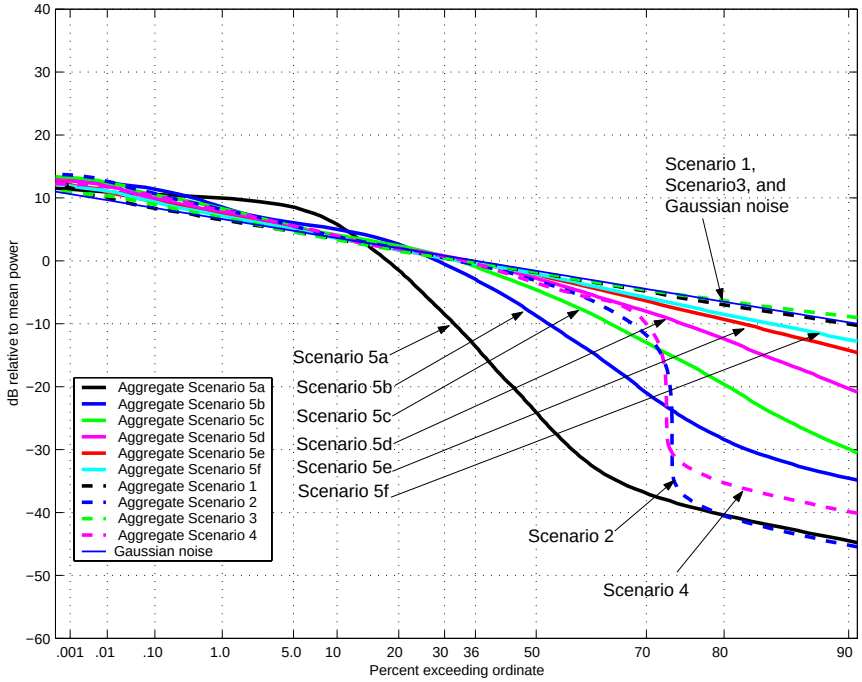

Figure C.3.30. APDs of aggregate UWB signals measured in a 3-MHz bandwidth.

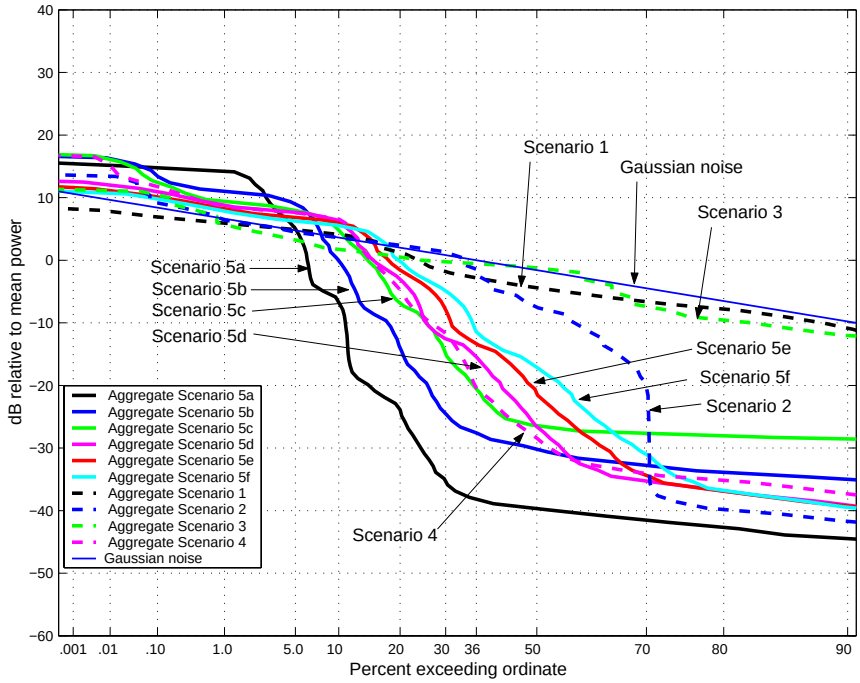

Figure C.3.31. APDs of aggregate UWB signals measured in a 20-MHz bandwidth.

APPENDIX D: THEORETICAL ANALYSIS OF UWB SIGNALS USING BINARY PULSE-MODULATION AND FIXED TIME-BASE DITHER

The theoretically derived spectra for fixed time-base dithered and binary pulse-modulated UWB signals were used to validate some of the test procedures described in this report. The calculated power spectral densities and examples showing how the analytical results compare to measurements are given below. The analytical results presented in this section are taken from [1].

Fixed time-base dithered UWB systems utilize short duration pulses transmitted at some nominal pulse period T. In this scheme, pulses are dithered about integer multiples of T. In the following discussion, it is assumed that the dither times are random variables 2_n that are independent and identically distributed over a fraction of the nominal pulse period with probability density $q(2_n)$. UWB signals may also include information bits by using binary pulse modulation in addition to the pulse dithering.

The power spectral density for a binary pulse-modulated fixed time-base dithered UWB signal is obtained by taking the Fourier transform of the autocorrelation function. Due to the periodic nature of the underlying pulsed signal, the process is *cyclostationary* with period T. Time averaging the autocorrelation function over a period yields the average power spectrum which depends only on the relative time delay. The time averaged power spectral density for a fixed time-base dithered UWB signal with binary pulse modulation is

$$\bar{R}_{xx}(f) = L + C$$
$$L = \frac{1}{T^2}\left|\sum_{k=0}^{1} g_k P_k(f)\right|^2 |Q(f)|^2 \sum_{n} \delta(f - n/T) \quad , \qquad \text{D.1}$$
$$C = \frac{1}{T}\left[\sum_{k=0}^{1} g_k |P_k(f)|^2 - \left|\sum_{k=0}^{1} g_k P_k(f)\right|^2 |Q(f)|^2\right]$$

where P_k is the Fourier transform of the signal pulse for the information bit having the value k, Q is the Fourier transform of probability density function that describes the dithering, and g_k is the probability that an information bit has the value k (e.g., g_o is the probability that an information bit is “0” and g_1 is the probability that the bit is a “1”). Note that L is discrete (i.e., spectral lines) and C is continuous.

D.1 Fixed Time-base Dither and Pulse Position Modulation

If the bit values are equiprobable (i.e., $g_k = ½$) and the pulse representing a 1 is a time delayed version of the pulse representing a 0 (i.e., $p_1(t+>) = p_0(t) = p(t)$), the power spectral density becomes

$$\bar{R}_{xx}(f) = L + C$$
$$L = \frac{1}{2T^2}\,|P(f)Q(f)|^2\,[1+\cos(2\pi>f)] \sum_n \delta(f-n/T) \quad , \qquad \text{D.2}$$
$$C = \frac{1}{T}\,|P(f)|^2 \left(1 - \frac{|Q(f)|^2[1+\cos(2\pi>f)]}{2}\right)$$

Note that the discrete and continuous components depend on both the pulse spectrum and $Q(f)$. When $Q(f) \approx 1$ (negligible dithering) and the information bits do not change, the continuous spectrum disappears leaving only a line spectrum as would be expected for a simple periodic pulsed signal.

The results of an example calculation using Equation D.2 when q is uniformly and continuously distributed between 0 and $T/2$ is given below. For this example, the signal consists of a short-duration pulse, shown in Figure D.1.1, transmitted at a 20 MHz rate. In this and following examples, it is assumed that > is small in comparison to the dithering, so that the effects of information bit modulation are negligible over the frequency range of interest.

The power spectral density over a frequency range of 1-5000 MHz is shown in Figure D.1.2. The magnitude of the spectrum is normalized to the peak of the continuous distribution (at about 250 MHz). The Fourier transform of the density function for this example is $Q(f) = \text{sinc}(\pi fT/2)$. This function has nulls at frequencies equal to $2k/T$ ($k = \pm1, \pm2, \pm3, ...$); hence the interval between discrete spectral lines is 40 MHz, as shown in the figures. For frequencies above about 40 MHz, the continuous spectrum is approximately the same as the pulse spectrum (i.e., $P(f)$).

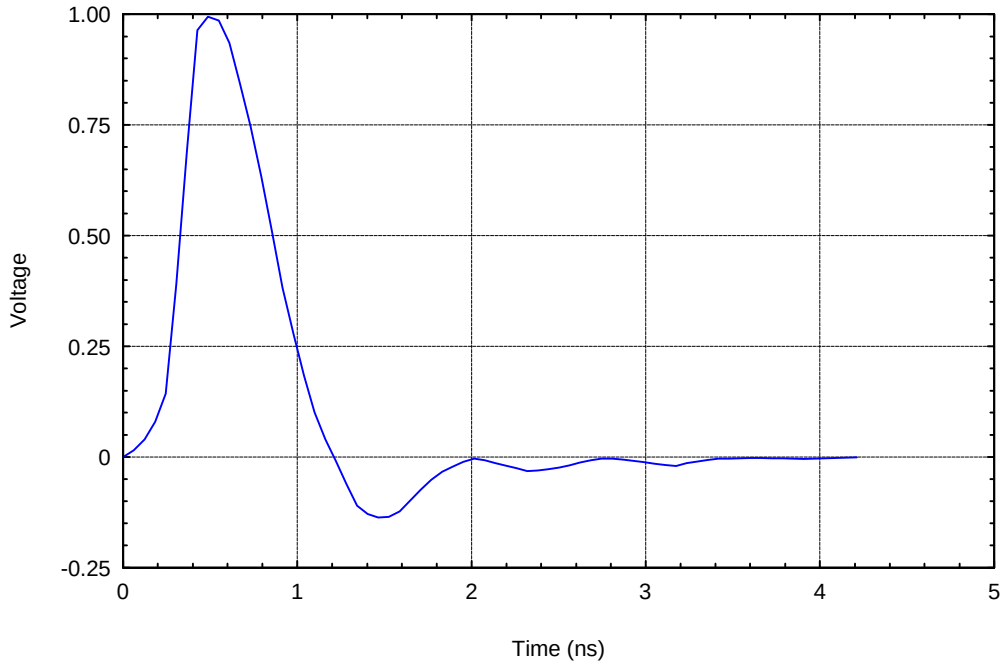

Figure D.1.1. Time-domain pulse shape.

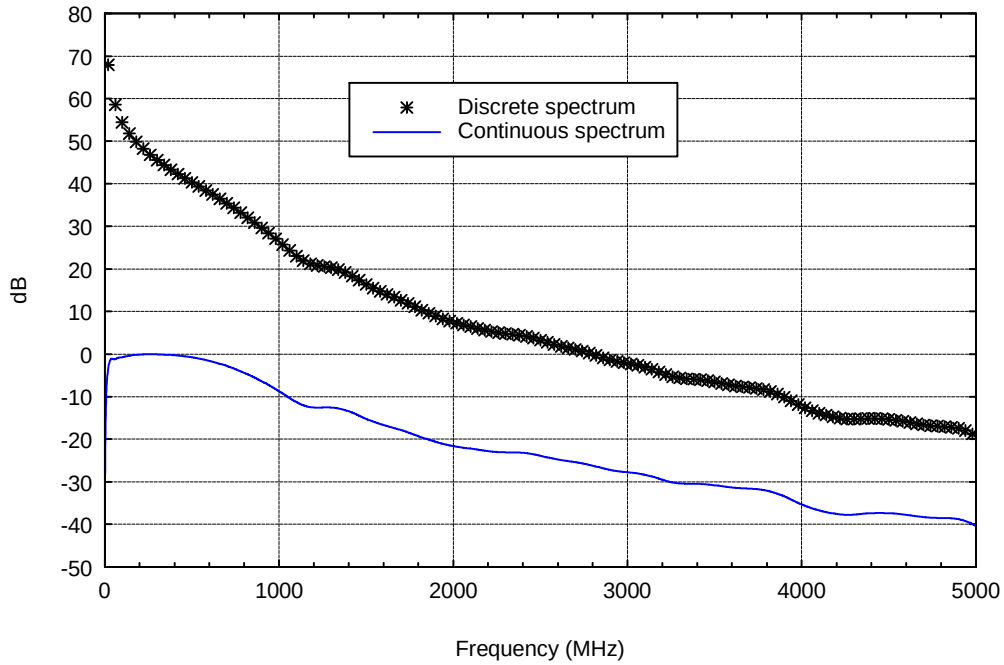

Figure D.1.2. Power spectral density for a fixed time-base dithered 10-MHz UWB signal. The pulse positions are continuously and uniformly distributed over 50% of the pulse repetition period.

The mean power in the bandwidth of a *narrowband* victim RF receiver as a function of frequency can readily be calculated from these results. For narrowband receivers where gains due to the UWB transmitter filters/antenna, propagation channel, and receiver are approximately constant over the receiver bandwidth, the received interference power can be calculated by applying the appropriate gain factors to the power in the receiver bandwidth at the center frequency of the receiver.

In the previous example, q is continuous and uniformly distributed over a fraction of the nominal period T. When the distribution is discrete so that the dithered pulse can only occur at particular times (e.g., $T - n\Delta$, where $n = 0, 1, 2, 3, \cdots, N - 1$) with equal probability, the density function can be written as

$$q(t) = \frac{1}{N} \sum_{n=0}^{N-1} \delta(t - n\Delta) \quad , \qquad \text{D.3}$$

with spectrum

$$|Q(t)|^2 = \left(\sum_{n=-4}^{4} \operatorname{sinc}[B N \Delta (f - n/\Delta)] \right)^2 \quad , \qquad \text{D.4}$$

which is a periodic function with period $1/\Delta$. For example, when $1/T = 20$ MHz, and the pulse is discretely dithered over one half of the pulse-repetition interval with $\Delta = 1$ ns, the spectrum is repeated at 1-GHz intervals as shown in Figure D.1.3. In this example, the receiver bandwidth is 1 MHz and the continuous spectrum is normalized to a maximum of 0 dB.

Note that for any integer m

$$|Q(m/\Delta)|^2 = \begin{cases} 1 & m = n \\ 0 & m \neq n \end{cases} \quad ,$$

hence, the continuous spectrum decreases to a minimum at integer multiples of 1 GHz. For these frequencies, the discrete spectrum tends to a local maximum and spectral lines are significant. Contrast this with the case where q is continuous (i.e., $Q(f) = \operatorname{sinc}(B f T/2)$) described previously. With continuous dithering, spectral lines at multiples of 1 GHz are not present, since they occur at nulls of $\operatorname{sinc}(B f T/2)$.

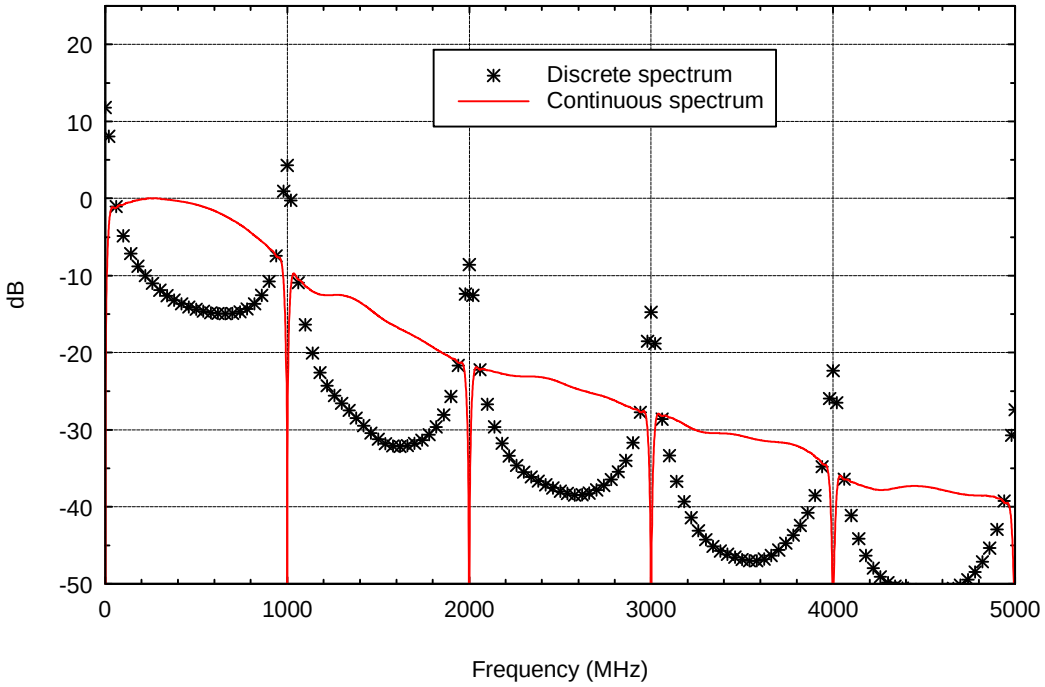

Figure D.1.3. Power spectral density for 20-MHz PRF 50% uniform discrete dithering with J = 1 ns.

A comparison of measured and predicted spectra for a discretely dithered UWB signal is shown in Figure D.1.4. The UWB signal is pulsed at a 20 MHz rate with uniform 50% discrete dithering with J = 1 ns. The measurement bandwidth is 1 MHz. As predicted, only three lines, the strongest at 1 GHz and two others at 1 GHz ± 20 MHz are visible in the measured signal. This figure shows good agreement between measurement and theory.

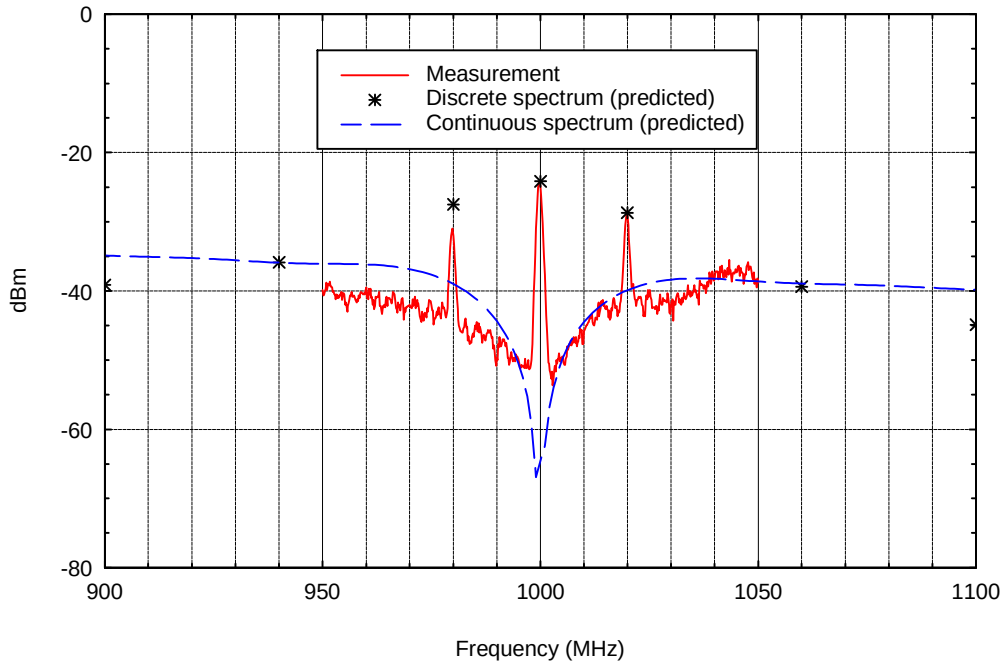

Figure D.1.4. Comparison of measured and predicted spectra for 20-MHz PRF 50% uniform discrete dithering with J = 1 ns.

D.2 Power Spectrum for On-off Keying Without Dithering

For binary pulse modulation using on-off keying without dithering, we set $P_0 = P(f)$, $P_1 = 0$, $Q(f) = 1$ and $g_0 = g_1 = ½$ in Equation D.1 and obtain

$$\bar{R}_{xx}(f) = L + C$$

$$L = \frac{|P(f)|^2}{4T^2} \sum_n \delta(f - n/T) \quad ,$$

$$C = \frac{|P(f)|^2}{4T}$$

When the signal is passed through a narrowband receiver with center frequency f_c and the bandwidth B, the received power is

$$\int_{f_c - B/2}^{f_c + B/2} \bar{R}_{xx}(f)\,df = \frac{|P(f_c)|^2}{4T^2}\left[N + TB\right] \quad ,$$

where N is the nominal number of lines in the filter passband. The ratio of the power in bandwidth B due to discrete and continuous components of the signal is simply $N(TB)^{-1}$.

Figure D.2.1 shows the spectrum of a signal generated by test equipment using on-off keying with equiprobable random bits and a pulse repetition frequency of 1 MHz. The signal was passed through a 20 MHz bandpass filter and a spectrum analyzer using a resolution bandwidth of B = 100 kHz. In this case N = 1, and hence, $(TB)^{-1}$ = 10 which is in agreement with Figure D.2.1 where the discrete spectrum is roughly 10 dB above the level of the continuous spectrum.

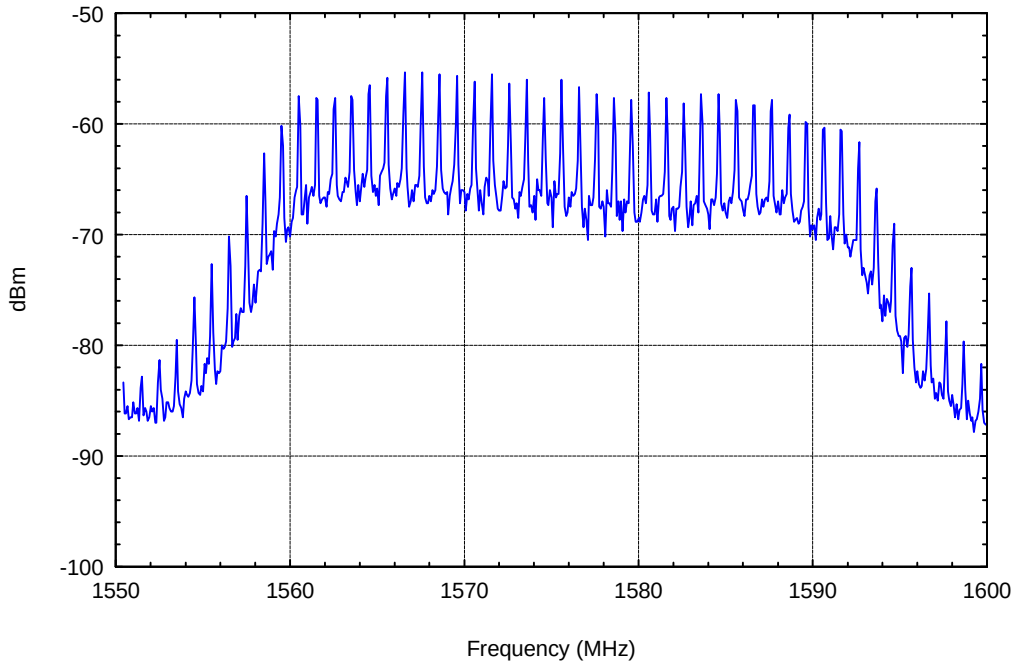

Figure D.2.1. Measured spectrum for on-off keying at 1-MHz PRF, B = 100 kHz.

References

[1] W.A. Kissick, Ed., "The temporal and spectral characteristics of ultrawideband signals," NTIA Report 01-383, Jan. 2001.

This Page Intentionally Left Blank

This Page Intentionally Left Blank

APPENDIX E. TUTORIAL ON USING AMPLITUDE PROBABILITY DISTRIBUTIONS TO CHARACTERIZE THE INTERFERENCE OF ULTRAWIDEBAND TRANSMITTERS TO NARROWBAND RECEIVERS

E.1 Introduction

The *amplitude probability distribution function* (APD) is used in radio engineering to describe signal amplitude *statistics*. The APD and its corresponding graph, shown in Figure E.1.1, succinctly express the probability that a signal amplitude exceeds a threshold. For example, the APD in Figure E.1.1 shows that the signal amplitude rarely exceeds high voltages. Statistics such as percentiles, deciles, and the median can be read directly from the APD. Other statistics such as average power can be computed with the APD.

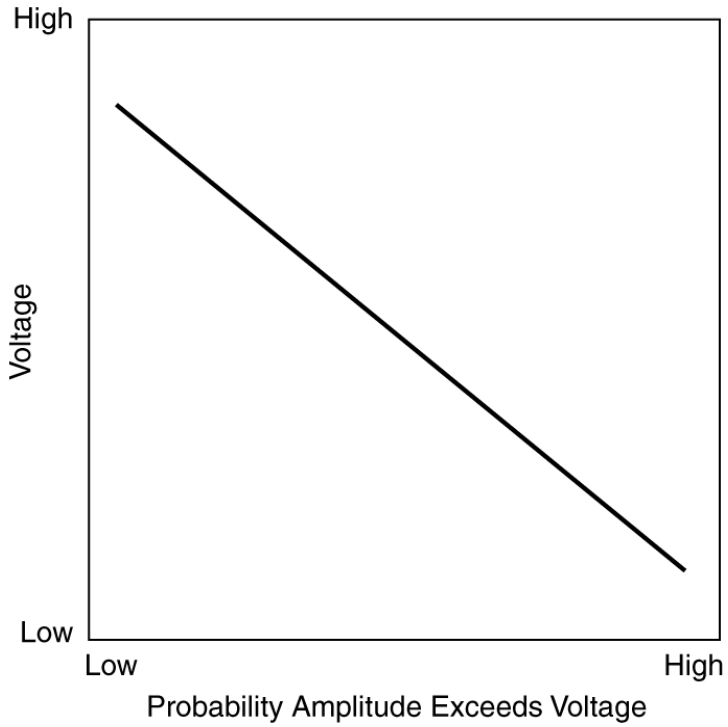

Figure E.1.1. Amplitude probability distribution.

The "signal" the APD characterizes is often noise or interference. For example, APDs are commonly used to characterize the amplitude statistics of *non-Gaussian* noise produced by lightning or unintentional emissions from man-made electrical or electronic devices. Numerous studies have shown that average noise power alone cannot predict the performance of receivers operating in non-Gaussian noise. APD statistics are needed for accurate predictions.

Today, many radio engineers are unfamiliar with the APD and its applications. This is because most modern receivers are designed to operate in bands with (zero-mean) *Gaussian* noise which is completely characterized by the average noise power statistic alone. Consequently, APD statistics are not needed for more accurate predictions.

Recently, Federal spectrum regulators have been asked to allow emissions from *ultrawideband* (UWB) transmitters to overlay bands licensed to services that use *narrowband* receivers. Critics have charged that UWB transmitters may cause interference to narrowband receivers. The amplitude statistics of this potential interference are dependent upon the specifications of the UWB signal and the band limiting filter in the narrowband receiver. The APD can be used to characterize this interference and correlate UWB signal and band limiting filter specifications to narrowband receiver performance.

The purpose of this tutorial is to introduce basic APD concepts to radio engineers and spectrum regulators who have not previously used the APD. It is hoped that these concepts will provide a firm basis for discussions on regulation of UWB transmitters. Emphasis is placed on understanding features likely to be found in band limited UWB signal APDs. These features are demonstrated with "tutorial" APDs of Gaussian noise, sinusoid (continuous wave) signals, and periodically pulsed sinusoid signals. Although the audience is intended to be broad, a limited number of mathematical expressions are used to avoid the ambiguity found in everyday language.

E.2 Signal Amplitude Characterization

E.2.1 APD Fundamentals

A *bandpass signal* is a signal whose bandwidth is much less than the *center frequency*. Bandpass signals are expressed mathematically as

$$s(t) = A(t)\cos(2\pi f_c + 2(t)) \quad ,$$

where $A(t)$ is the baseband amplitude, $2(t)$ is the baseband phase, and f_c is the center frequency. The amplitude and phase define the *complex baseband signal*, $A(t)e^{j2(t)}$, whose spectrum is centered about 0 Hz.

The amplitude is always positive and is considered to be a *random variable*, A, when characterized by an APD. Formally, a new random variable, A_n, is present at each sampling instant. The set $\{A_1, A_2, \ldots A_N\}$ is called the *random sample* of the random variable A if each

random variable is independent and identically distributed. Realizations or values of the random sample are denoted by the set $\{a_1,a_2, \ldots a_N\}$.

Associated with every random variable is a *probability density function* (PDF). The discrete PDF expresses the *probability* that a random variable "*A*" will have a realization equal to "a_i":

$$p(a_i) = P(A=a_i) \quad ,$$

where *P*() is the probability of its argument. PDF values are positive and the area under a PDF is equal to 1.0.

The *cumulative distribution function* CDF expresses the probability that a random variable "*A*" will have a realization less than or equal to "*a*":

$$c(a) = P(A\#a) \quad .$$

The discrete CDF is obtained by integrating the discrete PDF

$$c(a) = \sum_i p(a_i) \quad ,$$

for all a_i less than or equal to *a*. CDF values range from 0.0 to 1.0 .

Radio engineers are generally more concerned about how often a noise or interference amplitude exceeds a threshold. Thus they often prefer to use the complement of the CDF (CCDF) or APD. The APD function expresses the probability that a random variable "*A*" will have a realization greater than "*a*":

$$cc(a) = P(A>a) \quad .$$

The discrete APD is obtained by subtracting the discrete CDF from 1.0:

$$cc(a) = 1.0\text{-}c(a) \quad .$$

For clarification, Figure E.2.1.1 shows graphs of the discrete PDF, CDF, and APD for the random sample realizations:

$$\{a_1,a_2,\ldots a_{10}\} = \{1,2,3,3,1,4,4,3,4,3\} \text{ volts} \quad .$$

The discrete PDF is estimated from the histogram. By convention, the axes of the APD are oriented differently from the axes of the CDF and PDF.

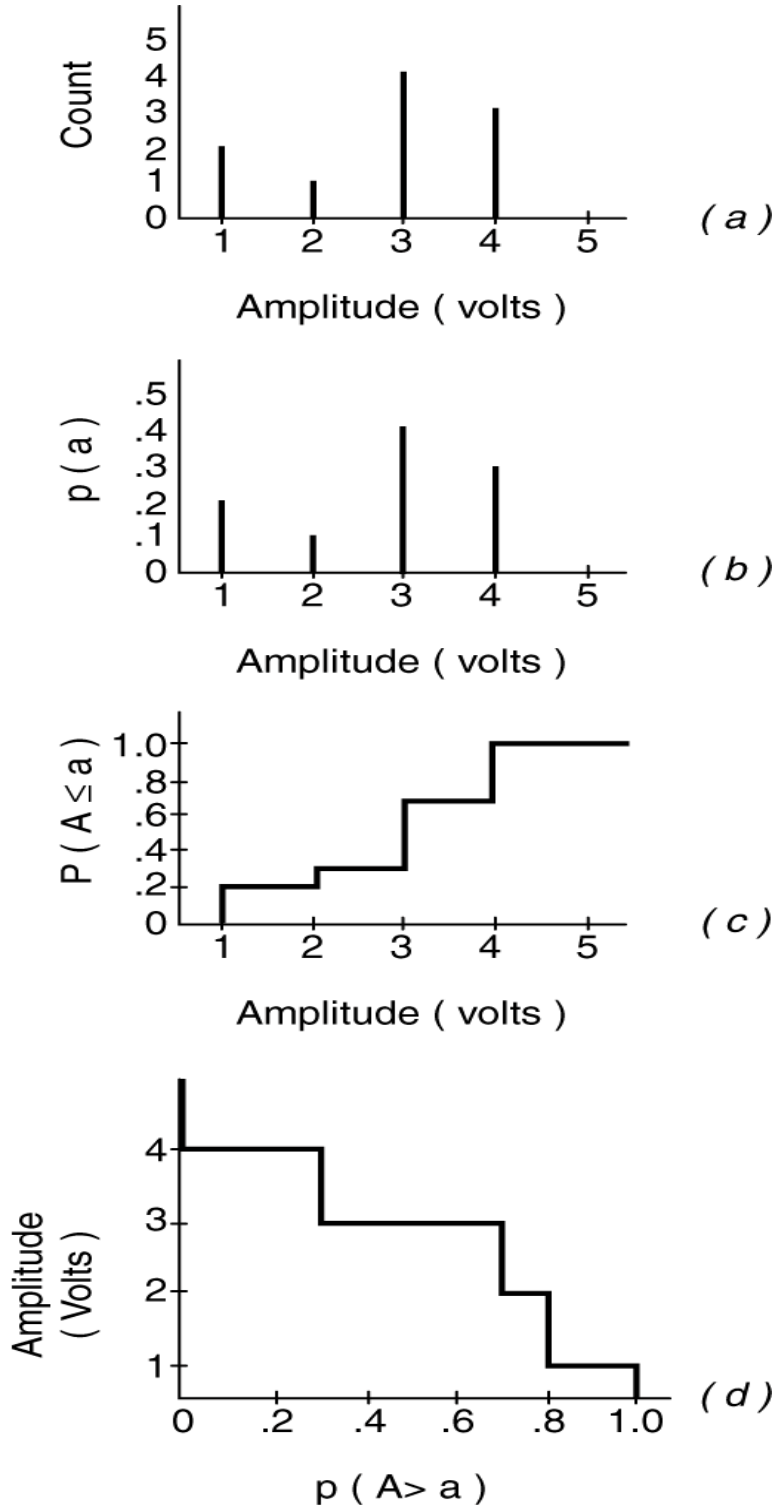

Figure E.2.1.1. Example histogram (a), probability density function (b), cumulative distribution function (c), and amplitude probability distribution function (d).

E.2.2 Statistical fundamentals

Statistics are functions that operate on the random sample. The *statistic value* is the result of a statistic operating on *random sample values*. Figure E.2.2.1 illustrates these relationships. Common statistical functions are percentile, mean or average, and root mean square (RMS). *First-order* statistics, addressed in this tutorial, assume the random variables are independent and identically distributed. *Second-order* statistics, not addressed in this tutorial, measure the correlation between these random variables. *Stationary* statistics are independent of time whereas *non-stationary* statistics are functions of time. Noise and interference amplitude statistics are non-stationary in many cases. Thus radio engineers sometimes measure the statistics of the amplitude statistics such as the median average noise power.

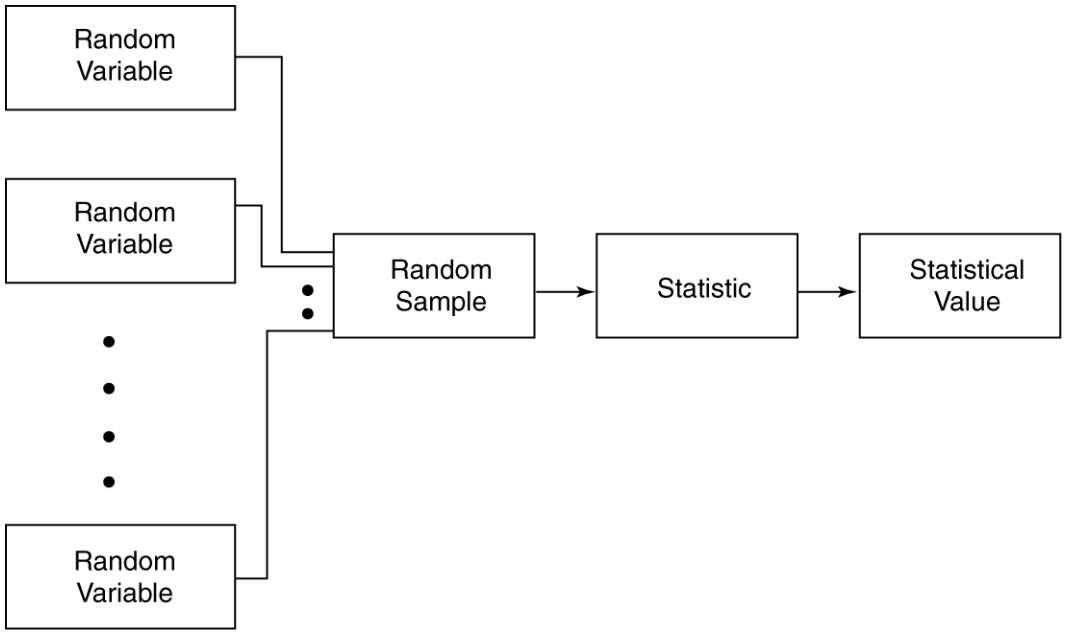

Figure E.2.2.1. Language of statistics.

Percentile amplitude statistics can be read directly from the APD. Peak and median amplitude statistics are the most widely used percentile statistics. The peak statistic is sometimes arbitrarily defined by the amplitude that is exceeded 0.0001% of the time:

$$V_p = cc^{-1}(0.000001) \quad ,$$

where $a = cc^{-1}(P(A>a))$. The median statistic is defined by the amplitude that is exceeded 50% of the time:

$$V_{median} = cc^{-1}(0.5) \quad .$$

The mean and RMS statistics are determined directly from the random sample values. The mean statistic is defined by:

$$V_{mean} = \frac{1}{N}\sum_{n} a_n \quad ,$$

where N is the number of samples. The mean-logarithm statistic is defined by:

$$V_{mean-\log} = \frac{1}{N}\sum_{n} \log_{10}(a_n) \quad ,$$

and the RMS statistic is defined by:

$$V_{RMS} = \sqrt{\frac{1}{N}\sum_{n} a_n{}^2} \quad .$$

The discrete APD and its corresponding discrete PDF can be used to calculate the mean and RMS statistics if the random sample values are no longer available. The choice of histogram bin size may affect the accuracy of these statistics. In this case the mean statistic is defined by:

$$V_{mean} = \sum_{i} a_i\, p(a_i) \quad ,$$

where a_i represents a discrete PDF value. The mean logarithm statistic is defined by:

$$V_{mean-\log} = \sum_{i} \log_{10}(a_i)\, p(a_i) \quad ,$$

and the RMS statistic is defined by:

$$V_{RMS} = \sqrt{\sum_{i} a_i{}^2\, p(a_i)} \quad .$$

As a reference, statistical values for the tutorial PDF presented in section E.2.1 are 4.0, 3.0, 2.8, 0.4, and 3.0 for the peak, median, mean, mean logarithm, and RMS statistics.

E.2.3 Graphing the APD

The APD of Gaussian noise is of particular interest to radio engineers because it is encountered in many practical applications. The amplitude of Gaussian noise is *Rayleigh distributed.* A Rayleigh distributed random variable is represented by a straight, negatively-sloped line on a *Rayleigh graph.* Figure E.2.3.1 shows the APDs of Gaussian and non-Gaussian noise on a Rayleigh graph.

The Rayleigh graph displays probability on the x-axis and amplitude on the y-axis. The probability is scaled by the function

$$x = 0.5 \log_{10}(-\ln(P(A>a))) \quad ,$$

and converted to percent to represent the "*percent (of samples or time) exceeding ordinate.*" The amplitude in volts is converted to units of power such as dBW, i.e., scaled by the function

$$y = 20 \log_{10}(A) \quad ,$$

or alternatively it is displayed in dB relative to a standard noise power density or noise power.

Figure E.2.3.1 shows the statistics of Gaussian noise on a Rayleigh graph. Gaussian noise average power or RMS voltage corresponds to the power or voltage that is exceeded 37% of the time. Gaussian noise peak voltage is approximately 10 dB above RMS voltage. Gaussian noise average voltage, median voltage, and average-logarithm voltage are approximately 1dB, 2 dB, and 2.5 dB below RMS voltage respectively.

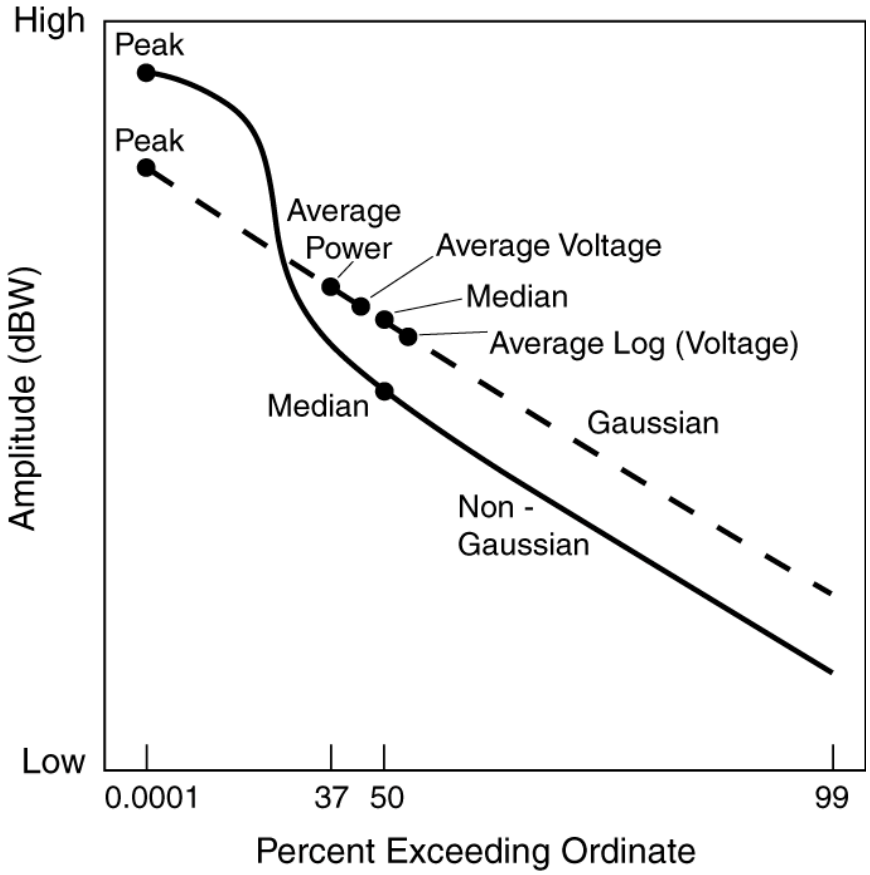

Figure E.2.3.1. Gaussian noise and non-Gaussian noise APDs plotted on a Rayleigh graph.

E.3 Tutorial APDs

E.3.1 Random Noise

Band limited random noise, i.e., the random noise present after a band limiting filter, is a random-amplitude and random-phase bandpass "signal" defined by

$$n(t) = A(t)\cos(2\pi f_c + 2(t)) \ .$$

Band limited random noise is represented in the frequency domain by a *power spectral density* (PSD) in units of watts/Hz. The random noise "signal," amplitude, and PSD are shown in Figure E.3.1.1.

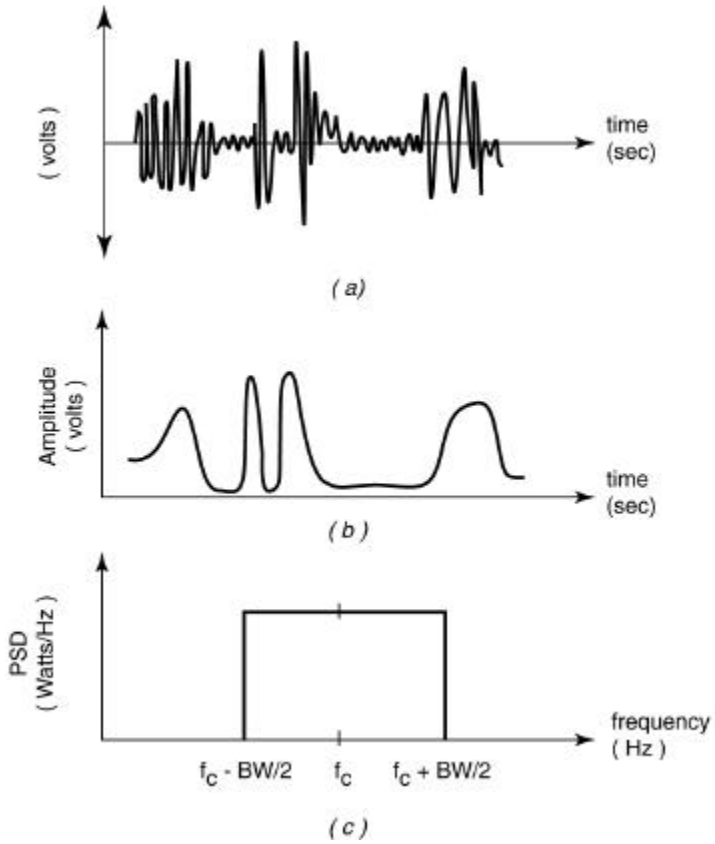

Figure E.3.1.1. Random noise (a), amplitude (b), and power spectral density (c).

Band limited noise average power is computed from the noise PSD:

$$P = \int_{f_c - BW/2}^{f_c + BW/2} N(f)\,df \quad ,$$

where $N(f)$ is the noise PSD in units of watts/Hz. Band limited *white* noise power density is

constant over the band limiting filter bandwidth. As a result, the average noise power is directly proportional to the filter bandwidth and the RMS amplitude is directly proportional to the square root of bandwidth. This is sometimes referred to as the "10 $\log_{10}$ bandwidth" rule. The amplitude of band limited Gaussian noise is Rayleigh distributed. Figure E.3.1.2 shows the APD of band limited white-Gaussian noise (WGN) for two different bandwidths on a Rayleigh graph.

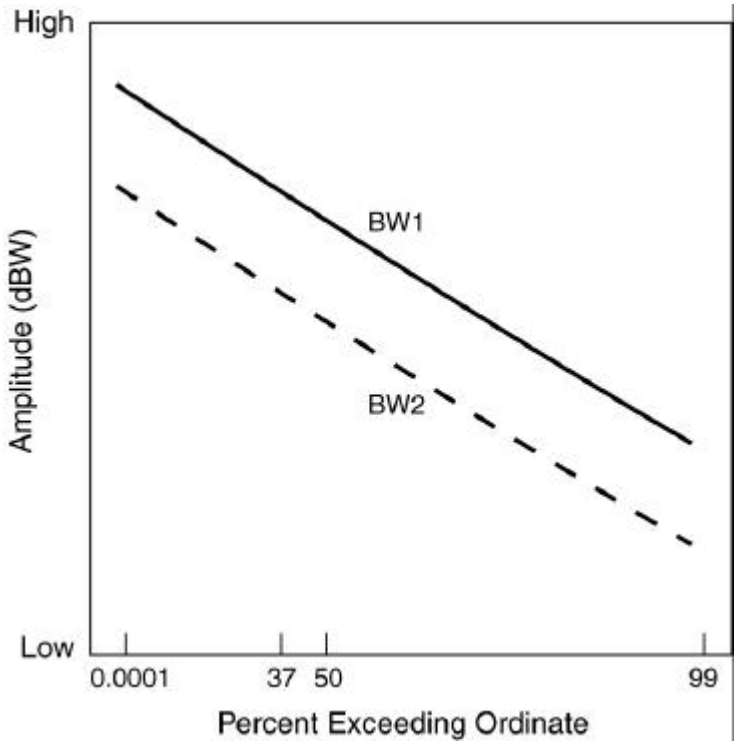

Figure E.3.1.2. Bandlimited Gaussian noise APDs with two different bandwidths. BW1 is greater than BW2.

E.3.2 Sinusoidal Signal

The sinusoid (continuous wave) signal is a narrowband, constant amplitude and constant phase signal. It is defined by

$$s(t) = A\cos(2\mathrm{B}f_c+2) \quad .$$

The signal, signal amplitude, and amplitude spectrum are shown in Figure E.3.2.1. The APD of the sinusoid signal is a flat line from the lowest to the highest percentile on a Rayleigh graph. Changing the receiver center frequency can change the amplitude of the sinusoidal signal.

Widening the bandwidth of a receiver filter in the presence of noise causes the statistics to be *Rician*. Rician statistics are dependent on the ratio of the sinusoid power to the noise power. The Rician APD corresponds to the sinusoid signal APD when noise is absent and the Rayleigh APD when the signal is absent. Sinusoid, Rician, and Rayleigh APDs are depicted in Figure E.3.2.2.

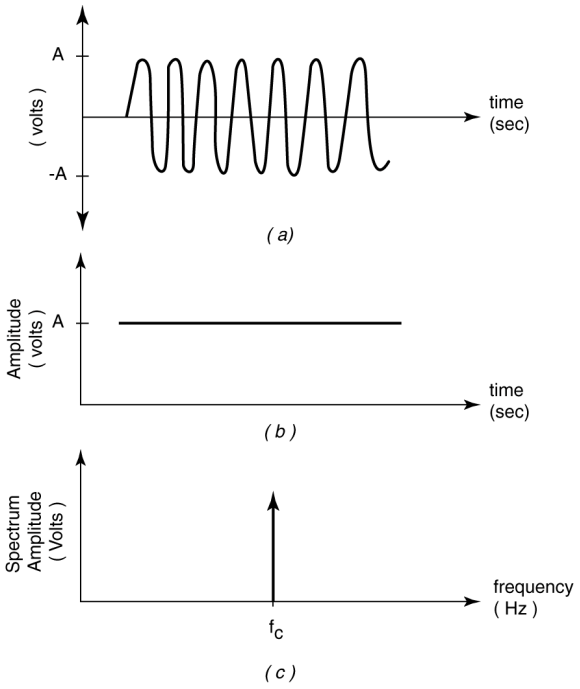

Figure E.3.2.1. Sinusoid signal (a), signal amplitude (b), and amplitude of the signal spectrum (c).

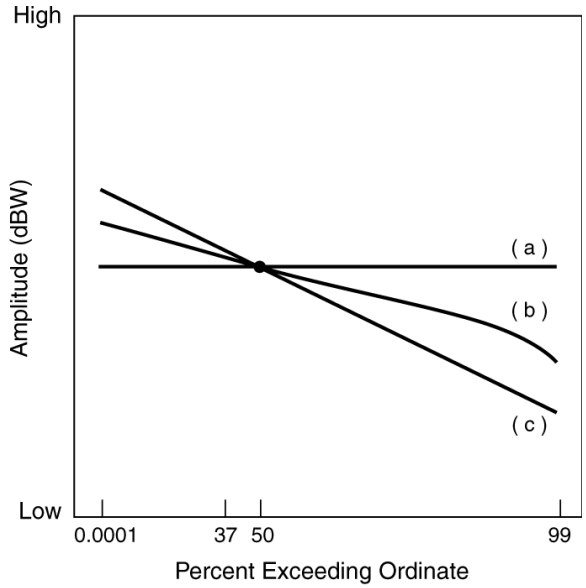

Figure E.3.2.2. Sinusoid signal APD without (a) and with (b) random noise. Sinusoid signal with random noise has Rician amplitude statistics. The Gaussian noise APD (c) is included for reference.

E.3.3 Periodically Pulsed Sinusoid

The periodically pulsed sinusoid is a deterministic, time-varying amplitude and constant phase signal defined by

$$s(t) = A(t)\cos(2\pi f_c + \theta) \quad .$$

The amplitude varies between 'on' and 'off' pulse states. The 'on' duration is the *pulse width* (PW) and the repetition rate of pulses is the *pulse repetition rate* (PRR) or the pulse repetition frequency (PRF). Amplitude spectrum *lines* are spaced at the PRF. Amplitude spectrum *nulls* are spaced by the reciprocal of the PW. The signal, signal amplitude, and amplitude of the signal spectrum are shown in Figure E.3.3.1.

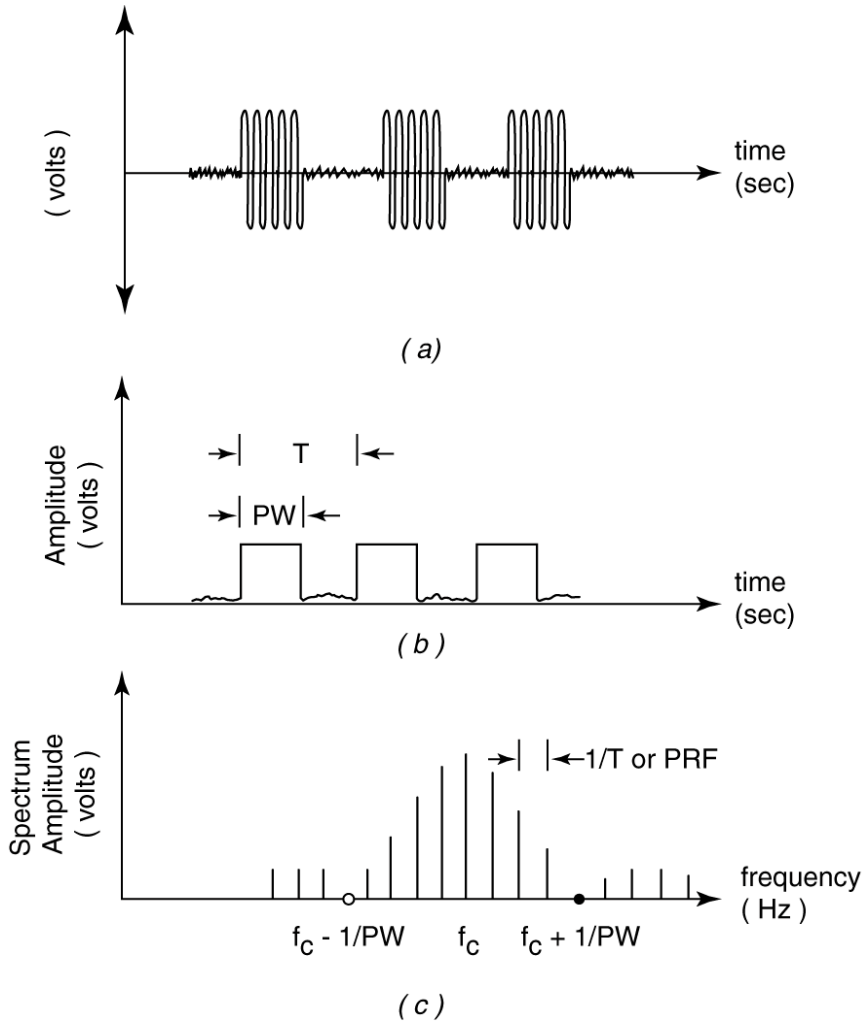

Figure E.3.3.1. Periodically pulsed sinusoid signal (a), signal amplitude (b), and amplitude of signal spectrum (c).

The APD of a periodically pulsed sinusoid is dependent on the receiver center frequency, band limiting filter parameters, and pulse parameters. *Pulse overlap distortion* is significant until the *band limited pulse* bandwidth (BW) exceeds the PRF. The band limited pulse is the pulse present at the output of the receiver filter. Analytically the band limited pulse is obtained by convolving the pulse shape with the receiver filter impulse response. Band limited pulses with minimal overlap are considered *independent* or *resolved*. The transmitted pulse shape is fairly well preserved when the filter BW is greater than 2/*PW*. The two graphs in Figure E.3.3.2. show a succession of APDs with the different receiver center frequency and BW combinations listed in Table E.3.3.1. The first graph has filter BWs less than the PRF while the second graph has filter BWs greater than the PRF.

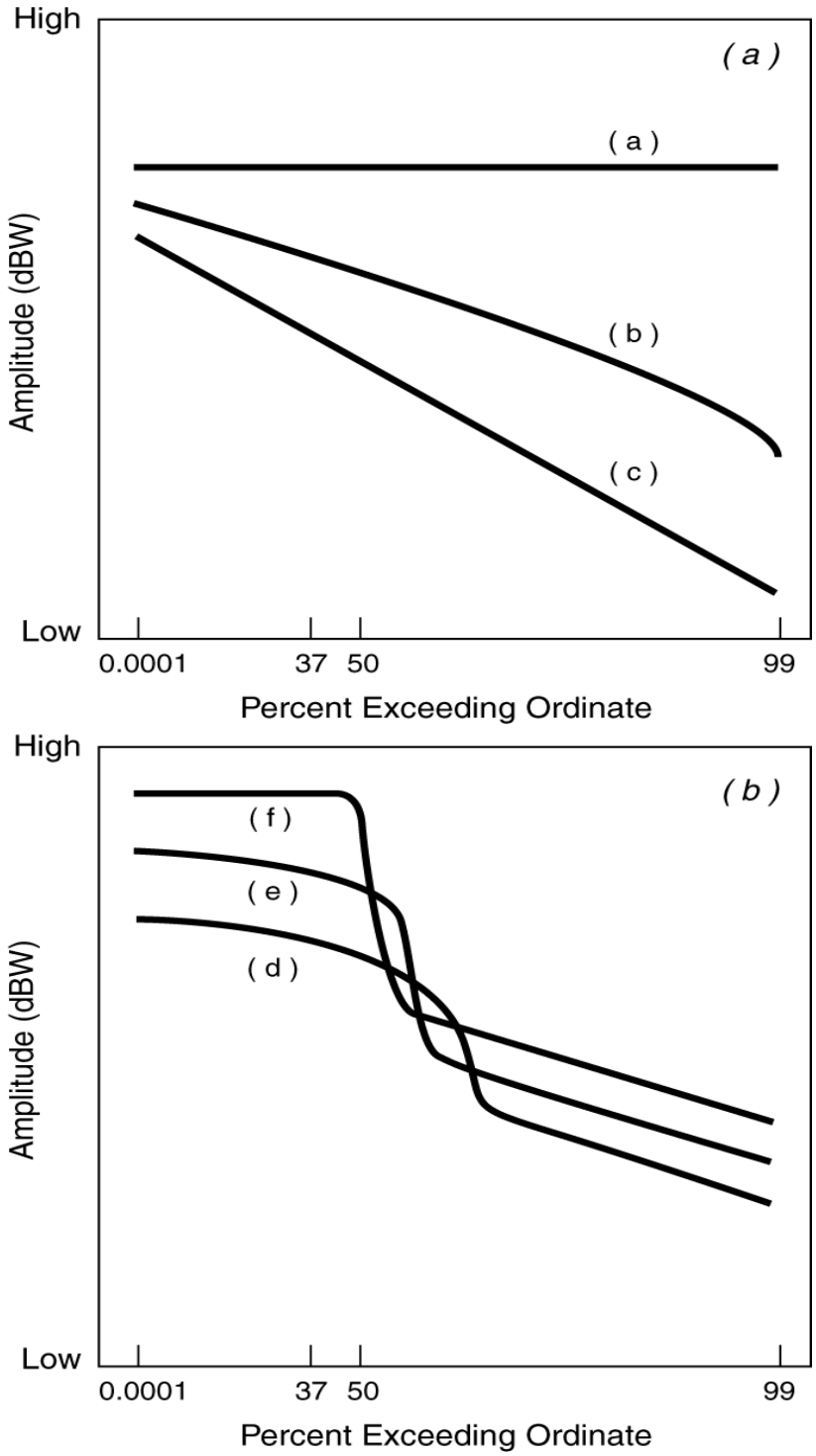

Figure E.3.3.2. Periodically pulsed sinusoid APD with receiver filter bandwidth less than (a) and greater than (b) the pulse repetition frequency. See Table E.3.3.1 for receiver center frequency and filter bandwidth conditions for curves a-f.

Table E.3.3.1. Figure E.10 APD Conditions

Figure, Curve	**Receiver Center Frequency**	**Bandwidth**
E.3.3.2a, a	Tuned to spectral line	Filter BW<< PRF
E.3.3.2a, b	Tuned to spectral line	Filter BW< PRF
E.3.3.2a, c	Tuned off spectral line	Filter BW< PRF
E.3.3.2b, d	Tuned to pulse center frequency	Band limited pulse BW>PRF
E.3.3.2b, e	Tuned to pulse center frequency	Band limited pulse BW>>PRF
E.3.3.2b, f	Tuned to pulse center frequency	Band limited pulse BW > 2/PW

The APD takes on three characteristics when the filter bandwidth is less than the PRF, as shown in Figure E.3.3.2a. If the center frequency is tuned to a spectral line frequency and the filter bandwidth is able to *resolve* the line, it has a sinusoid APD (a). If the center frequency is tuned to a spectral line frequency, but the filter bandwidth is wider than necessary to resolve the line, it can have a Rician APD (b). If the center frequency is tuned to avoid a spectral line frequency, it has a Rayleigh APD (c).

Pulse overlap distortion decreases as the band limited pulse BW increases beyond the PRF as shown in Figure E.3.3.2b. The APDs are clearly non-Gaussian. The APD is somewhat curved at the lower probabilities for narrow filter bandwidths where there is pulse overlap (d). The APD flattens at low probabilities for wider filter bandwidths where the pulse overlap is minimal (f).

The low probability amplitudes correspond to the band limited pulse amplitudes. The high probability amplitudes correspond to the receiver noise amplitudes. The amplitudes at low probabilities are proportional to filter BW corresponding to a '20 $\log_{10}$ bandwidth rule'. The amplitudes at high probabilities are proportional to the square root of filter BW corresponding to the '10 $\log_{10}$ bandwidth rule.' The transition probability between these two domains is related to the band limited pulse duty cycle.

E.3.4 Summary Table

Table E.3.4.1. summarizes the APD dependencies for the three tutorial signals.

Table E.3.4.1. Tutorial Signal APD Dependencies

Signal	**Receiver Center Frequency**	**Receiver Filter**	**Other Parameters**
WGN	No	BW	
Sinusoid with WGN	Yes	BW	
Periodically-pulsed sinusoid with WGN	Yes	BW	PW, PRF

E.4 Band Limited UWB APDs

E.4.1 UWB Signals

The UWB signal is a train of pulses whose widths (in time) are "ultrashort" and bandwidths (in frequency) are "ultrawide." Like the periodically pulsed sinusoid, the pulses are defined by a PW and PRF. Unlike the periodically pulsed sinusoid, the impulses do not modulate a carrier frequency prior to being transmitted.

For some applications the pulse train may be pulse position modulated by a *time-dither sequence*. Time-dithering attenuates the discrete spectral line PSD component caused by periodic pulse transmission and introduces a continuous, random noise PSD component. The effectiveness of dithering is dependent on time-dither characteristics such as the distribution of dithering times, the reference time of the time-dithered pulse (absolute or relative to the last pulse), and the length of the time-dither sequence.

UWB signals are used in radar and communication devices. These devices reduce power requirements and alleviate spectral congestion by "gating" the pulse train off when continuous transmissions are not needed. They also use uncorrelated dither sequences to minimize interference to other UWB devices operating in the same room or building.

Figure E.4.1.1 shows a UWB undithered pulse train, a dithered pulse train, and a gated and dithered pulse train. Figure E.4.1.1 also shows an example UWB signal PSD with continuous and discrete components.

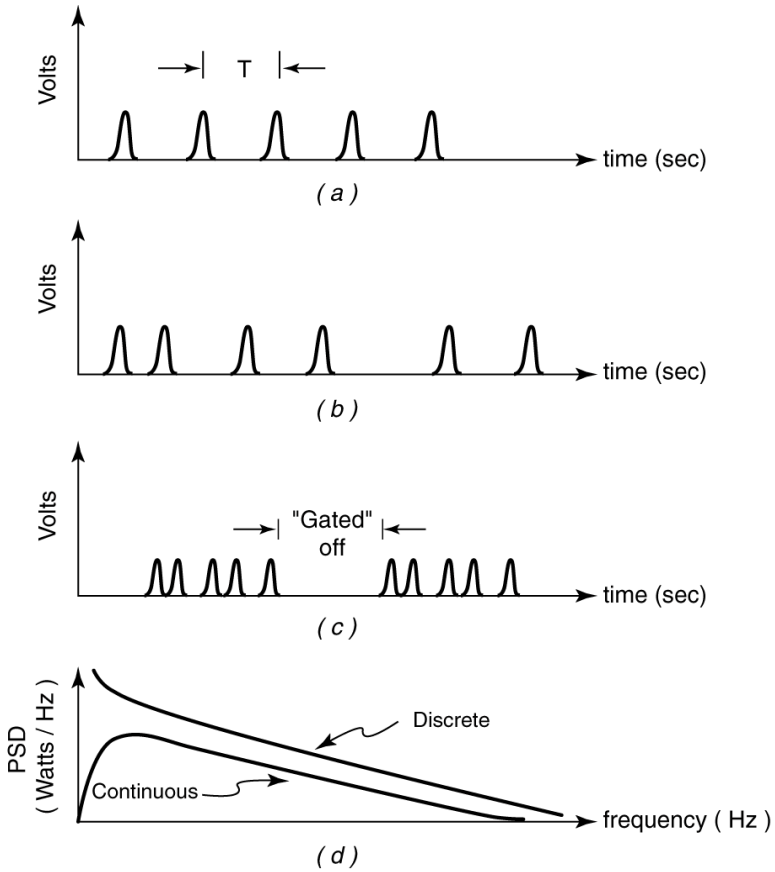

Figure E.4.4.1. Undithered (a), dithered (b), and dithered and gated (c) ultawideband signal. Dithered ultrawideband signal power spectral density (d) showing discrete and continuous components. The discrete components are represented as a curve because the lines cannot be resolved graphically.

E.4.2 Band Limited UWB Signals

The bandwidth of the interfering UWB signal is typically several orders of magnitude wider than that of the band limiting filters in the victim narrowband receiver. Thus the pulse shape and BW of the band limited pulse corresponds to the impulse response and BW of the receiver filter. Pulses are independent or resolved when the filter BW is greater than the PRF. Pulses that were independent or resolved before dithering may not be when dithering is introduced. To remain resolved, the pulse repetition period must be greater than the sum of the pulse duration and the maximum dither time.

Band limiting can occur in several of the narrowband receiver functions including demodulation, detection, and signal parameter estimation. Signal parameter estimation is necessary to provide frequency, phase, amplitude, and timing information to the demodulation and detection functions. The bandwidths associated with each of these functions may differ by several orders of magnitude. The relationships among these functions are shown in Figure E.4.2.1.

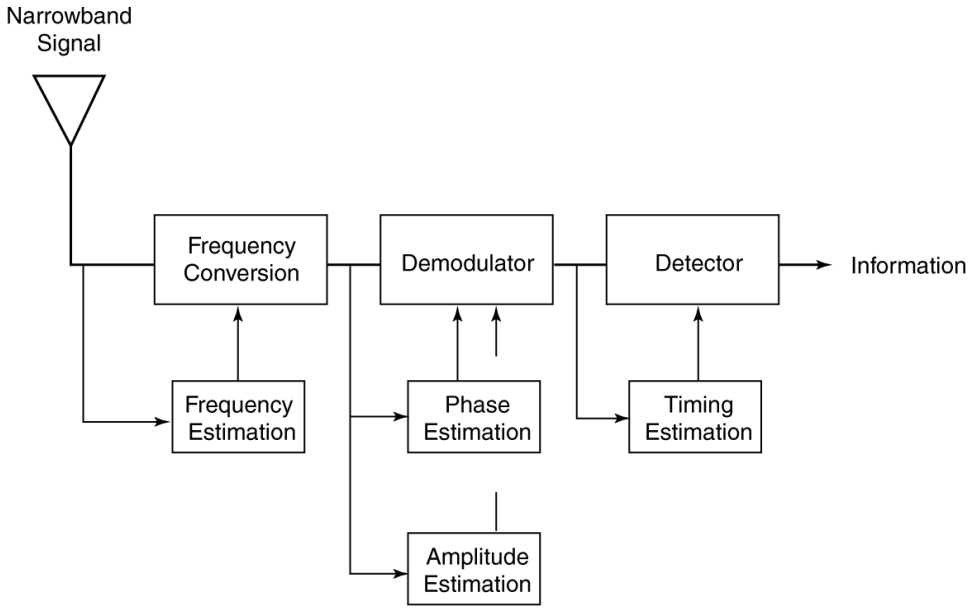

Figure E.4.2.1. Locations of band limiting filters in narrowband receivers.

E.4.3 Band Limited UWB Signal APDs

The undithered UWB signal APD will behave similarly to the periodically pulsed sinusoid APD as the filter bandwidth is varied from less than the PRF towards filter bandwidths much greater than the PRF. The dithered UWB signal APD will also behave similarly to the periodically pulsed sinusoid APD as long as the dithered pulses remain resolved. Figure E.4.3.1 shows an example of the changes that might happen to an unresolved dithered UWB signal APD when dithering is varied and BW is constant. These effects of dithering are only one possibility among many which are dependent on frequency, dithering distribution, dither reference time, length of dither sequence, gating, modulation, and filtering. In filter bandwidths less than the PRF increased dithering caused this APD to progress from the sinusoid APD to the Rician APD and finally to the Rayleigh APD. The receiver center frequency in this case was tuned to a spectral line. This progression is illustrated in Figure E.4.3.1a. In filter bandwidths comparable to the PRF, increased dithering caused this APD to progress from the non-Gaussian noise APD towards the Gaussian noise APD with Rayleigh distributed amplitudes. This progression is illustrated in Figure E.4.3.1b.

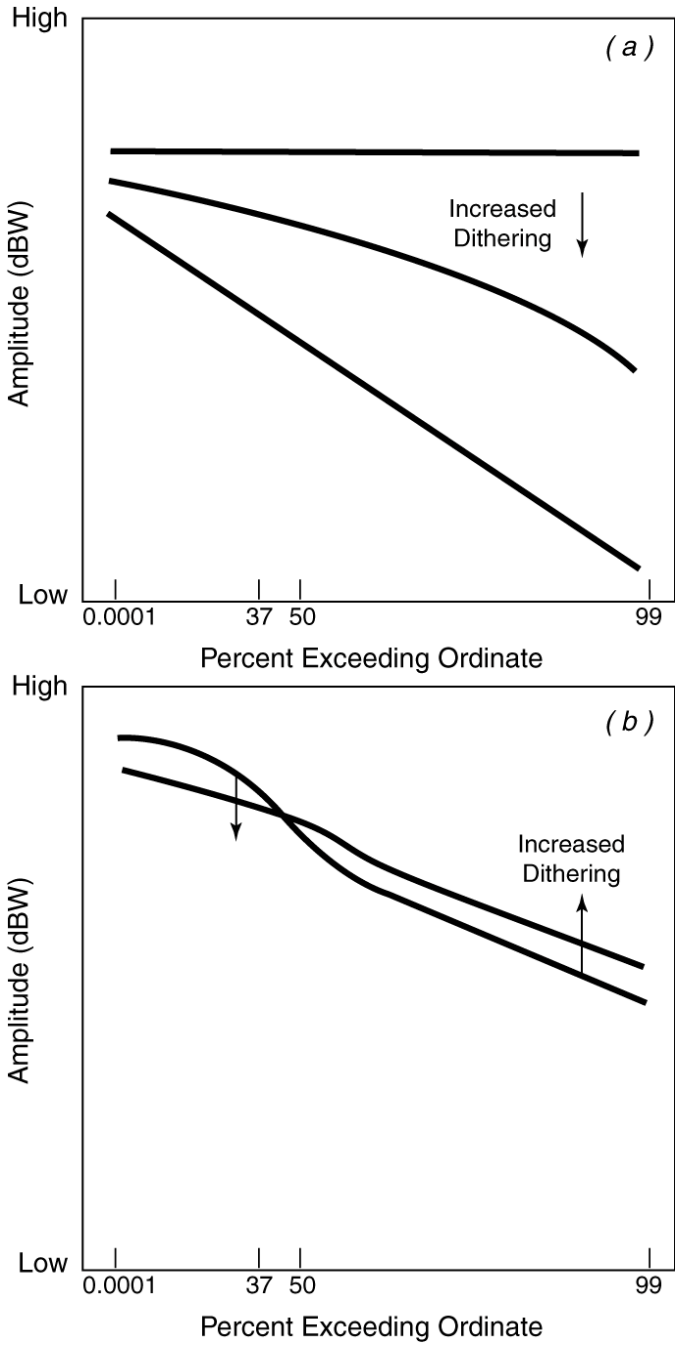

Figure E.4.3.1. Effects of increased dithering when band limiting filter bandwidth is less than (a) and comparable to (b) the pulse repetition frequency.

E.5 APD Special Topics

E.5.1 APD Measurement

Spectrum analyzer measurements can be used to estimate the APD or an amplitude statistic such as peak voltage. A block diagram of a spectrum analyzer is shown in Figure E.5.1.1. The received signal is converted to an intermediate frequency, band limited by the variable resolution bandwidth filter, and compressed by the log amplifier. Compression by the log amplifier extends the dynamic range of the measurement. The envelope detector extracts the amplitude from the band limited and compressed signal. The video bandwidth filter is used to (video) average the amplitude. The peak detector holds the highest amplitude since it was last reset.

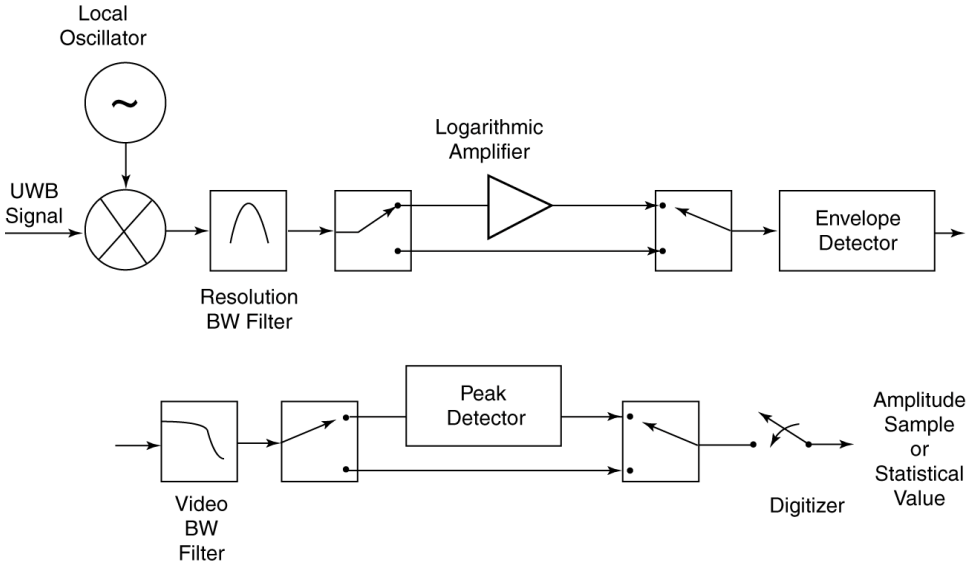

Figure E.5.1.1. Spectrum analyzer block diagram.

The statistics of the APD are derived from independent amplitude measurements. The amplitude measurements are considered independent if the sample time is 5 to 10 times the resolution bandwidth. The peak detector is bypassed and video averaging is disabled during an APD measurement. A histogram of the amplitude measurements is used to estimate the APD as shown in Section E.2.1.

The peak voltage statistic is measured with the peak detector. Video averaging is disabled during peak detection. Average voltage statistics are measured with the video bandwidth filter. The log amplifier is bypassed and the peak detector is disabled for this measurement. The integration-time of the video bandwidth filter is long enough to suppress variation but surely more than the reciprocal of the resolution bandwidth. Average logarithm voltage statistics are measured in the same manner as the average voltage; however, the signal is log amplified.

E.5.2 APD of the Sum of Band Limited UWB Signals

APDs of band limited UWB signals are often collected individually in a laboratory setting. These APDs are useful for studying the interference of one UWB signal. However, in everyday life, more than one UWB device may be transmitting at a time. The statistics of the aggregate signal are conditional on the distributions of the individual band limited UWB signals and the number of signals that are to be added. Assuming the phases of the band limited UWB signals are uniformly distributed, four cases of interest emerge as shown in Table E.5.2.1.

Table E.5.2.1. Distributions of Four Aggregate APD Cases

	Distributions of band limited UWB signals	
Number of UWB signals	**Rayleigh**	**Any Distribution**
Few	(1) Rayleigh	(3) Non-Rayleigh
Many	(2) Rayleigh	(4) Rayleigh

In cases 1 and 2 all the band limited UWB signals have Rayleigh distributions and the aggregate is also Rayleigh distributed. Case 4 is Rayleigh distributed by virtue of the central limit theorem of statistics. In cases 1, 2, and 4 the aggregate power is simply the sum of the individual UWB signal powers. Measurement system average noise power can be removed from individual APDs before summing. In addition, the average power of the individual APD may have to be reduced by attenuation due to the propagation channel to compensate for differences in location.

Case number 3 is more difficult for two reasons. First, measurement system noise statistics cannot be removed from the measured statistics. Second, the computation of the aggregate APD requires using the joint statistics of a band limited UWB signal amplitude and phase distributions. For these reasons it is best to measure these statistics as an aggregate.

E.5.3 Performance Prediction

Characterizing the band limited UWB signal with an APD is not enough. Ultimately the effect that the amplitude statistics have on victim receiver performance has to be determined. The band limited UWB interference takes three guises: sinusoidal interference, Gaussian noise with Rayleigh distributed amplitudes, and non-Gaussian noise. The APD is particularly useful for predicting the performance of non-Gaussian noise.

For example, Figure E.5.3.1. shows how the non-Gaussian noise APD can be used to predict bit error rate (BER) for non-coherent binary frequency-shift keying. The straight, sloped APD is the result of band limited Gaussian noise produced in the receiver. The stepped APD is the result of band limited non-Gaussian interference. The average receiver noise power is represented by a horizontal line on the graph. The signal-to-noise ratio (SNR) is represented as another horizontal line SNR dB above the noise power line. The BER is approximately one-half the probability where the SNR line intersects the APD curve.

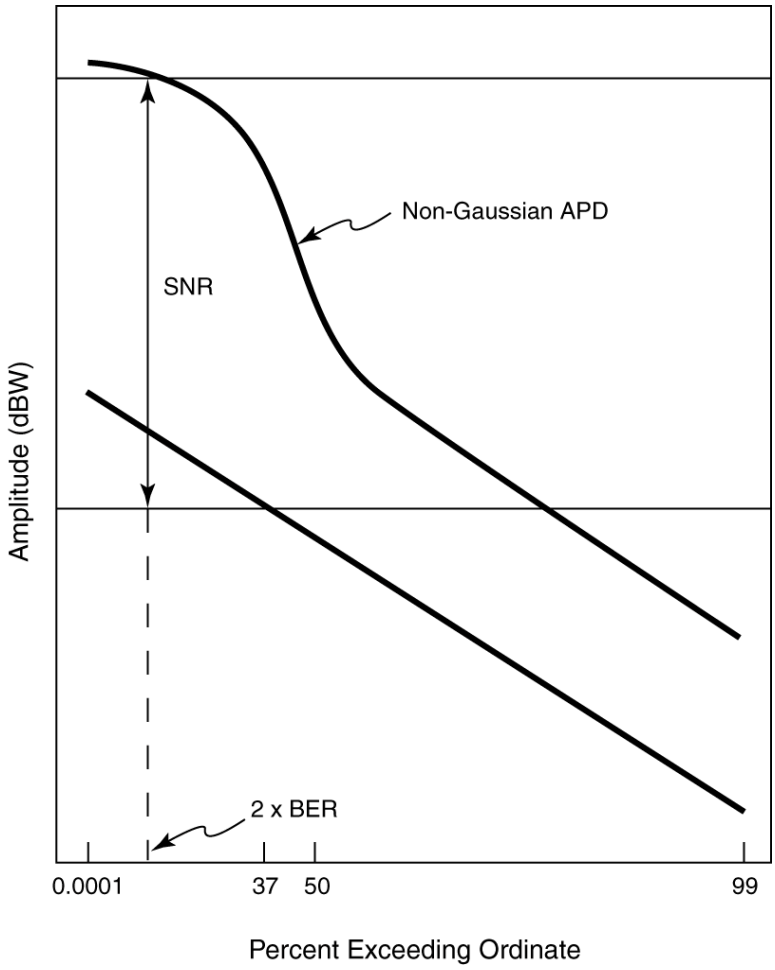

Figure E.5.3.1. Estimation of bit error rate from a non-Gaussian noise APD.

Many modern digital receivers use elaborate error correction and time-interleaving techniques to correct errors in the received bit sequence. In such receivers, the corrected BER delivered to the user will be substantially different from the received BER. Computation of BERs in these receivers will require much more detailed interference information than is contained in the

APDs. For example, second-order statistics of noise amplitudes describing the time of arrival of noise amplitudes may be needed.

E.6 Concluding Remarks

This tutorial has shown that the APD is a useful tool for describing the UWB signal and analyzing UWB signal interference to victim narrowband receivers. It is useful because it 1) is measurable, 2) provides a variety of statistical values, and 3) can be used to aid in receiver performance prediction.

The APD gives insight to the potential interference from UWB signals in a wide variety of receiver bandwidths and UWB characteristics, especially when the combination of interferer and victim produces non-Gaussian interference in the victim receiver. If the interference is Gaussian, victim receiver performance degradation is correlated to the interfering signal average power alone and there is no need for further analysis using the APD. If the interference is non-Gaussian or sinusoidal, information in the APD may be critical to quantifying its effect on victim receiver performance degradation. Band limited UWB interference becomes increasingly non-Gaussian as the victim narrowband receiver bandwidth increases beyond the UWB signal PRF. Band limited UWB interference becomes increasingly sinusoidal as the victim narrowband receiver bandwidth decreases below the UWB signal PRF and a spectral line is present within the receiver bandwidth.

Spectrum regulators frequently use amplitude statistics such as peak, RMS, or average logarithm voltage to regulate transmitters. Further work is needed to determine if these statistics are strongly correlated to narrowband receiver performance. If these statistics are not correlated to receiver performance, it may be necessary to set regulatory limits in terms of the APD itself.

E.7 Bibliography

[1] A.D. Spaulding and R.T. Disney, “Man-made radio noise, part 1: Estimates for business, residential, and rural areas,” OT Report 74-38, Jun. 1974.

[2] A.D. Spaulding, “Digital system performance software utilizing noise measurement data,” NTIA Report 82-95, Feb. 1982.

[3] A.D. Spaulding,”The natural and man-made noise environment in personal communication services bands,” NTIA Report 96-330, May 1996.

[4] R.J. Achatz, Y. Lo, P.B. Papazian, R.A. Dalke, and G.A. Hufford, “Man-made noise in the 136-138-MHz VHF meteorological satellite band,” NTIA Report 98-355, Sep. 1998.

[5] R.A. Dalke, “Radio Noise,” in the *Wiley Encyclopedia of Electrical and Electronics Engineering*, Vol. 18., J.G. Webster, Ed., John Wiley & Sons, Inc., New York: N.Y., 1998, pp. 128-140.

[6] R.J. Matheson, “Instrumentation problems encountered making man-made electromagnetic noise measurements for predicting communication system performance,” *IEEE Transactions on Electromagnetic Compatibility*, Volume EMC-12, Number 4, Nov. 1970.

[7] J.S. Bendat and A.G. Piersol, *Measurement and Analysis of Random Data*, New York, NY: John Wiley & Sons, Inc, 1966.

[8] P.L. Meyer, *Introductory Probability and Statistical Applications*, Second Edition, Reading, Mass: Addison-Wesley Publishing Company, 1970.

APPENDIX F: GPS PERFORMANCE MEASUREMENT RESULTS

Each figure in this appendix illustrates a comprehensive summary of measured GPS performance degradation for a given receiver exposed to a UWB signal permutation. Due to time constraints, not all scenarios were measured, as summarized in Tables F.1 and F.2.

Table F.1. Single-Source UWB Interference Measurement Figure List

Interference	Rx 1		Rx 2	
Spacing / PRF(MHz) / DC(%)	BL	RQT	BL	RQT
Gaussian noise	F.1.1	F.1.1	F.2.1	F.2.1
UPS / 20 / 100, 20	F.1.2, 3	N/A	F.2.2, 3	N/A
UPS / 5 / 100, 20	F.1.4, 5	N/A	N/A	N/A
UPS / 1 / 100, 20	F.1.6, 7	N/A	N/A	N/A
UPS / 0.1 / 100, 20	F.1.8, 9	F.1.8, 9	F.2.4, 5	F.2.4, 5
OOK / 20 / 100, 20	F.1.10, 11	N/A	F.2.6, 7	N/A
OOK / 5 / 100, 20	F.1.12, 13	N/A	N/A	N/A
OOK / 1 / 100, 20	F.1.14, 15	N/A	N/A	N/A
OOK / 0.1 / 100, 20	F.1.16, 17	F.1.16, 17	F.2.8, 9	F.2.8, 9
50%-ARD / 20 / 100, 20	F.1.18, 19	F.1.18, 19	F.2.10, 11	F.2.10, 11
50%-ARD / 5 / 100, 20	F.1.20, 21	F.1.20, 21	F.2.12, 13	F.2.12, 13
50%-ARD / 1 / 100, 20	F.1.22, 23	F.1.22, 23	F.2.14, 15	F.2.14, 15
50%-ARD / 0.1 / 100, 20	F.1.24, 25	F.1.24, 25	F.2.16, 17	F.2.16, 17
2%-RRD / 20 / 100, 20	F.1.26, 27	F.1.26, 27	F.2.18, 19	F.2.18, 19
2%-RRD / 5 / 100, 20	F.1.28, 29	F.1.28, 29	F.2.20, 21	F.2.20, 21
2%-RRD / 1 / 100, 20	F.1.30, 31	F.1.30, 31	F.2.22, 23	F.2.22, 23
2%-RRD / 0.1 / 100, 20	F.1.32, 33	F.1.32, 33	F.2.24, 25	F.2.24, 25

Table F.2. Aggregate UWB Interference Measurement Summary

Interference (See Table 4.1.2.2 for details)	Rx 1		Rx 2	
	BL	RQT	BL	RQT
Aggregate 1	F.1.34	F.1.34	N/A	N/A
Aggregate 2	F.1.35	F.1.35	N/A	N/A
Aggregate 3	F.1.36	F.1.36	N/A	N/A
Aggregate 4	F.1.37	F.1.37	N/A	N/A
Aggregate 5(a)	F.1.38	F.1.38	N/A	N/A
Aggregate 5(b)	F.1.39	F.1.39	N/A	N/A
Aggregate 5(c)	F.1.40	F.1.40	N/A	N/A
Aggregate 5(d)	F.1.41	F.1.41	N/A	N/A
Aggregate 5(e)	F.1.42	F.1.42	N/A	N/A
Aggregate 5(f)	F.1.43	F.1.43	N/A	N/A

F.1. C/A-code Receiver Results

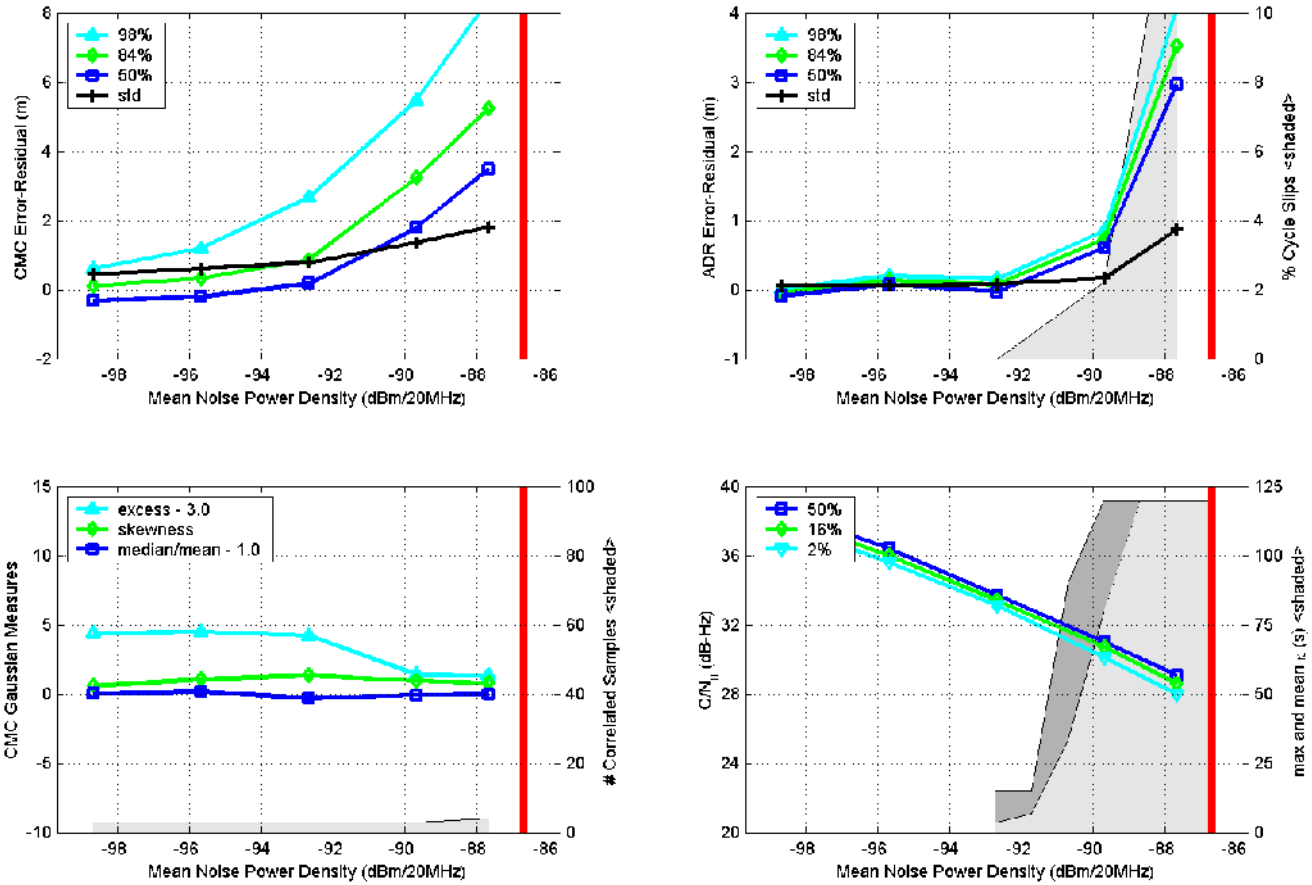

Figure F.1.1. Measured GPS parameters (Rx 1) as a function of Gaussian-noise interference.

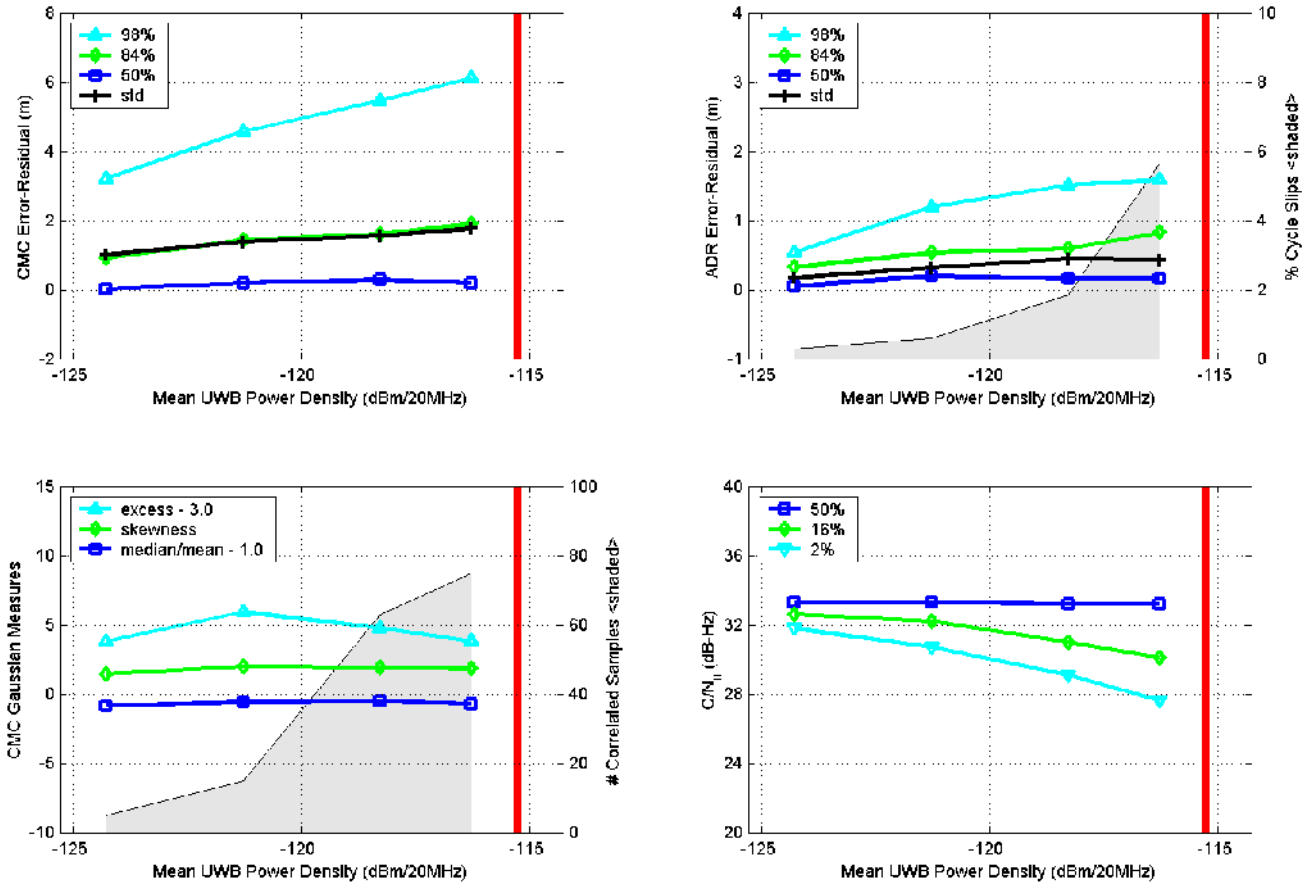

Figure F.1.2. Measured GPS parameters (Rx 1) as a function of 20-MHz PRF, UPS, non-gated UWB interference.

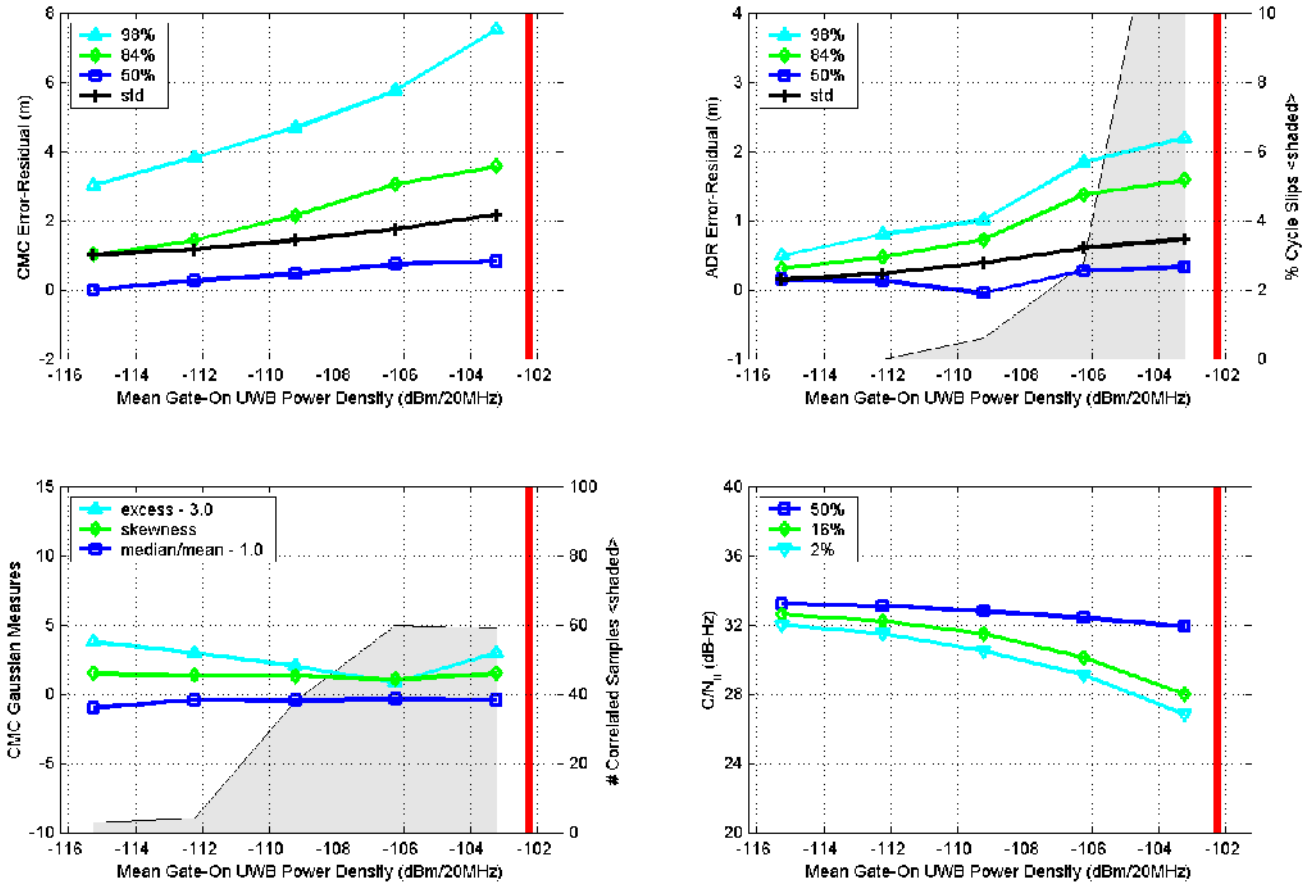

Figure F.1.3. Measured GPS parameters (Rx 1) as a function of 20-MHz PRF, UPS, gated (20% duty cycle) UWB interference.

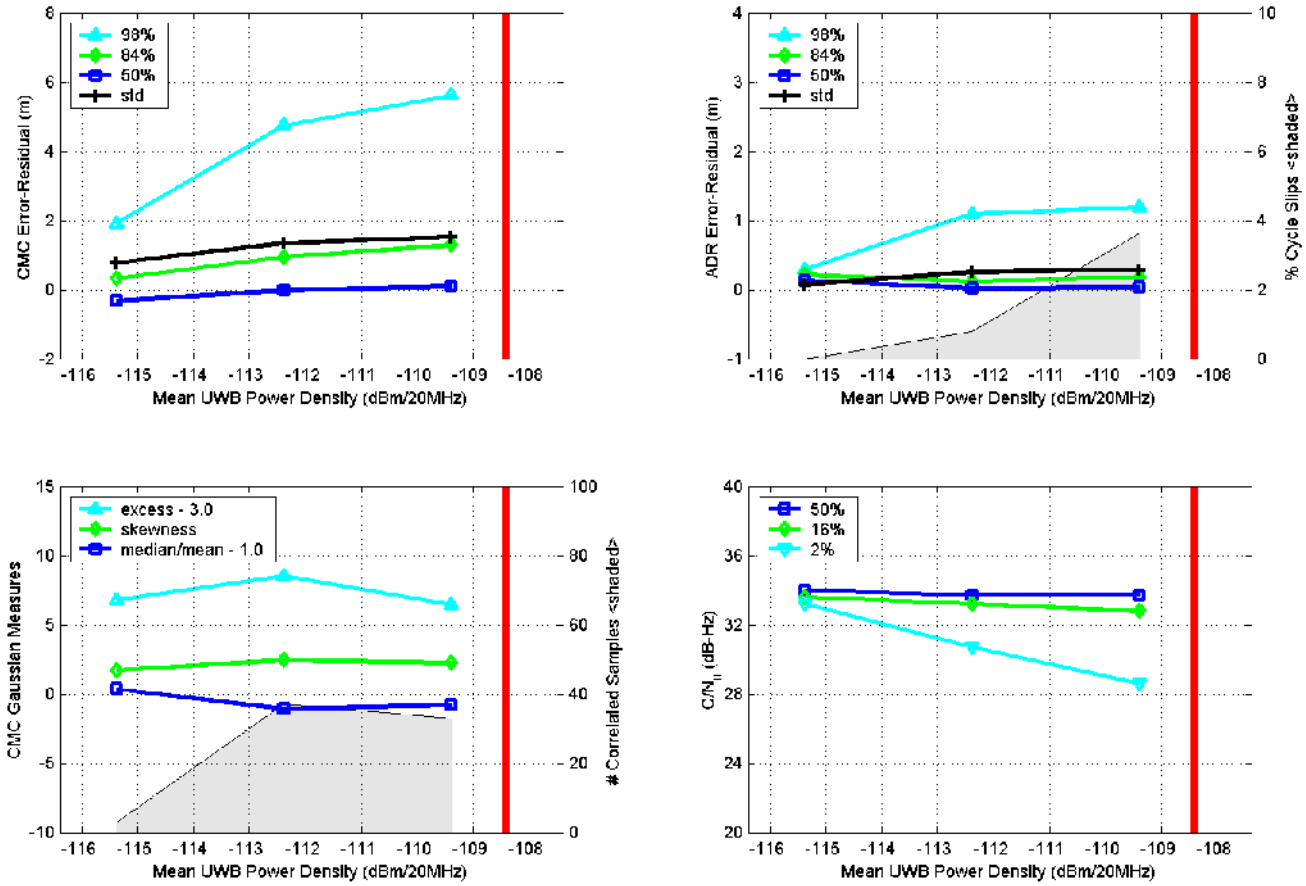

Figure F.1.4. Measured GPS parameters (Rx 1) as a function of 5-MHz PRF, UPS, non-gated UWB interference.

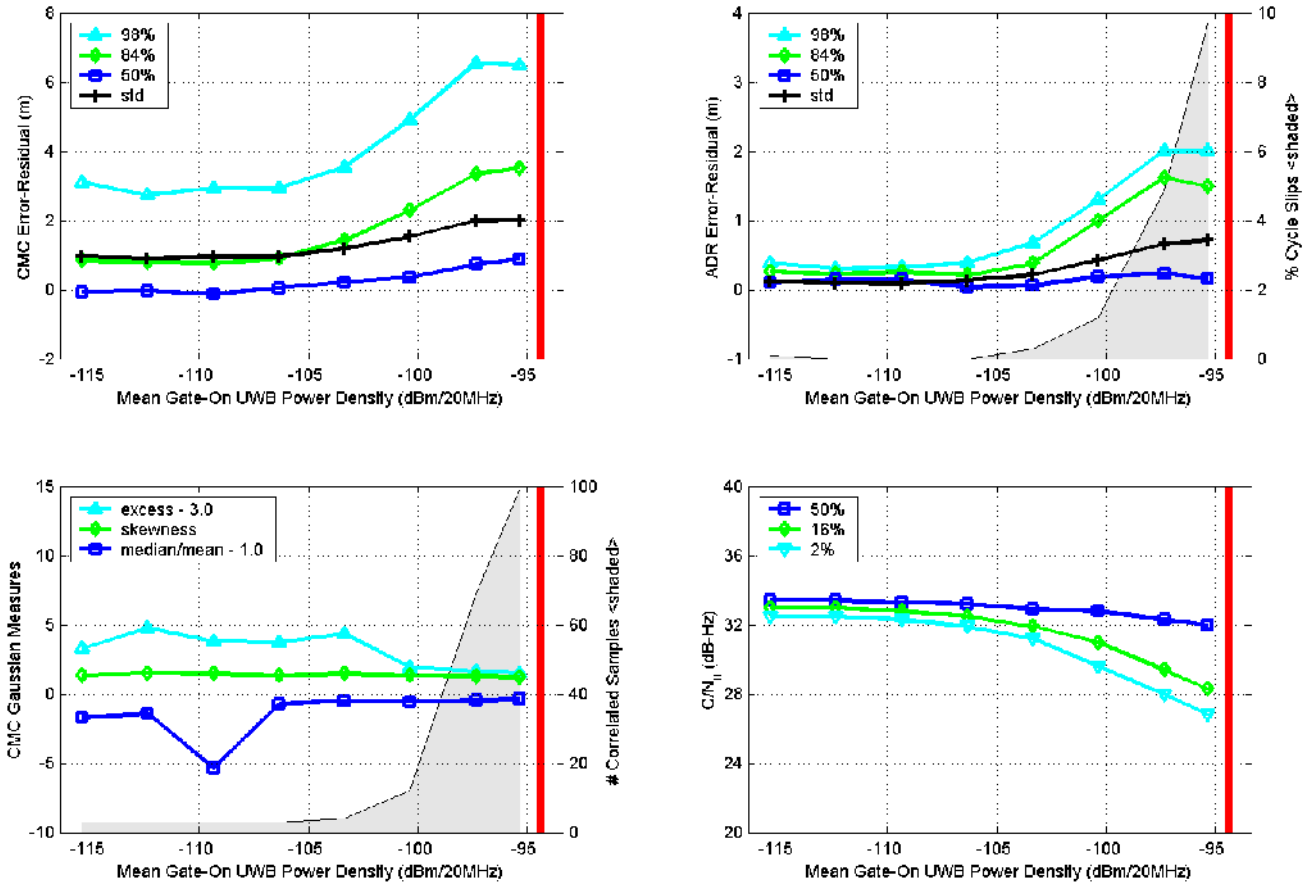

Figure F.1.5. Measured GPS parameters (Rx 1) as a function of 5-MHz PRF, UPS, gated (20% duty cycle) UWB interference.

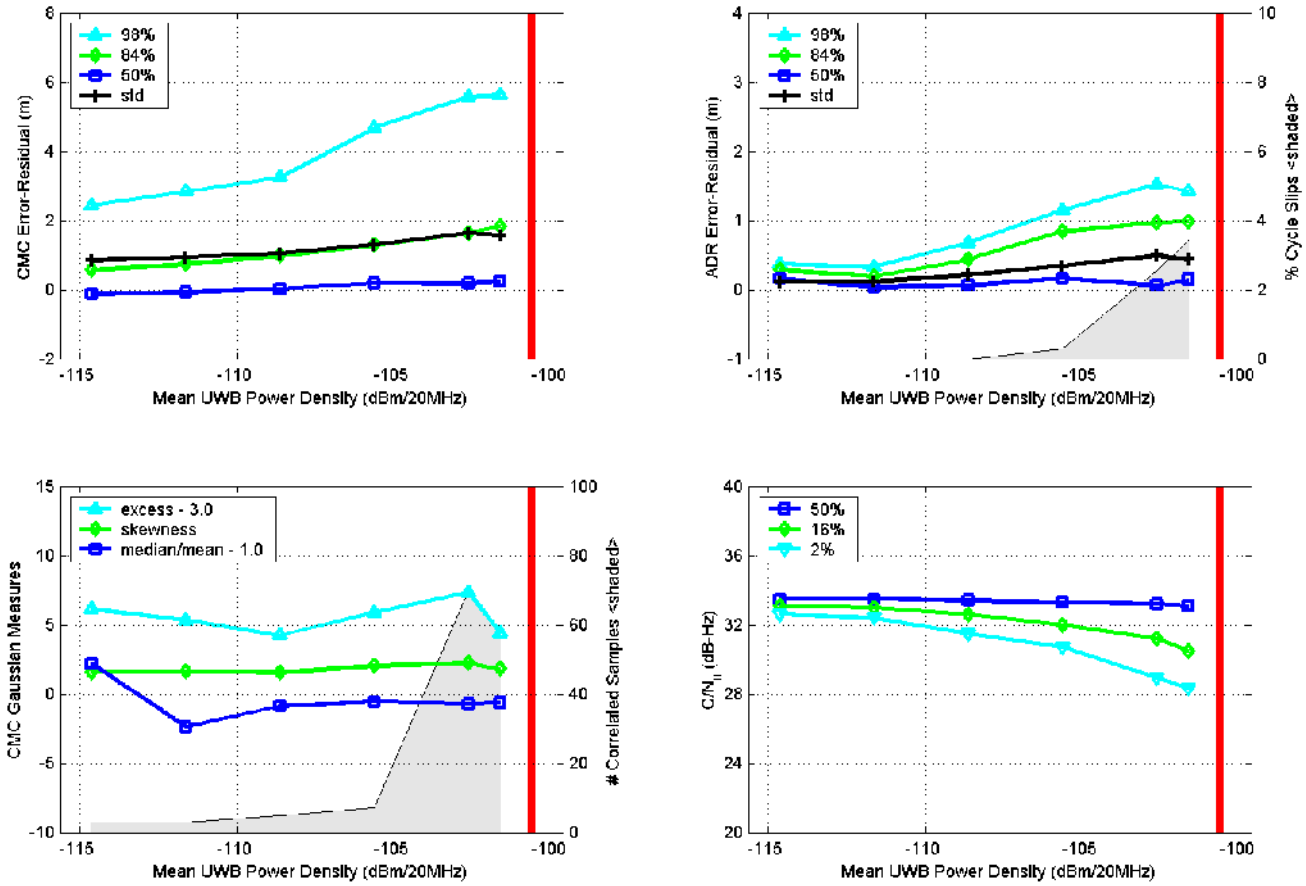

Figure F.1.6. Measured GPS parameters (Rx 1) as a function of 1-MHz PRF, UPS, non-gated UWB interference.

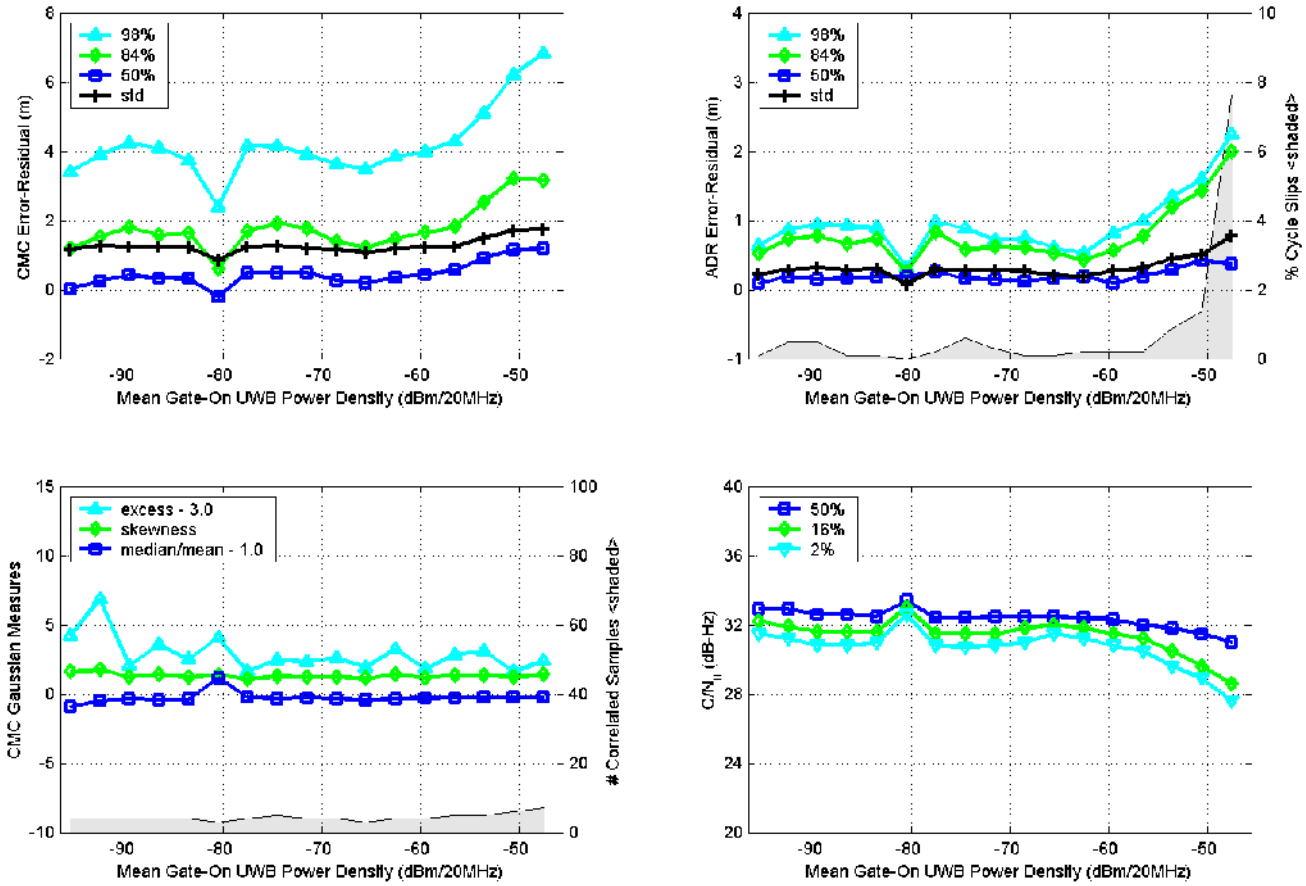

Figure F.1.7. Measured GPS parameters (Rx 1) as a function of 1-MHz PRF, UPS, gated (20% duty cycle) UWB interference.

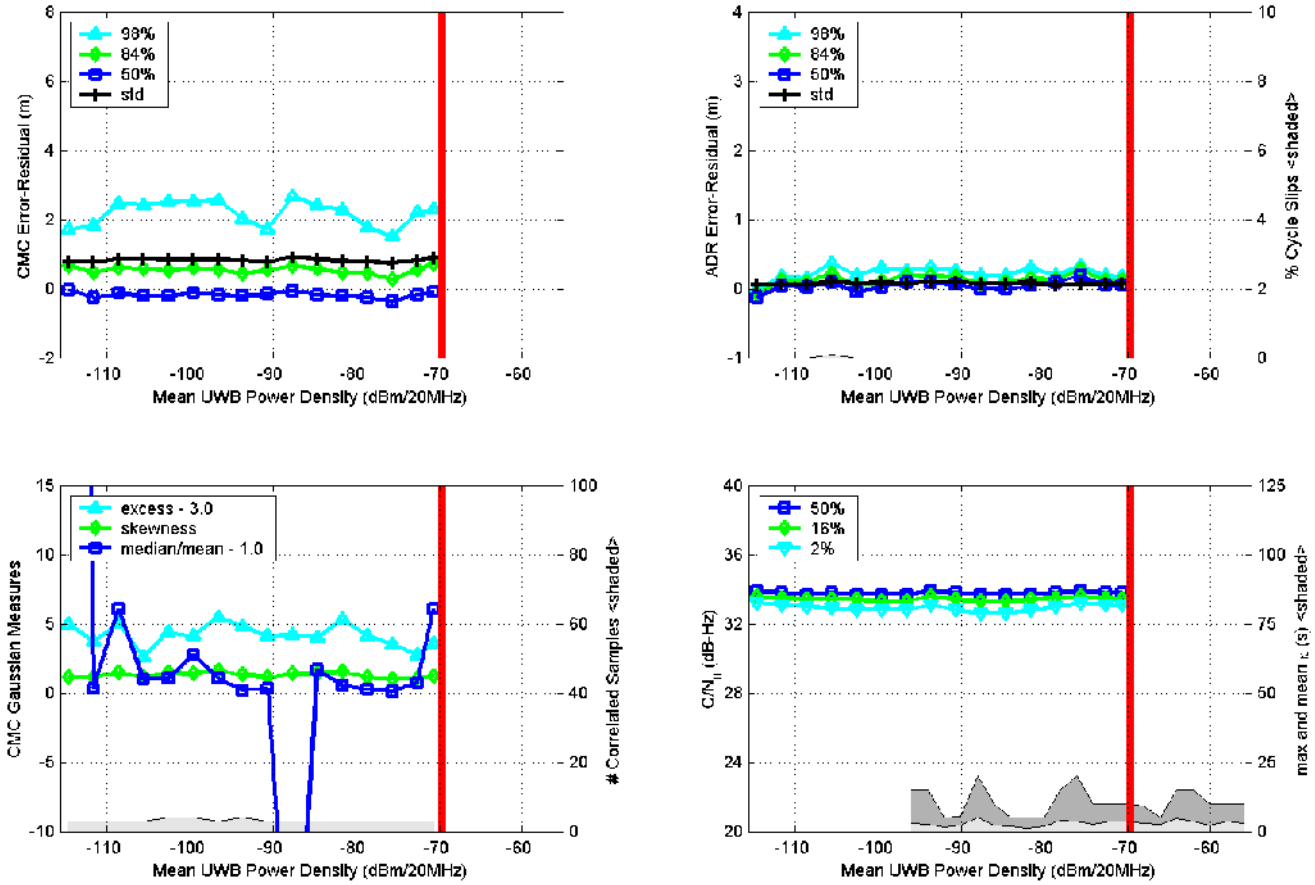

Figure F.1.8. Measured GPS parameters (Rx 1) as a function of 0.1-MHz PRF, UPS, non-gated UWB interference.

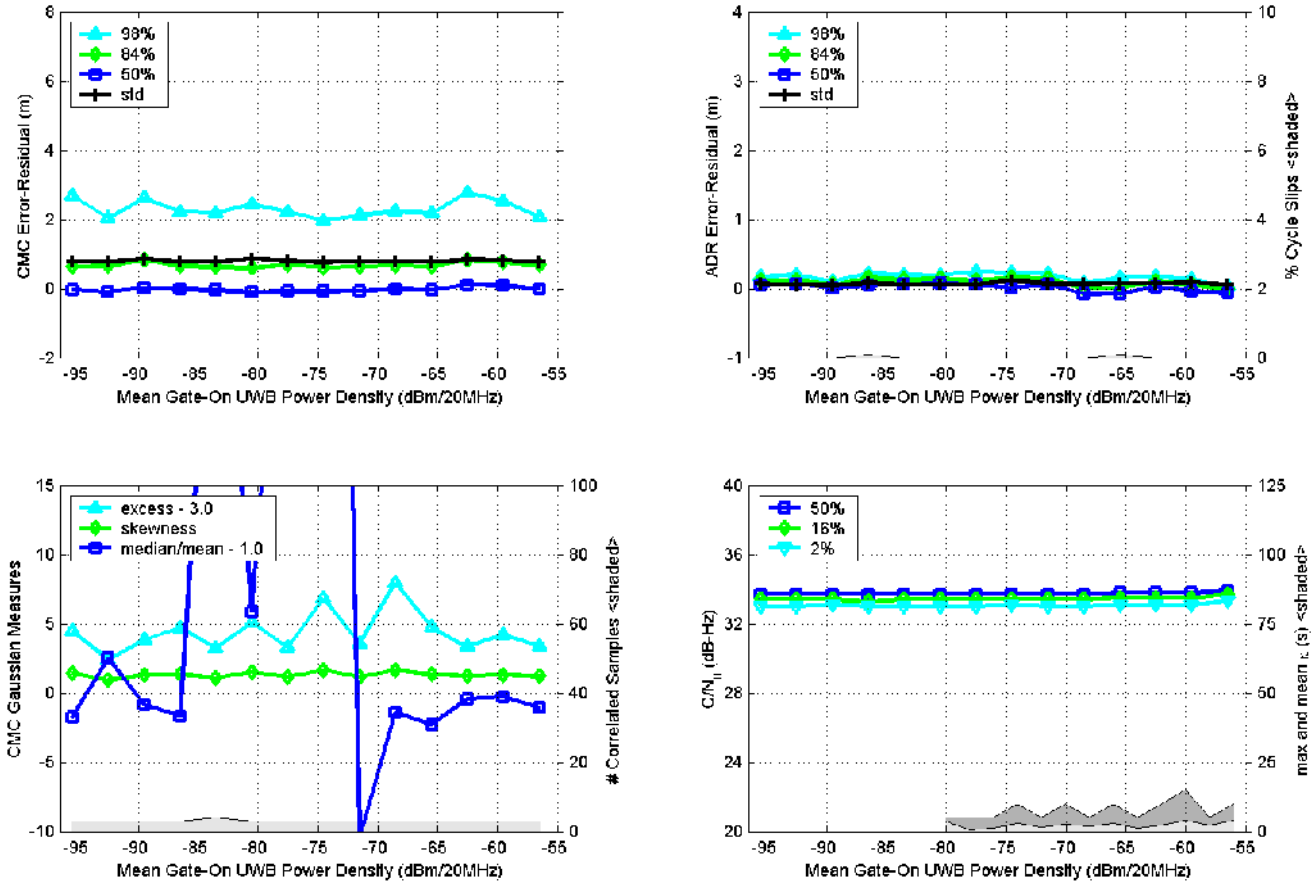

Figure F.1.9. Measured GPS parameters (Rx 1) as a function of 0.1-MHz PRF, UPS, gated (20% duty cycle) UWB interference.

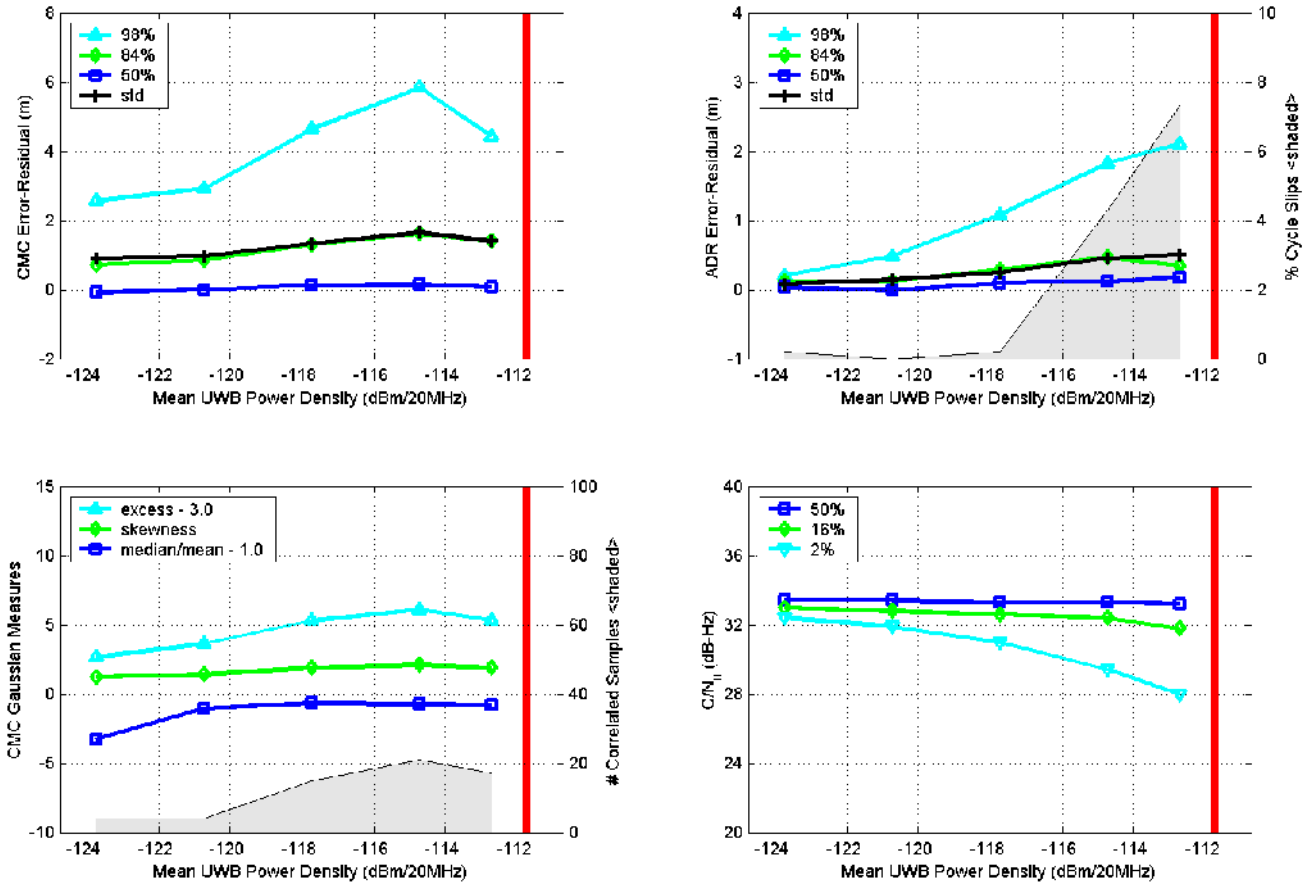

Figure F.1.10. Measured GPS parameters (Rx 1) as a function of 20-MHz PRF, OOK, non-gated UWB interference.

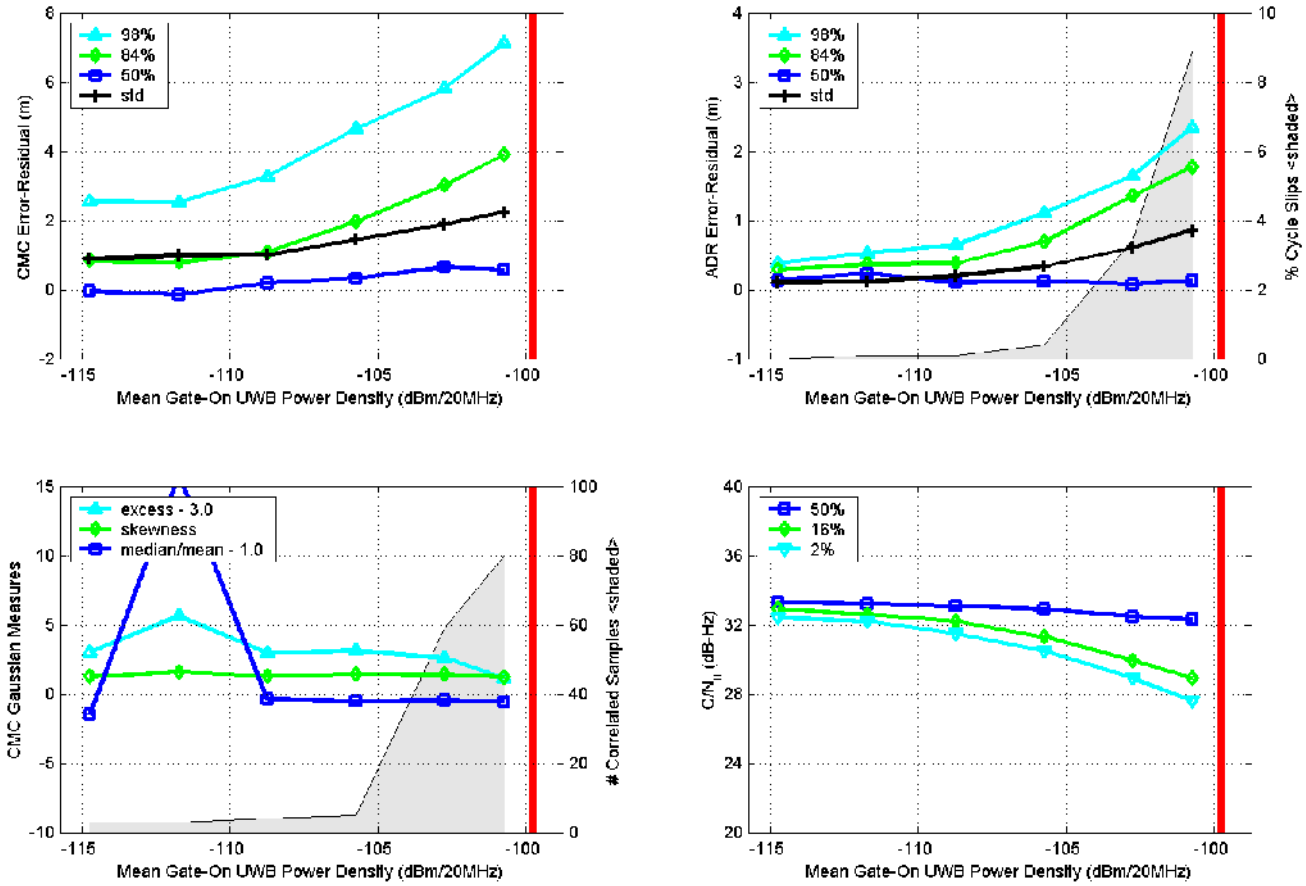

Figure F.1.11. Measured GPS parameters (Rx 1) as a function of 20-MHz PRF, OOK, gated (20% duty cycle) UWB interference.

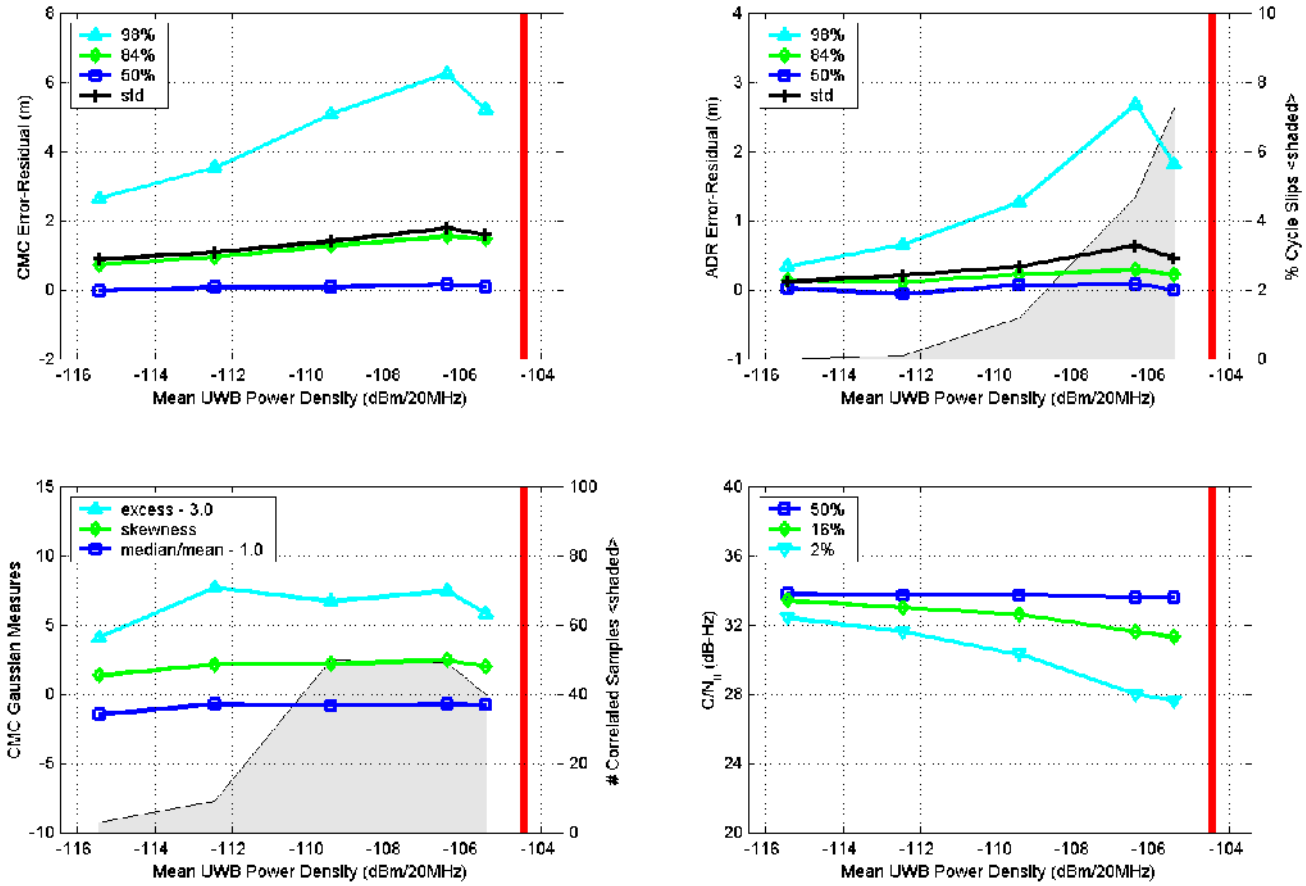

Figure F.1.12. Measured GPS parameters (Rx 1) as a function of 5-MHz PRF, OOK, non-gated UWB interference.

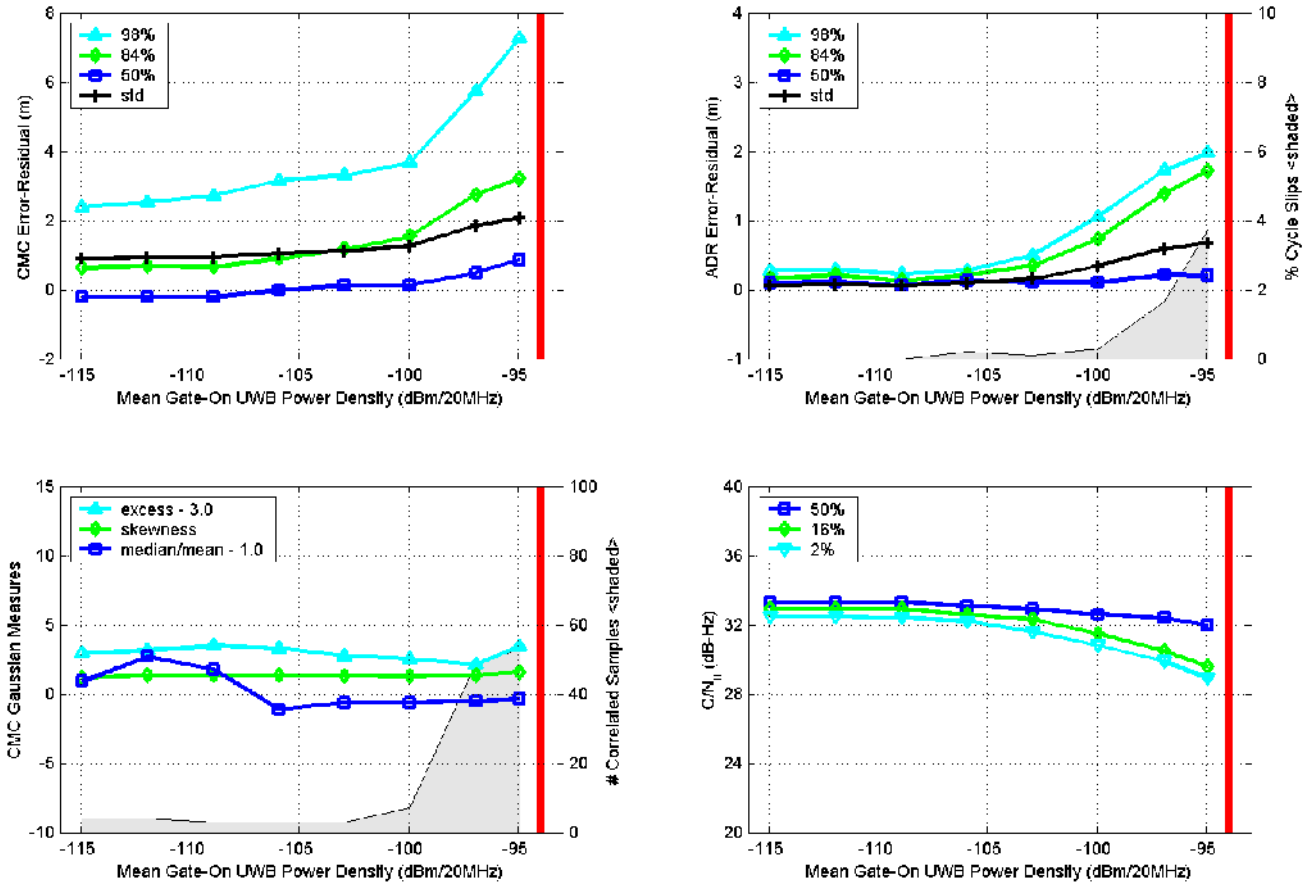

Figure F.1.13. Measured GPS parameters (Rx 1) as a function of 5-MHz PRF, OOK, gated (20% duty cycle) UWB interference.

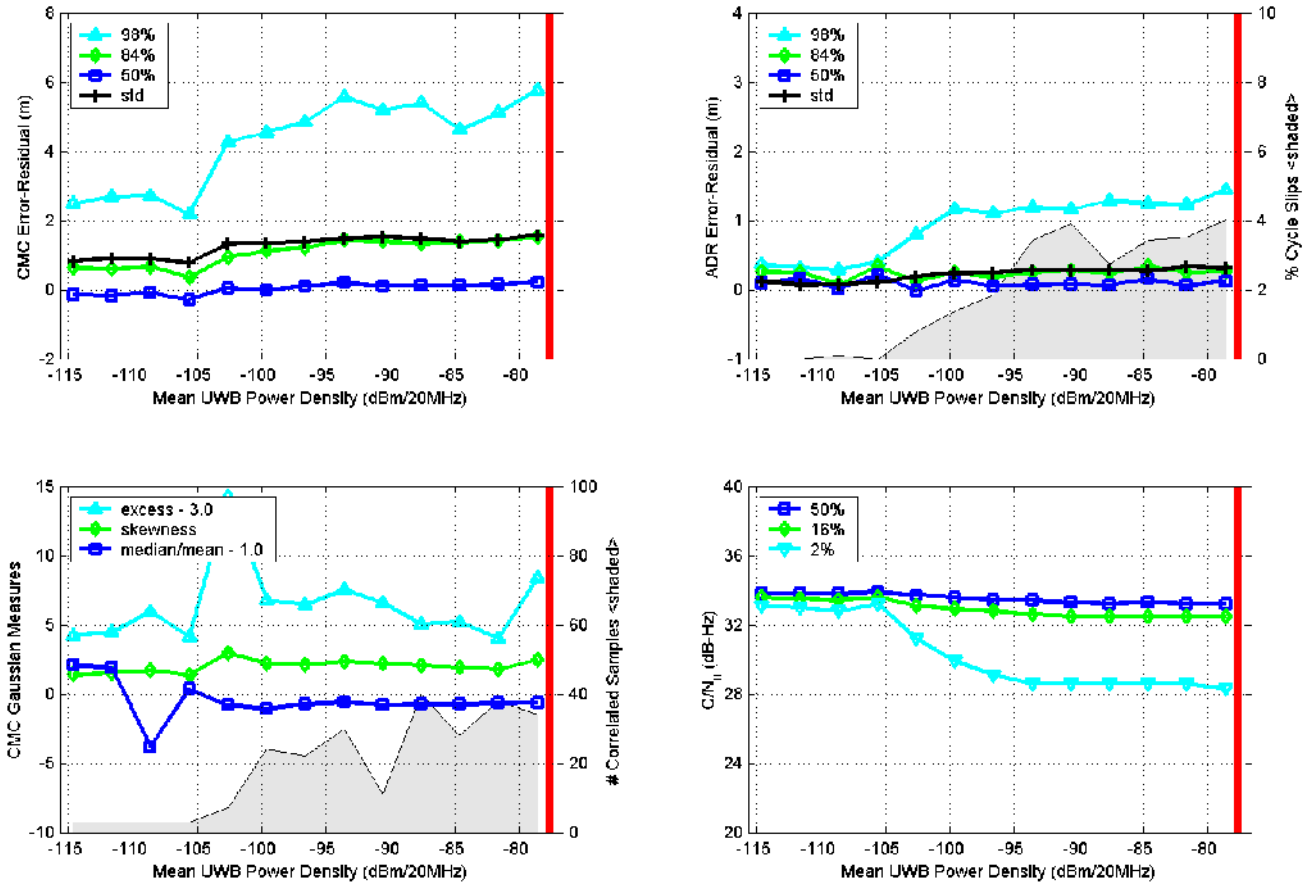

Figure F.1.14. Measured GPS parameters (Rx 1) as a function of 1-MHz PRF, OOK, non-gated UWB interference.

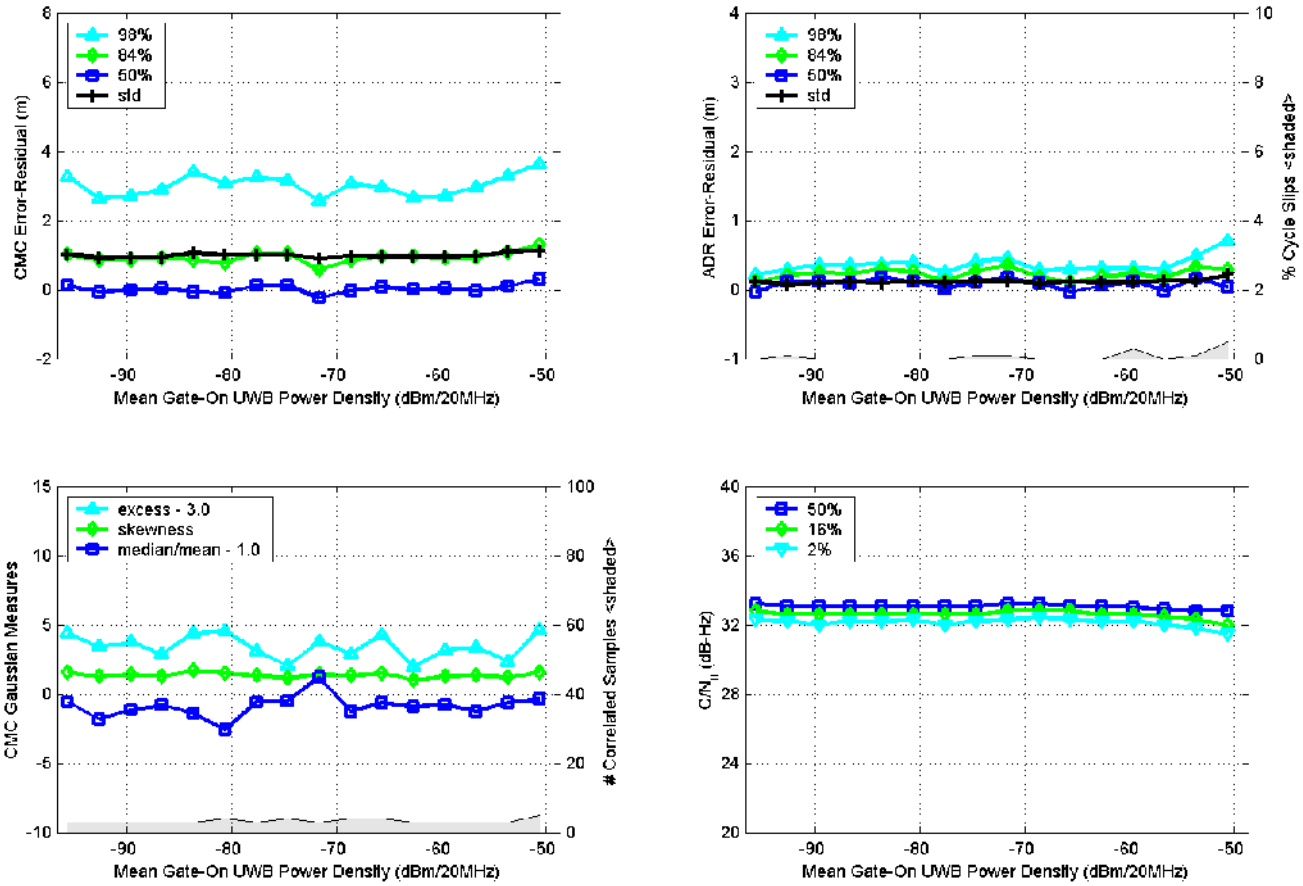

Figure F.1.15. Measured GPS parameters (Rx 1) as a function of 1-MHz PRF, OOK, gated (20% duty cycle) UWB interference.

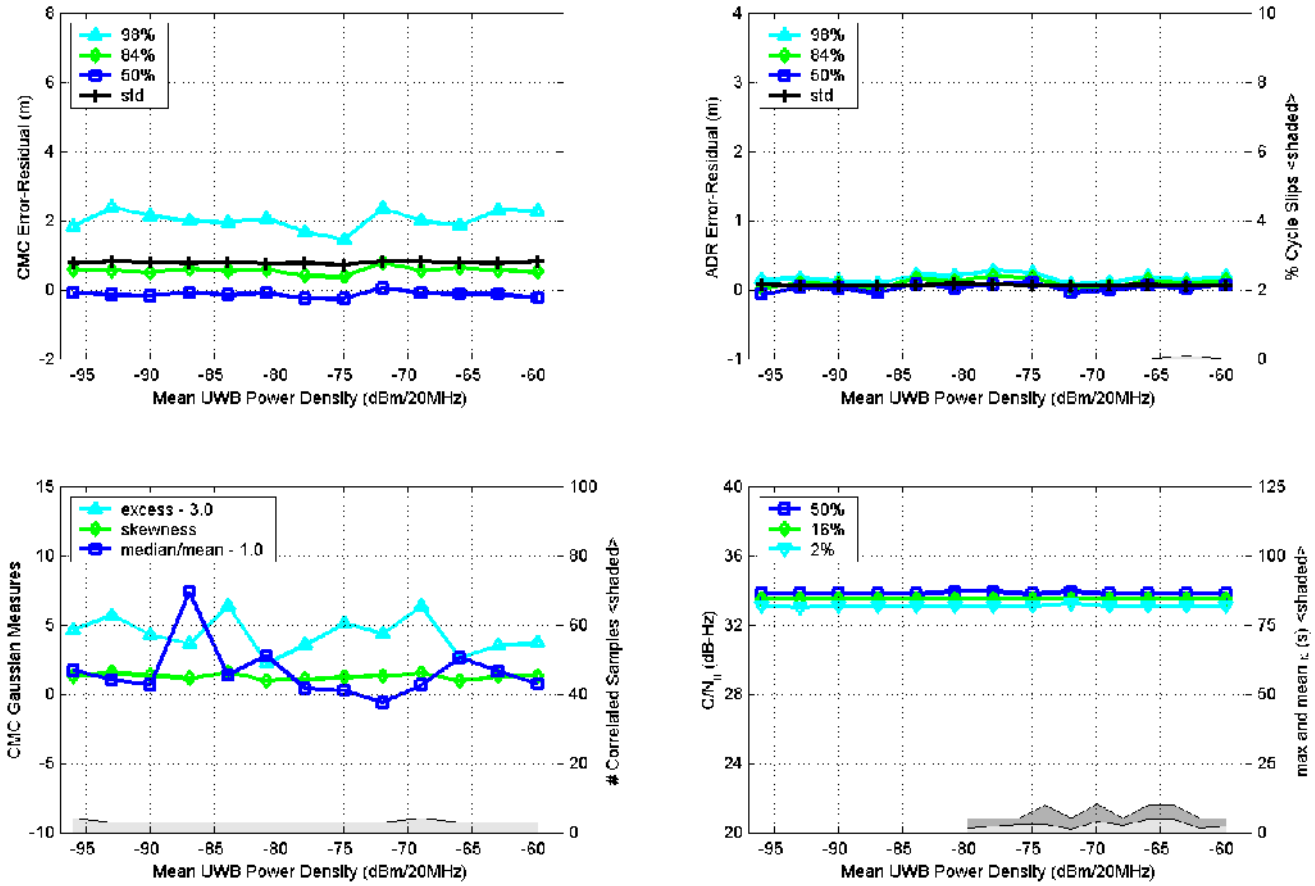

Figure F.1.16. Measured GPS parameters (Rx 1) as a function of 0.1-MHz PRF, OOK, non-gated UWB interference.

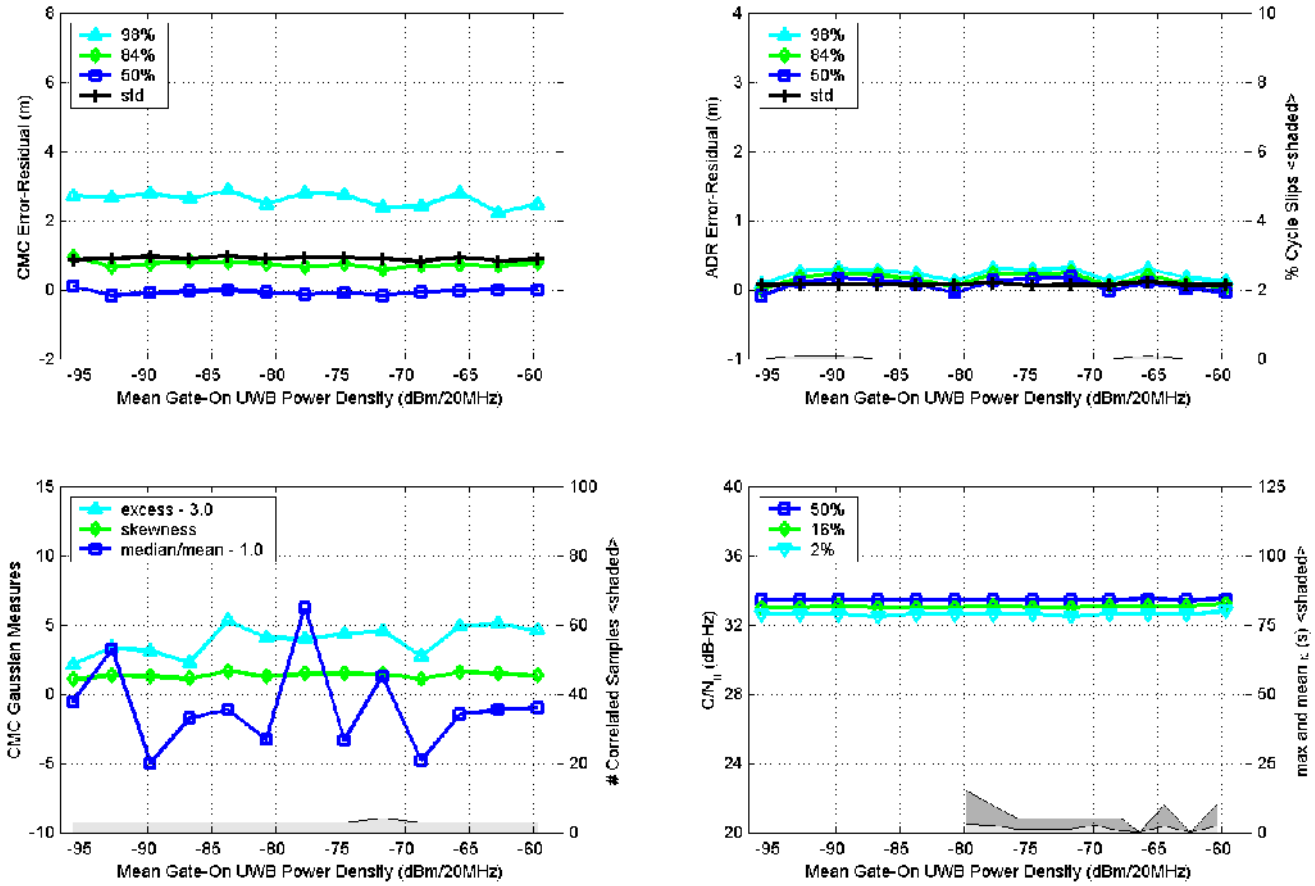

Figure F.1.17. Measured GPS parameters (Rx 1) as a function of 0.1-MHz PRF, OOK, gated (20% duty cycle) UWB interference.

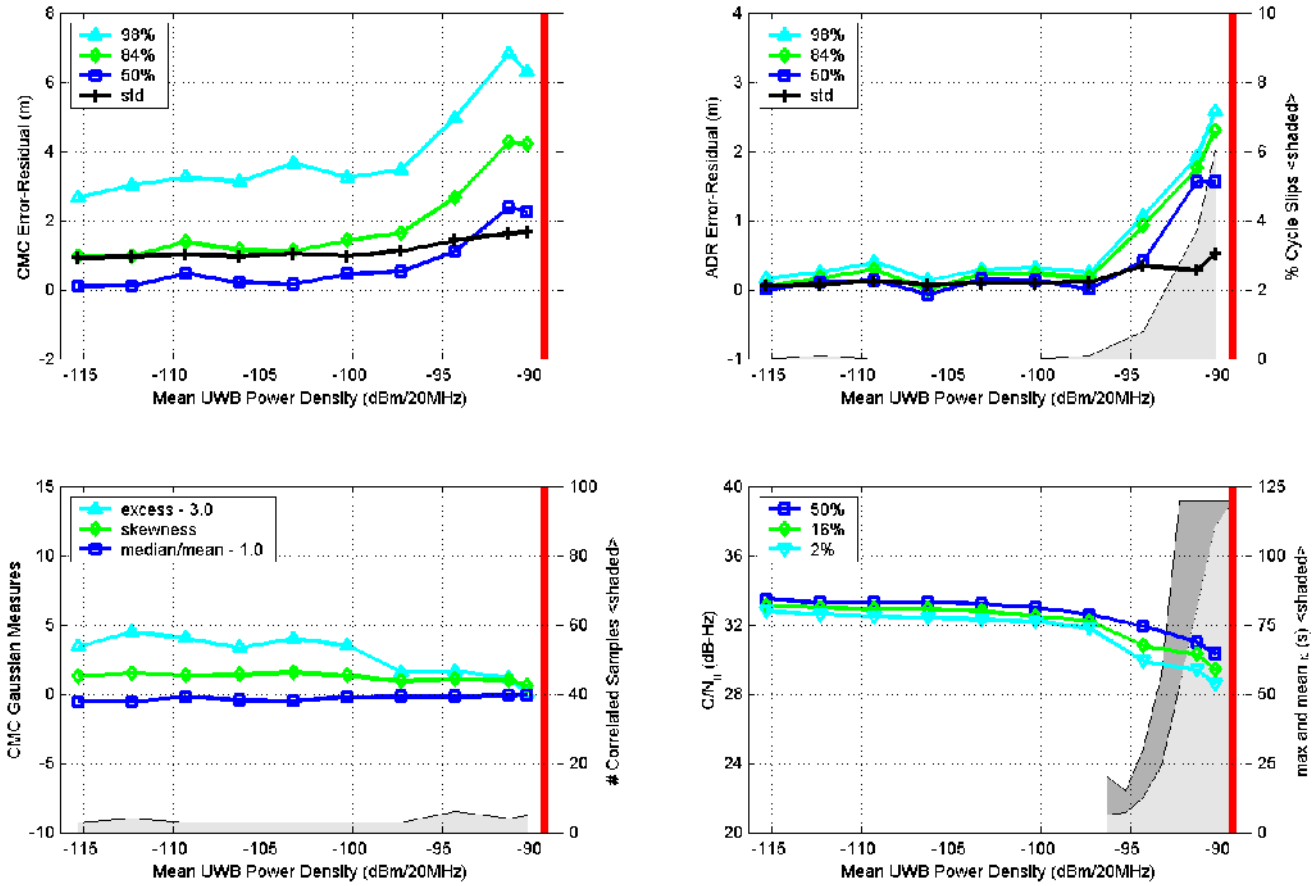

Figure F.1.18. Measured GPS parameters (Rx 1) as a function of 20-MHz PRF, 50%-ARD, non-gated UWB interference.

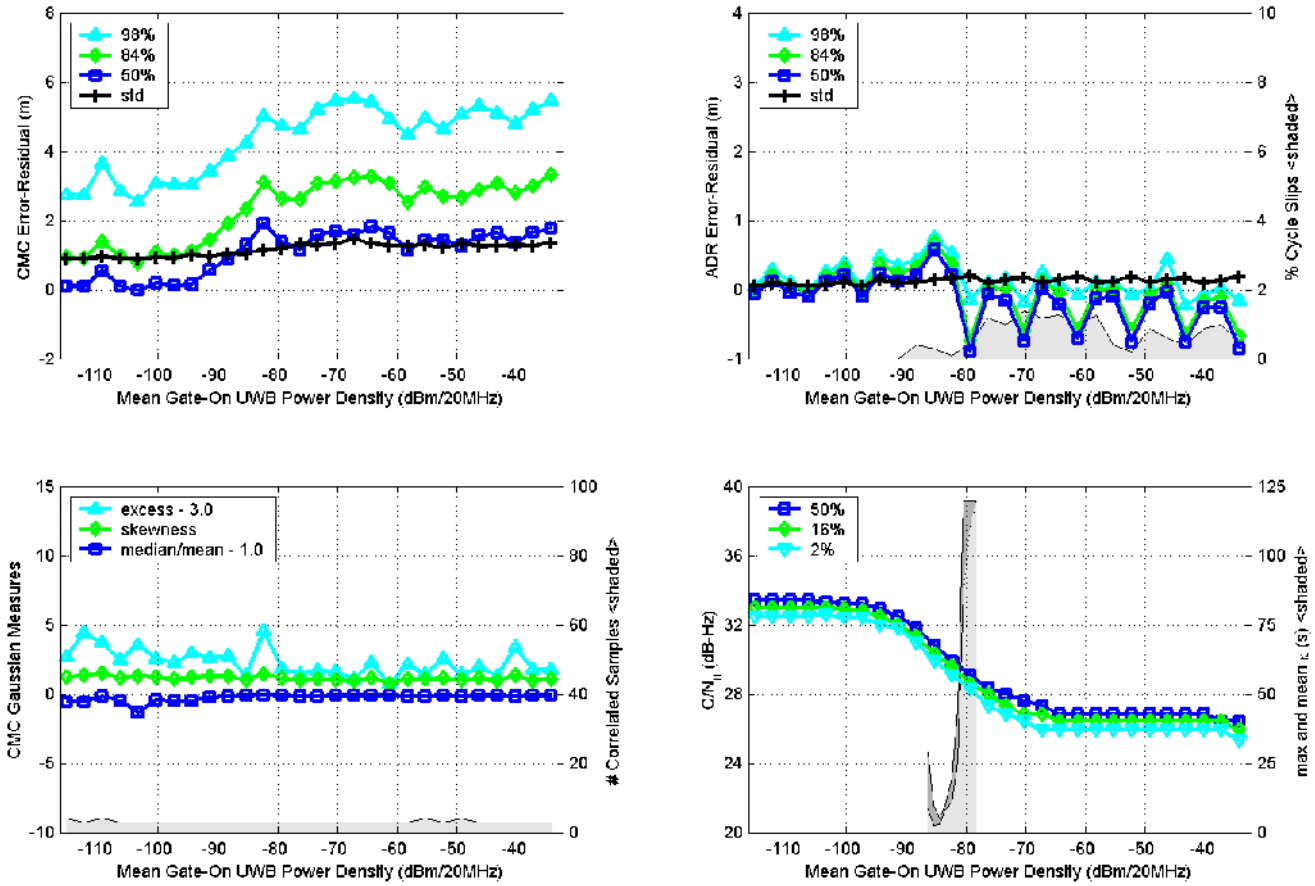

Figure F.1.19. Measured GPS parameters (Rx 1) as a function of 20-MHz PRF, 50%-ARD, gated (20% duty cycle) UWB interference.

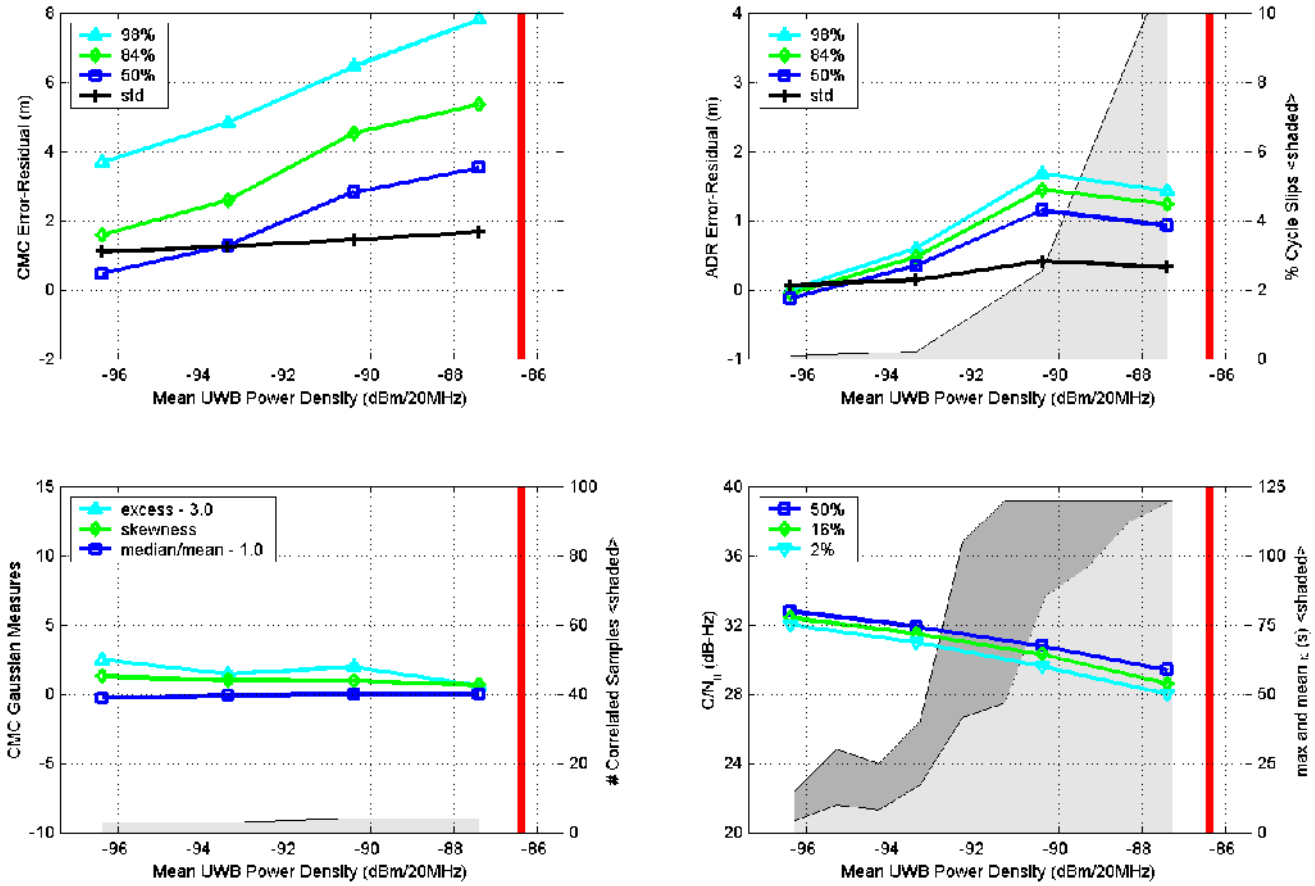

Figure F.1.20. Measured GPS parameters (Rx 1) as a function of 5-MHz PRF, 50%-ARD, non-gated UWB interference.

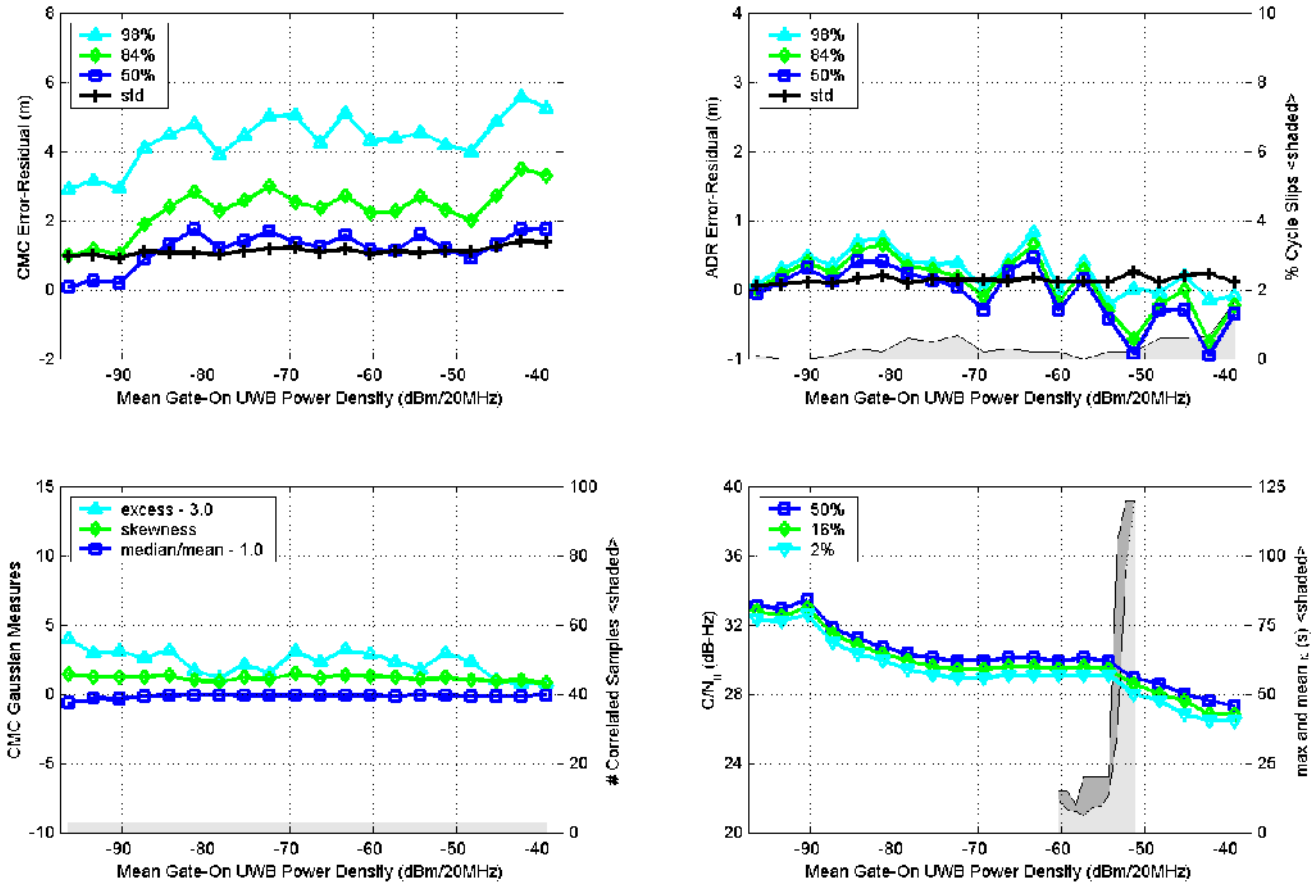

Figure F.1.21. Measured GPS parameters (Rx 1) as a function of 5-MHz PRF, 50%-ARD, gated (20% duty cycle) UWB interference.

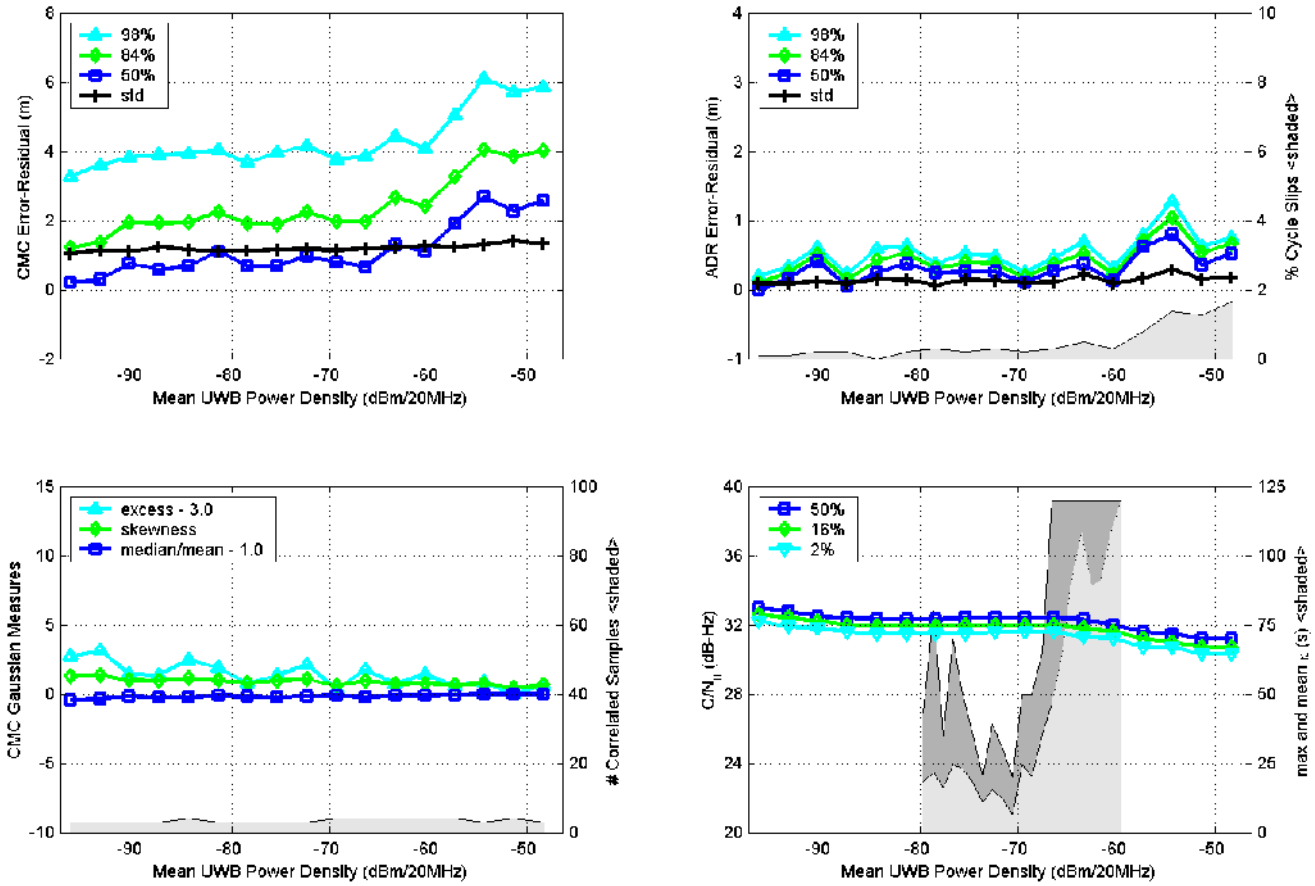

Figure F.1.22. Measured GPS parameters (Rx 1) as a function of 1-MHz PRF, 50%-ARP, non-gated UWB interference.

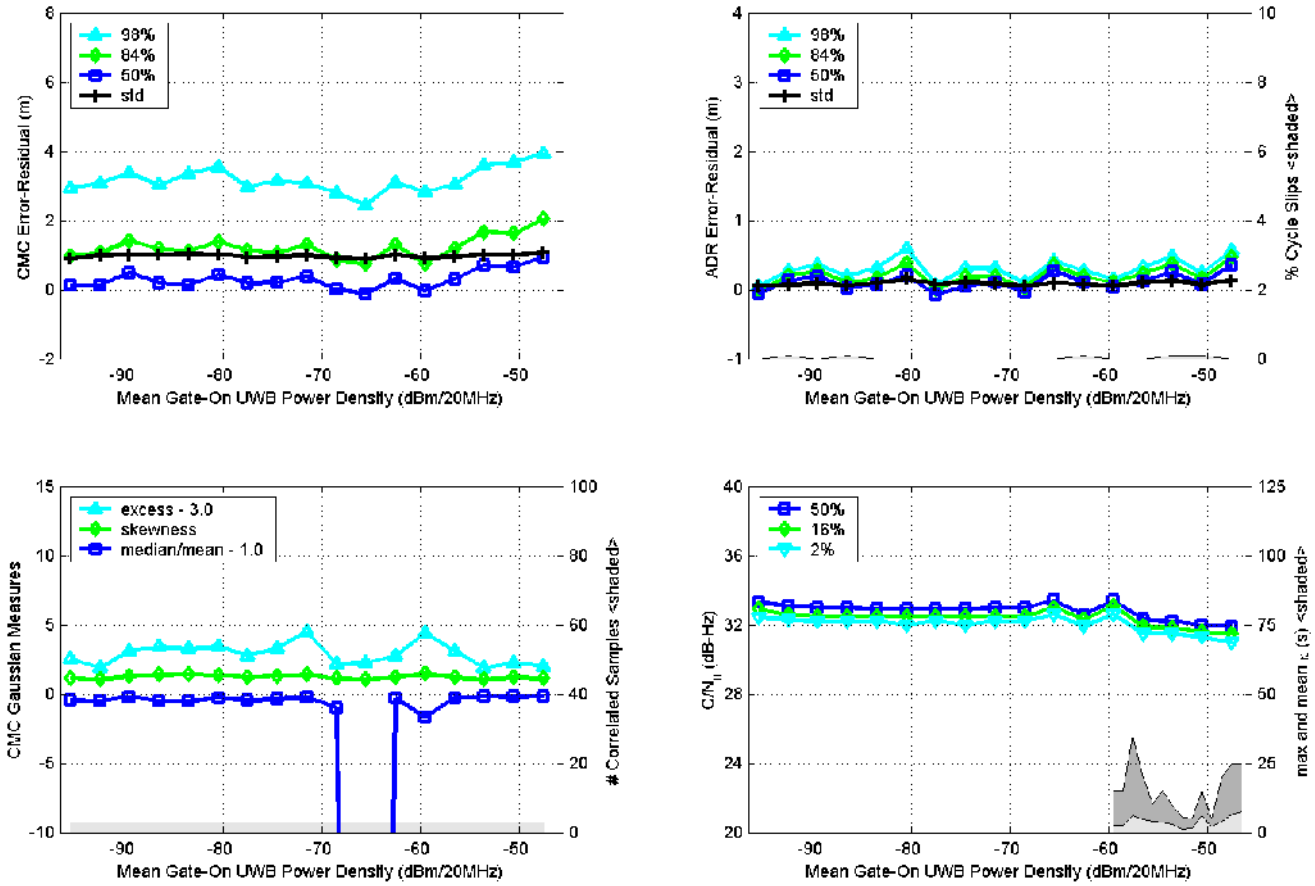

Figure F.1.23. Measured GPS parameters (Rx 1) as a function of 1-MHz PRF, 50%-ARD, gated (20% duty cycle) UWB interference.

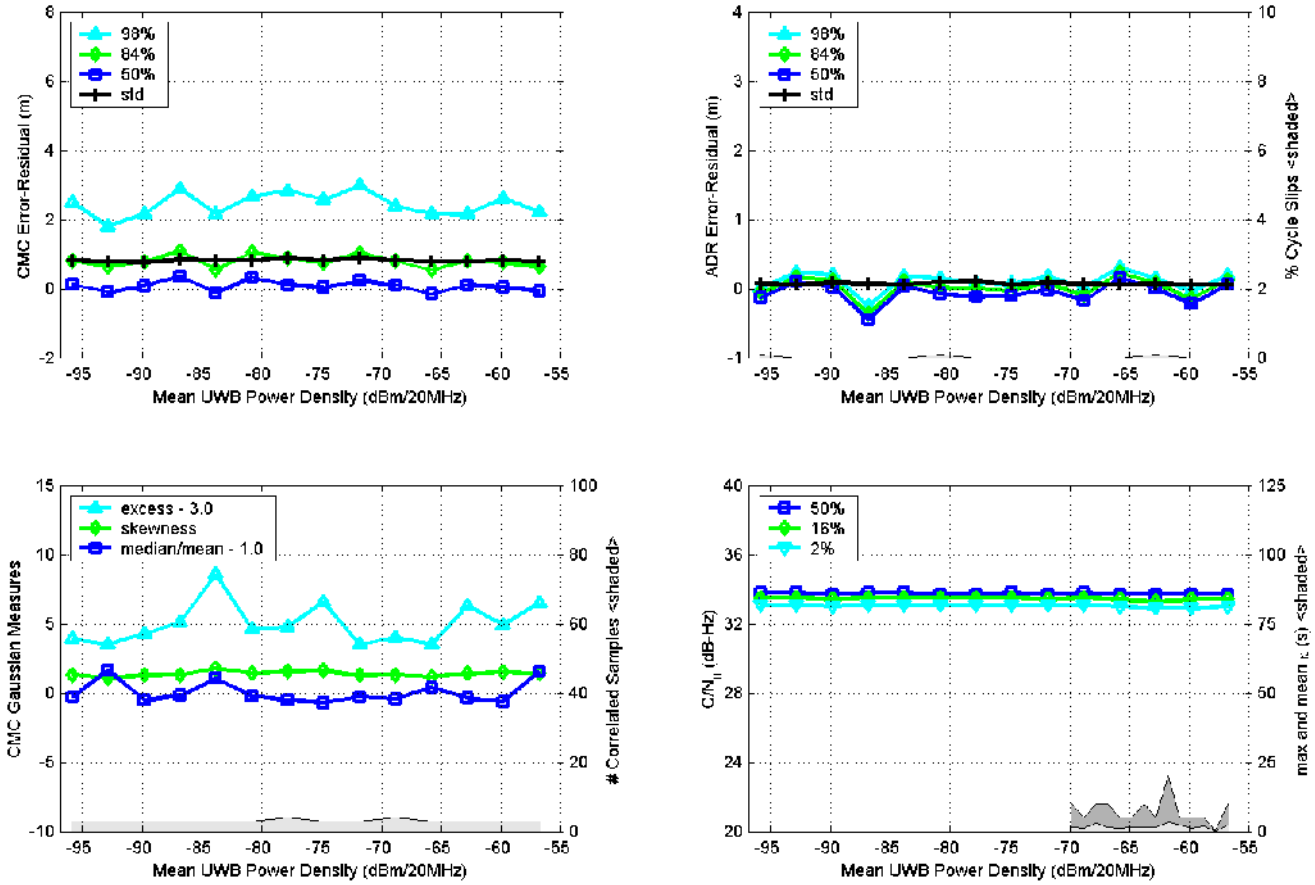

Figure F.1.24. Measured GPS parameters (Rx 1) as a function of 0.1-MHz PRF, 50%-ARD, non-gated UWB interference.

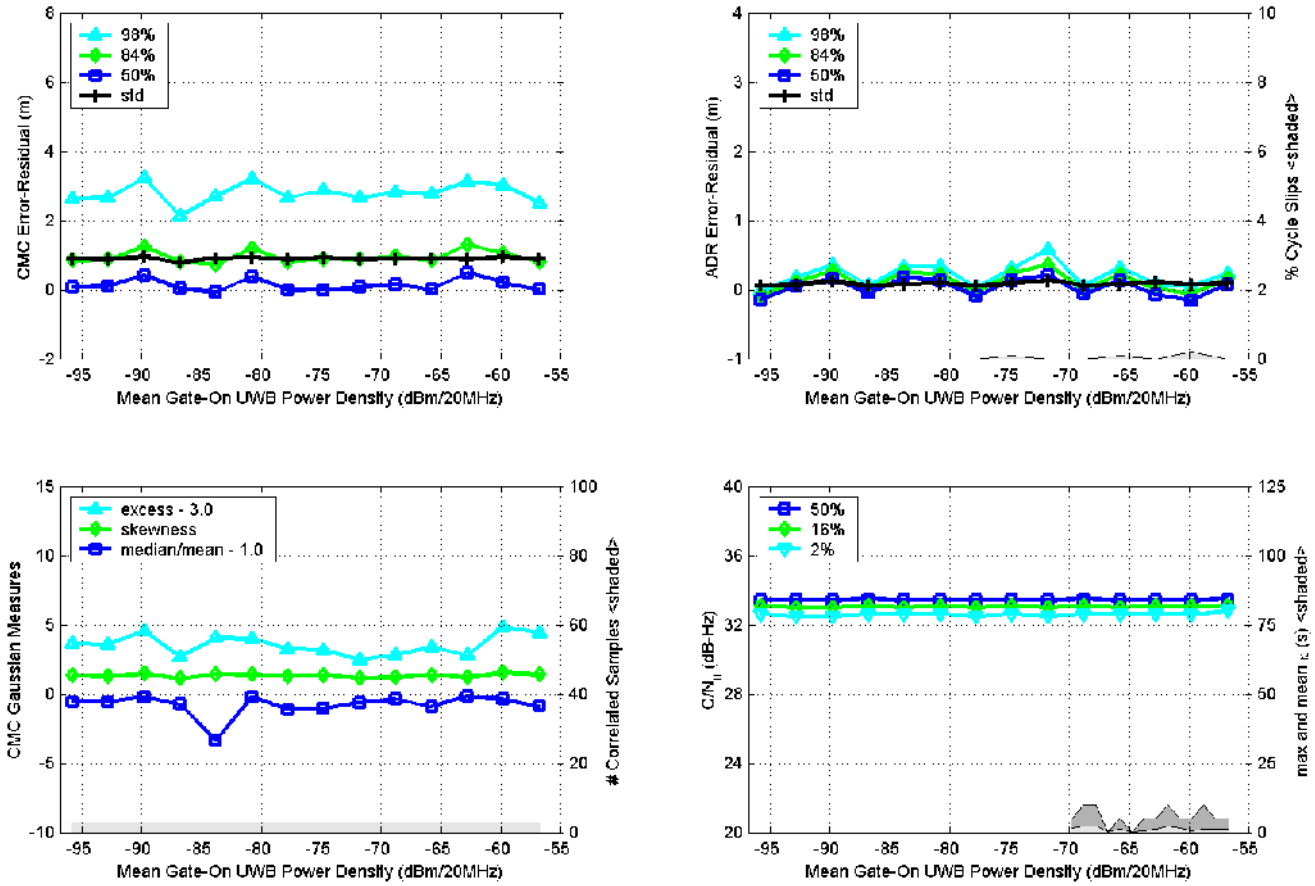

Figure F.1.25. Measured GPS parameters (Rx 1) as a function of 0.1-MHz PRF, 50%-ARD, gated (20% duty cycle) UWB interference.

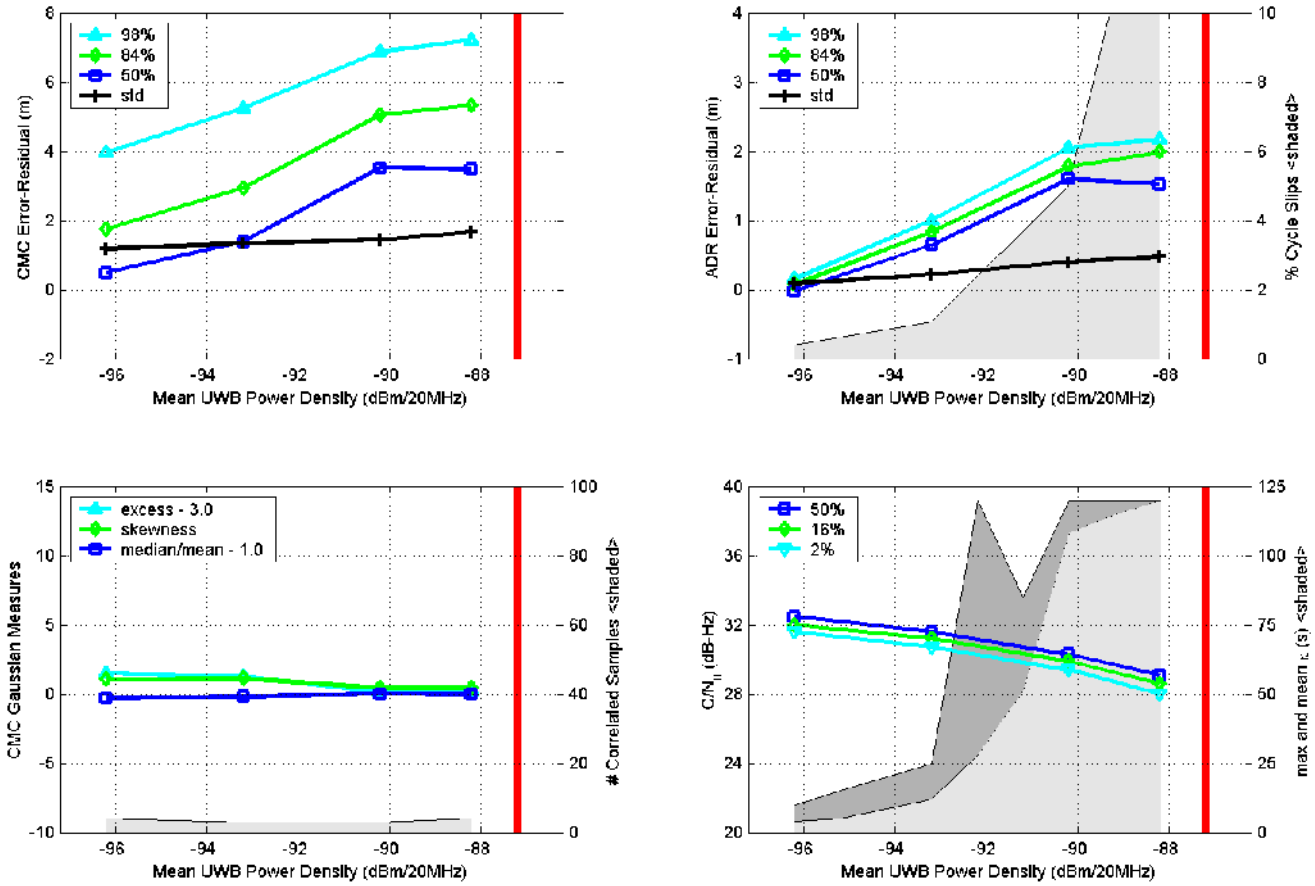

Figure F.1.26. Measured GPS parameters (Rx 1) as a function of 20-MHz PRF, 2%-RRD, non-gated UWB interference.

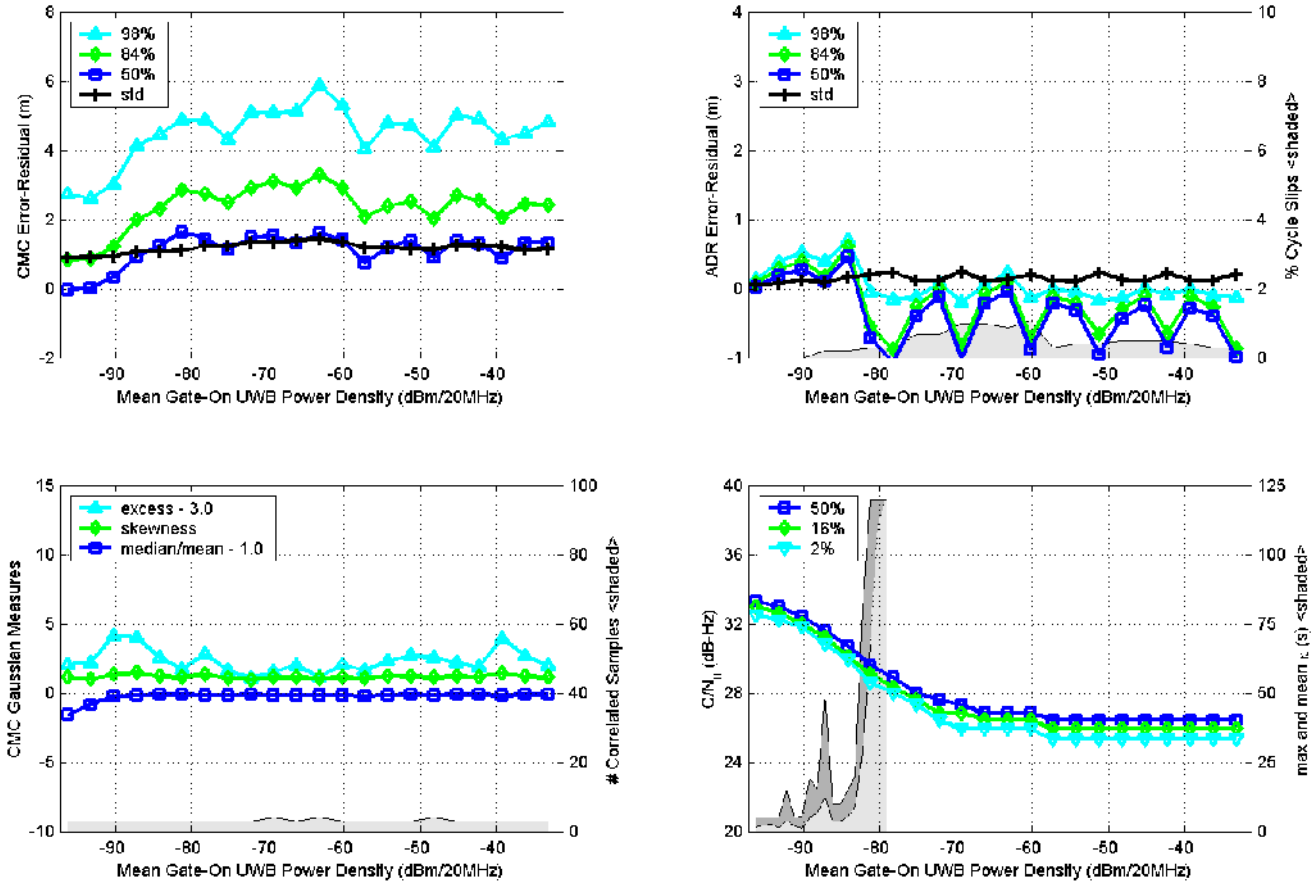

Figure F.1.27. Measured GPS parameters (Rx 1) as a function of 20-MHz PRF, 2%-RRD, gated (20% duty cycle) UWB interference.

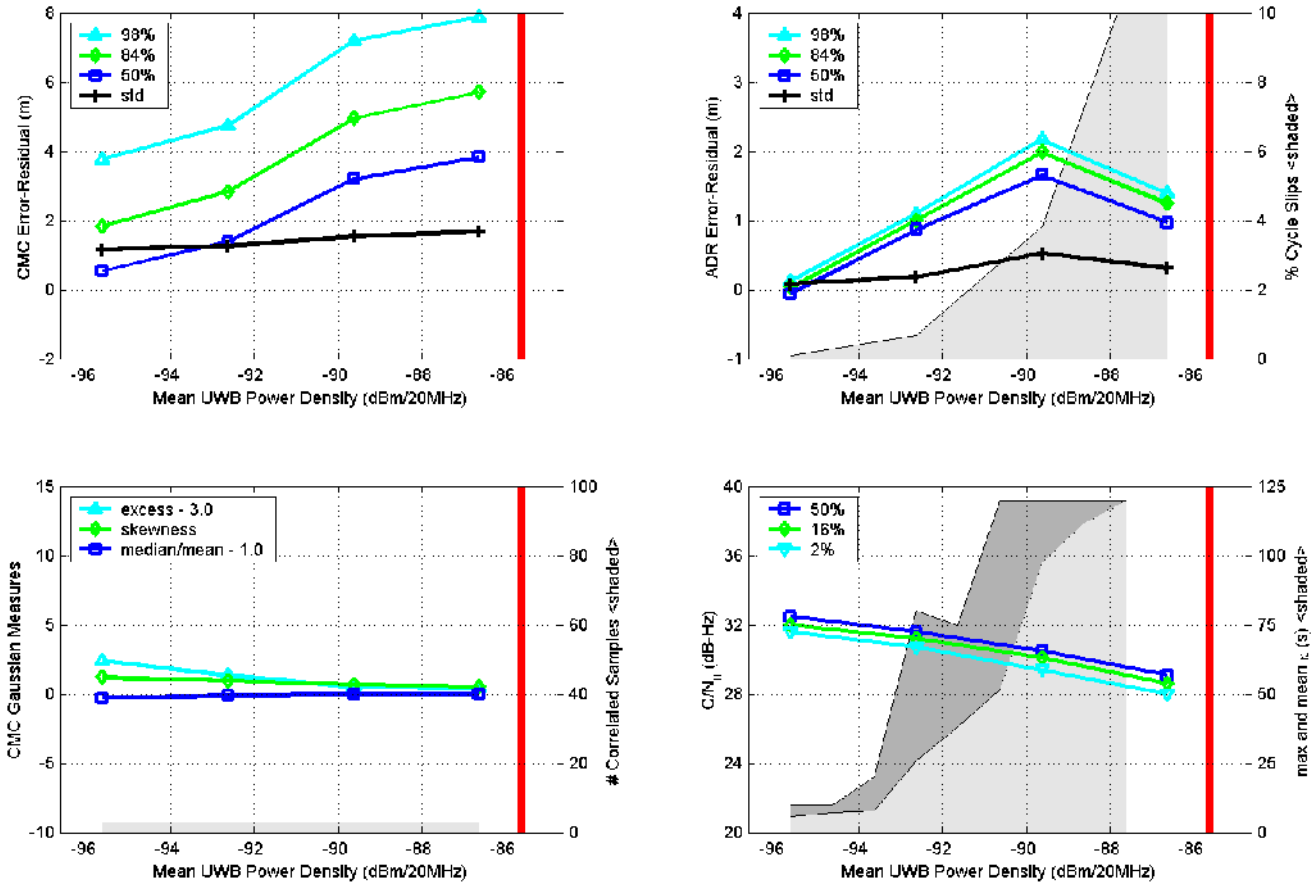

Figure F.1.28. Measured GPS parameters (Rx 1) as a function of 5-MHz PRF, 2%-RRD, non-gated UWB interference.

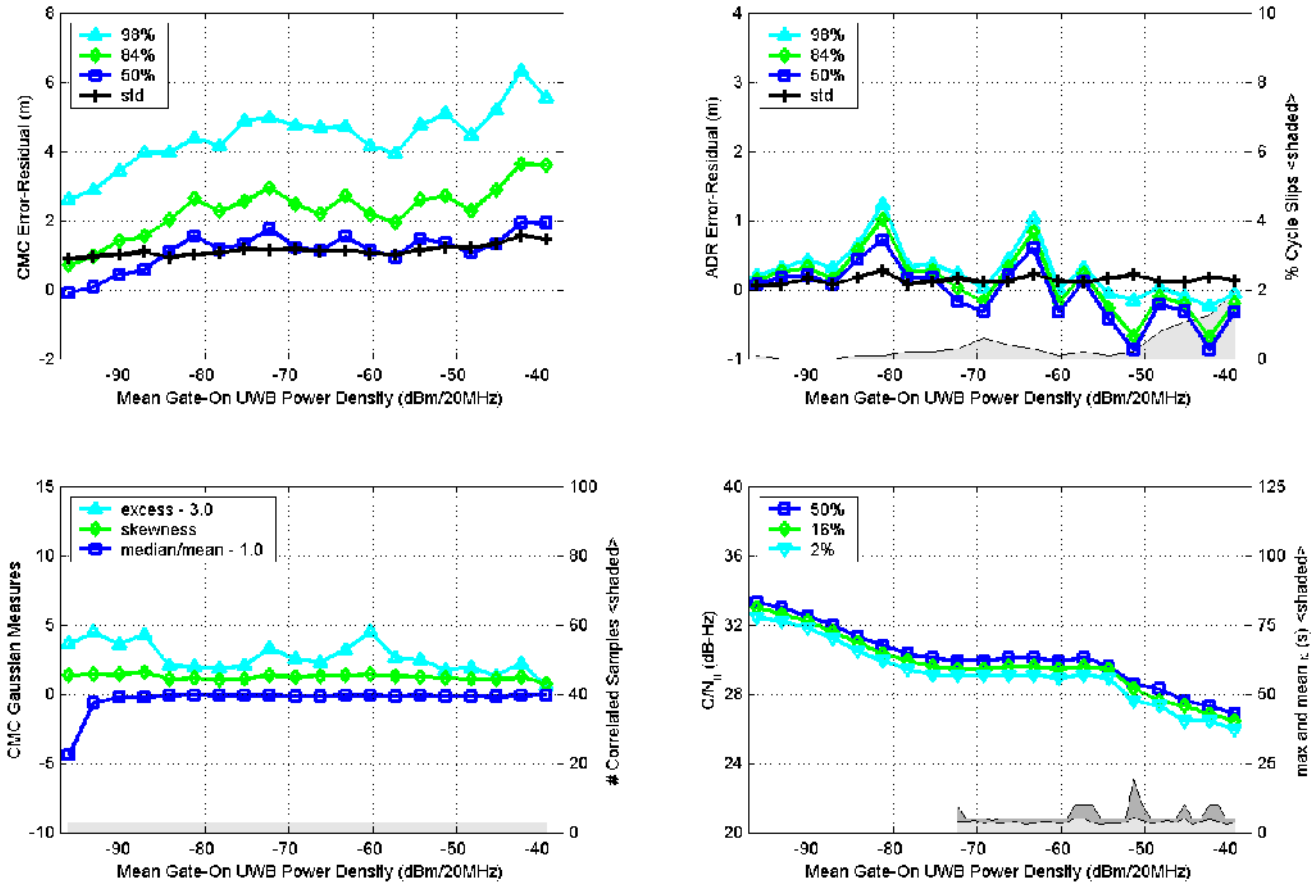

Figure F.1.29. Measured GPS parameters (Rx 1) as a function of 5-MHz PRF, 2%-RRD, gated (20% duty cycle) UWB interference.

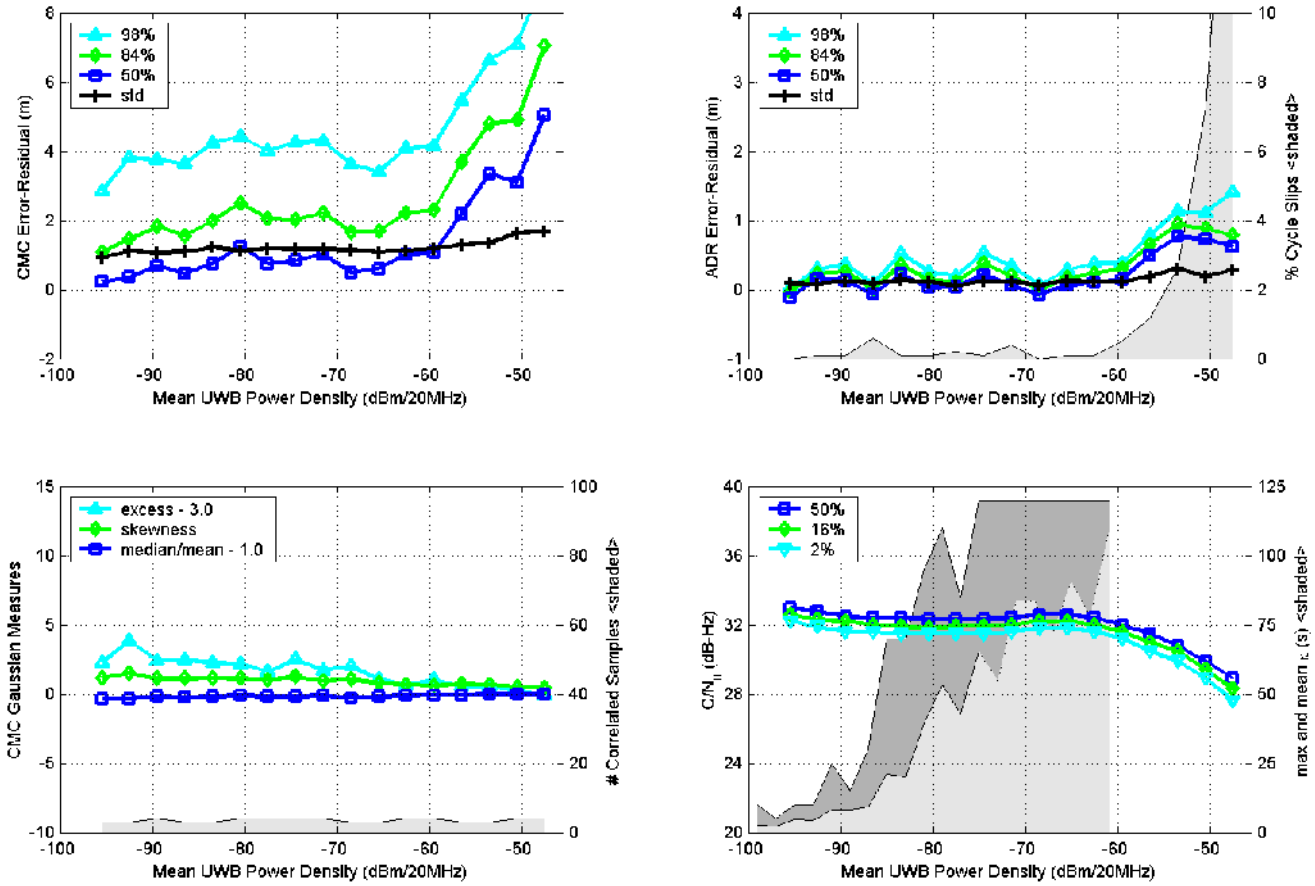

Figure F.1.30. Measured GPS parameters (Rx 1) as a function of 1-MHz PRF, 2%-RRD, non-gated UWB interference.

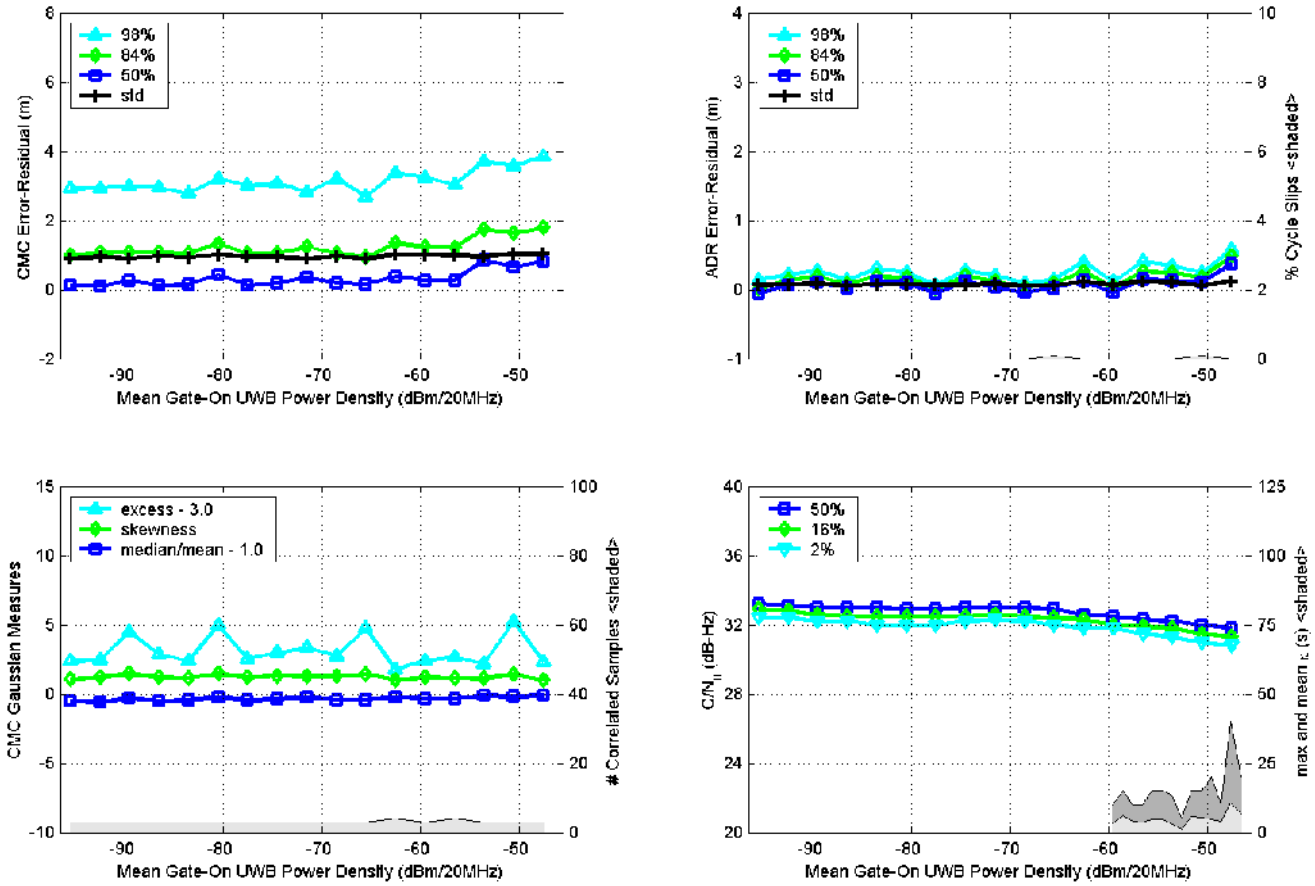

Figure F.1.31. Measured GPS parameters (Rx 1) as a function of 1-MHz PRF, 2%-RRD, gated (20% duty cycle) UWB interference.

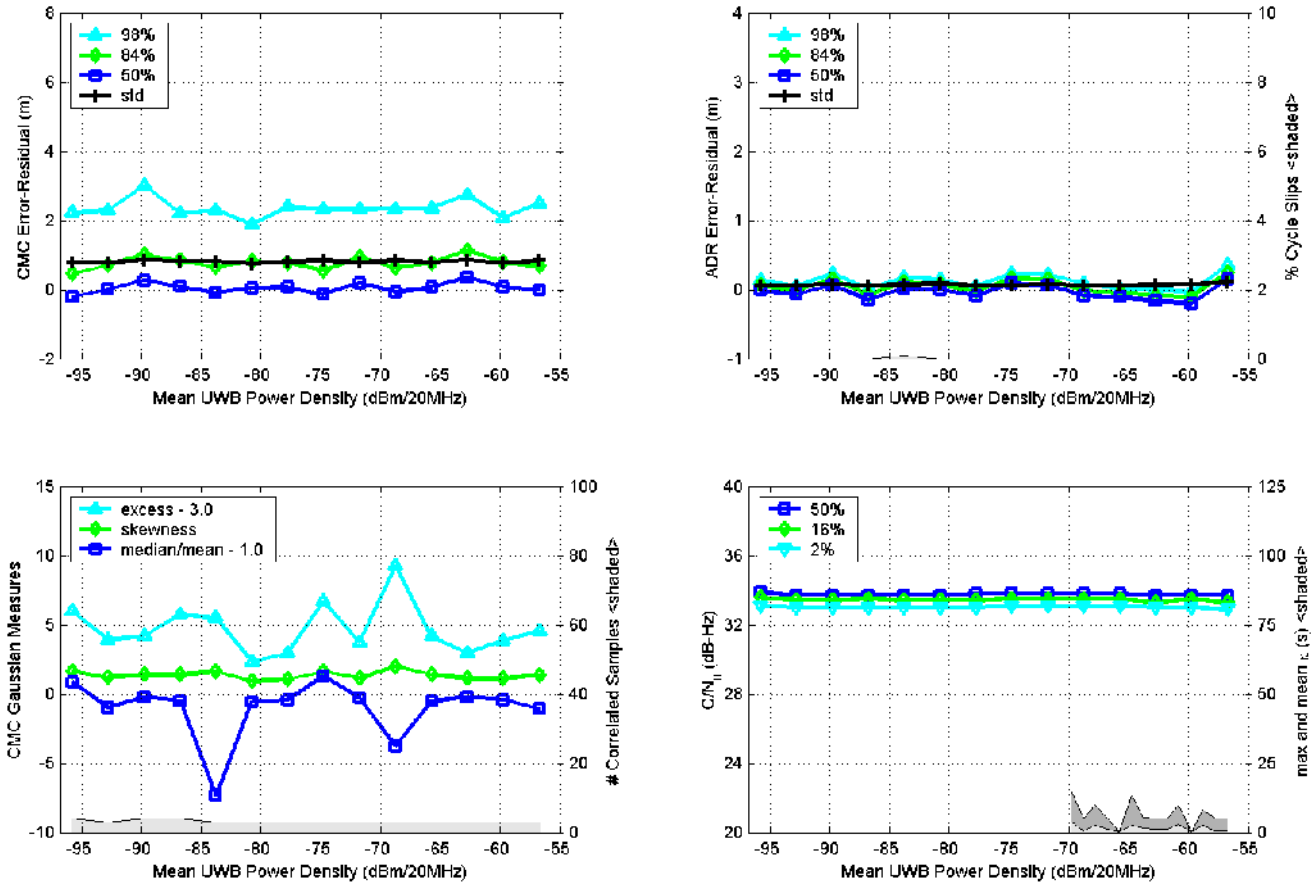

Figure F.1.32. Measured GPS parameters (Rx 1) as a function of 0.1-MHz PRF, 2%-RRD, non-gated UWB interference.

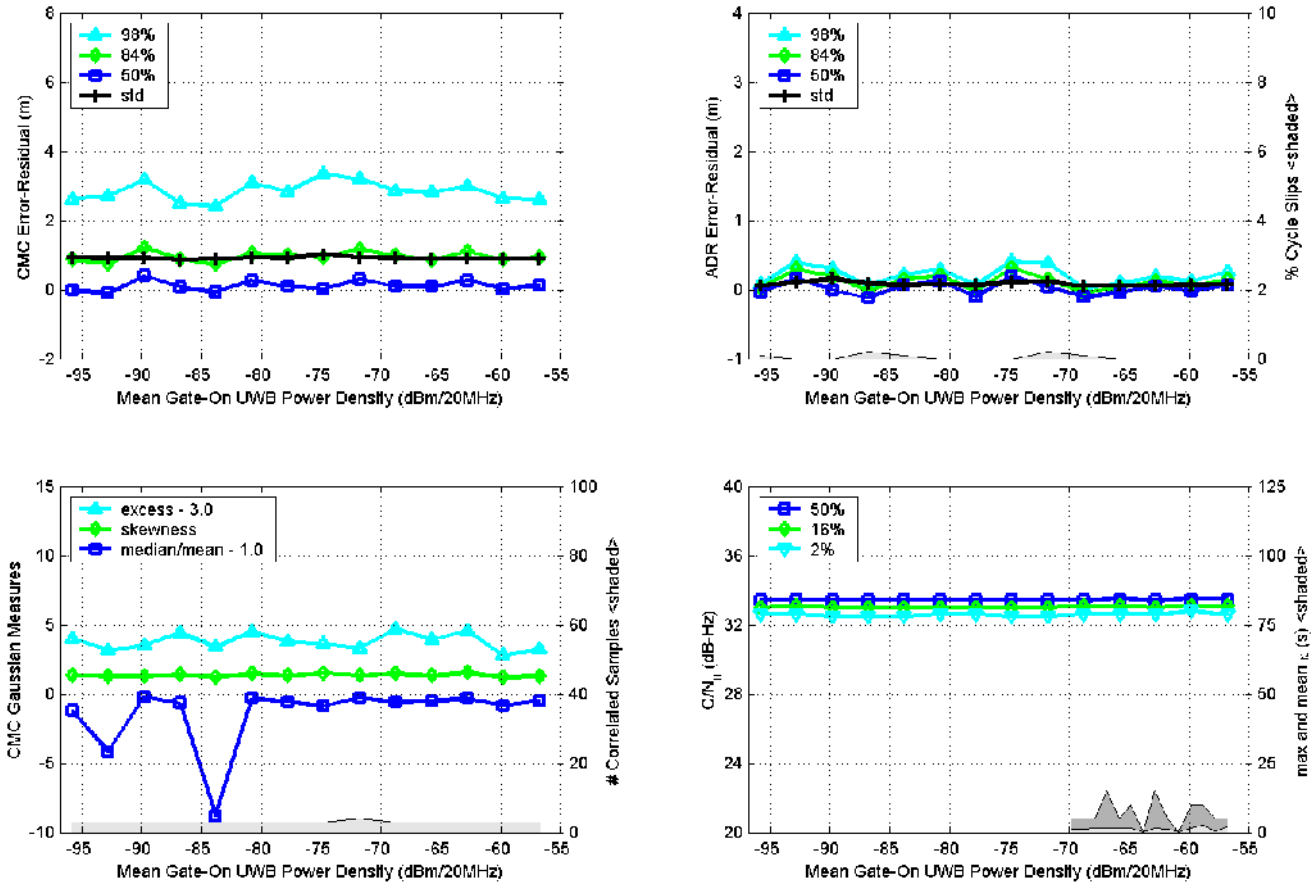

Figure F.1.33. Measured GPS parameters (Rx 1) as a function of 0.1-MHz PRF, 2%-RRD, gated (20% duty cycle) UWB interference.

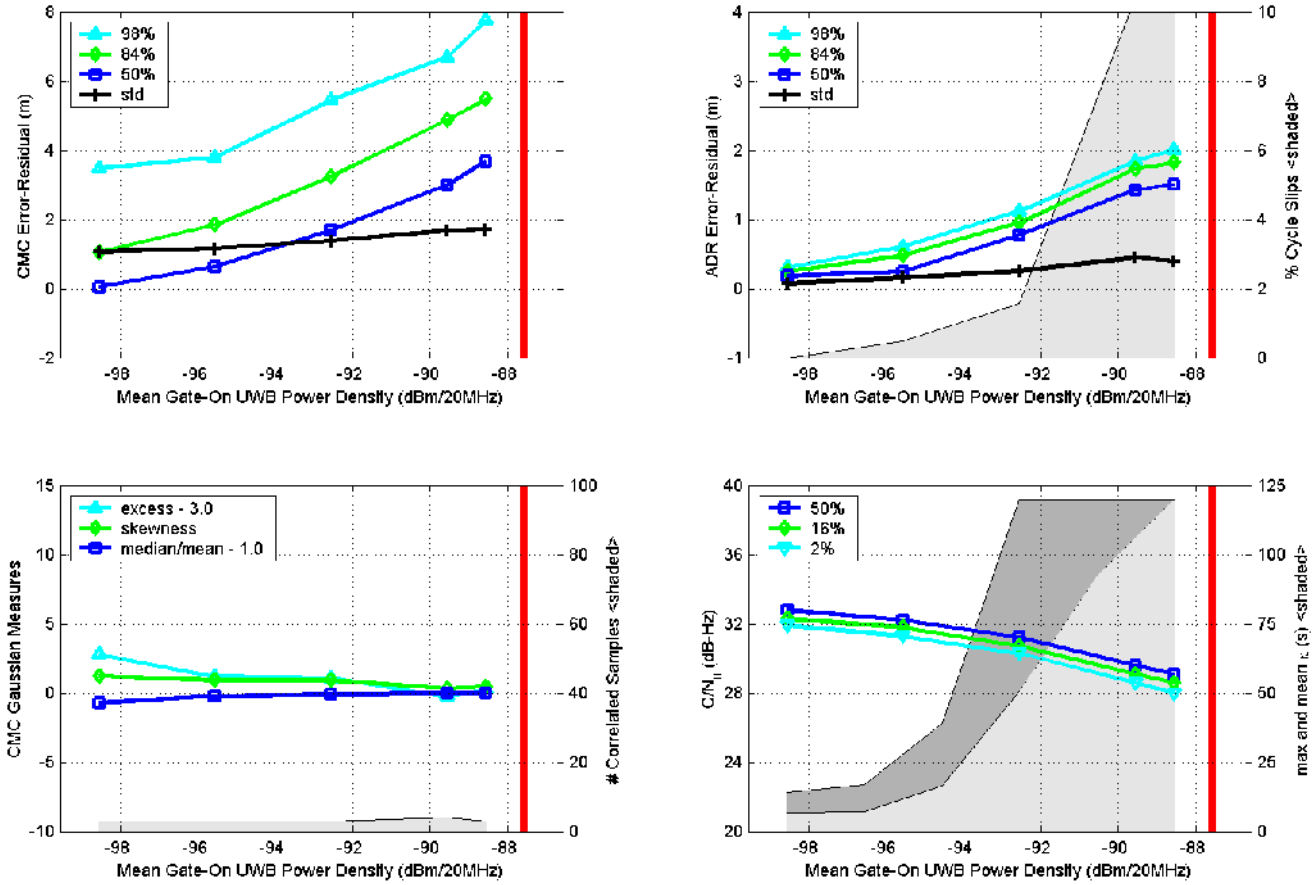

Figure F.1.34. Measured GPS parameters (Rx 1) as a function of Aggregate-1 UWB interference. Aggregate 1 is the combination of six 10-MHz PRF, 2%-RRD, non-gated UWB signals.

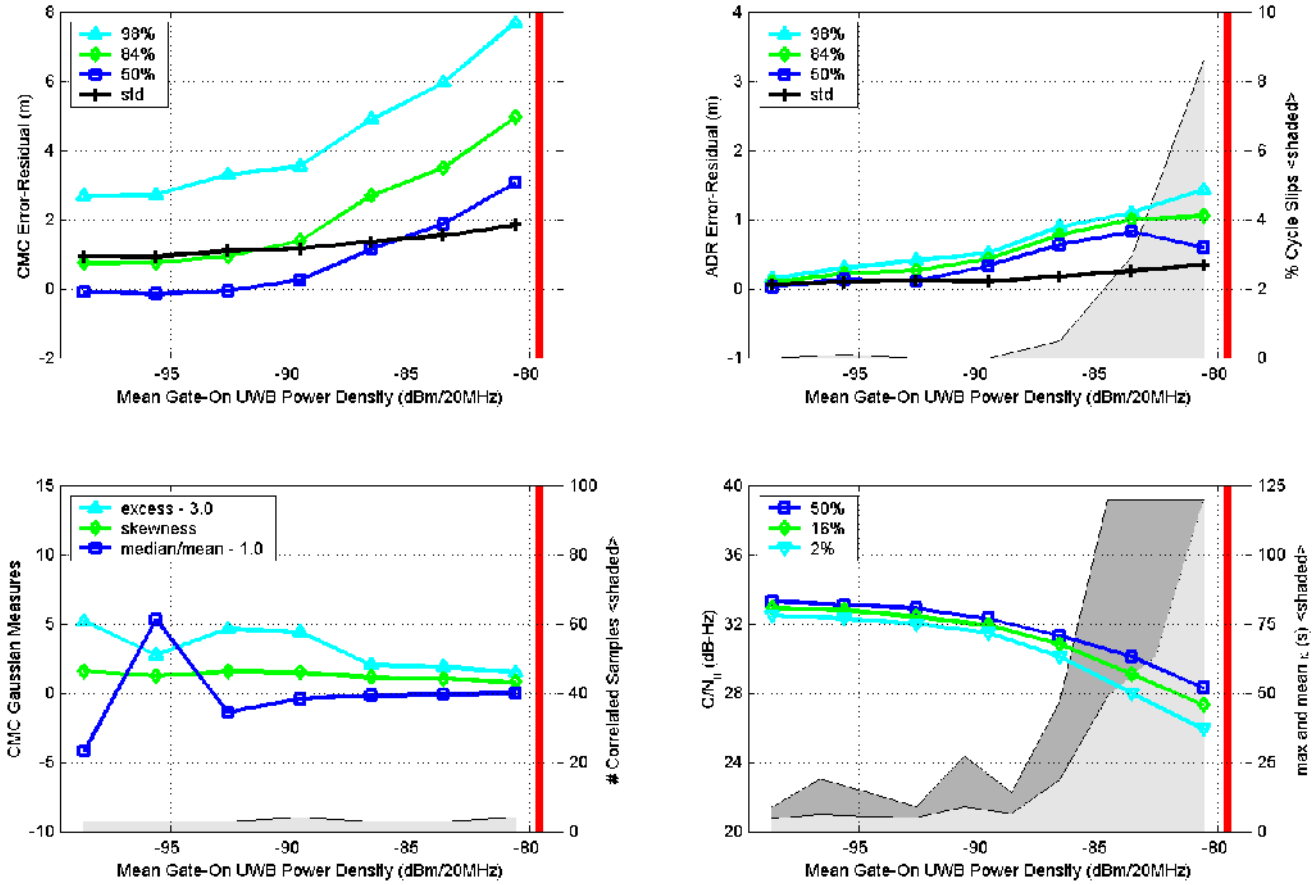

Figure F.1.35. Measured GPS parameters (Rx 1) as a function of Aggregate-2 UWB interference. Aggregate 2 is the combination of six 10-MHz PRF, 2%-RRD, gated UWB signals.

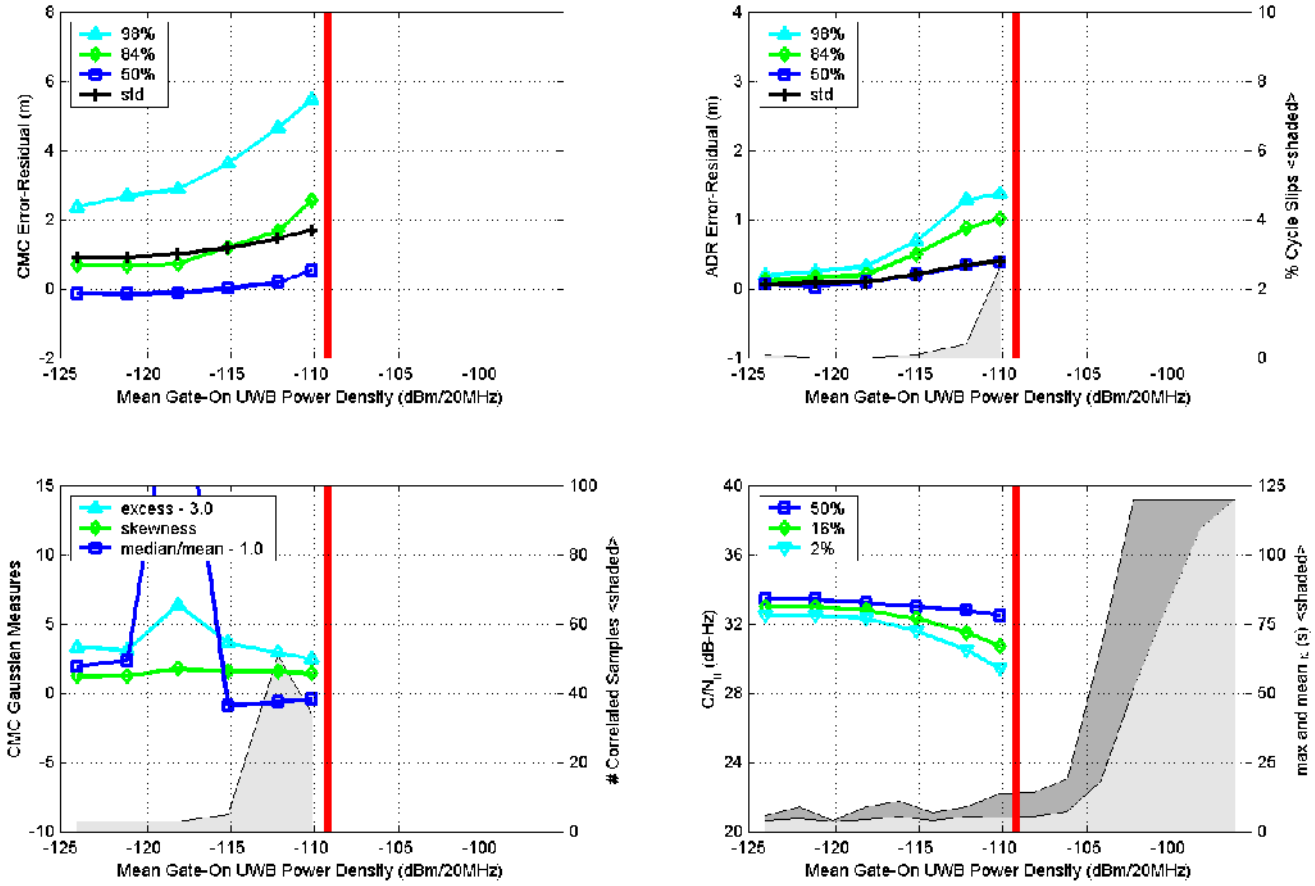

Figure F.1.36. Measured GPS parameters (Rx 1) as a function of Aggregate-3 UWB interference. Aggregate 3 is the combination of two 10-MHz PRF, UPS, non-gated UWB signals plus one 3-MHz PRF, UPS, non-gated UWB signal plus three 3-MHz PRF, 2%-RRD, gated UWB signals.

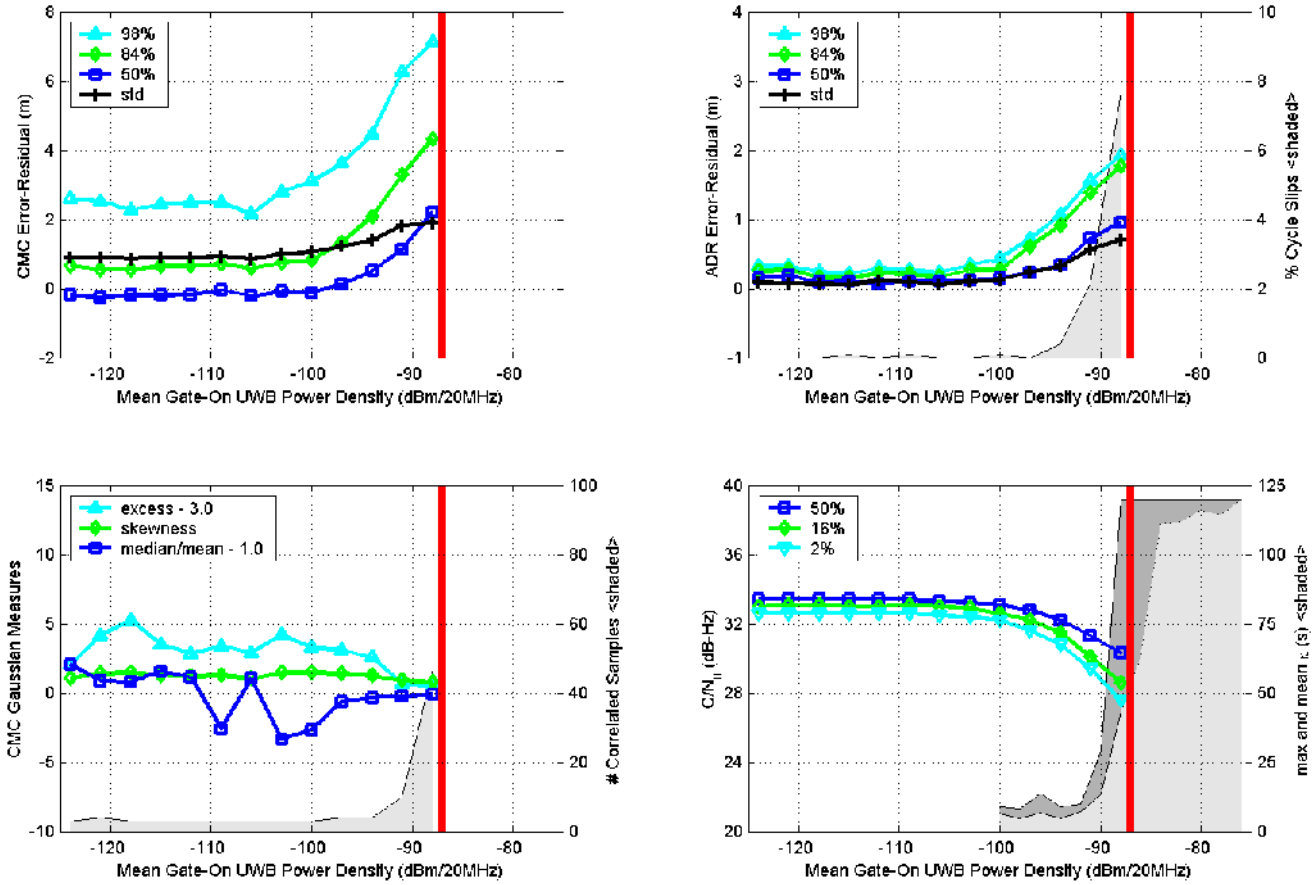

Figure F.1.37. Measured GPS parameters (Rx 1) as a function of Aggregate-4 UWB interference. Aggregate 4 is the combination of three 3-MHz PRF, UPS, gated UWB signals plus three 3-MHz PRF, 2%-RRD, gated UWB signals.

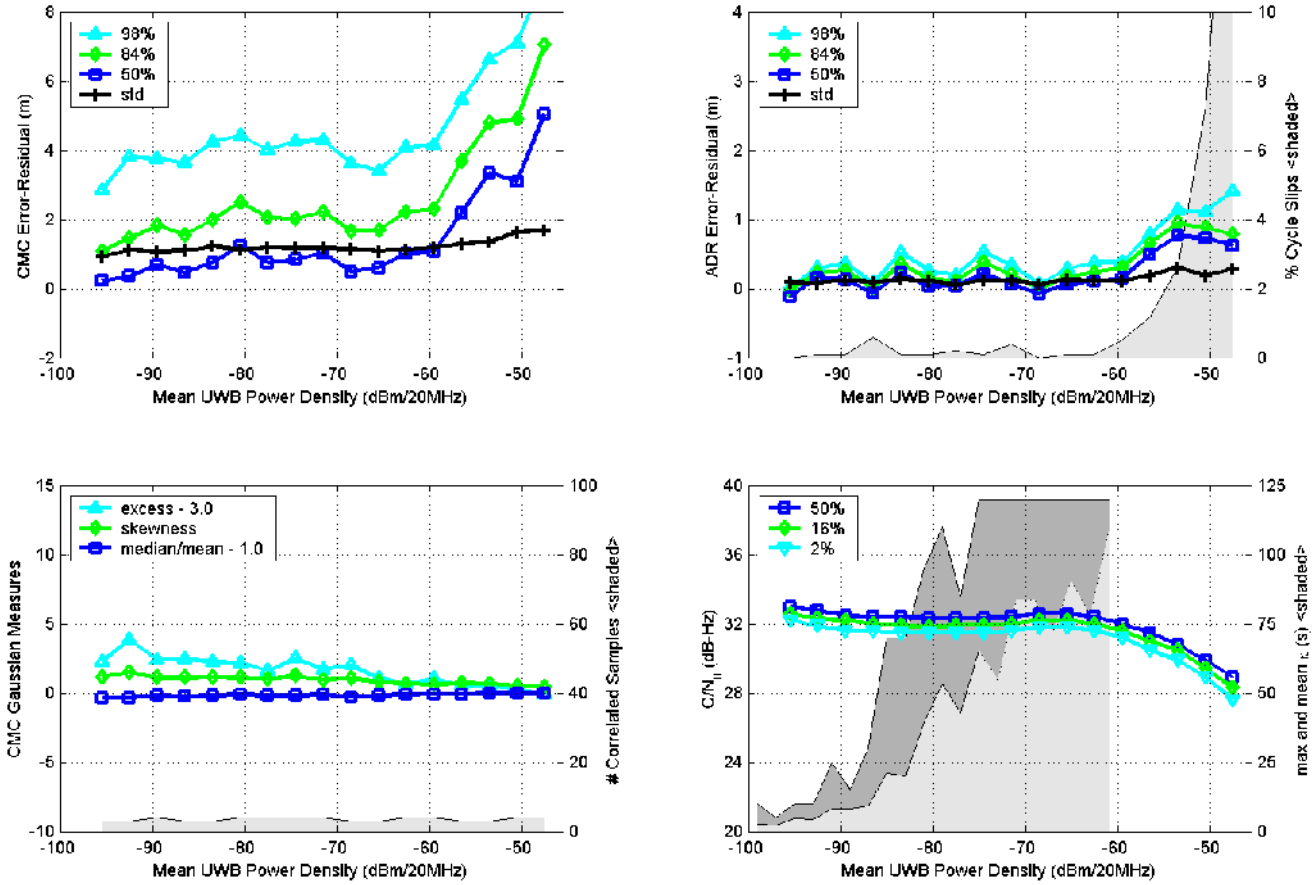

Figure F.1.38. Measured GPS parameters (Rx 1) as a function of Aggregate-5(a) UWB interference. Aggregate 5(a) is one 1-MHz PRF, 2%-RRD, non-gated UWB signal.

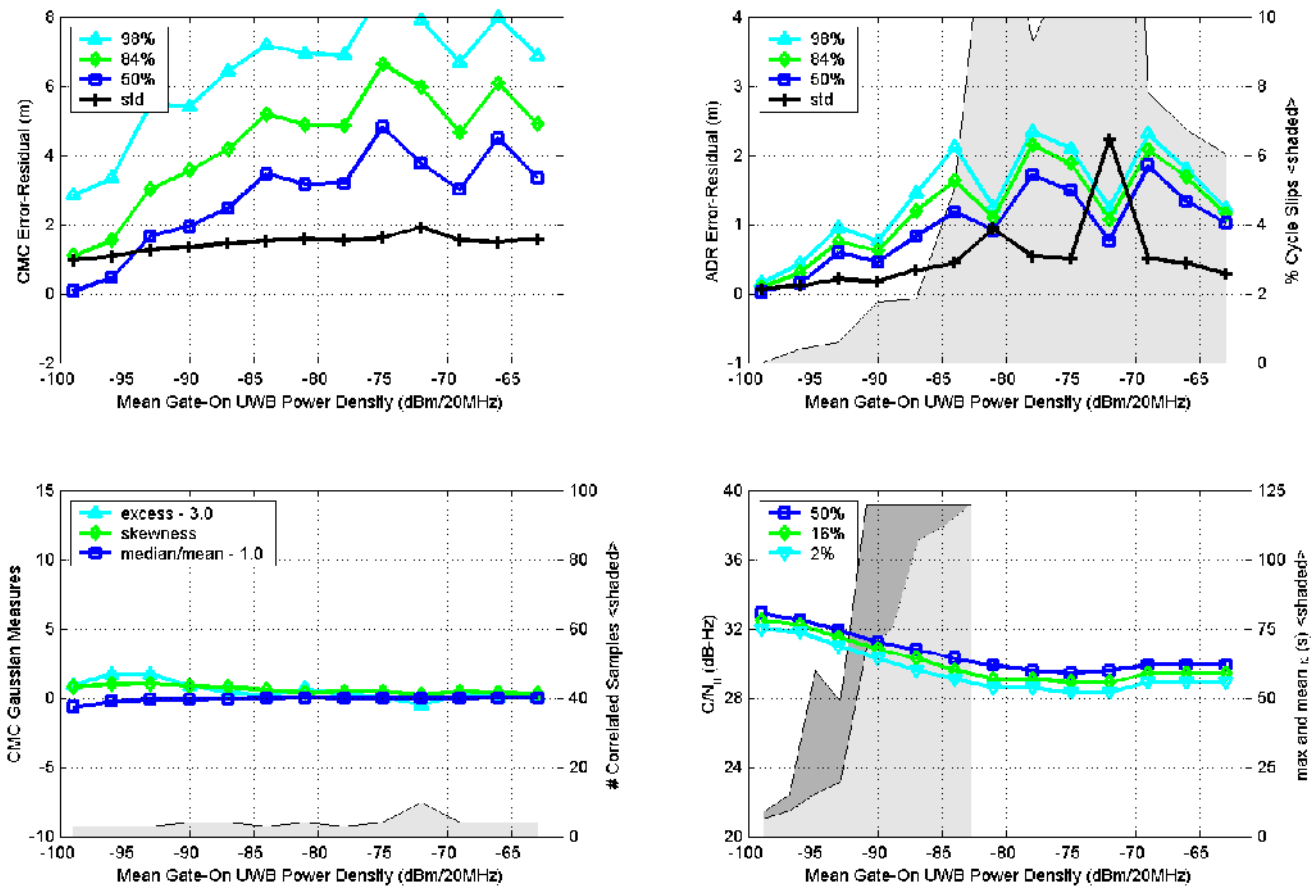

Figure F.1.39. Measured GPS parameters (Rx 1) as a function of Aggregate-5(b) UWB interference. Aggregate 5(b) is the combination of two 1-MHz PRF, 2%-RRD, non-gated UWB signals.

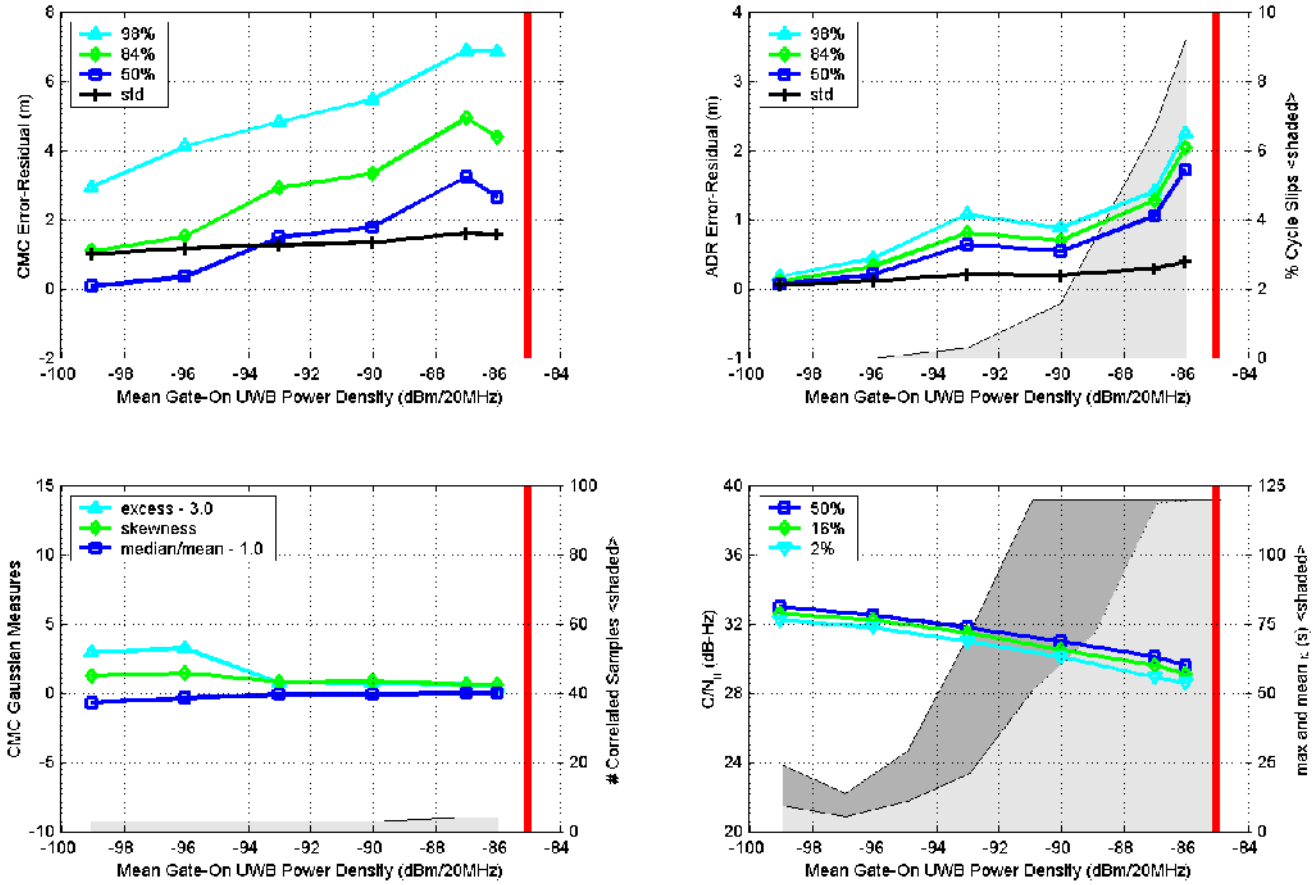

Figure F.1.40. Measured GPS parameters (Rx 1) as a function of Aggregate-5(c) UWB interference. Aggregate 5(c) is the combination of three 1-MHz PRF, 2%-RRD, non-gated UWB signals.

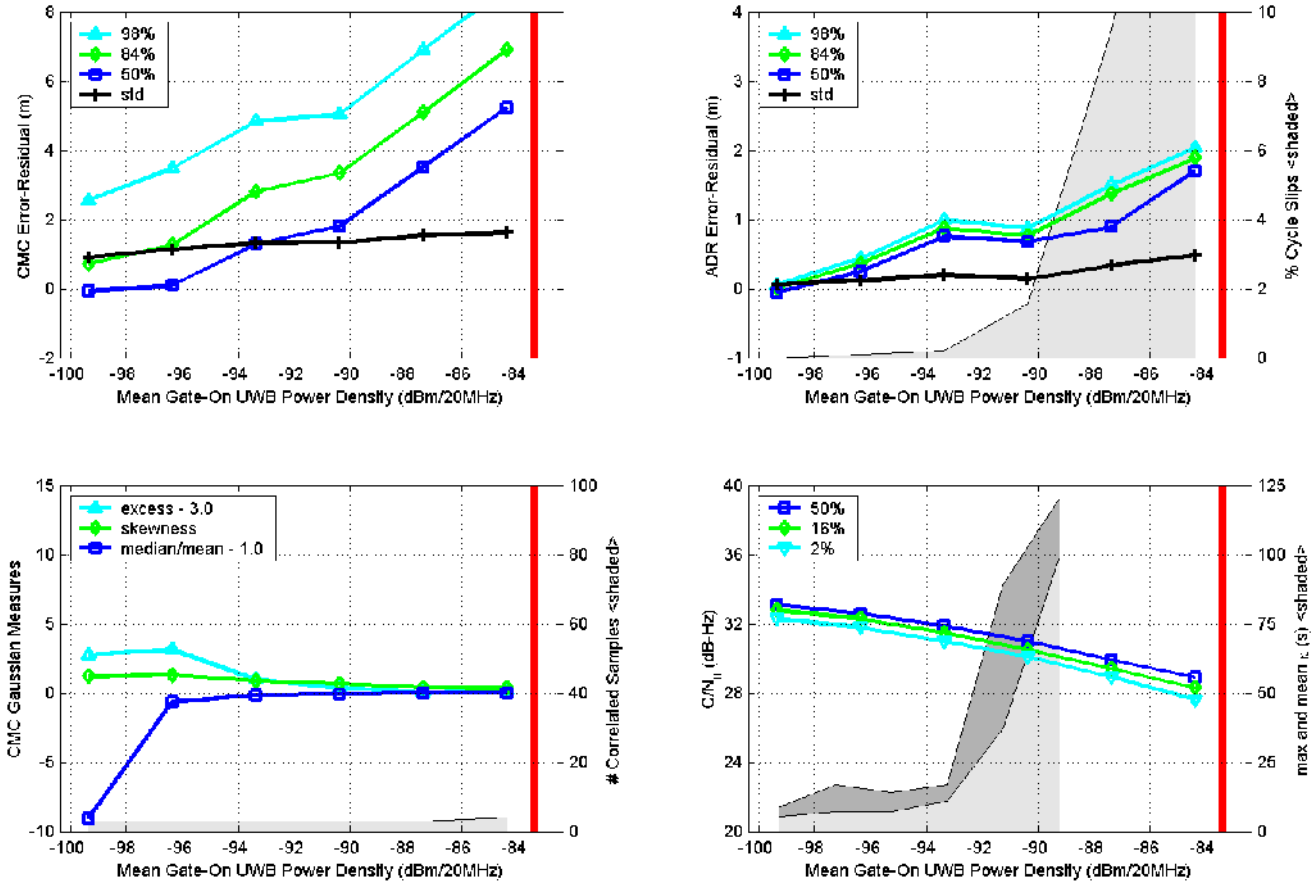

Figure F.1.41. Measured GPS parameters (Rx 1) as a function of Aggregate-5(d) UWB interference. Aggregate 5(d) is the combination of four 1-MHz PRF, 2%-RRD, non-gated UWB signals.

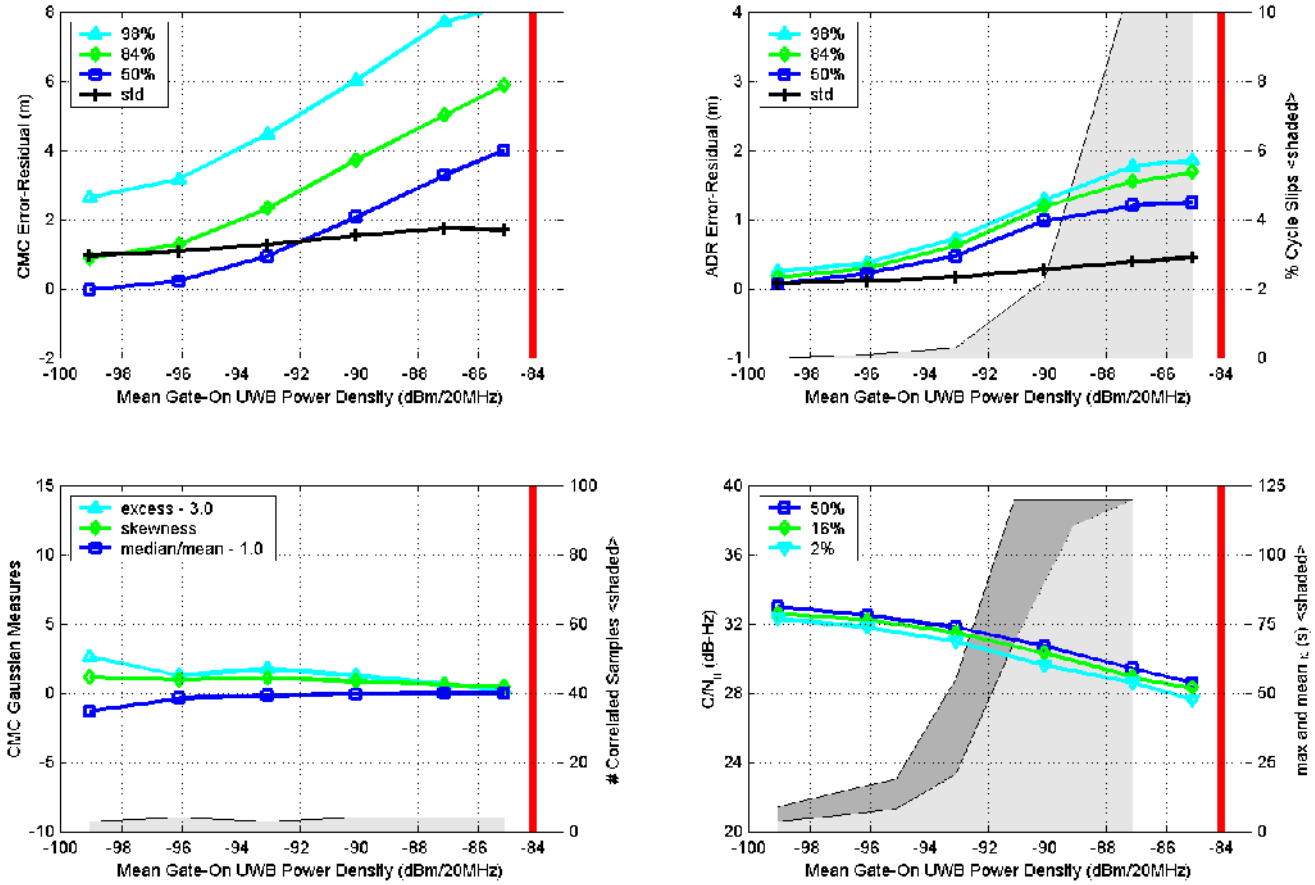

Figure F.1.42. Measured GPS parameters (Rx 1) as a function of Aggregate-5(e) UWB interference. Aggregate 5(e) is the combination of five 1-MHz PRF, 2%-RRD, non-gated UWB signals.

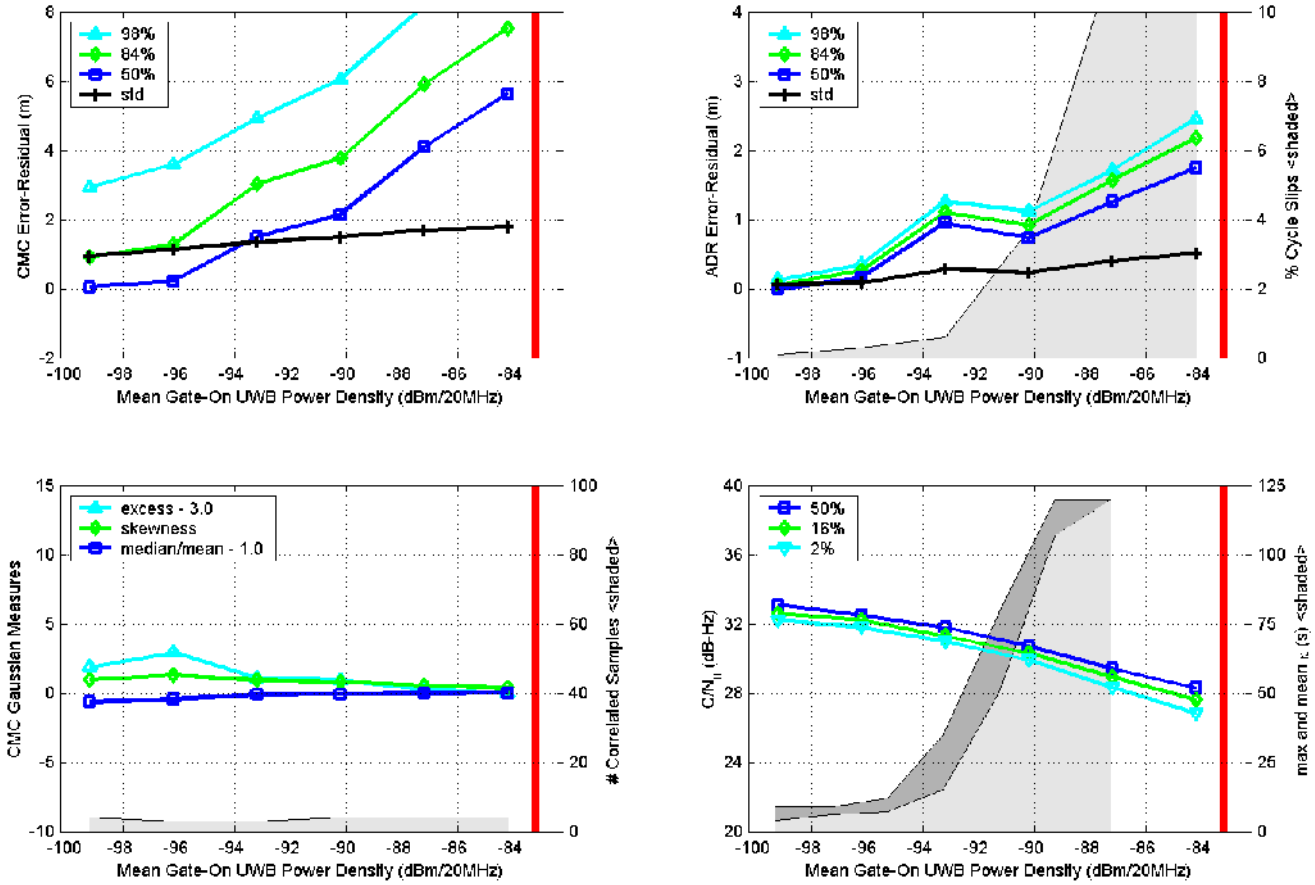

Figure F.1.43. Measured GPS parameters (Rx 1) as a function of Aggregate-5(f) UWB interference. Aggregate 5(f) is the combination of six 1-MHz PRF, 2%-RRD, non-gated UWB signals.

F.2. Semi-Codeless Receiver (Rx 2) Results

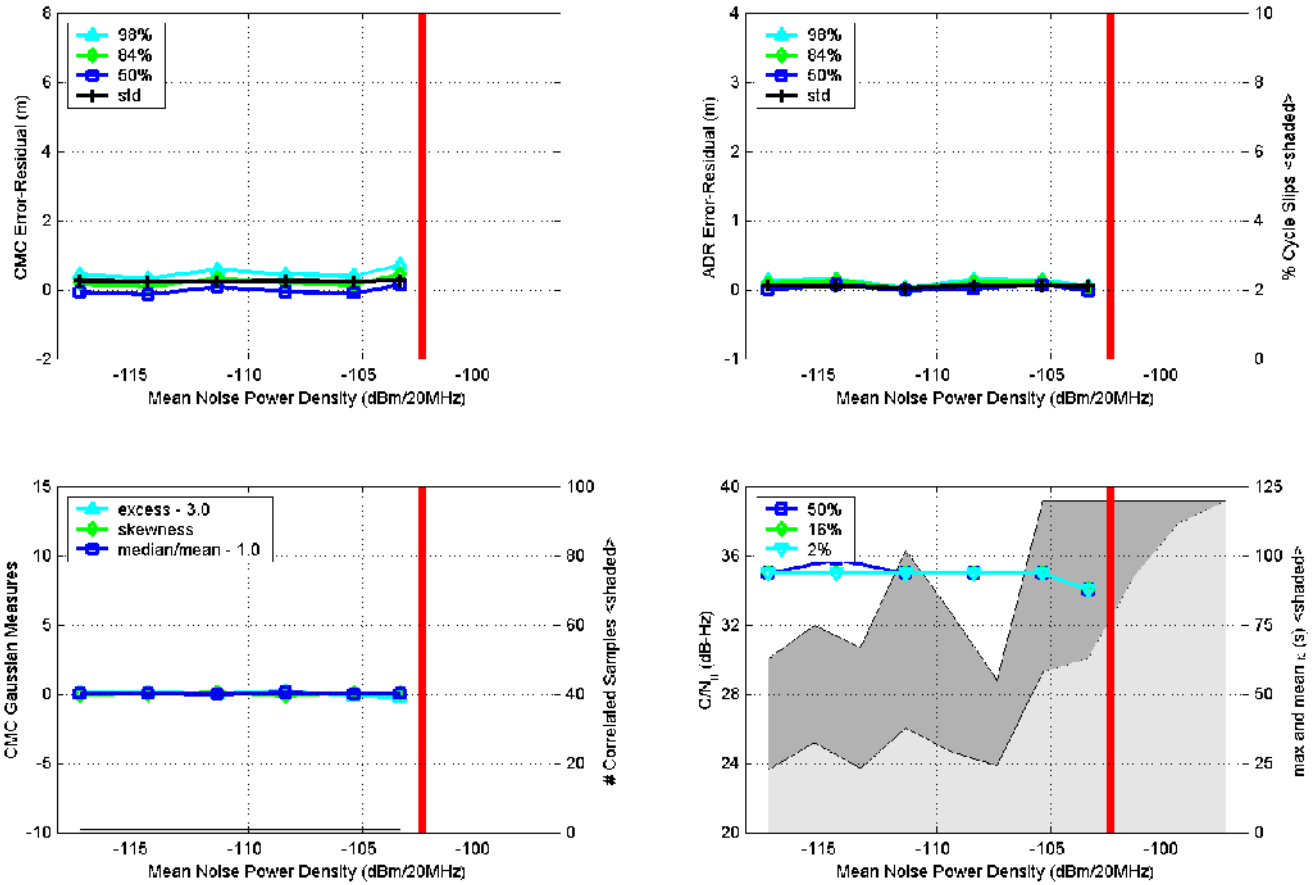

Figure F.2.1. Measured GPS parameters (Rx 2) as a function of Gaussian-noise interference.

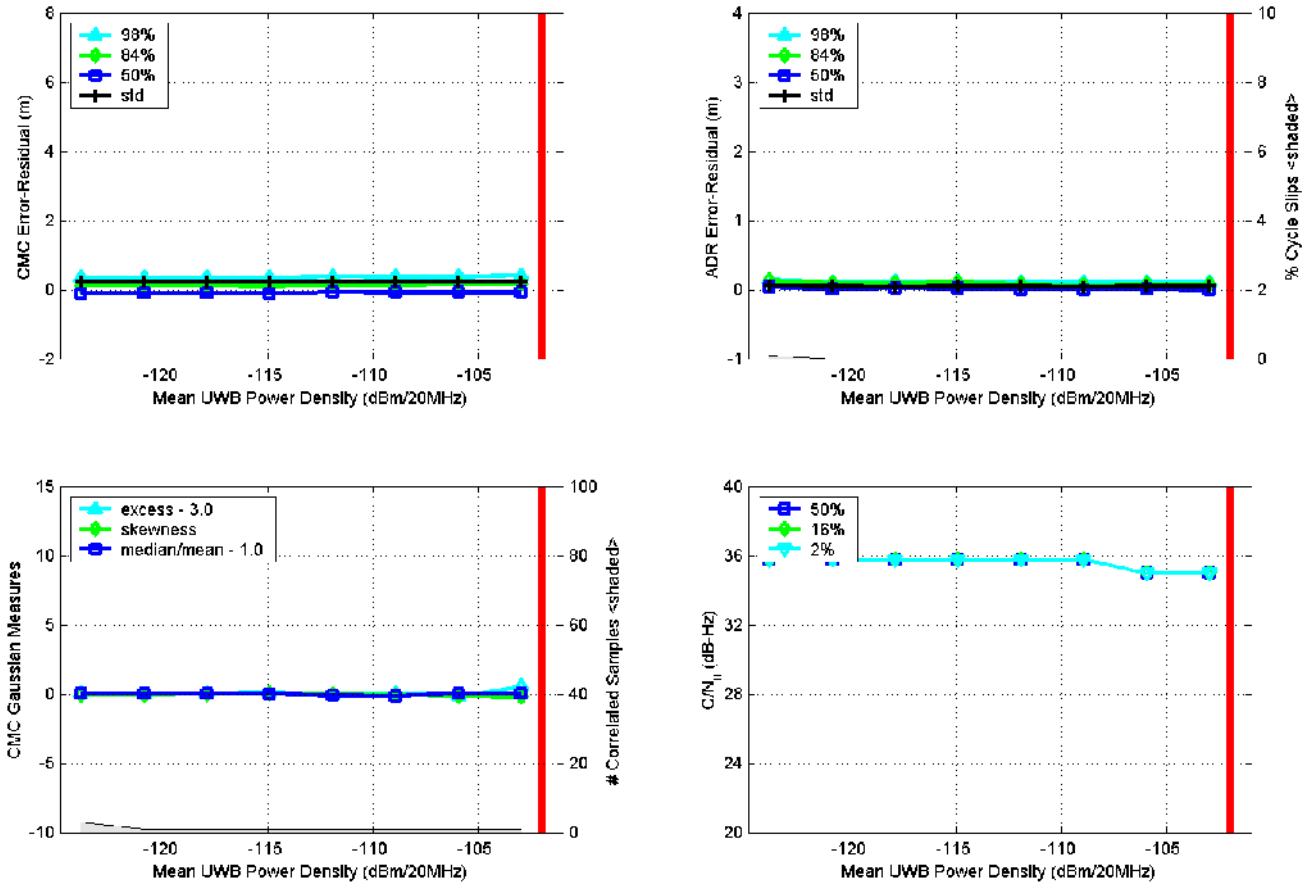

Figure F.2.2. Measured GPS parameters (Rx 2) as a function of 20-MHz PRF, UPS, non-gated UWB interference.

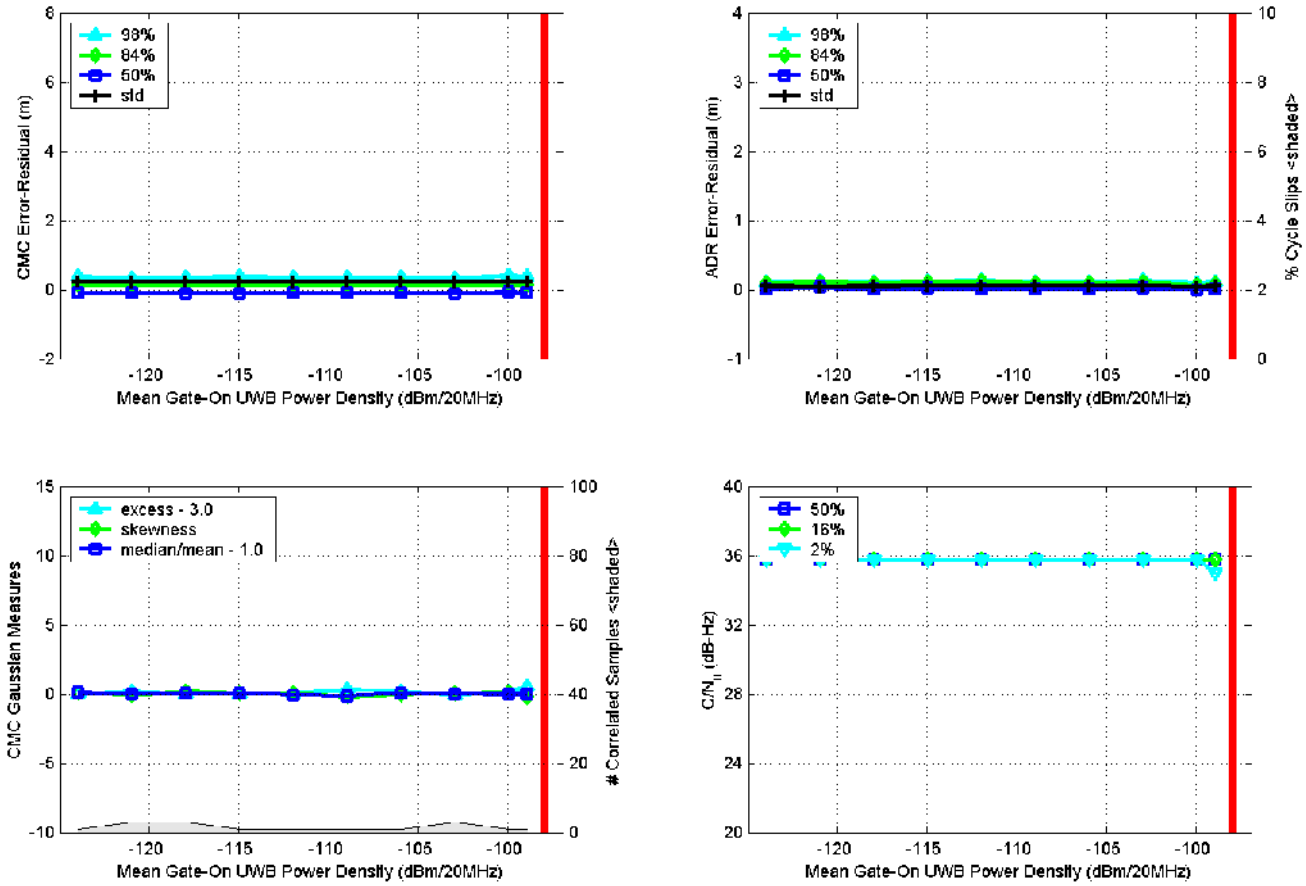

Figure F.2.3. Measured GPS parameters (Rx 2) as a function of 20-MHz PRF, UPS, gated (20% duty cycle) UWB interference.

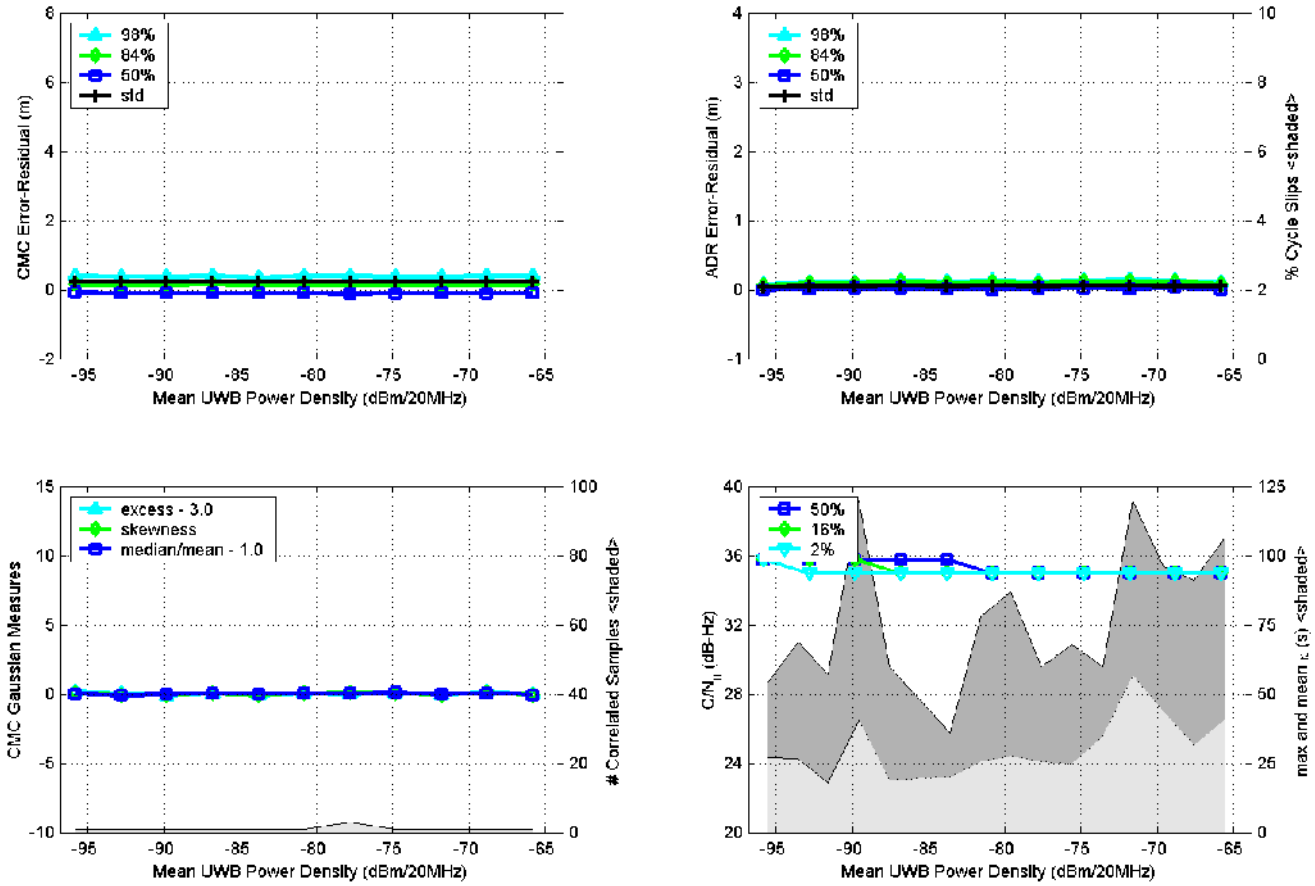

Figure F.2.4. Measured GPS parameters (Rx 2) as a function of 0.1-MHz PRF, UPS, non-gated UWB interference.

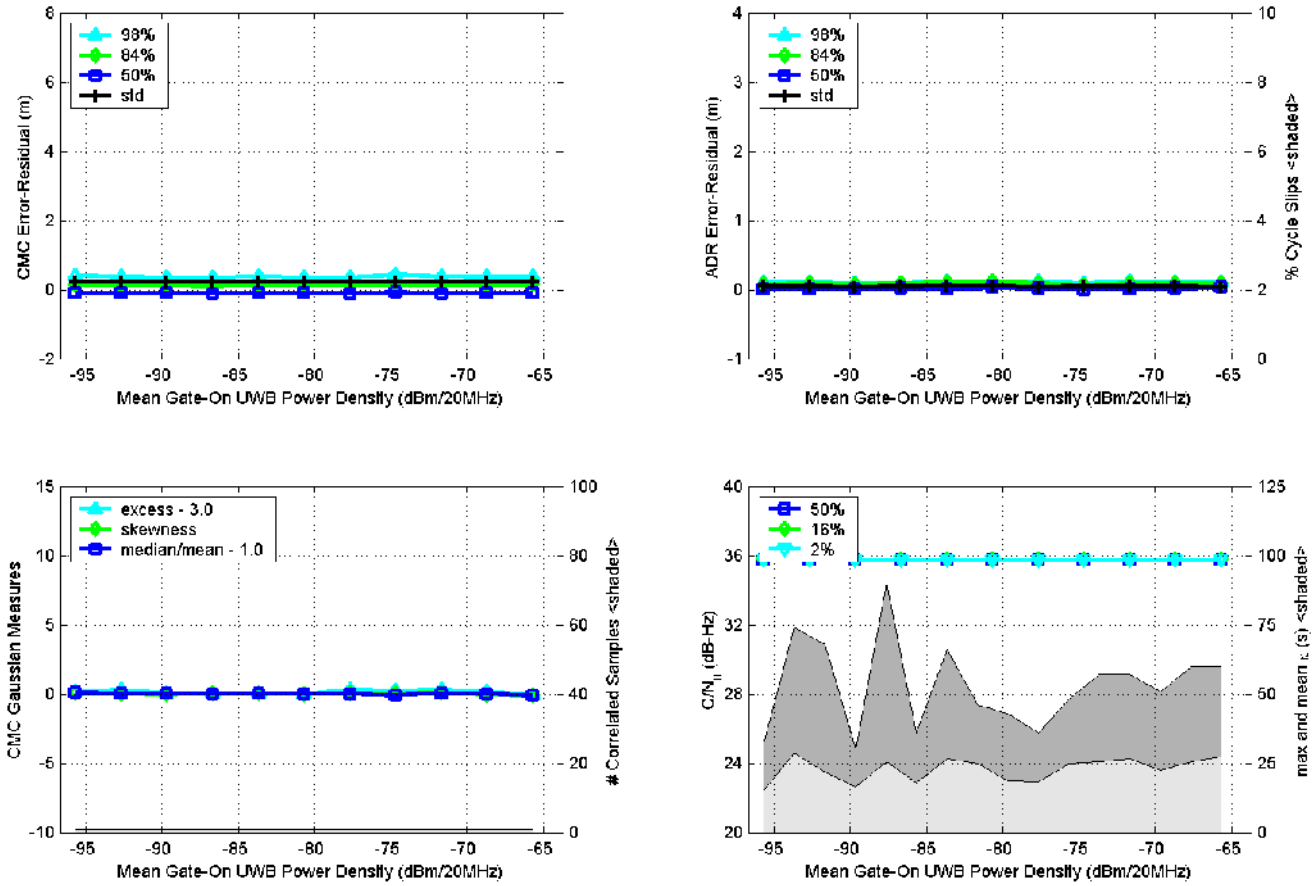

Figure F.2.5. Measured GPS parameters (Rx 2) as a function of 0.1-MHz PRF, UPS, gated (20% duty cycle) UWB interference.

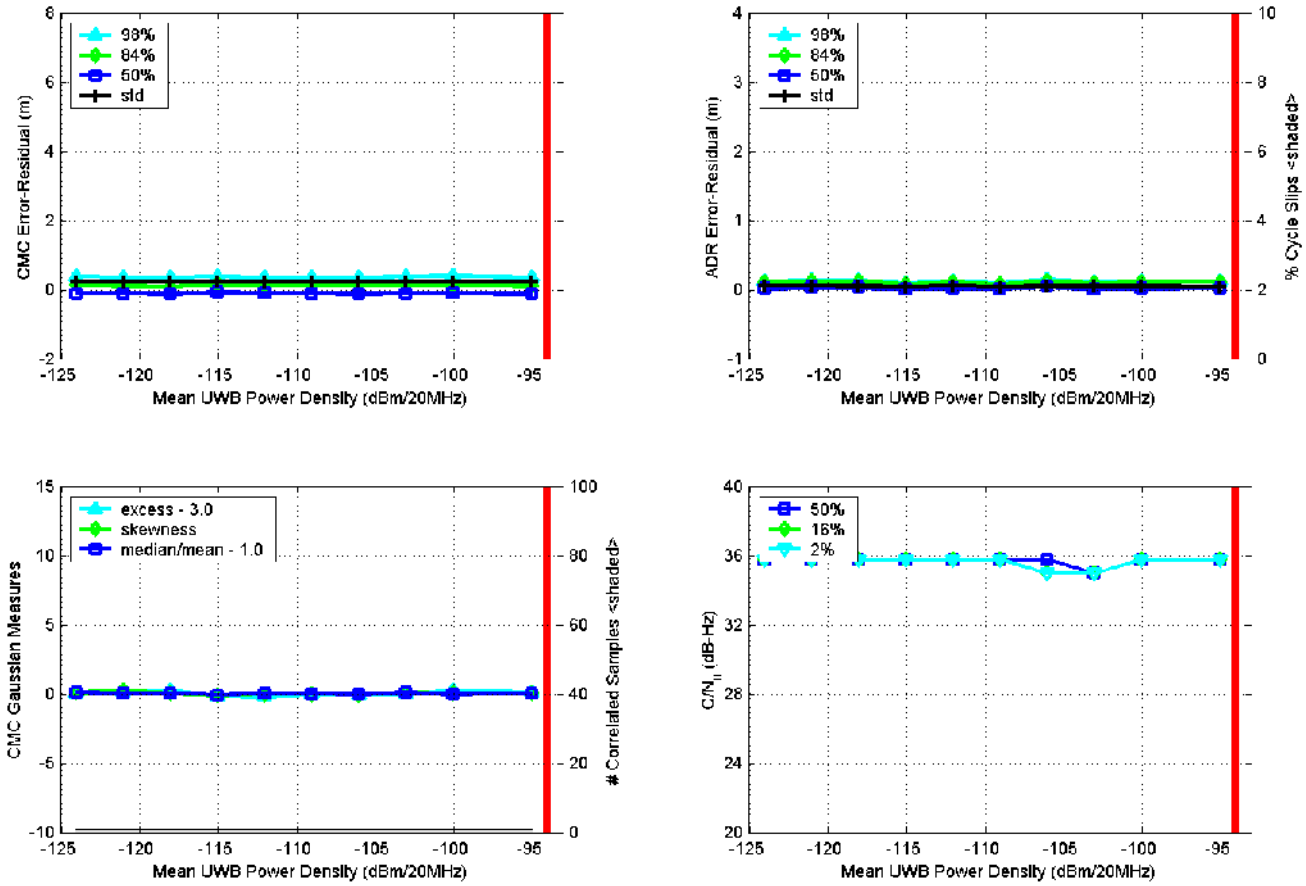

Figure F.2.6. Measured GPS parameters (Rx 2) as a function of 20-MHz PRF, OOK, non-gated UWB interference.

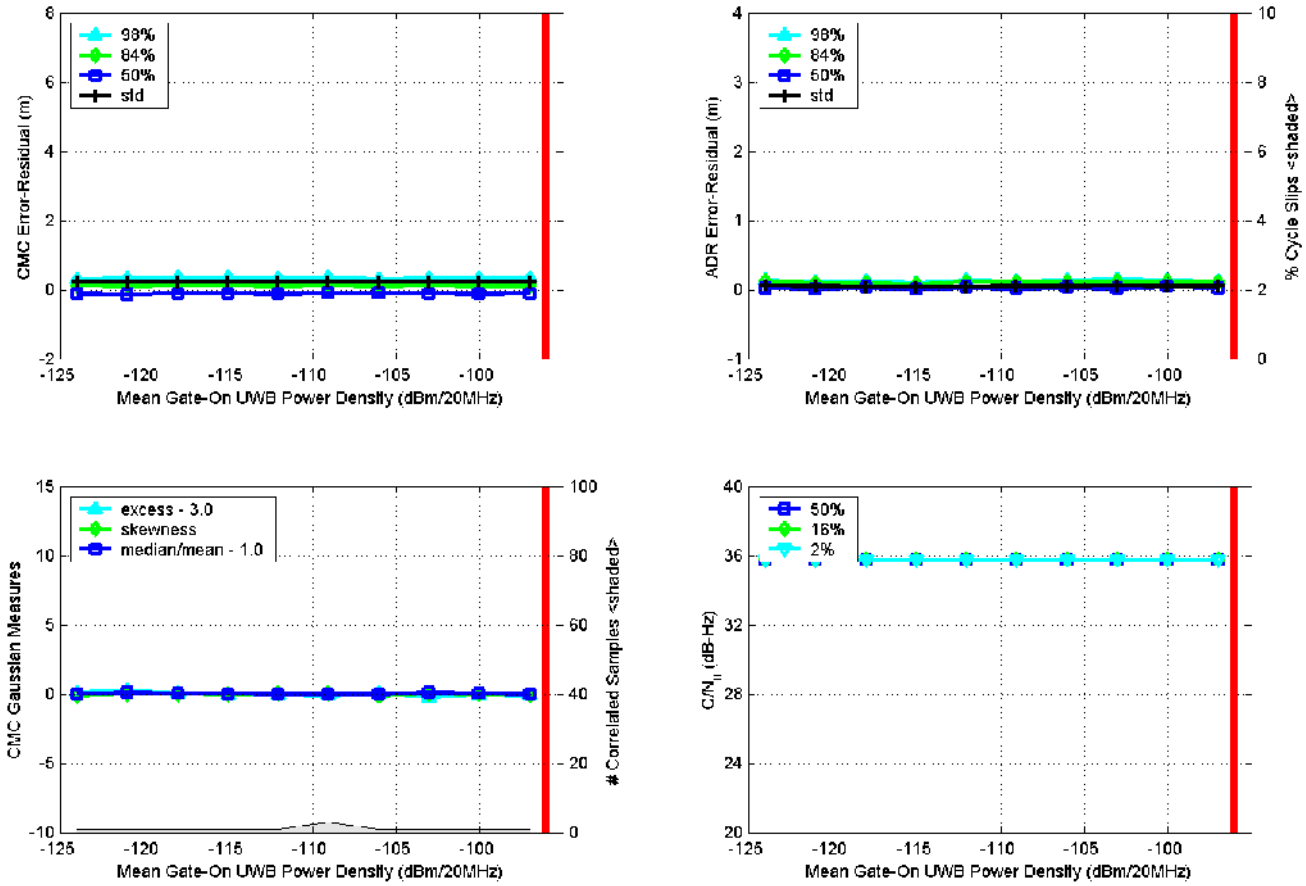

Figure F.2.7. Measured GPS parameters (Rx 2) as a function of 20-MHz PRF, OOK, gated (20% duty cycle) UWB interference.

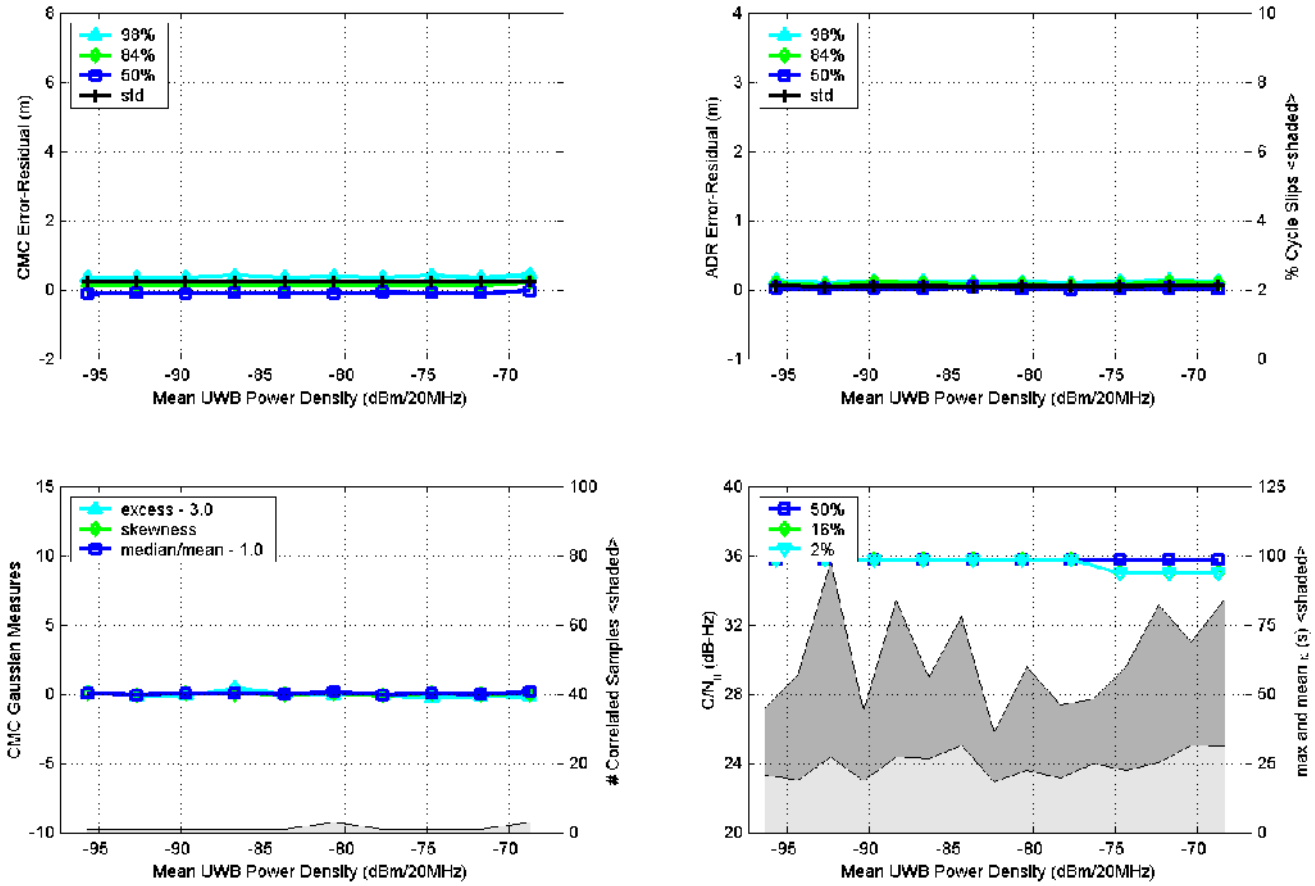

Figure F.2.8. Measured GPS parameters (Rx 2) as a function of 0.1-MHz PRF, OOK, non-gated UWB interference.

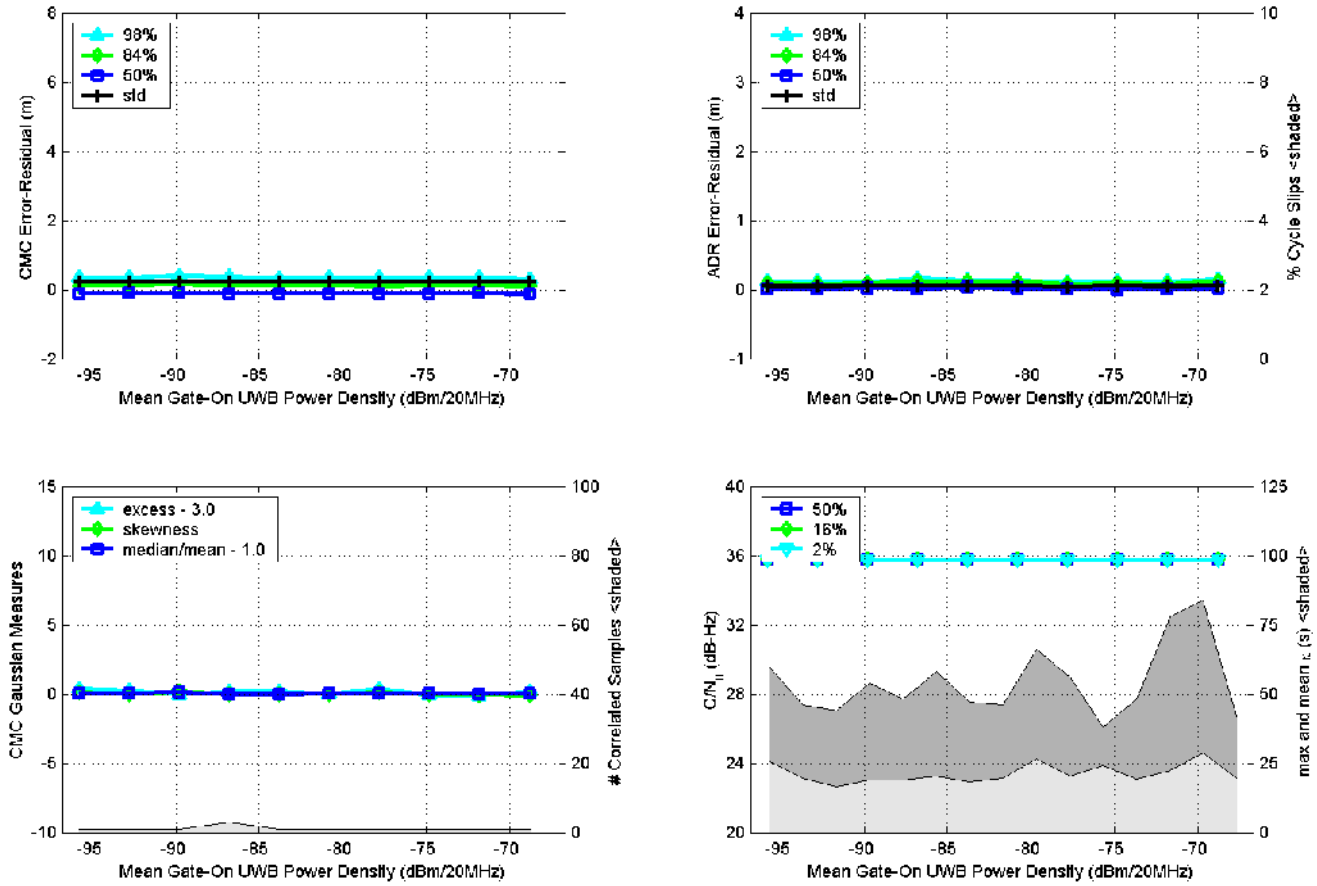

Figure F.2.9. Measured GPS parameters (Rx 2) as a function of 0.1-MHz PRF, OOK, gated (20% duty cycle) UWB interference.

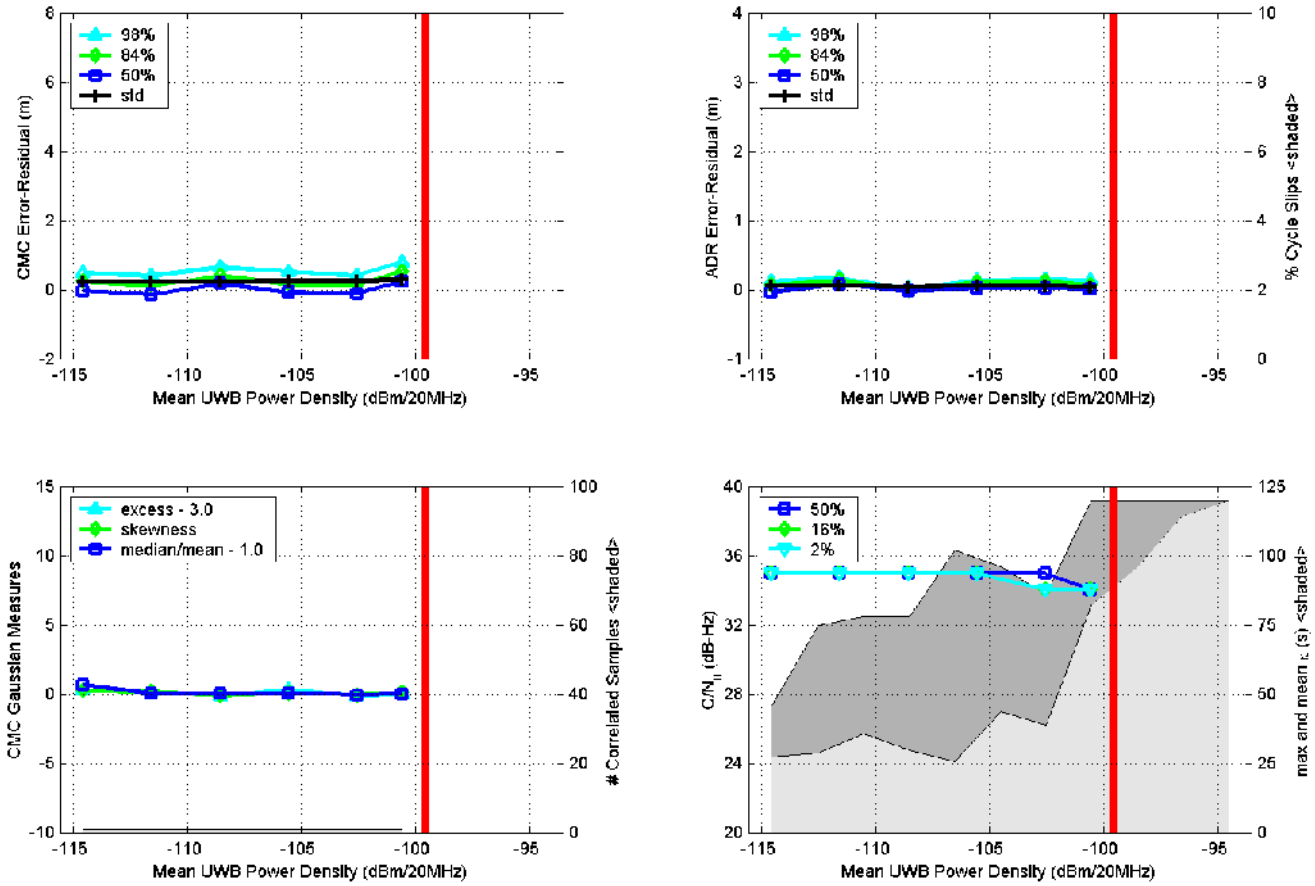

Figure F.2.10. Measured GPS parameters (Rx 2) as a function of 20-MHz PRF, 50%-ARD, non-gated UWB interference.

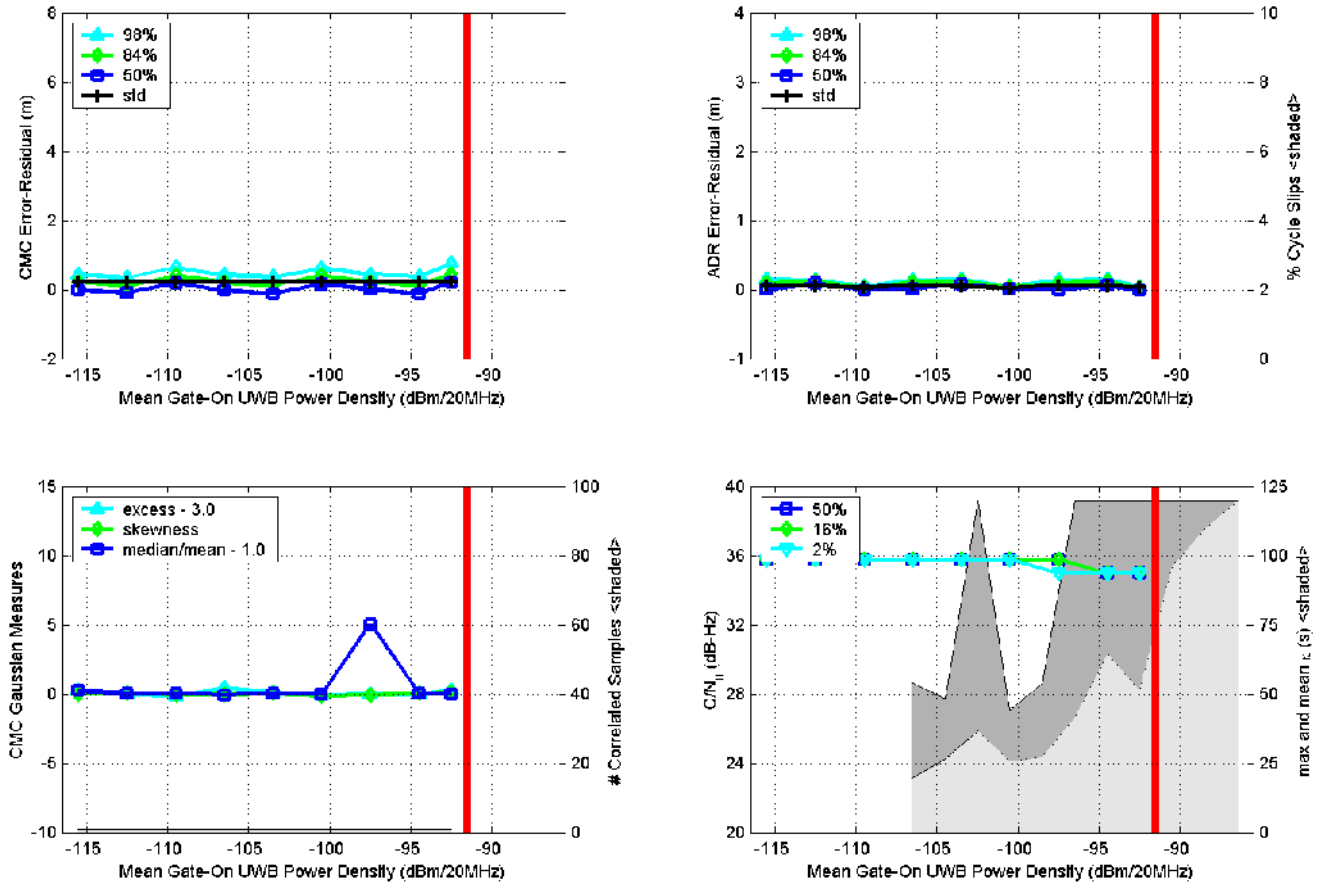

Figure F.2.11. Measured GPS parameters (Rx 2) as a function of 20-MHz PRF, 50%-ARD, gated (20% duty cycle) UWB interference.

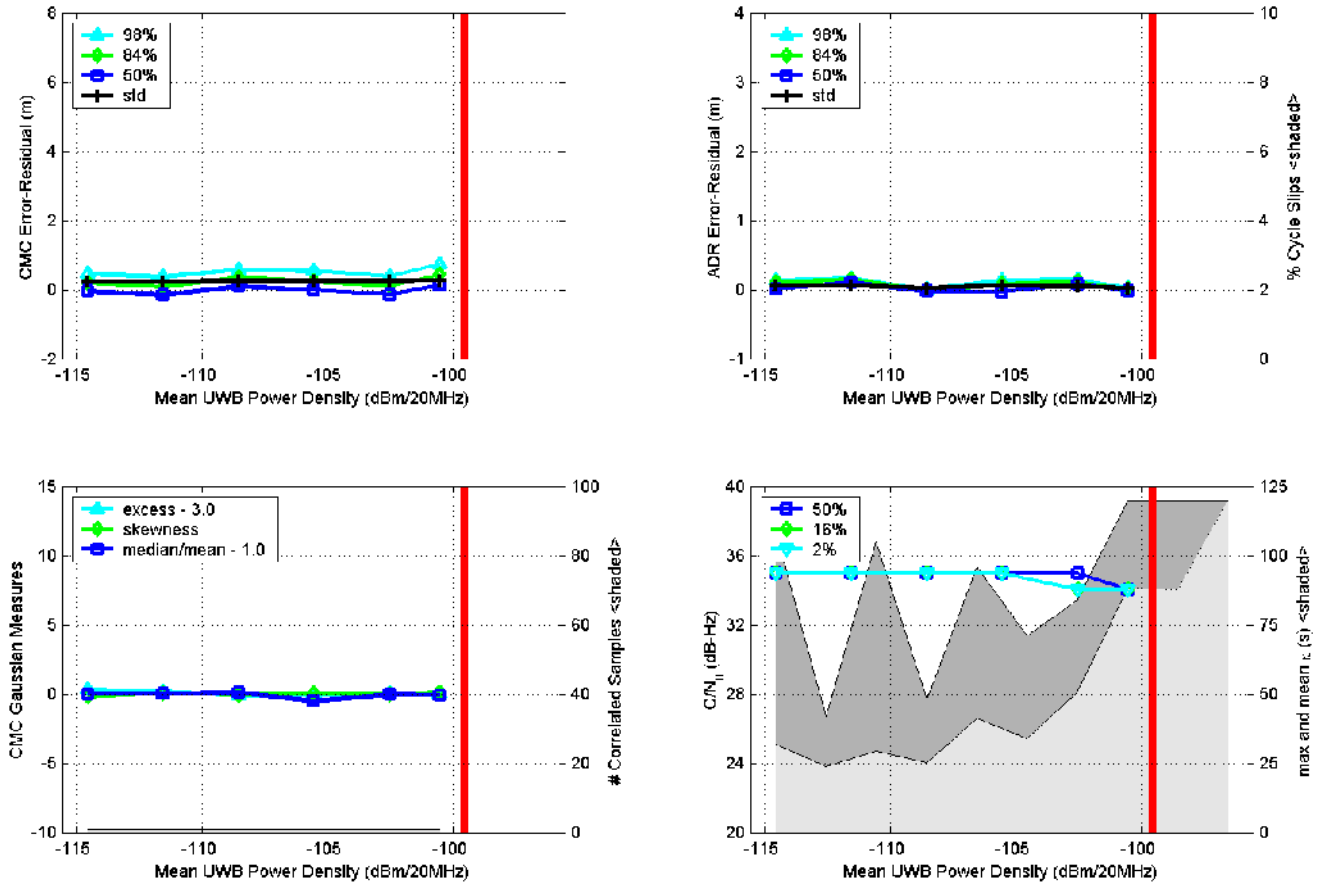

Figure F.2.12. Measured GPS parameters (Rx 2) as a function of 5-MHz PRF, 50%-ARD, non-gated UWB interference.

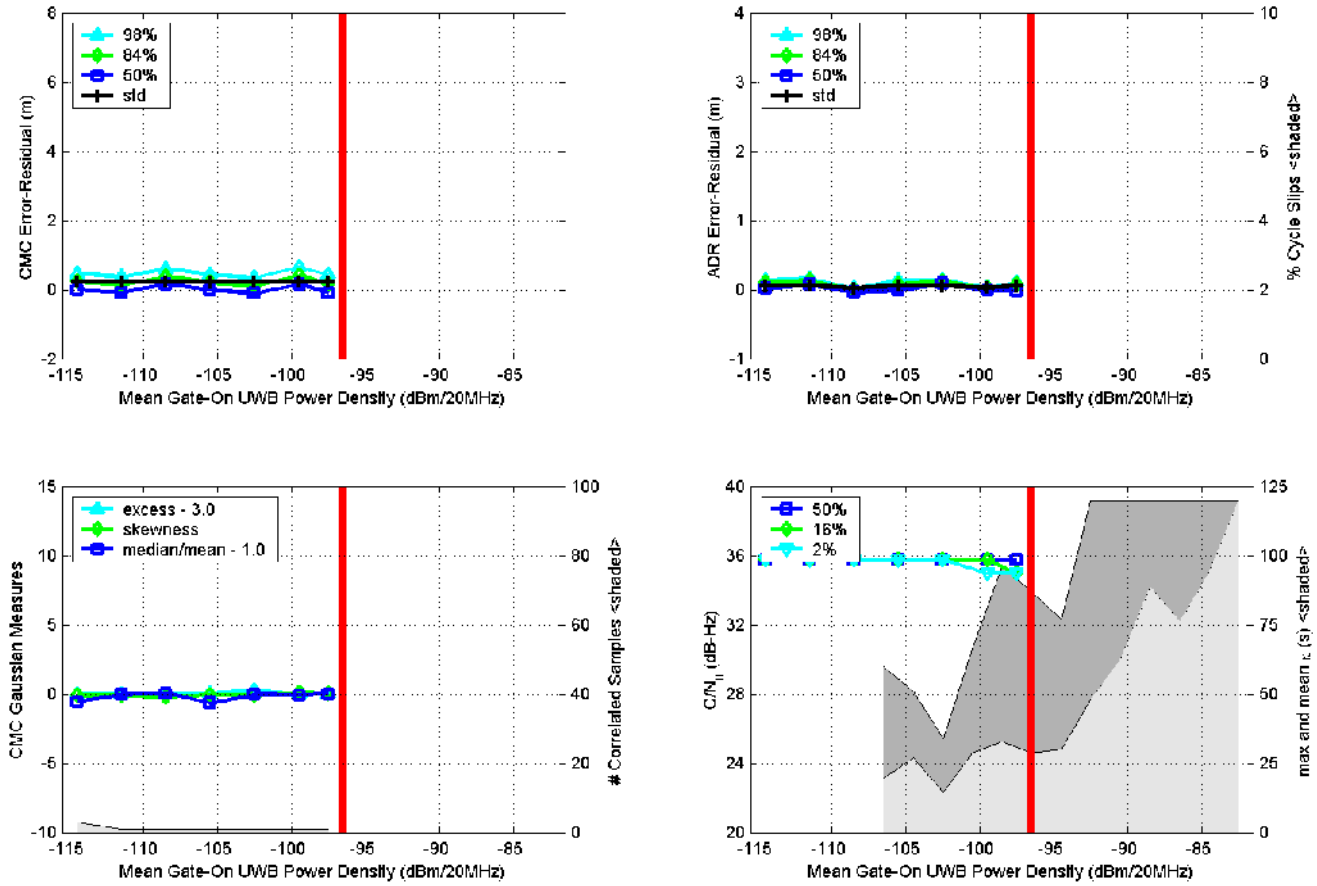

Figure F.2.13. Measured GPS parameters (Rx 2) as a function of 5-MHz PRF, 50%-ARD, gated (20% duty cycle) UWB interference.

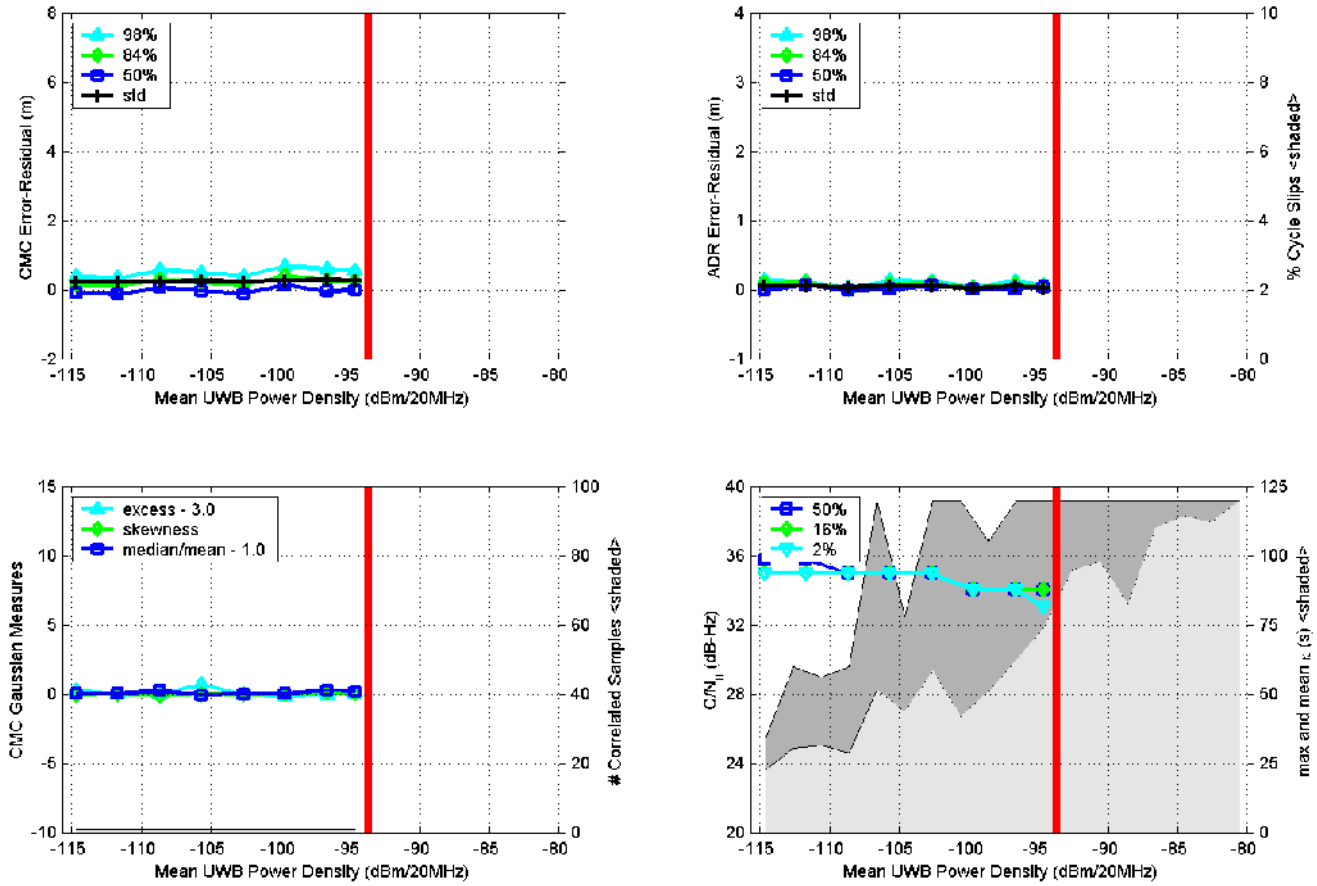

Figure F.2.14. Measured GPS parameters (Rx 2) as a function of 1-MHz PRF, 50%-ARP, non-gated UWB interference.

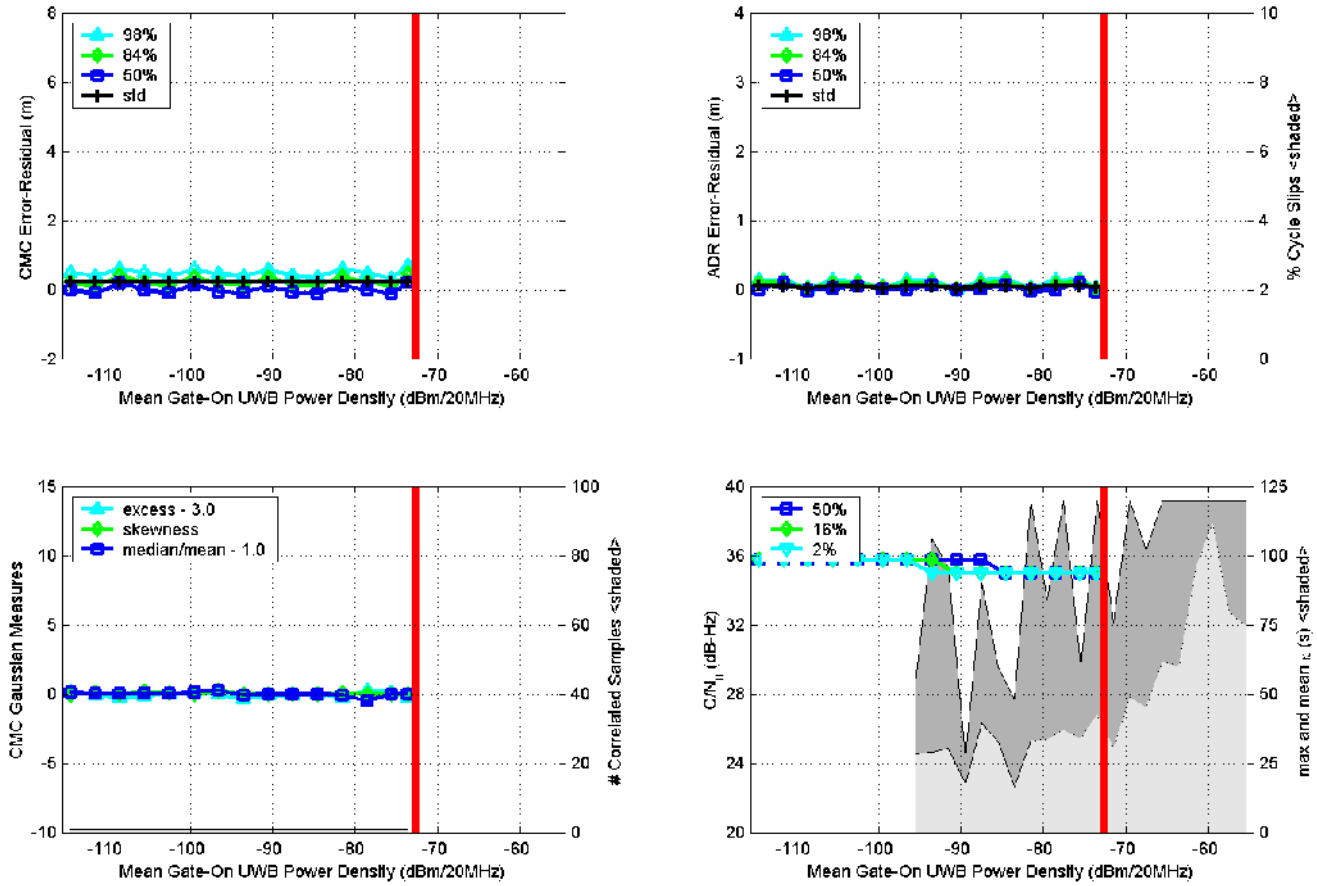

Figure F.2.15. Measured GPS parameters (Rx 2) as a function of 1-MHz PRF, 50%-ARD, gated (20% duty cycle) UWB interference.

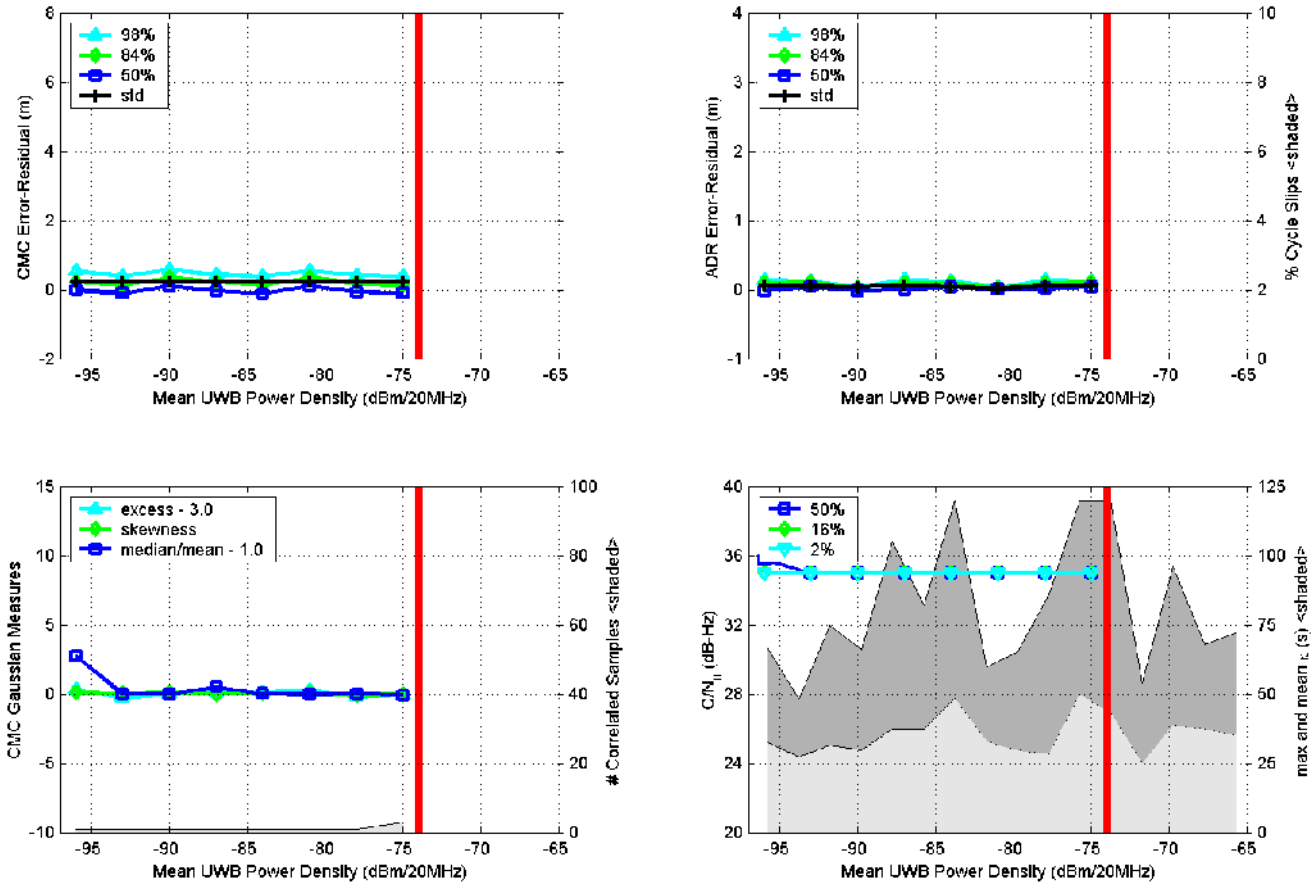

Figure F.2.16. Measured GPS parameters (Rx 2) as a function of 0.1-MHz PRF, 50%-ARD, non-gated UWB interference.

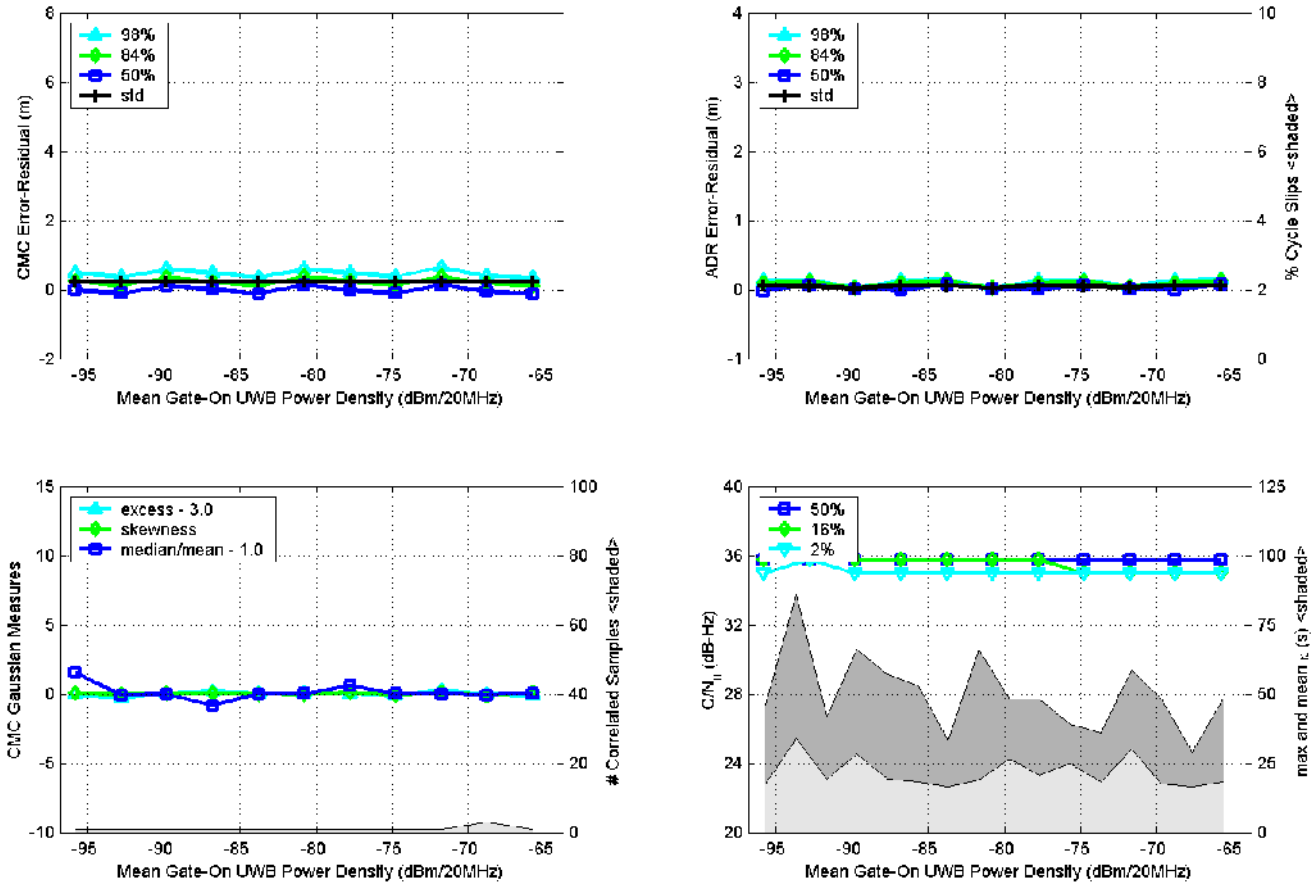

Figure F.2.17. Measured GPS parameters (Rx 2) as a function of 0.1-MHz PRF, 50%-ARD, gated (20% duty cycle) UWB interference.

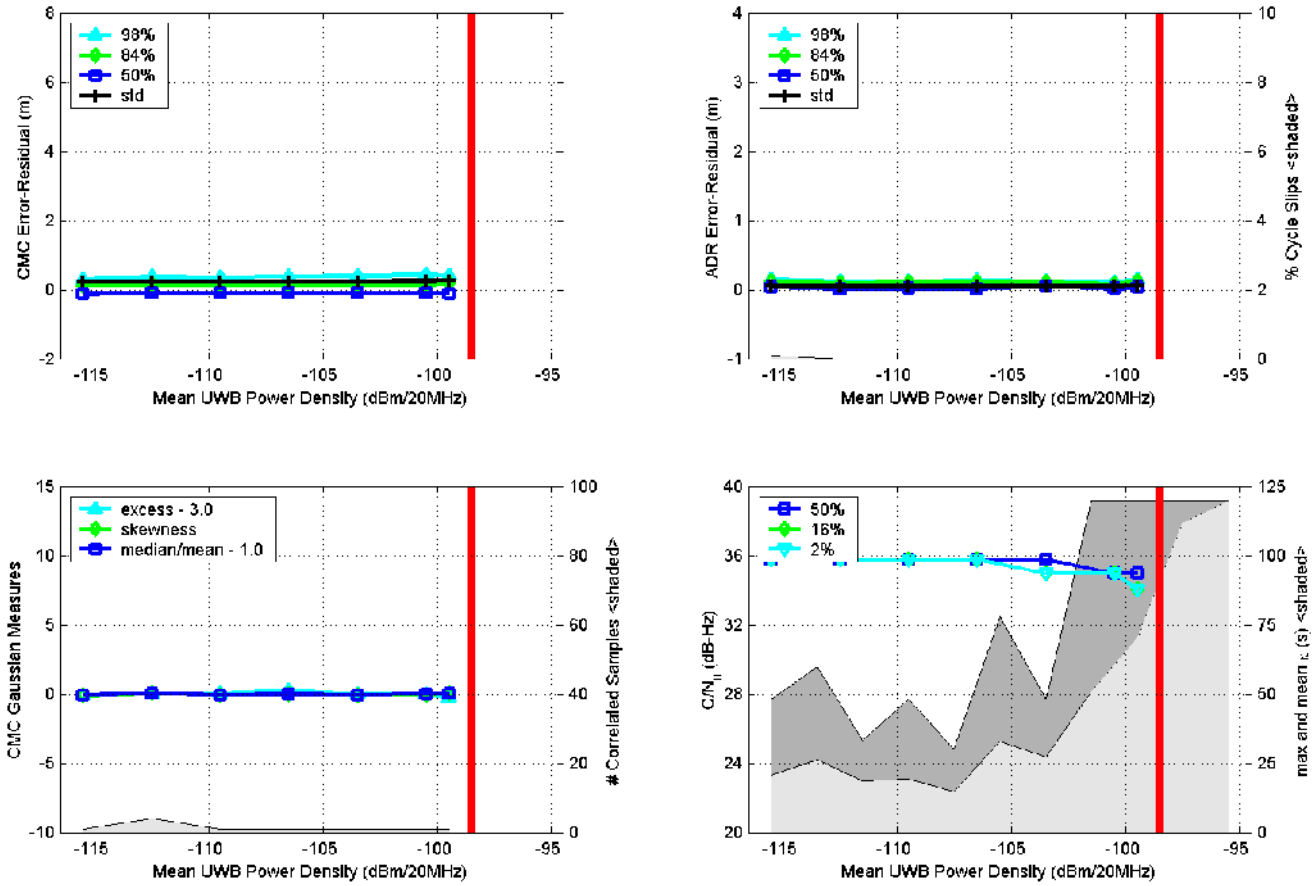

Figure F.2.18. Measured GPS parameters (Rx 2) as a function of 20-MHz PRF, 2%-RRD, non-gated UWB interference.

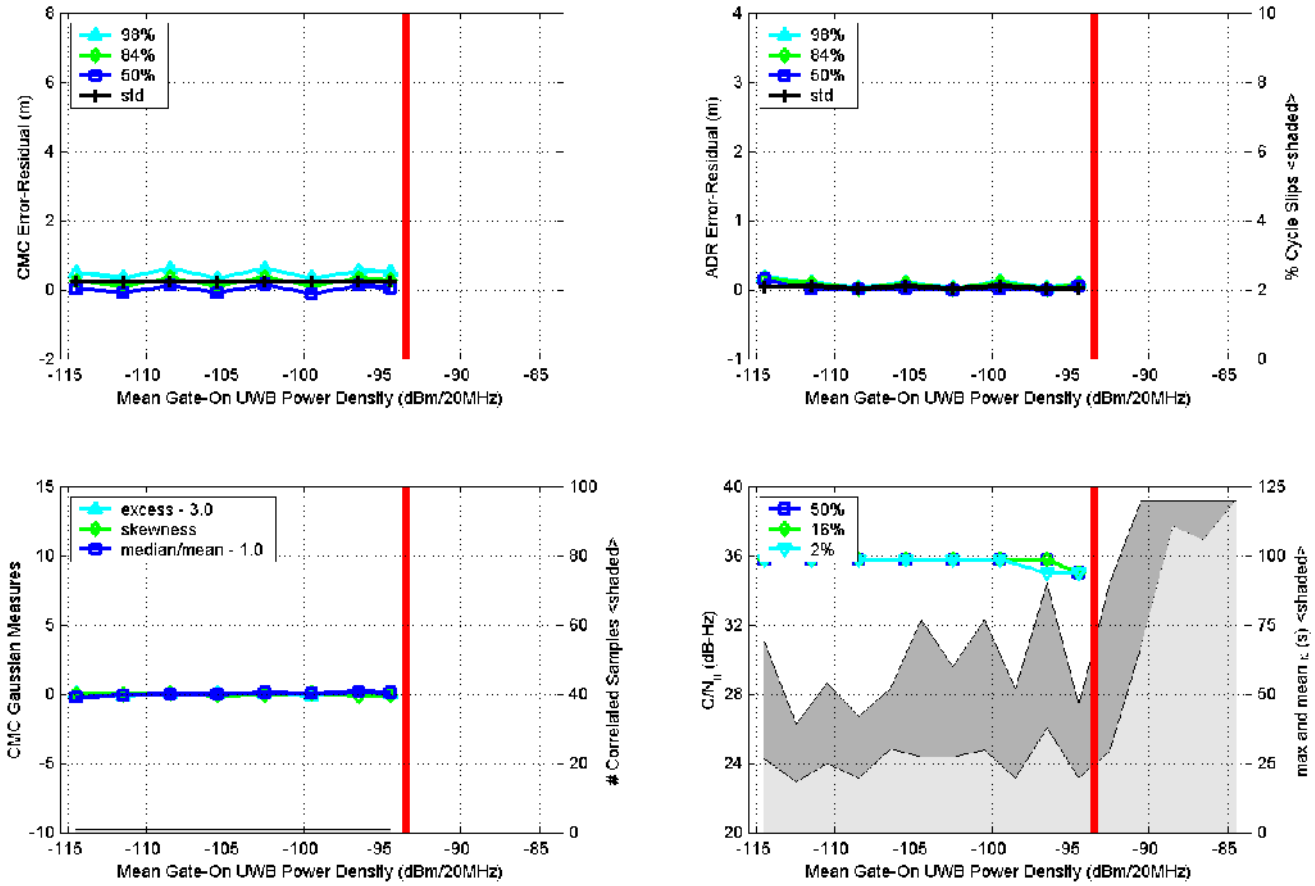

Figure F.2.19. Measured GPS parameters (Rx 2) as a function of 20-MHz PRF, 2%-RRD, gated (20% duty cycle) UWB interference.

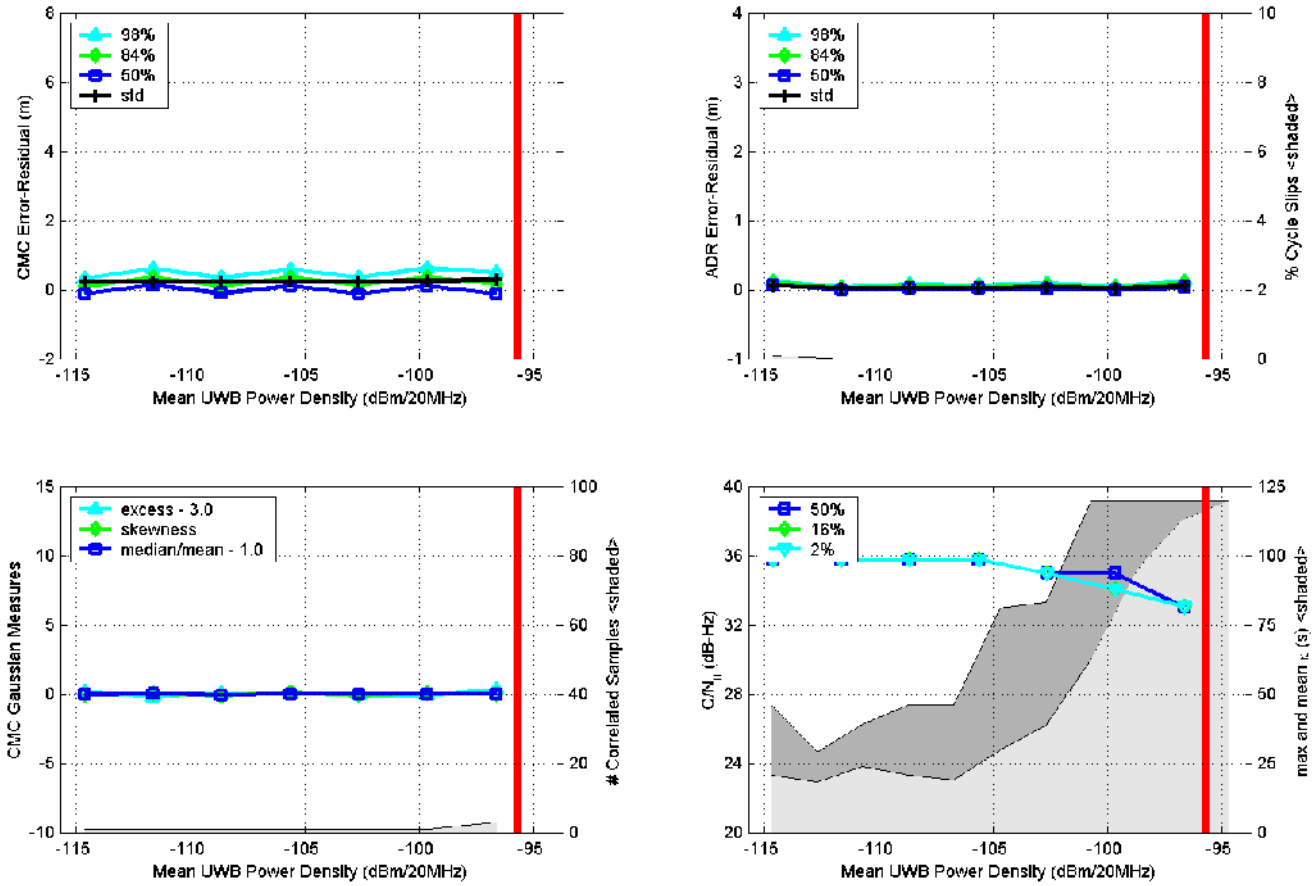

Figure F.2.20. Measured GPS parameters (Rx 2) as a function of 5-MHz PRF, 2%-RRD, non-gated UWB interference.

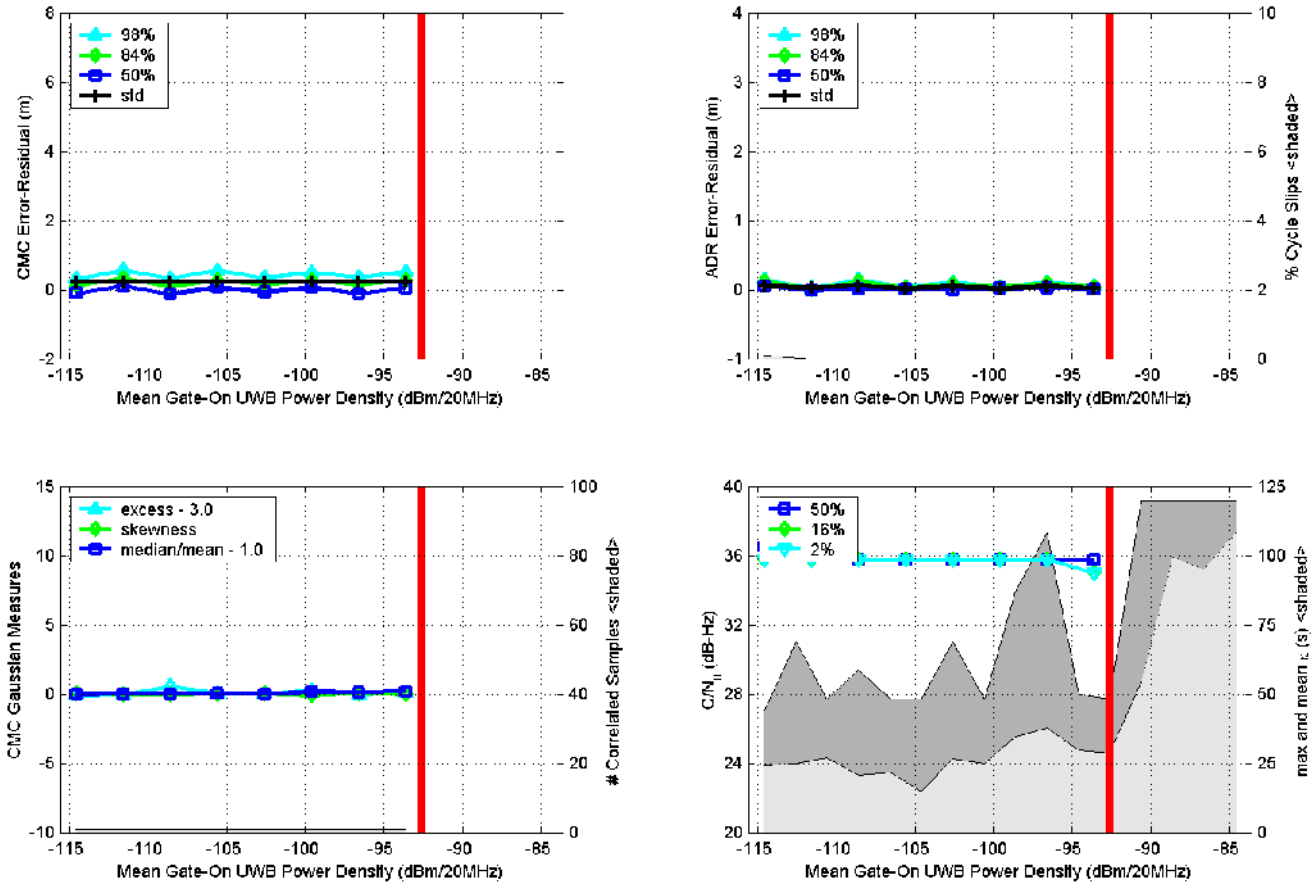

Figure F.2.21. Measured GPS parameters (Rx 2) as a function of 5-MHz PRF, 2%-RRD, gated (20% duty cycle) UWB interference.

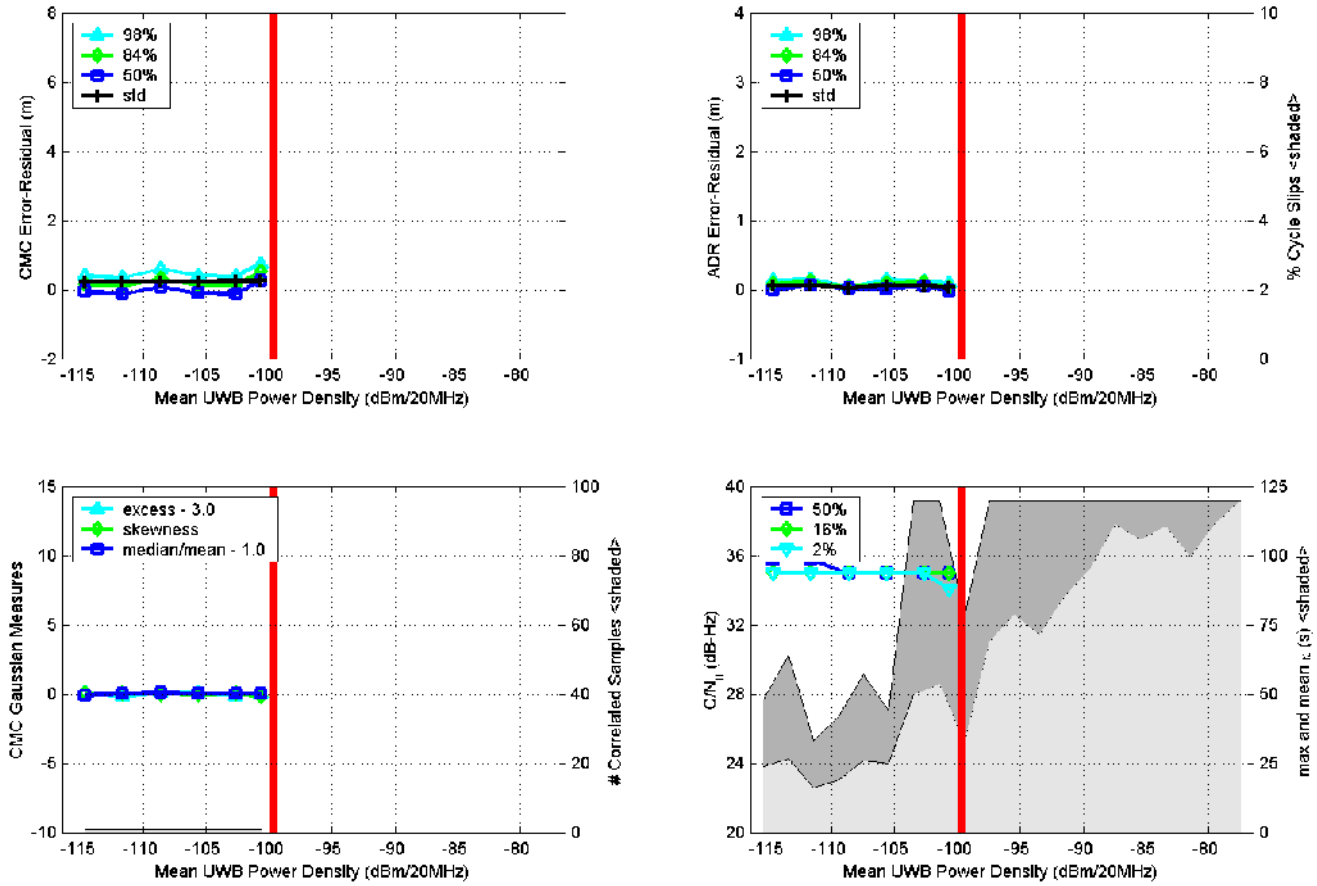

Figure F.2.22. Measured GPS parameters (Rx 2) as a function of 1-MHz PRF, 2%-RRD, non-gated UWB interference.

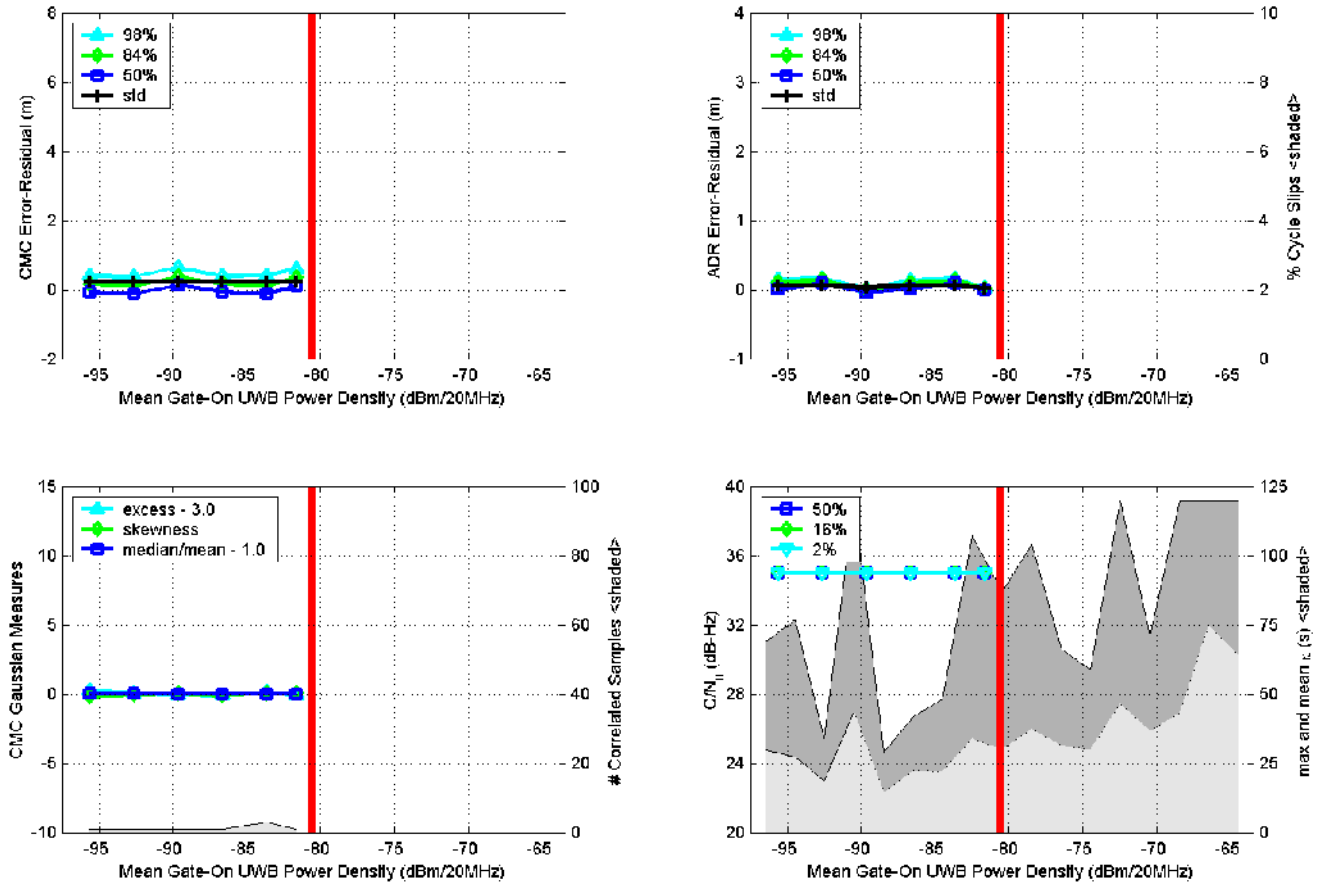

Figure F.2.23. Measured GPS parameters (Rx 2) as a function of 1-MHz PRF, 2%-RRD, gated (20% duty cycle) UWB interference.

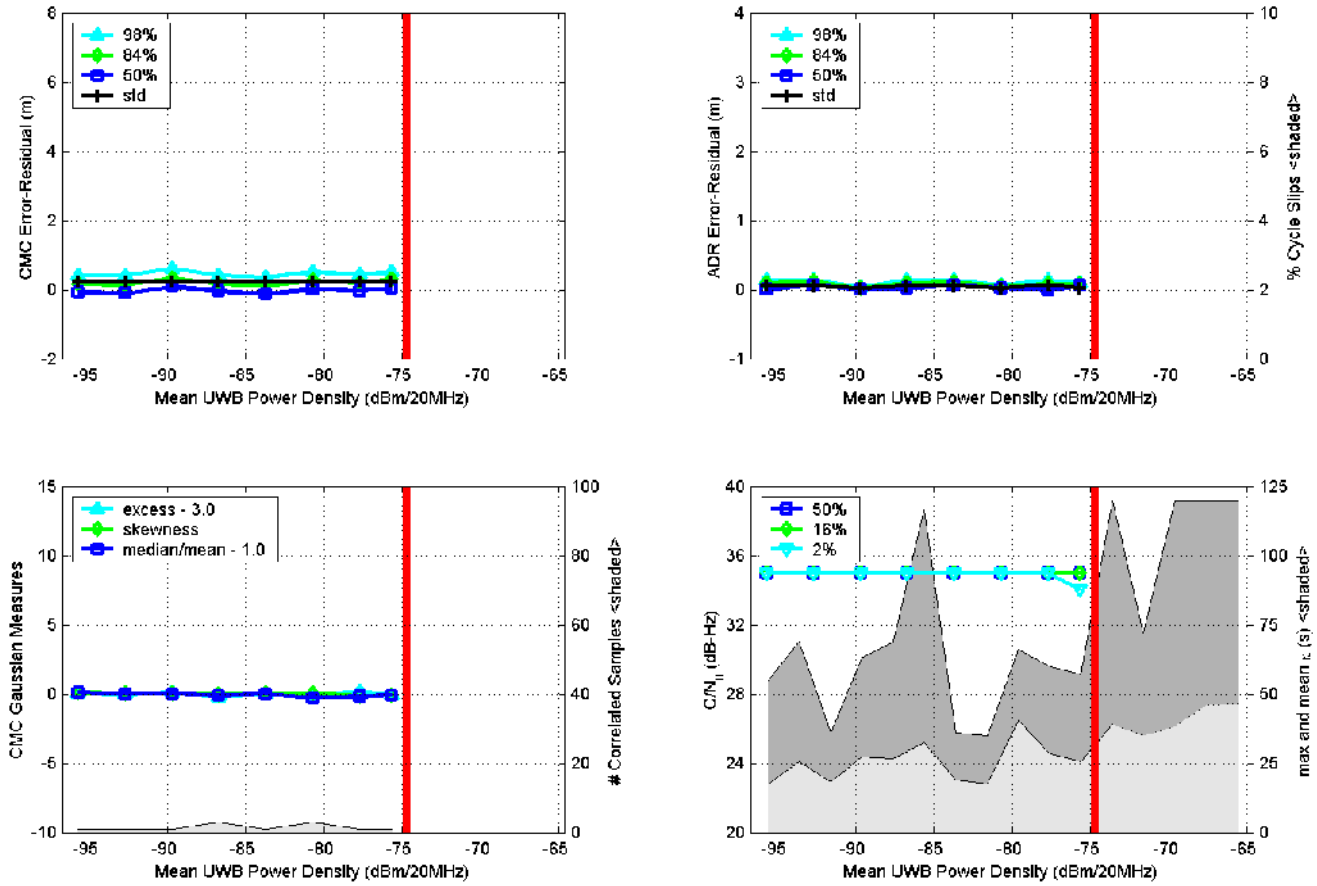

Figure F.2.24. Measured GPS parameters (Rx 2) as a function of 0.1-MHz PRF, 2%-RRD, non-gated UWB interference.

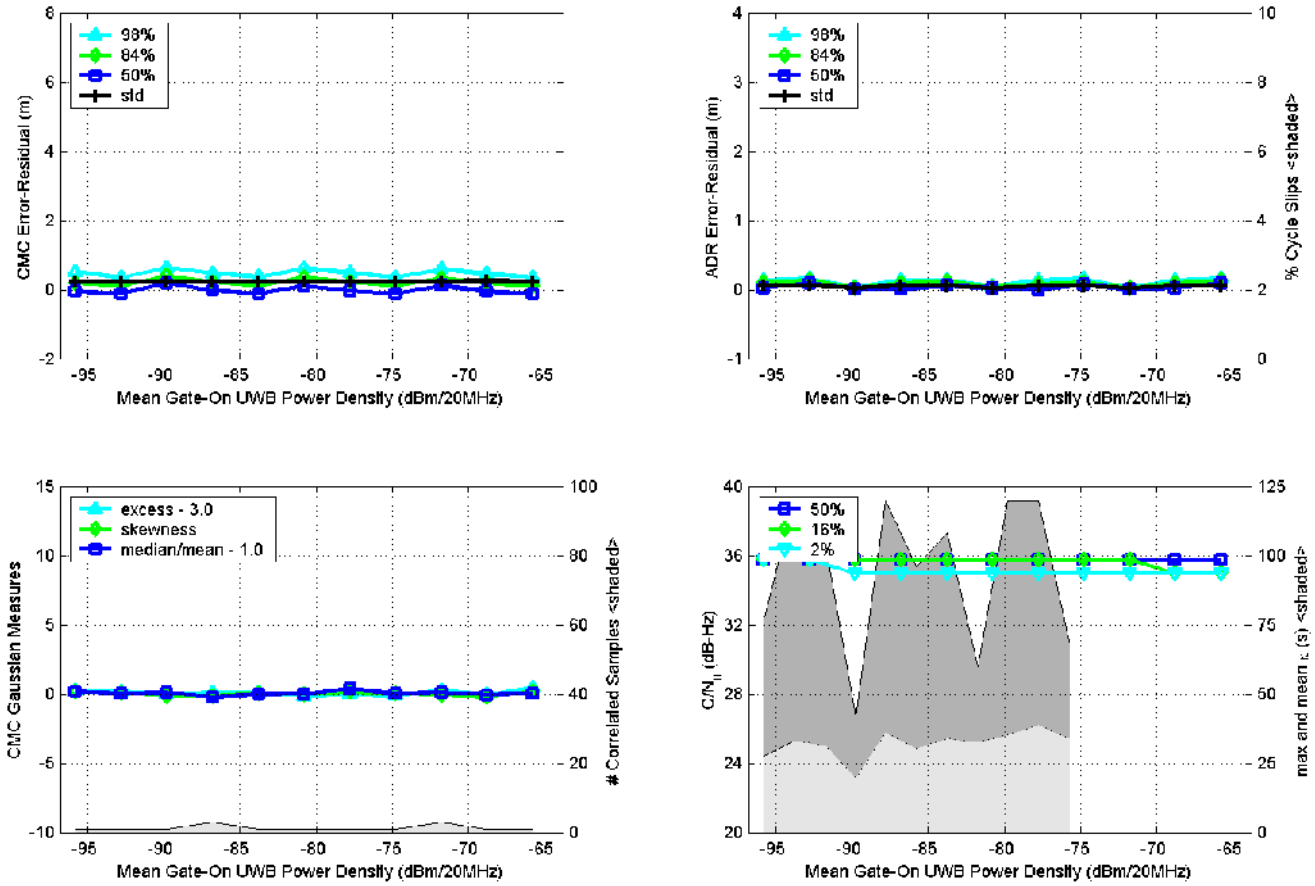

Figure F.2.25. Measured GPS parameters (Rx 2) as a function of 0.1-MHz PRF, 2%-RRD, gated (20% duty cycle) UWB interference.